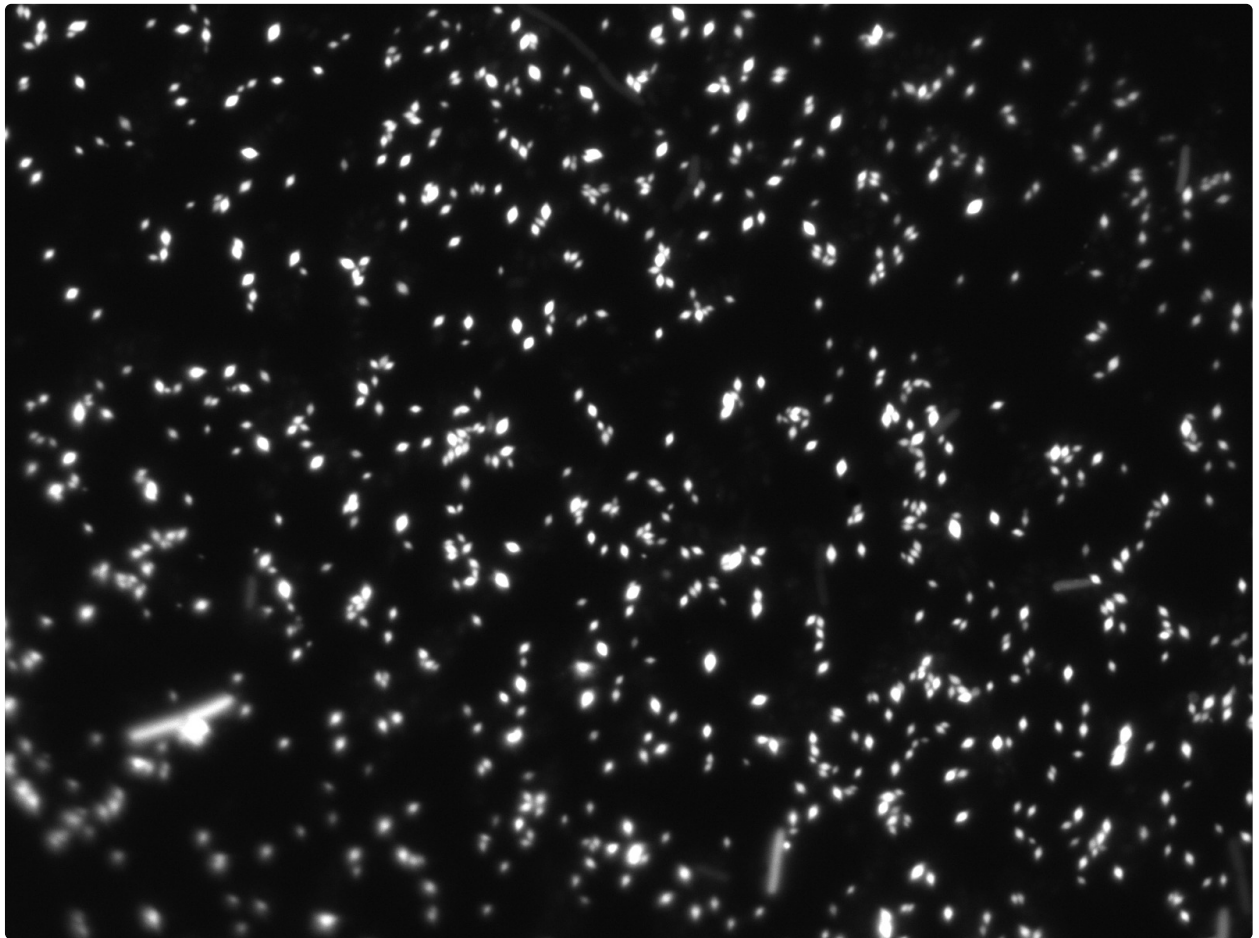


# Spore-forming bacteria as pharmaceutical factories

David Lee Joshua Baynard



May 2019

Emmanuel College

This thesis is submitted for the degree of Doctor of Philosophy.



## Preface

This thesis is the result of my own work and includes nothing which is the outcome of work done in collaboration except as declared in the Preface and specified in the text.

It is not substantially the same as any that I have submitted, or, is being concurrently submitted for a degree or diploma or other qualification at the University of Cambridge or any other University or similar institution except as declared in the Preface and specified in the text. I further state that no substantial part of my thesis has already been submitted, or, is being concurrently submitted for any such degree, diploma or other qualification at the University of Cambridge or any other University or similar institution except as declared in the Preface and specified in the text.

It does not exceed the prescribed word limit for the relevant Degree Committee.

Some laboratory work was performed under my academic supervision by undergraduate students Joshua Cozens and Luke Vinter, and by masters student Tayla Gordon. This is indicated in the text.



## Summary

Many *Bacilli* form dormant structures, spores, which routinely survive physical, chemical and biological challenge. How do spores encapsulate their contents, and could it be possible to mimic or adapt them to make better drug products?

Key spore component 2,6-dipicolinic acid (DPA) is necessary for protein stability, but investigation of its role is confounded with that of water content. Tests replacing DPA with chemical analogues were not successful, but led to the novel approach of doping spores with extra DPA.

Various *Bacillus* species, in the main *B. subtilis* and *B. thuringiensis*, have been engineered to produce, for the first time, fragments of a humanized monoclonal antibody: kindly provided by Medimmune. It is possible to produce antibodies inside the spore core.

This work proposes for the first time that such therapeutic spores might lack an outer coat, and demonstrates that antibody production continues. It is understood they continue to resist most challenges including wet heat, which damages proteins, yet they become susceptible to lysozyme. Such spores, further developed to lyse in presence of intestinal, though not gastric fluid, may have use in oral delivery.

Cry1Ac of *B. thuringiensis* offers an alternative; large protein crystals are produced during sporulation. Here, various fluorescent fusions that maintain fluorescence over months were developed and investigated in detail. For the first time, fluorescent antibody crystals were produced. In addition to drug delivery, these fusions offer a novel approach to crystallization of intransigent proteins, for structural studies.

This work shows that it might be feasible to use spores as pharmaceutical formulations. A number of challenges remain: from fabrication, through limits of current good manufacturing practice, to engineering biology to protect the environment and commercial interests. Bacterial spores have for the past century and a half been known for their dormancy, and it's about time engineers took advantage.

## Colophon

Except where otherwise noted, this work, *Spore-forming bacteria as pharmaceutical factories*, by David Lee Joshua Baynard, is licensed under the Creative Commons Attribution-ShareAlike 4.0 International License, CC BY-SA 4.0 (<http://creativecommons.org/licenses/by-sa/4.0/>).



The diagram in figure 1.5 is Copyright © 1976, American Society for Microbiology.

Figure 1.7, too, is Copyright © 1976, American Society for Microbiology.

Figure 1.8 is Copyright © 1959, Rockefeller University Press.

Figure 1.9 is Copyright © 2014, John Wiley and Sons.

Figure 1.10, *Electron micrograph of the coat of a wild-type and a cotE mutant spore*, by Zheng *et al.* (1988), is licensed by Cold Spring Harbor Laboratory Press under CC BY-NC 4.0 (<https://creativecommons.org/licenses/by-nc/4.0/>).

✪

This thesis was rendered from source with Pandoc (<https://pandoc.org/>) and typeset using Prince (<https://www.princexml.com/>).

✪

The cover image is a fluorescence micrograph of spores of *B. thuringiensis* subsp. *kurstaki* HD-73::3130.

To those who stayed the course, and those who could not.





## Acknowledgements

I thank my supervisor, Graham Christie, who fought for me from the very first grant application, to the completion of this thesis. With metaphorical and literal sniff tests, he demonstrated the importance of quality in research. His supervision was complemented by my advisor, Krish Mahbubani, who asked the tough questions about my direction and development, and gave me confidence in my answers.

I'm grateful to Ljiljana Fruk and Simon Cutting for their professional, punctual and pertinent work as my second examiners. This thesis has benefited from exposure to Prof. Cutting's unique domain expertise and from Dr Fruk's constructive and focused feedback.

I must thank CEB for providing an EPSRC doctoral training grant to support my research, and MedImmune (now AZ Biologics) for extending that support to the end of my research contract. MedImmune provided laboratory funding, technical suggestions and a career-shaping insight into a leading pharmaceutical company.

My fellow molecular microbiologists have been sources of solidarity, lab supplies and technical support: Srishti, Işik, Julia, Mo, Bahja, Henry, Xu Ke, Abhi, Irîs, Manja, Amin and Sina. Luke and Josh did a fantastic job on their undergraduate research project, as did Tayla for her MPhil. Ever the source of quiet reassurance, quick quips and Q5 polymerase, Dave Bailey kept my work at the forefront of what was possible.

Thanks to Christine, Debbie, Jason, Lee, Maggie, Phil, Roz, Simon, Sue and Tom, the equipment and processes just worked. Everything was clean, save the jokes. Only with good fortune will I again find such professional and dedicated technical support. I extend my thanks to Amanda, Elena, Iain, Laura, Michaela and Robin, who resolved the miscellany of non-laboratory issues quickly and with good humour. Finally, Amberley, Colin, Fanny, Fernando, Hendrik, Jethro, Laurie and Santi all offered welcome guidance, as did Eric and my former directors of studies: Bart and Patrick.

Emmanuel college has been a home for the past twelve years, where thanks to academics and staff, alumni and my contemporaries, I've grown professionally and personally. Fiona Reynolds and Richard Wilson have proffered extremely helpful career advice, and my long-serving graduate tutor, Jeremy Caddick, has offered a reassuring voice (and the proverbial big stick). I'm grateful to Pete and Mary Twitchett, and all those involved with EBC; to the porters Dave, Donna, Karen, Monty, Paul, Peter and Stuart, who could brighten even the

darkest day; and to Faith, JuG and Nick from the Emmanuel Society. My greatest privilege was to represent the graduate student body, as president and treasurer of the MCR, where I learned when to smile politely and when to fight.

I'm grateful to all those whose love and friendship proved invaluable during this time. My friends, in particular Alice, Beth, Bobby, Delphine, Emily, Mark, Sam, Sarah, Sophie, Tom, Veronika and Zac, have shared the apogees and perigees of this turbulent process. I thank Alison, Mark, Sam and Shanna, for hosting me while I sought somewhere to live, and Paul too — both for this and for his reviewing my thesis, as I bridged the fourteen month gap between submission and *viva*. Nathan, Becky and Tara invited me to join their scrappy (now profitable) start-up, showed how I can do good and well, and (with Vincent, Alex and Marek) offered mentorship and friendship in this difficult world.

I thank Sara and Elana, my sisters, who knew when to put an arm on my shoulder and when to give me a kick in the rear: my brothers-in-law, too, despite their bias towards the latter. Dad, I shall neither help your buddy set up his CBD QC lab, nor quit my job to trade cryptocurrencies, but don't stop trying. Mum, I hope I've made the most of the opportunities you've given me. I have come a very long, yet also very short way from singing times tables with you in the car. Thank you (and David) for your patience. I'm happy Anne got to see me start the PhD, and Nat saw me submit the thesis, twice. I hope to make you proud.

Contents	11
List of Figures	15
List of Tables	17
Abbreviations	19
Nucleic acid codes	23
Amino acid codes	24
Units	25
1 Introduction	27
1.1 Bacterial endospores	28
1.1.1 Spores and humans	29
1.1.2 Spores as insecticides	30
1.1.3 Spores in industry	30
1.2 Therapeutic proteins	31
1.2.1 Monoclonal antibodies	32
1.2.2 Bacterial production of therapeutic proteins	32
1.2.3 Failings of formulations	35
1.2.4 How to stabilize a protein	35
1.2.5 Quantifying protein quality	36
1.3 Spore biology	38
1.3.1 Sporeformers in biotechnology	38
1.3.2 The sporulation-germination cycle	38
1.3.3 Crystal proteins	44
1.3.4 Spore survival	46
1.3.5 Protein stability in spore cores	51
1.4 Spores as delivery vehicles	57
1.4.1 Spores protect their protein contents	57
1.4.2 Spores can produce vast quantities of protein	58
1.4.3 Prior art	59
1.5 This thesis	63

2	Methods	67
2.1	Materials & Equipment	68
2.1.1	Antibiotics	68
2.1.2	Antibodies	69
2.1.3	Ladders	69
2.1.4	Plasmids	69
2.1.5	Strains	69
2.1.6	Equipment	71
2.1.7	Buffers	71
2.1.8	Media	81
2.2	Basic microbiology	88
2.2.1	Culture	88
2.2.2	Gradient plate analysis	88
2.2.3	Promoter analysis	89
2.3	Cloning	90
2.3.1	<i>In silico</i> design	90
2.3.2	Producing DNA fragments	90
2.3.3	Assembly	92
2.3.4	Verification of constructs	92
2.3.5	Transformation	94
2.3.6	Isolation of desired recombinant <i>B. megaterium</i>	97
2.3.7	Plasmid extraction	98
2.3.8	<i>I-SceI</i> digestion	98
2.4	Strain construction	100
2.4.1	<i>B. megaterium</i>	100
2.4.2	<i>B. thuringiensis</i>	101
2.4.3	<i>B. cereus</i>	104
2.4.4	<i>B. subtilis</i>	104
2.5	Spore-specific microbiology	111
2.5.1	Sporulation	111
2.5.2	Spore washing	112
2.6	Microscopy	114
2.6.1	Slide preparation	114
2.6.2	Phase contrast	114
2.6.3	Fluorescence	115
2.6.4	Image processing	115
2.7	Protein processing	116
2.7.1	Spore disruption	116
2.7.2	Isolation of soluble protein fraction	116

2.7.3	SDS-PAGE	.	.	.	.	.	.	.	.	116
2.7.4	Purification	.	.	.	.	.	.	.	.	118
2.7.5	Buffer exchange	.	.	.	.	.	.	.	.	118
2.8	Spore assays	.	.	.	.	.	.	.	.	119
2.8.1	DPA assay	.	.	.	.	.	.	.	.	119
2.8.2	Lysozyme susceptibility	.	.	.	.	.	.	.	.	119
2.8.3	Wet heat susceptibility	.	.	.	.	.	.	.	.	119
2.8.4	Spore viability count	.	.	.	.	.	.	.	.	120
3	The effects of dipicolinic acid on spores	.	.	.	.	.	.	.	.	121
3.1	Introduction	.	.	.	.	.	.	.	.	122
3.2	Results & discussion	.	.	.	.	.	.	.	.	124
3.2.1	Spores lacking the putative DPA synthetase	.	.	.	.	.	.	.	.	124
3.2.2	Scavenging of DPA during sporulation	.	.	.	.	.	.	.	.	129
3.2.3	Inhibition of sporulation by DPA	.	.	.	.	.	.	.	.	130
3.2.4	Wet heat susceptibility	.	.	.	.	.	.	.	.	131
3.2.5	Spores grown in DPA analogue-doped media	.	.	.	.	.	.	.	.	134
3.2.6	Experimental design	.	.	.	.	.	.	.	.	138
3.3	Conclusion	.	.	.	.	.	.	.	.	142
4	Therapeutic proteins in sporulating <i>Bacillus subtilis</i>	.	.	.	.	.	.	.	.	145
4.1	Introduction	.	.	.	.	.	.	.	.	146
4.2	Results & discussion	.	.	.	.	.	.	.	.	148
4.2.1	Antibody expression by sporulating <i>B. subtilis</i>	.	.	.	.	.	.	.	.	148
4.2.2	Behaviour of the $\Delta cotE$ strain	.	.	.	.	.	.	.	.	154
4.2.3	Inducible competence and counter-selection	.	.	.	.	.	.	.	.	159
4.2.4	Nanobodies expressed by sporulating <i>B. subtilis</i>	.	.	.	.	.	.	.	.	162
4.2.5	Path to a commercially viable product	.	.	.	.	.	.	.	.	165
4.3	Conclusions	.	.	.	.	.	.	.	.	169
5	Cry protein fusions	.	.	.	.	.	.	.	.	171
5.1	Introduction	.	.	.	.	.	.	.	.	172
5.2	Results & discussion	.	.	.	.	.	.	.	.	173
5.2.1	Cry1Ac subdomain fusions	.	.	.	.	.	.	.	.	173
5.2.2	Cry1Ac-antibody fusions	.	.	.	.	.	.	.	.	183
5.2.3	Expression in other <i>Bacilli</i>	.	.	.	.	.	.	.	.	186
5.2.4	Expression of the <i>cry1Ac</i> operon in <i>E. coli</i>	.	.	.	.	.	.	.	.	190
5.2.5	Solubilization of crystal proteins	.	.	.	.	.	.	.	.	194
5.3	Conclusions	.	.	.	.	.	.	.	.	197

6	Bacterial spores as a commercially viable therapeutic product	·	·	199
6.1	The effects of DPA	·	·	200
6.2	Therapeutic proteins in the spore core	·	·	201
6.3	Crystal protein fusions	·	·	203
6.4	Final conclusions	·	·	205
	References	·	·	207
A1	Appendix	·	·	225
A1.1	DPA Assay	·	·	226
A1.2	<i>B. megaterium</i> colony counts	·	·	229
A1.3	Spores grown with DPA analogues	·	·	231
A1.4	Pop-out calculation	·	·	232
A1.5	Fusions	·	·	234
A1.6	Nanobodies	·	·	235
A1.7	Inducibly (super-)competent <i>B. subtilis</i>	·	·	236
A1.8	$\Delta cotE$ mutants	·	·	239

## List of Figures

1.1	Phase contrast micrographs of sporulating <i>B. subtilis</i> .	28
1.2	Therapeutic antibodies disrupt disease pathways.	31
1.3	Cartoon representation of an IgG (immunoglobulin G).	33
1.4	Camelid heavy chain antibodies.	34
1.5	The structure of a <i>B. megaterium</i> spore.	39
1.6	The chemical structure of DPA (2,6-dipicolinic acid).	39
1.7	A summary schematic of the sporulation stages.	41
1.8	A schematic of the sporulation process for <i>B. thuringiensis</i> subsp. <i>alesti</i> .	41
1.9	The annotated crystal structure of Cry1Ac.	44
1.10	Electron micrographs of <i>B. subtilis</i> spores, with $\Delta cotE$ mutation.	47
1.11	DPA, interacting specifically with arginine residues in hen egg white lysozyme.	53
1.12	SpoVAD, forming a gated DPA channel in <i>B. subtilis</i> .	56
2.1	Allelic exchange via Campbell-type homologous crossover between the vector and target genome.	97
2.2	Map of plasmid pDBT30, based on pHT315.	101
2.3	Plasmid pDBT71e, constructed to delete <i>cotE</i> from <i>B. subtilis</i> .	108
3.1	Map of the pDBT21s plasmid, used to disrupt the <i>spoVF</i> operon in <i>B. megaterium</i> by allelic exchange.	124
3.2	Phase contrast micrographs of <i>B. megaterium</i> spores, from strains with <i>spoVF</i> deletions.	126
3.3	Results of the DPA assays, for <i>B. megaterium</i> spores.	128
3.4	Micrographs showing failure to sporulate with excessive DPA in the sporulation medium.	130
3.5	Colony counts for germinated <i>B. megaterium</i> spores, grown in standard or DPA-supplemented medium.	133
3.6	Survival plots for <i>B. megaterium</i> spores, grown in standard or DPA-supplemented medium.	134
3.7	Chemical structures of DPA (2,6-dipicolinic acid) and some chemical analogues.	135
3.8	Outcome of sporulation screening, in analogue-supplemented SNB.	137
4.1	Representative pDBT61* plasmid for expressing NIP109 fragments under control of promoter $P_{sspB}$ .	149
4.2	Micrographs of <i>B. subtilis</i> 168::61* spores, containing antibody fragments.	150
4.3	Western blot of NIP109 fragments, extracted from <i>B. subtilis</i> 168::61* spores.	151
4.4	Fractionated crude lysates from WT coat and $\Delta cotE$ <i>B. subtilis</i> spores containing antibody fragments.	154

4.5	Micrographs of these <i>B. subtilis</i> spores, challenged with lysozyme.	155
4.6	Gradient plates of 5-fluorouracil, spread with <i>B. subtilis</i> .	161
4.7	Western blot of nanobodies, extracted from <i>B. subtilis</i> spores.	163
4.8	Western blot showing <i>B. subtilis</i> can produce a chromobody.	163
4.9	Fractionated, purified extracts of nanobodies, from <i>B. subtilis</i> spores.	164
5.1	The domains of the Cry1Ac protein.	173
5.2	Plasmid pDBT310, for expression of (His-tagged) Cry1Ac, from its native operon.	174
5.3	Polyacrylamide gel of solubilized spore-crystal slurries, containing Cry1Ac-mCherry fusions.	175
5.4	Micrographs of <i>B. thuringiensis</i> HD-73 spores, not containing Cry1Ac-mCherry fusions.	177
5.5	Micrographs of <i>B. thuringiensis</i> HD-73 spores, containing Cry1Ac-mCherry fusions.	178
5.6	Electron micrographs of Cry1Ac crystals.	180
5.7	Micrographs of <i>B. thuringiensis</i> HD-73::3110 spores, bearing a leader-mCherry fusion.	179
5.8	Micrographs of <i>B. thuringiensis</i> HD-73::3140 spores, bearing the leader-toxic core-mCherry fusion.	181
5.9	Micrographs of antibody fusion crystals in <i>B. thuringiensis</i> spore cultures.	184
5.10	Polyacrylamide gel of Cry1Ac-mCherry-NIP109 triple fusions.	185
5.11	<i>B. thuringiensis</i> YBT-020 spore cultures, engineered to express Cry fusions.	187
5.12	<i>B. cereus</i> spore cultures, engineered to express Cry fusions.	188
5.13	<i>B. subtilis</i> spore cultures, engineered to express Cry fusions.	189
5.14	Micrographs of <i>B. subtilis</i> 690::31610 spores, bearing His-tagged mCherry.	189
5.15	Micrographs of <i>E. coli</i> , having assembled pDBT31* vectors.	190
5.16	Streaks of <i>E. coli</i> Turbo colonies, bearing pDBT31* plasmids.	192
5.17	Micrographs of <i>B. thuringiensis</i> HD-73, following attempts to dissolve crystal proteins.	195
A1.1	Calibration curve for DPA assay.	226
A1.2	Micrographs of <i>B. megaterium</i> 1551::21s+, sporulated in DPA analogue-supplemented SNB.	231
A1.3	Probability density distributions, for cells undergoing pop-out.	233
A1.4	The <i>upp</i> locus, following a successful indel mutation.	236
A1.5	Plasmid pDBT69d for construction of supercompetent <i>B. subtilis</i> .	237
A1.6	The <i>upp</i> locus, after integration of plasmid pDBT69d into <i>B. subtilis</i> 168.	238



## List of Tables

1.1	Factors that induce germination, and their mechanisms.	42
2.1	Antibiotics, used in this project.	68
2.2	Base plasmids, used in this project.	69
2.3	Further plasmids used, but not designed, as part of this work.	69
2.4	Plasmids, constructed as part of this project and referenced in this thesis.	69
2.5	Background strains, used in this thesis.	69
2.6	<i>B. megaterium</i> strains, engineered to test behaviour of DPA.	70
2.7	<i>B. subtilis</i> strains, with coat mutation or for antibody expression.	70
2.8	Strains, for work with <i>cry1Ac</i> operon.	70
2.9	Laboratory equipment.	71
2.10	Transforming buffer ( <i>E. coli</i> ).	74
2.11	T-base buffer ( <i>B. subtilis</i> ).	74
2.12	Electroporation buffer ( <i>B. cereus</i> family).	76
2.13	Base for PDMR (PDM, ratio optimized), with C:N ratio of 2.8:1.	81
2.14	Supplement for PDMR, added before use.	81
2.15	Composition of RHAF (Hadlaczky Alföldi Fodor) broth ( <i>B. megaterium</i> ).	82
2.16	Recipes for SpC and SpII media ( <i>B. subtilis</i> ).	82
2.17	Electroporation recovery medium.	82
2.18	Composition of SNB, supplemented nutrient broth ( <i>B. megaterium</i> ).	83
2.19	Supplements for 2×SG and 2×SGR medium ( <i>B. subtilis</i> ).	84
2.20	Base CCY (casein casein yeast) medium ( <i>B. cereus</i> family).	84
2.21	CCY salts, to supplement base medium.	84
2.22	SM (Sterlini-Mandelstam) growth medium.	85
2.23	SM (Sterlini-Mandelstam) resuspension medium.	85
2.24	CH I + II, for SM (Sterlini-Mandelstam) medium ( <i>B. subtilis</i> ).	85
2.25	PCR primers, to construct plasmid pDBT21s.	100
2.26	PCR primers, to construct plasmid pDBT30.	101
2.27	PCR primers, to construct <i>cry1Ac-mCherry</i> plasmids.	102
2.28	PCR primers, to construct <i>cry1Ac-NIP109</i> plasmids.	102
2.29	PCR primers, to construct pDBT6* plasmids.	105
2.30	PCR primers, to construct nanobody plasmids.	105
2.31	PCR primers, to construct pDBT69? plasmids.	106
2.32	PCR primers, to construct pDBT12u and pDBT71e? plasmids.	108
2.33	Promoters switched, in constructing pDBT316* plasmids.	109
2.34	Lenses and corresponding magnifications, for optical microscopy.	114
2.35	Fluorophores, used in fluorescence microscopy.	115
3.1	<i>B. megaterium</i> strains, used in this chapter.	124
4.1	Fragments of the NIP109 antibody.	148

4.2	Nanobodies, used in this chapter.	162
5.1	Schematic representation of mutant <i>cry1Ac</i> fusion operons.	173
5.2	Fluorescence phenotypes of <i>B. thuringiensis</i> HD-73 strains bearing <i>cry1Ac</i> fusion operons.	176
5.3	Schematic representation of Cry1Ac–NIP109 fusion operons.	183
A1.1	Paired comparisons test, of differences in DPA content with or without $\Delta spoVF$ mutation.	226
A1.2	Paired comparisons test of differences in DPA content with (✓) or without (✗) exogenous DPA.	226
A1.3	Data, for DPA assay plot.	226
A1.4	Colony count data for <i>B. megaterium</i> mutants.	229
A1.5	Paired comparisons test, of differences in OD <sub>600</sub> in $\Delta cotE$ strains.	239

## Abbreviations

5-FU	fluorouracil
ADCC	antibody dependent cell-mediated cytotoxicity
AMP	adenosine monophosphate
API	active pharmaceutical ingredient
ATP	adenosine triphosphate
BEST	Bayesian estimation [that] supersedes the <i>t</i> -test
BGSC	Bacillus Genetic Stock Centre
BiFC	bimolecular fluorescence complementation
BSA	bovine serum albumin
CAIC	Cambridge Advanced Imaging Centre
CCD	charge-coupled device
CCY	casein casein yeast
CDVAX	<i>C. difficile</i> vaccine
cGMP	current good manufacturing practice
CHO	Chinese hamster ovary
CLE	cortex lytic enzyme
CSTR	continuous stirred tank reactor
Ctx	cortex
DAP	diaminopimelic acid
DHDPA	dihydrodipicolinic acid
DLS	dynamic light scattering
DLVO	Derjaguin Landau Verwey Overbeek
DMSO	dimethyl sulfoxide
DNA	deoxyribonucleic acid
dNTP	deoxy-nucleoside triphosphate
DPA	dipicolinic acid
DSC	differential scanning calorimetry
DTT	dithiothreitol
DXO	double crossover
EDTA	ethylenediaminetetraacetic acid
ELM	ellipsoid localization microscopy
EM	electron microscopy
Ex	exosporium
FASTA	fast-all
FU	fluorouracil

GALT	gut associated lymphatic tissue
gDNA	genomic DNA
GFP	green fluorescent protein
GR	germinant receptor
HEPES	4-(2-hydroxyethyl)-1-piperazineethanesulphonic acid
HTDA	4-hydroxy-tetrahydro-dipicolinic acid
IC	inner coat
IDA	iminodiacetic acid
IgG	immunoglobulin G
IM	inner membrane
IPA	isophthalic acid
KAM	Klenow assembly method
LB	lysogeny broth
LDS	lithium dodecyl sulphate
L-ASA	L-aspartate semi-aldehyde
mAb	monoclonal antibody
MBP	maltose binding protein
MES	2-(N-morpholino)ethanesulphonic acid
MOPS	3-(N-morpholino)propanesulphonic acid
mRNA	messenger RNA
NIP	4-hydroxy-3-iodo-5-nitrophenylacetic acid
NMR	nuclear magnetic resonance
NNPP	neural network promoter prediction
NTA	nitrilotriacetic acid
OC	outer coat
OF	oil flowable
ORF	open reading frame

PA	picolinic acid
PAGE	polyacrylamide gel electrophoresis
PCR	polymerase chain reaction
PD-L1	programmed death–ligand 1
PDB	Protein Data Bank
PDM	plasmid DNA medium
PDMR	PDM, ratio optimized
PEG	poly–ethylene glycol
PGA	phosphoglyceric acid
PIPES	piperazine–N,N'–bis(2–ethanesulphonic acid)
PMSF	phenylmethylsulfonyl fluoride
PVDF	polyvinylidene difluoride
P <sub>i</sub>	inorganic phosphate
RBS	ribosome binding sequence
RHAF	Hadlaczky Alföldi Fodor
ROS	reactive oxygen species
SASP	small acid–soluble protein
SAXS	small angle x–ray scattering
SC	liquid suspension concentrate
scFv	single chain variable fragment
SDS	sodium dodecyl sulphate
SLS	static light scattering
SM	Sterlini–Mandelstam
SNB	supplemented nutrient broth
SOB	super optimal broth
SP	spore photoproduct
SXO	single crossover
TAE	tris acetate EDTA
TBS	tris–buffered saline
TEM	transmission electron micrograph
TMB	3,3',5,5'–tetramethylbenzidine
tRNA	transfer RNA
TSB	tryptone soy broth
UC	undercoat
UV	ultraviolet
VPO	vapour phase osmometry
WG	wettable granule
WP	wettable powder
WT	wild type

YFP

yellow fluorescent protein

## Nucleic acid codes

Symbol	Mnemonic	Adenine	Cytosine	Guanine	Thymine	Uracil
A	Adenine	✓				
C	Cytosine		✓			
G	Guanine			✓		
T	Thymine				✓	
U	Uracil					✓
N	aNy	✓	✓	✓	✓	✓
.	none					
K	Keto			✓	✓	✓
Y	pYrimidine		✓		✓	✓
S	Strong		✓	✓		
W	Weak	✓			✓	✓
R	puRine	✓		✓		
M	aMino	✓	✓			
B	not Adenine		✓	✓	✓	✓
D	not Cytosine	✓		✓	✓	✓
H	not Guanine	✓	✓		✓	✓
V	not Thymine/ Uracil	✓	✓	✓		

Source: Evett (2004).

## Amino acid codes

Symbol	3-letter code	Amino acid
A	Ala	Alanine
B	Asx	Asparagine/aspartate
C	Cys	Cysteine
D	Asp	Aspartic acid
E	Glu	Glutamic acid
F	Phe	Phenylalanine
G	Gly	Glycine
H	His	Histidine
I	Ile	Isoleucine
K	Lys	Lysine
L	Leu	Leucine
M	Met	Methionine
N	Asn	Asparagine
P	Pro	Proline
Q	Gln	Glutamine
R	Arg	Arginine
S	Ser	Serine
T	Thr	Threonine
V	Val	Valine
W	Trp	Tryptophan
X	—	Unknown or other
Y	Tyr	Tyrosine
Z	Glx	Glutamine/glutamate

Source: IUPAC-IUB Comm. on Biochem. Nomencl. (1968).



## Units

Symbol	Name	Quantity
$\Omega$	Ohm	Electrical resistance
bn	billion	
bp	base pair	Nucleotides
$^{\circ}\text{C}$	degree centigrade	Temperature
cfu	colony forming unit	Microbial viability
Da	Dalton	Atomic mass unit
F	Farad	Capacitance
kg	kilogram	Mass
L	litre	Volume
ml	millilitre	Volume
h	hour	Time
kmol	kilomole	Number of atoms
V	Volt	Potential
m	metre	Length
M	molar	Concentration
min	minute	Time
mol%	percentage by mole	Proportion
nt	nucleotide	Nucleotides
Pa	Pascal	Pressure
PSI	pound per square inch	Pressure
rpm	revolution per minute	Rate of rotation
s	second	Time
% v/v	percentage by volume	Proportion
% v/w	volume percentage by total mass	Proportion
% w/v	mass percentage of total volume	Proportion
% w/w	percentage by mass	Proportion



# Chapter 1

## Introduction

Is it possible to use bacterial spores for drug delivery? *Bacillus* species form dormant structures, which very effectively protect their contents from a range of physical and chemical stresses — and this is an attractive feature of a biopharmaceutical formulation. What follows is an exploration of this idea, from a study of the scientific literature concerning its context, through patent literature on applications, laboratory investigation into some of the possibilities, and a discussion of the gap between the outcome of such research and having a finished product that could save lives.

## 1.1 Bacterial endospores

*Bacilli* and *Clostridia* differentiate into endospores to become the most robust biological structures known (figure 1.1). They lie dormant for millennia, *i.e.* with no metabolic activity, yet throughout that time they passively sense their environment. Within minutes of the environment becoming hospitable, they germinate, once more becoming growing, *vegetative* cells (Abel-Santos, 2012; Setlow, 2014).

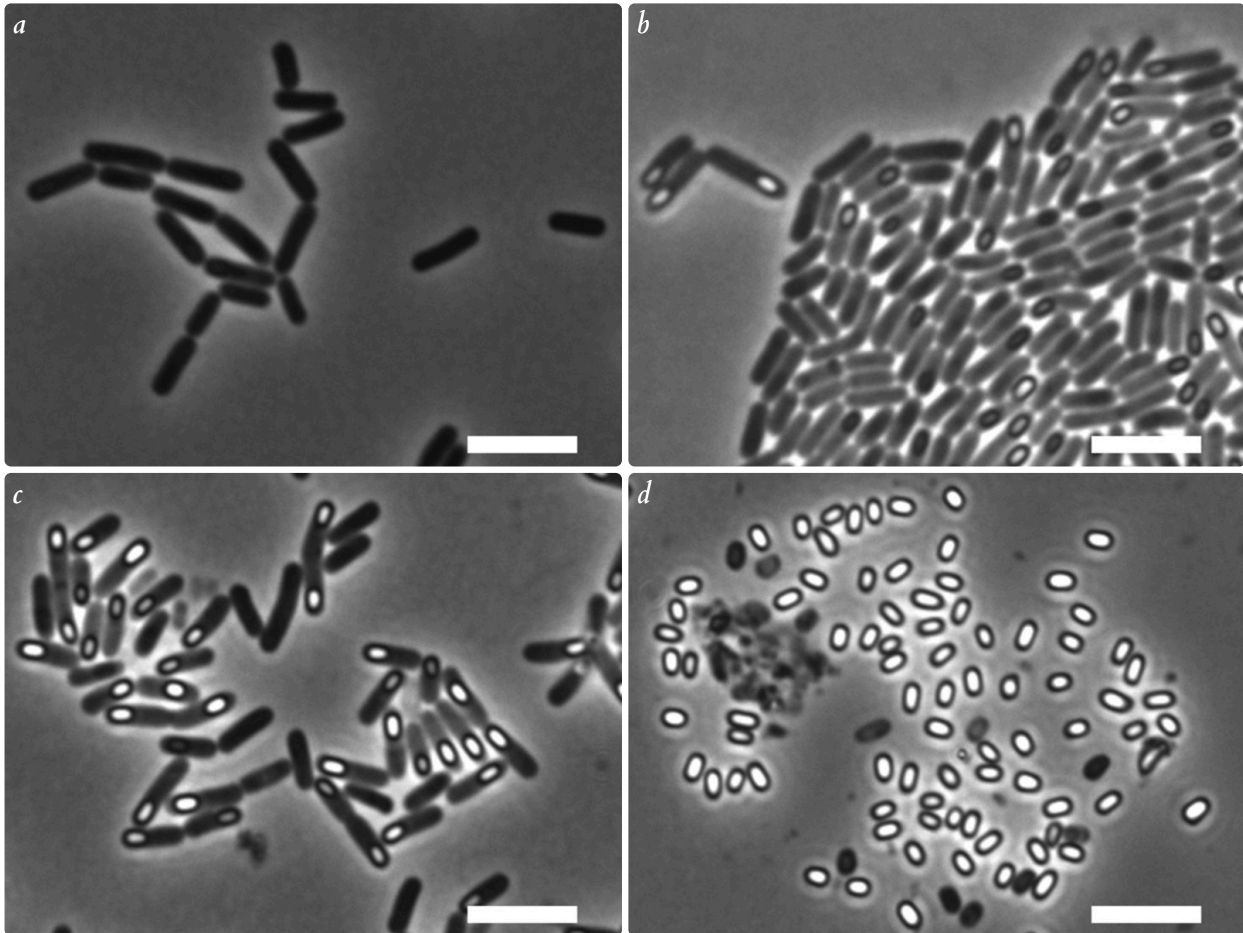


Figure 1.1: Phase contrast micrographs of sporulating *B. subtilis*. (a) shows vegetative cells, 3h after inoculation; (b) shows a sporangium with forming forespores (4h); (c) shows bright forespores (5h); (d) shows free spores and some debris (25h) The bright regions of the spores have high refractive indices, indicating low water content. Spores were produced using the synchronous resuspension technique. Scale bars are  $5\ \mu\text{m} \times 1\ \mu\text{m}$ .

The convention for naming proteins and genes is as follows: proteins begin with an upper case letter and are typeset as the surrounding text; genes begin with a lower case letter and are emphasised (*e.g.* Protein, *gene*).

In a review of bacterial endospore coats, McKenney *et al.* (2012) described other dormant bacterial ‘resting cells’. *Metabacterium polyspora* forms two (usually) and up to three spores per cell. For *Streptomyces*, exospores form from a multinucleate cell at the tip of a hypha. *Myxococcus* and some cyanobacteria form myxospores and heterocysts respectively, which involve no cell division. The authors commented that though desiccation resistance is common, resistances to other challenges vary. Like fungal spores and plant spores, these various resting cells shall not be considered further.

*Bacillus* species are allochthonous. Much of their life cycle is spent as saprophytes, though there remains much that is unknown about their behaviour in soil. The range of habitats of sporeformers extends beyond just soil. A recent paper from a multidisciplinary team reviewed, in part, the ecology of *B. anthracis*, reporting its ability to induce germination of grass seeds by itself germinating nearby; this behaviour is typically shown by *B. cereus*, yet the authors suspect *B. anthracis* has evolved to take advantage of the subsequent arrival of grazers (Carlson *et al.*, 2018). *Bacillus* species have been isolated from within walls of buildings, and from rocks — both at Earth’s surface and up to 3 km below. It is not clear to what extent this corresponds to cultures growing and sporulating within the rocks versus spores filtering through the pores (Nicholson, 2002). The remainder of the life cycle often includes passage through gastrointestinal systems of larger organisms. *Bacillus* species are frequently found within mammalian gut flora, where sporulation is critical to development of the GALT (gut associated lymphatic tissue) required for immune sampling (Tam *et al.*, 2006).

### 1.1.1 Spores and humans

Spores’ resistance to typical sterilization techniques has inspired much research. John Tyndall lends his name to one technique to kill bacterial spores. Tyndallization encourages spores to germinate and uses heat to kill the subsequently-vulnerable vegetative cells (Gould, 2006). The finest line on the industrial approach to spores must surely go to Grahame Warwick Gould, who wrote:

‘Newer’ processes such as treatment with ionizing radiation (first proposed in 1905) and high hydrostatic pressure (first proposed in 1899) may be introduced if consumer resistance and some remaining technical barriers could be overcome.

— Gould (2006)

### 1.1.2 Spores as insecticides

Some bacterial spores are a desirable presence, in agriculture. *B. thuringiensis* is widely used as a biopesticide for its highly specific pathogenicity (Sansinenea, 2012), though its shelf life, stability and ease of production and application no doubt played a role in its popularity. The role extends beyond agriculture, to forestry and mosquito control. The toxic components are the Cry and Cyt proteins (see section 1.3.3).

### 1.1.3 Spores in industry

The ABE process is not the only example of sporeformers in industry. *Bacillus* spores have themselves been used to test equipment and processes designed to disinfect or sterilize; *B. subtilis* (and even the opportunistic pathogen *B. cereus*) is used as a probiotic; and the vital agricultural role of *B. thuringiensis* is discussed. A comprehensive, and not quite dated, review of *Bacillus* species as industrial fermenters is by Schallmeyer *et al.* (2004).

Duc *et al.* (2003) reported the first example of a spore as a vaccine delivery system, and that work has continued, some as part of the doctoral thesis of Lin (2017) from the Christie group. The pitch is straightforward: immune sampling in the gastrointestinal system, predominantly at Peyer's patches, identifies pathogens and raises an adaptive immune response with greater efficacy against future mucosal infection than does injection. A spore would both protect the antigens through the stomach and act as an adjuvant, enhancing the immune response, once it reaches its destination.

Recently Martine Vandermarlière (2016) presented her work for amatsiQBiologicals on production of recombinant spores. The specific focus was cGMP (current good manufacturing practice): a framework for ensuring that the quality of a biopharmaceutical product meets the requirements of regulators and patients. The company has been working on a multidisciplinary project, aiming to use *B. subtilis* spores as a *C. difficile* vaccine, CDVAX (Cutting, 2013).

## 1.2 Therapeutic proteins

Therapeutic proteins, or *biologics*, can drastically improve health and quality of life of patients with many diseases and conditions. They are often valuable because of their multifunctional mechanisms (e.g. immuno-oncology, figure 1.2). However, there are difficult formulation challenges: these proteins can be difficult to produce correctly, and maintain their quality during formulation, transport and storage. It matters that the proteins have their correct form, as damaged proteins vary in behaviour — from ineffective, to acutely harmful.

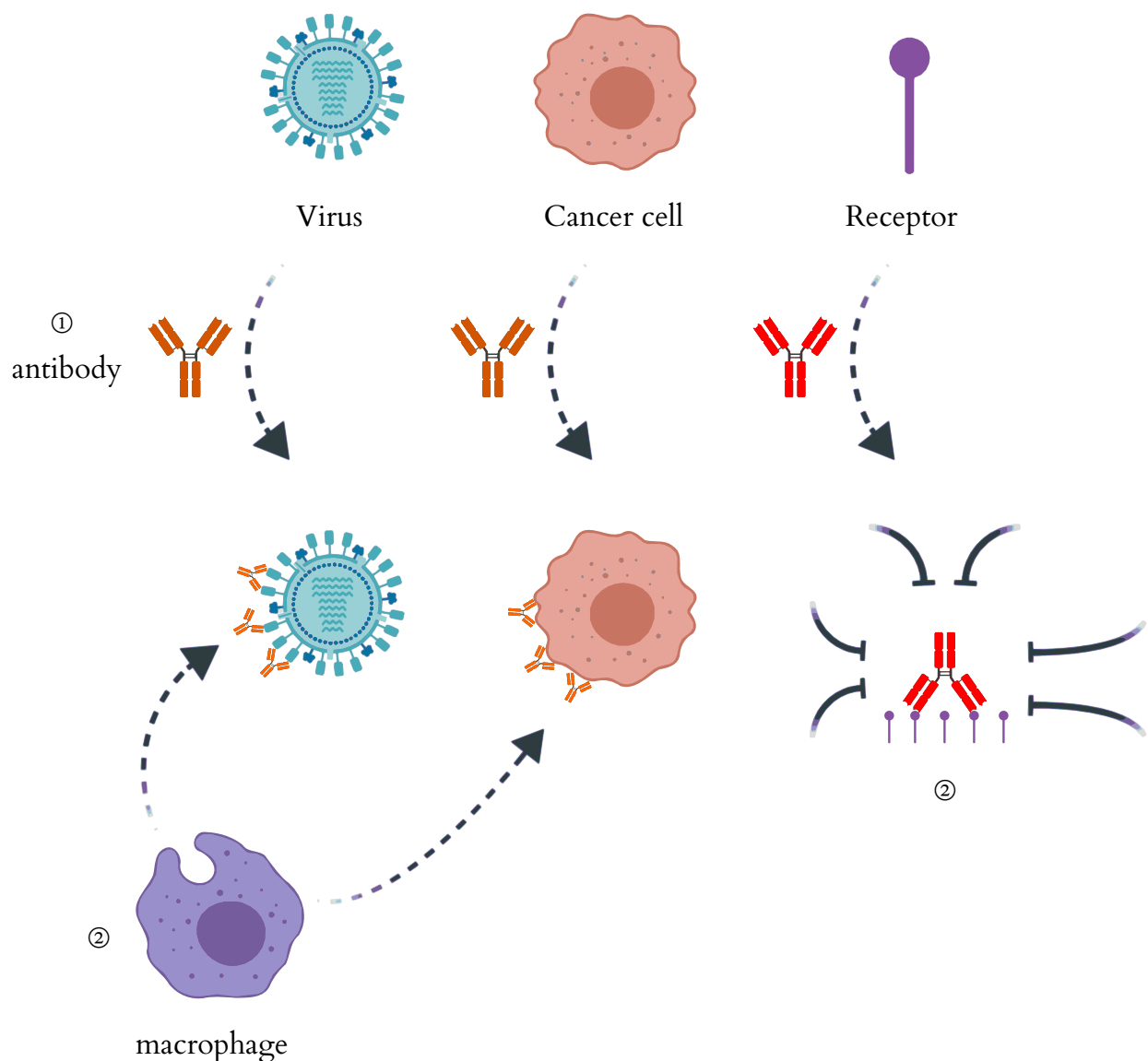


Figure 1.2: Therapeutic binding proteins, such as antibodies, disrupt processes which cause disease. ① The binding protein binds a target. ② The protein recruits an effector (such as a macrophage) or prevents other molecules from binding the target. For example, in immuno-oncology, antibodies flag cancerous cells and the ADCC (antibody dependent cell-mediated cytotoxicity) response marks them for phagocytosis, by macrophages.

The state of the art is as follows: mammalian cell lines produce proteins that are extracted, purified, and concentrated as a solution that needs to be stored below 4°C. That's often not possible, and the protein must be lyophilized (freeze-dried) and reconstituted directly before injection into a patient. This process is particularly complicated — and (importantly) it is impossible to guarantee quality on reconstitution.

### 1.2.1 Monoclonal antibodies

A mAb (monoclonal antibody) is a Y-shaped macromolecule, an immunoglobulin (figure 1.3), which binds with one end (paratope) to specific targets (epitopes) on antigens: typically pathogens or receptors. From a formulation perspective, they can be considered amphoteric polyelectrolytes: globular proteins which can aggregate to cause inactivation and immunogenicity (Arzenšek *et al.*, 2012). The production complexities required to avoid such an outcome is a major factor in the costs of mAbs (monoclonal antibody). Those costs can be prohibitive. For example, the PD-L1 (programmed death–ligand 1) inhibitor durvalumab (MedImmune) is estimated to cost \$180 000 per patient per year, for a year of fortnightly treatments (Optum Inc., 2017).

There are alternatives to mAbs. Antibody fragments such as scFvs (single chain variable fragments) lack effector functions (such as for ADCC), making them a good choice for interference with receptors. Newer alternatives, such as the camelid V<sub>H</sub>H antibodies' single domain variable fragments, *nanobodies*, are small enough for fast renal clearance (they are ~25 kDa and the upper kidney threshold is ~50 kDa, De Meyer *et al.*, 2014, see figure 1.4). These face many of the same production challenges, though, as full IgGs.

High production costs are in part a consequence of the industry standard, in which CHO (Chinese hamster ovary) cells produce antibodies in fermentors. There is much research on using bacteria as fermenters, instead.

### 1.2.2 Bacterial production of therapeutic proteins

The production of proteins, whether by bacteria or higher organisms, is termed *expression*. *Escherichia coli* are the most common bacterial expression host, but others, in particular the Gram-positive *Bacilli*, produce greater protein quantities, and with easier downstream



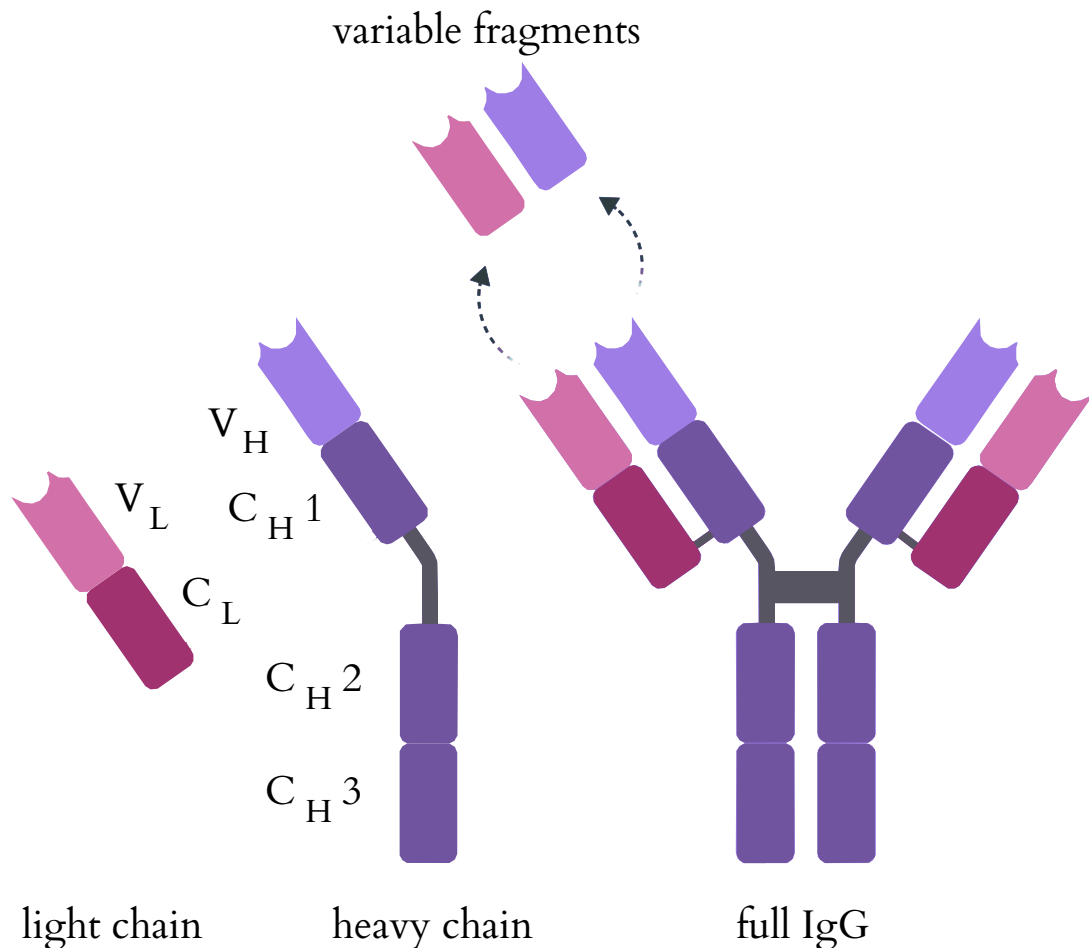


Figure 1.3: Cartoon representation of an IgG (immunoglobulin G). The light chain contains two domains, the heavy chain four. The variable domains,  $F_v$  (two sets of two, one per branch), contain the paratope, which recognises the antigen (epitope). The branch made from the light chain and corresponding  $C_L$  and  $C_{H1}$  heavy chain domains is known as the  $F_{ab}$  domain. The branch made from the pairs of  $C_{H2}$  and  $C_{H3}$  heavy chain domains is known as the  $F_c$  domain, and it is this which both binds Protein A and recruits effector functions.

processing (Terpe, 2006). Bacterial expression systems benefit from the fast, easy growth on cheap substrates and relatively simple genetics of bacteria, as compared with eukaryotes (in particular, mammalian cells).

For proteins expressed by *E. coli*, the chosen mechanisms usually deposit the product in the cytoplasm (Terpe, 2006). The periplasmic space is an alternative, which is more suitable for proteins requiring oxidized cysteines; osmotic shock or cell wall permeabilization then release proteins from the periplasm.

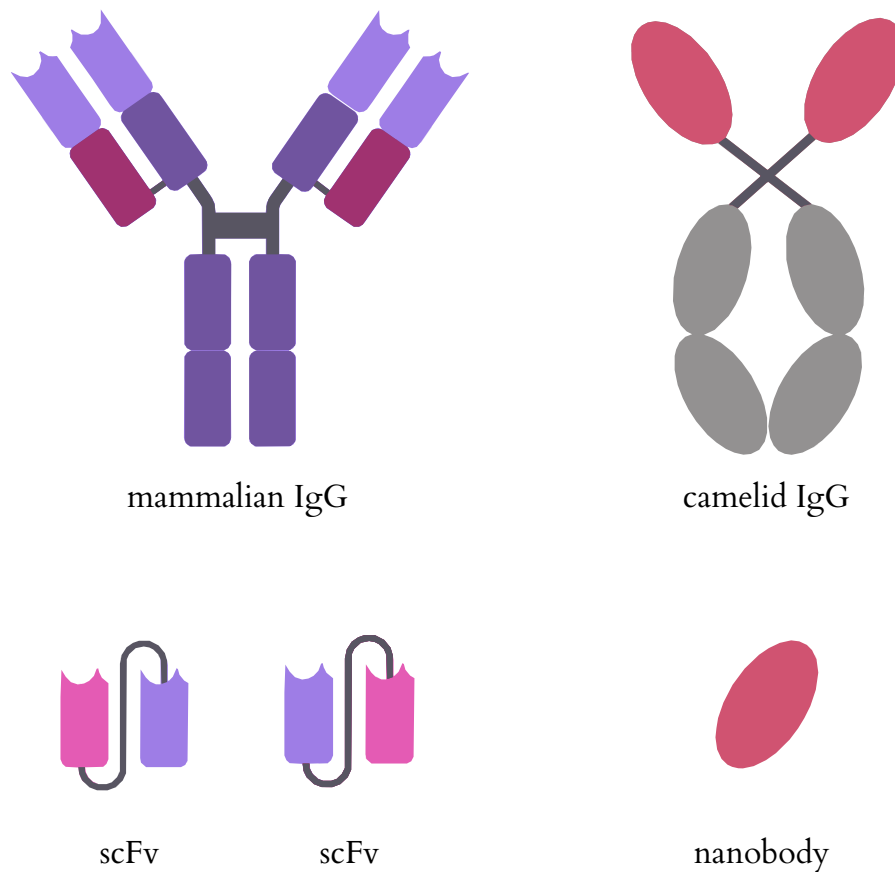


Figure 1.4: Nanobodies are to camelid heavy chain antibodies as scFvs are to typical mammalian IgGs. The single domain to the lower right is the  $V_{HH}$  domain, the nanobody. Unlike for the individual variable domain fragments of IgG, this single domain is sufficiently stable by itself for practical use.

*Bacillus* species offer an alternative. The *Bacilli*, being Gram-positive, secrete (extracellular) protein directly into their medium, which usually suits industrial production better than the periplasmic expression of *E. coli* (Schallmeyer *et al.*, 2004), with titres of up to  $1.5 \text{ g L}^{-1}$  in *B. megaterium* (Biedendieck *et al.*, 2011). An inherent advantage over *E. coli* is that *Bacillus* species produce no lipopolysaccharide.

*B. megaterium* has been shown to produce a higher quantity of higher quality antibody fragments than *E. coli* (Jordan *et al.*, 2007); in the absence of lipopolysaccharide, such proteins were also simpler to purify. Protein production brings this particular ‘big beast’ to the fore (Biedendieck *et al.*, 2011; Korneli *et al.*, 2013). At  $4 \mu\text{m}$  long, cells have a volume 100× that of *E. coli*; indeed single cell analysis is relatively straightforward as *B. megaterium* cells are big enough for flow cytometry. The main factors that make *B. megaterium* a great host for recombinant proteins include the ability to maintain plasmids without selection, lack of (alkaline) proteases and endotoxin, high yields of intracellularly folded protein and high protein export capability. *B. subtilis* is another important industrial *Bacillus* (Liu *et al.*, 2013).

Bacteria as a whole are at a disadvantage when it comes to post-translational modification. Even bacteria that glycosylate their proteins do so at different residues, and with different moieties, to mammalian cells. With antibodies, one can customise the F<sub>c</sub> domain to render N-glycosylation unnecessary (Robinson *et al.*, 2015).

Overall, the advantages in using bacteria, especially *Bacillus* species, for producing therapeutic proteins are significant. Production is only part of the challenge, though; downstream processing is just as important. The purpose of downstream processing is to recover the protein from its source, and formulate it such that it can reach the patient in good condition.

### 1.2.3 Failings of formulations

The main purpose of a biopharmaceutical formulation is to protect the therapeutic protein it contains. Proteins are chains of amino acids, folded in three spatial dimensions to produce highly specific shapes. This 3D conformation is mediated by interactions between residues, and with the environment. Solvents, other proteins, co-solutes and interfaces can stabilize or destabilize that structure. At low salt concentrations, electrostatic forces dominate all these interactions, but at higher, physiologically relevant salt concentrations, short range non-electrostatic ion forces (including polarizability) dominate behaviour. The effect is non-linear, meaning conventional DLVO (Derjaguin Landau Verwey Overbeek) theory fails to predict interactions, and like protein folding, protein-solvent-solute interactions are hard to model (Boström *et al.*, 2005).

These effects all pose challenges, for which formulation scientists have many techniques to overcome.

### 1.2.4 How to stabilize a protein

A drug product is more than just the API (active pharmaceutical ingredient) — for example, a therapeutic protein. Fillers, buffers, antimicrobials and viscosity modifiers (e.g. binders & disintegrants) make a product suitable for patients. These excipients must protect the API during storage, transport and delivery, affecting neither pharmacokinetics nor efficacy. In practice, these goals often contradict. Storage during transit imposes requirements on stability, e.g. a limit on vibration as shear and cavitation enhance damage at interfaces (Manning *et al.*, 2010); consequently the producer will often freeze-dry the product for

reconstitution moments before delivery. There are harms associated with the large changes of local environment on lyophilization and reconstitution (Manning *et al.*, 2010), which the drug manufacturer cannot always quantify; this loss of control over quality is a problem for producers.

The most valuable APIs are the mAbs (see section 1.2.1). The hinge region is susceptible to non-enzymatic, non-metal ion catalysed hydrolysis (Cordoba *et al.*, 2005). Glutamate is a common N-terminal residue on the light chain; pyroglutamic acid forms from nucleophilic attack of the N-terminal amine on the side chain carbonyl. This degradation increases during storage. Tryptophan photooxidation has been shown to reduce immunoglobulin activity, as does disulphide scrambling of cysteine residues. Oxidation in general is particularly problematic as it has been known to destabilize immunoglobulin conformations and enhance aggregation (Manning *et al.*, 2010). Such outcomes can occur without oxidation — antibodies adsorb on plastic, complicating processing, and aggregate destructively on freeze-thaw. In addition, the importance of the problem of reversible self-association is increasing in line with prevalence of sub-cutaneous formulations. These require a mass of antibody greater than 100 mg in a volume smaller than 2 ml, i.e.  $> 50 \text{ mg ml}^{-1}$  (Dobson *et al.*, 2016) and so excipients which can prevent such degradation are in high demand. Arginine and glutamate allow proteins to remain soluble at concentrations an order of magnitude above their previous solubility limit (Golovanov *et al.*, 2004).

### 1.2.5 Quantifying protein quality

It is illustrative to consider how formulation scientists measure protein quality. A number of techniques assess antibody structure; DLS (Dynamic Light Scattering), SLS (static light scattering), DSC (differential scanning calorimetry), VPO (vapour phase osmometry) and SAXS (small angle x-ray scattering) are preferred (C. F. van der Walle, personal communications, 2016). The (high throughput) scattering techniques investigate aggregation; when the aggregation properties of the correctly folded antibodies are known one can infer the nature and variation in structure of those proteins measured. With VPO one infers a change in water activity, also determined by antibody structure, and DSC identifies energies of interactions as it scans the temperature range (Arzenšek *et al.*, 2012; Boström *et al.*, 2005; Schneider *et al.*, 2011).

With these techniques, formulation scientists can measure the quality of proteins they have produced, and thus infer the consequences for a whole drug product itself. These measurements and inference techniques do not all transfer beyond the established formulation techniques; they certainly do not transfer across to using spores to formulate therapeutics. In order to understand the ways in which a spore-based biopharmaceutical may differ, one must consider the biology of the spores themselves.

## 1.3 Spore biology

The morphology and behaviour of spores has fascinated researchers for over a century. As one example, the model organism *B. subtilis* is particularly well studied, and its genome well characterized (Losick, 2015). Though there are significant differences across the genera, much has been conserved. This section shall review features of spore-forming bacteria, and their spores, that are relevant to designing therapeutic formulations.

### 1.3.1 Sporeformers in biotechnology

Prokaryotes, especially bacteria, and especially *B. subtilis*, are highly amenable to genome editing. It is straightforward to introduce mutations — insertions, deletions, combinations thereof — by transforming cells with suitable DNA (linear or as circular plasmids). Many mutations rely on native promoters, which, when bound by  $\sigma$  factors (*e.g.* the vegetative cell cycle factor  $\sigma^A$ ), lead to transcription of the attached operons. There are also heterologous promoters: most importantly the inducible promoters, which cause transcription in the presence of a specific chemical (the inducer). Harwood & Cutting (1990) have provided a list of techniques for working with *Bacillus* species.

Such biotechnological work, like much work that uses *B. subtilis* as a model organism, typically considers the vegetative cell cycle exclusively.

### 1.3.2 The sporulation-germination cycle

Sporulation is the process by which vegetative cells differentiate to become endospores. Germination is the opposite: the process by which spores resume a vegetative life cycle.

All endospores formed by species in the genera *Bacillus* and *Clostridium* have the same minimum structure of core, inner membrane, cortex, and coat (figure 1.5). The core contains the genome, half the spore's proteins, the ribosomes, tRNAs, a pool of 3-PGA and complexed with  $\text{Ca}^{2+}$  and other divalent ions, 2,6-DPA (dipicolinic acid) (figure 1.6). The critical biological macromolecules are protected; a spore must preserve in its core all the functional components it needs to once again become a vegetative cell (Bassi *et al.*, 2012).

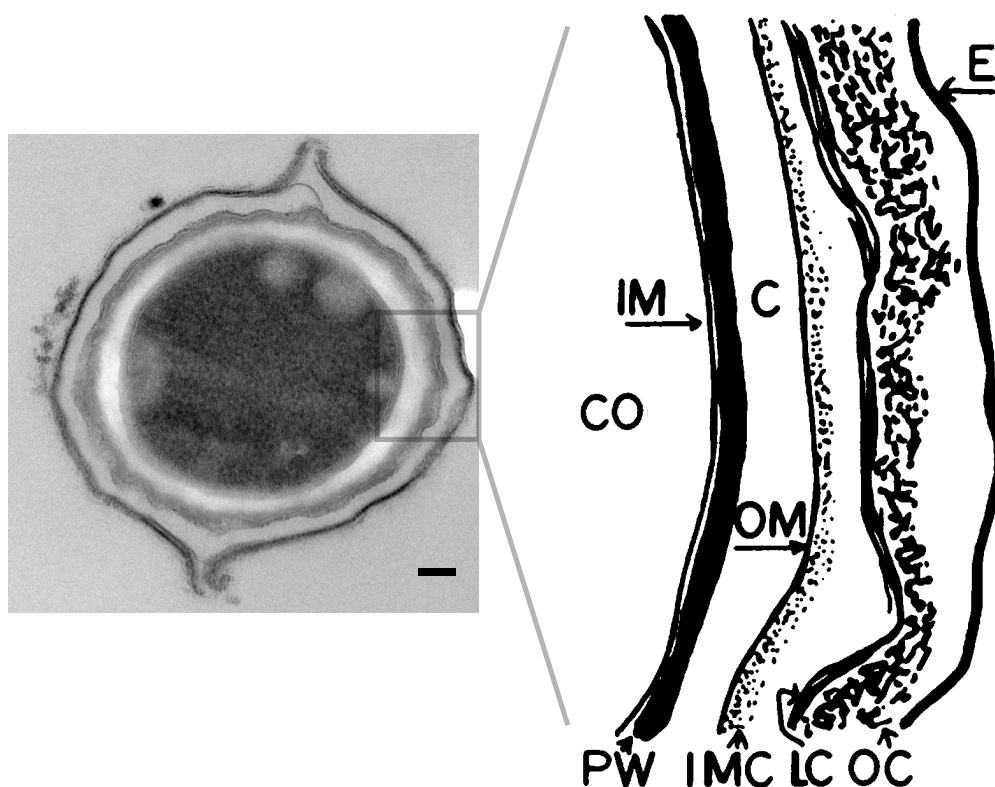


Figure 1.5: The structure of a *Bacillus megaterium* spore. The TEM (transmission electron micrograph) on the left is a *B. megaterium* spore (Source: G. Christie, personal communications, 2013–2019). The expanded diagram (derived from the diagram of mature spores of *B. thuringiensis*, Bechtel & Bulla, 1976) shows the layers of the spore, from inside to out (left to right). Abbreviations in the diagram: CO, core; IM, inner membrane; PW, primordial cell wall; C, cortex; OM, outer membrane; IMC, incorporated mother cell cytoplasm; LC, lamellar spore coat; OC, outer spore coat; E, exosporium. The scale bar is 100 nm.

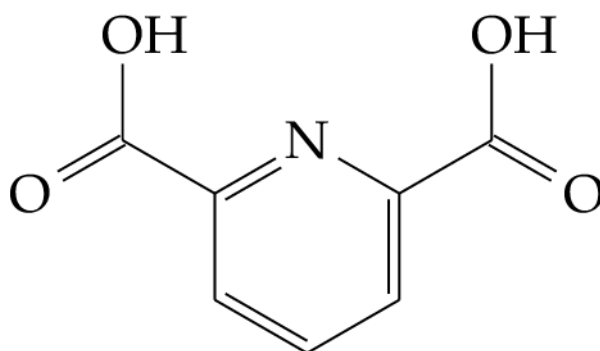


Figure 1.6: The chemical structure of DPA (2,6-dipicolinic acid).

## Sporulation

Sporulation is the process by which cells, anticipating unsustainable conditions, use the last of their free energy to form these dormant survival structures. For *B. subtilis* and *B. megaterium*, this takes roughly twelve hours. The layers of the spore structure are

synthesized by both forespore and mother cell, which communicate via channels (Camp & Losick, 2009). The properties of the environment significantly affect the properties of the spores produced (Xu Zhou *et al.*, 2017).

The sporulation process is shown in figure 1.7; see figure 1.1 for phase contrast micrographs of this process in *B. subtilis*. Sporulation is initiated through nutrient stress, at a sufficient population density, and at the appropriate point in the vegetative cell cycle (Errington, 1993). Cells aggregate as a *sporangium*. Spo0A and  $\sigma^H$  promote transcription of the initial sporulation genes. The early mother cell sporulation genes are controlled by  $\sigma^E$ ; as the forespore begins to form, the genes there are controlled by  $\sigma^F$ . The engulfed forespore begins to see  $\sigma^G$ -dependent transcription. This includes the SASPs (small acid-soluble proteins), and GRs (germinant receptors). Synthesis of the cortex, and then the coat, begin during these stages. Finally,  $\sigma^K$  controls expression in the late mother cell. At this point, DPA is synthesized, in the mother cell, and transported into the forespore. The forespore, having acquired the properties of the mature spore, is released from the mother cell.

The forespore begins its process of isolating from the mother cell at stage I and compartmentalizes fully by stage III, a point at which it is neither fully formed nor contains sufficient nutrients to complete sporulation. As a result there must be some mechanism by which free energy is supplied from the mother cell, and so Camp & Losick (2009) proposed what they called the *feeding tube model*. Subsequent work has indicated genes and channels which might be involved but it is not yet clear how to use this research to increase forespore protein productivity (Camp *et al.*, 2011; Crawshaw *et al.*, 2014)

The various stages are illustrated too for *B. thuringiensis* by Young & Fitz-James (1959), reproduced here as figure 1.8. These species produce crystal proteins (see section 1.3.3) in the mother cell. There are binding sites for both the mother cell  $\sigma^E$  and  $\sigma^K$  factors in the promoter of *cry1Aa*, from *B. thuringiensis* HD-1 (Adams *et al.*, 1991).

Crops of spores — even when strictly isogenic, and produced under the same conditions — are heterogeneous (Setlow *et al.*, 2012). In addition to potential microenvironments and quorum effects, stochastic variation is significant, especially when there may only be one or two molecules of mRNA per gene within a sporulating cell. GRs make a good example; the number of receptors for a specific nutrient in mature spores may vary three to four times, which can have a dramatic effect where there are only tens of receptors present in the first place. As a result, even in identical environments, spore populations will show heterogeneity.



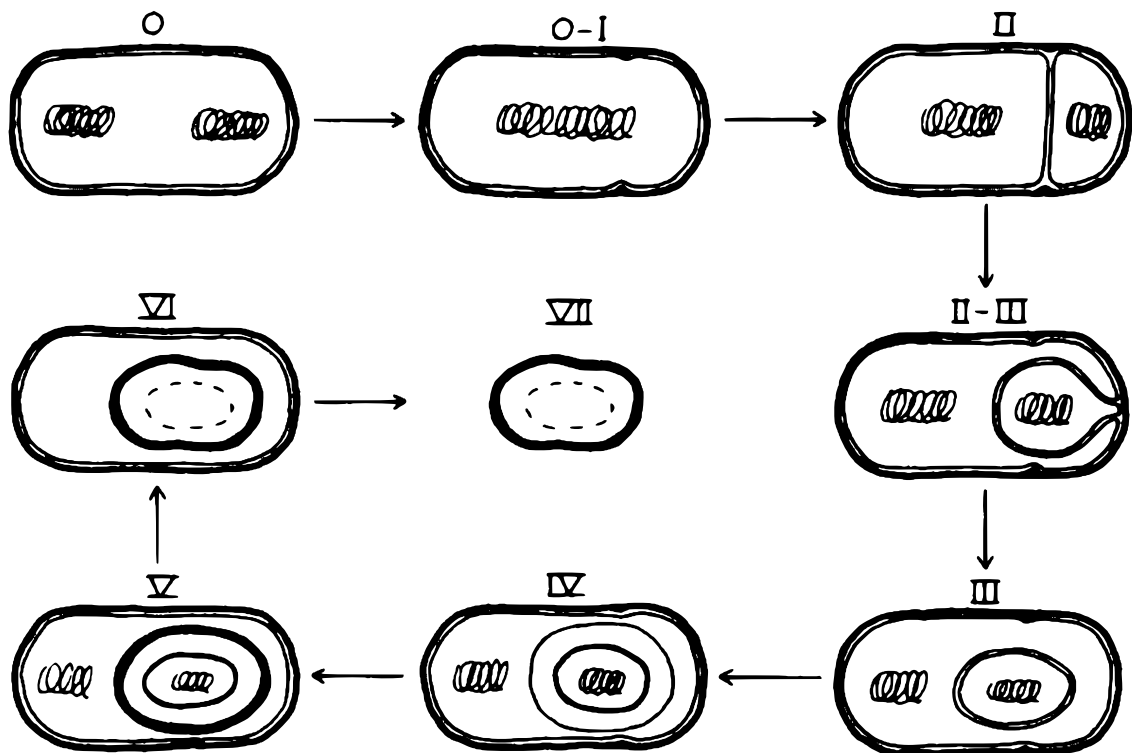


Figure 1.7: A summary schematic of the sporulation stages. 0, vegetative cells,  $\sigma^H$  active; 0-I,  $\sigma^E$  active; I, cell separated by septum,  $\sigma^F$ ; II, III, engulfment of pre-spore,  $\sigma^G$  in forespore; IV, cortex synthesis begins; V, coat synthesis begins,  $\sigma^K$  in mother cell; VI, maturation, acquisition of resistance properties; VII, release. The genomic DNA is shown at each stage until stage VI, where the dashed outline of the spore core is shown in its place. Original image from Piggot & Coote (1976).

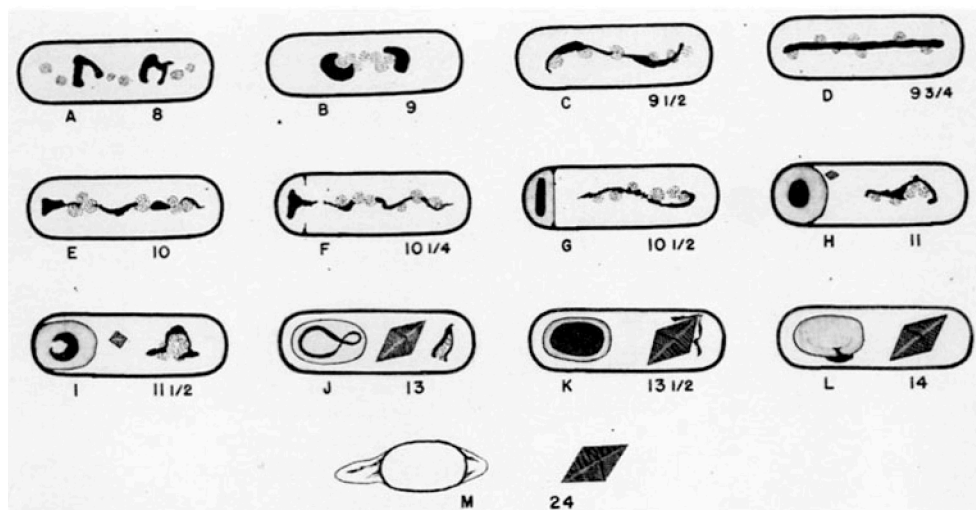


Figure 1.8: A schematic of the sporulation process for *B. thuringiensis* subsp. *alesti*. Cells proceed from A-M, and the numbers to the lower right of each spore correspond to hours following inoculation at 30 °C. The chromosome divides, resulting chromatids condense and then separate into the forespore (left) and mother cell. A bipyramidal crystal initially forms at the forespore (H). The result is a phase bright spore, with a loose-fitting exosporium, and a protein crystal. Reproduced from Young & Fitz-James (1959), who knew this strain as *B. cereus* var. *alesti*.

Some spores — typically 1 to 3% (Ghosh *et al.*, 2009) — are just hardier, in that they show greater resistance to heat and less sensitivity to germinants. Spores demonstrating the latter, termed *superdormant*, will resist Tyndallization-type approaches (see section 1.1.1; though these spores are still viable — they germinate in response to dodecylamine and Ca-DPA). For example, while spores of *B. anthracis* resist antibiotics that easily kill *B. anthracis* cells, heterogeneity within the spore population means that treatment must be timed to ensure cells are exposed to a lethal, rather than a selective, dose. Properties of the spores which vary include size ( $\pm 25\%$ ), composition, staining behaviour, water content, requirement for heat activation and germination response (Setlow *et al.*, 2012).

The heterogeneity extends beyond variation within a spore population. Not all cells in a population will sporulate, and some spores will germinate immediately. In the laboratory, spores must usually be washed free of nutrients, cell debris (sporangia) and any remaining vegetative cells (Church *et al.*, 1954), before analysis.

## Germination

Though spores resist many challenges, under specific conditions they give up their resistance and germinate, resuming the vegetative cycle. For *B. subtilis* and *B. megaterium*, germination and outgrowth together take close to three hours; the initial phase darkening (hydration) lags the addition of nutrients (termed germinants) by 5–25 min and then takes just 30 s to complete (Abel-Santos, 2012; Setlow *et al.*, 2012). A variety of factors can induce germination, through a number of routes (table 1.1, sourced from Setlow, 2014; Shah *et al.*, 2008). In germination, the IM permeability increases. The stores of  $H^+$ ,  $K^+$  and  $Na^+$  are released, then all Ca-DPA. The cortex lyses, and over a matter of minutes the water content of the spore core rises from 25–55% w/w to 80% w/w (*c.f.* 75–80% w/w for vegetative cells, Abel-Santos, 2012).

Spores commit to germination — they still germinate after germinant removal. Even pulses of germinants, individually insufficient to trigger germination, have an additive effect (Setlow, 2016). Commitment is when the act of blocking GRs (e.g. with competitive inhibition, or acidification) no longer prevents germination; this step precedes Ca-DPA release by minutes. Setlow (2014) suggests that it is the IM that changes, on commitment. Heat, too, reversibly promotes GR-dependent germination — this is termed *heat activation*.

The next step is the aforementioned release of DPA. SpoVA appears to form a Ca-DPA IM channel. SpoVAC is mechanosensitive (Velásquez *et al.*, 2014); SpoVAEa and SpoVAD are IM associated, likely on the outer IM surface; and SpoVAD binds DPA (Setlow, 2014). In

Table 1.1: Factors that induce germination, and their mechanisms. Abbreviations: GR (germinant receptor), CLE (cortex lytic enzyme).

Factor	Mechanism
Nutrients	GR activation
150–250 MPa hydrostatic pressure	GR activation
Ca-DPA	CwlJ, a CLE
Dodecylamine	SpoVA channel
500–1000 MPa hydrostatic pressure	SpoVA channel
Peptidoglycan fragments	PrkC, a Ser/Thr protein kinase

principle a channel, such as this, could permit other small molecules, but likely candidates AMP (adenosine monophosphate), Pi (inorganic phosphate) and 3-PGA (phosphoglyceric acid) remain in the spore during early germination. The mechanism by which the channel operates remains a research problem.

Another mystery concerns the behaviour of the CLEs (cortex lytic enzymes), which degrade the cortex following DPA release. The *Bacillus* enzyme CwlJ is activated by Ca-DPA, though this mechanism too is unknown (Paidhungat *et al.*, 2001). It is neither clear whether a direct chemical reaction causes the activation, nor how activation is suppressed during spore maturation. The precise mechanism of the other CLE in *Bacillus*, the lytic glycosylase SleB, remains a mystery too, despite the publication of crystal structures for several *Bacilli* (Setlow, 2014).

What follows cortex lysis are rehydration of the core, resumption of enzymatic activity — including ATP (adenosine triphosphate) synthesis and degradation of the SASPs (small acid-soluble proteins) — and finally, outgrowth of the new vegetative cell (Moir, 2003).

★★

The sporulation–germination cycle as a whole allows sporeformers to survive challenging local conditions, through dormancy, and resume their vegetative state when conditions are more favourable. From an evolutionary perspective, this behaviour has allowed spore-forming species to survive existential threats.

### 1.3.3 Crystal proteins

The highly specific, insecticidal component of crystalliferous strains of *B. thuringiensis* is the Cry crystal protein. This inclusion is formed in the mother cell and usually released from the sporangium in a ratio of one crystal per spore (Sansinenea, 2012) although they can form within the exosporium (Zhu *et al.*, 2011) or even as an alternative to the spore (Deng *et al.*, 2014). Agaisse & Lereclus (1996) review the key factors enhancing crystal production. The full length crystal structure of Cry1Ac (figure 1.9), produced by *B. thuringiensis* subsp. *kurstaki* HD-73, was published by Evdokimov *et al.* (2014).

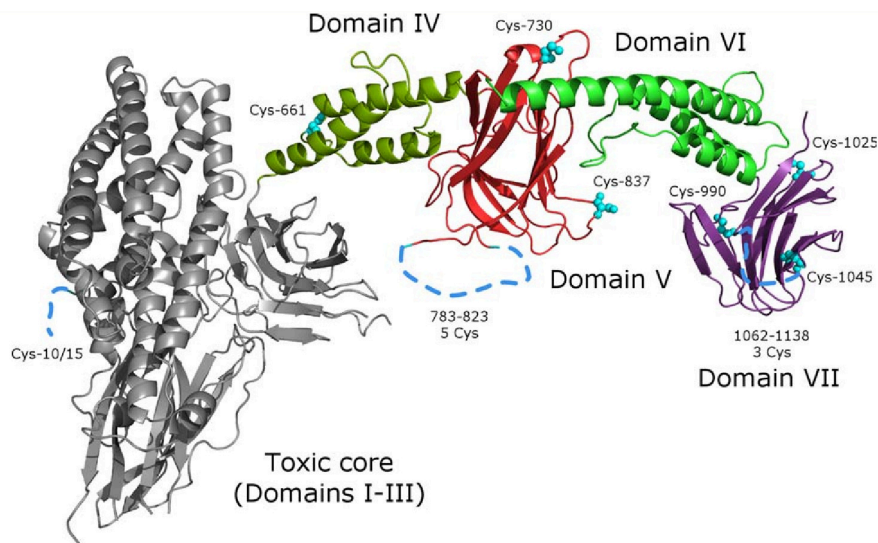


Figure 1.9: The annotated crystal structure of Cry1Ac. The majority of interactions are between residues in the protoxin domains, IV–VII. The toxic core (the N-terminus) has the insecticidal properties. Only recently have researchers solved the full structure, in part as previous research focussed exclusively on the toxin. Technically, the crystals are of a cysteine poor variant, developed to overcome the ‘pernicious’ aggregation of the native protein. (Reproduced from Evdokimov *et al.*, 2014).

#### Highly specific toxicity

Cry toxins bind highly (species) specific–receptors, (hetero-)oligomerize, change conformation to penetrate the epithelial plasma membrane, and then insert — opening a non-selective ion channel and killing gut cells (Pardo-López *et al.*, 2013). The three-domain Cry toxins are highly specific, affecting neither vertebrates (including humans) nor plants. There are two-varieties: 65 kDa and 130 kDa; the latter has a C-terminus that gut proteases cleave. (In the case of engineered, Cry-containing *Bt-corn*, plant enzymes perform this role). The active toxin is ~600 residues, preceded by a 20–60 amino acid N-terminal fragment (possibly a signal peptide) and the overall structure is highly conserved. Knowles & Ellar (1987) propose the toxins form a non-selective ion channel, leading to osmotic death.

Indeed the Cry toxins hetero-oligomerize to form a membrane penetrating structure (the “umbrella model”, Pardo-López *et al.*, 2013); this typically depends on cadherin protein on the gut epithelium of sensitive organisms. Not all Cry variants behave like this. Cry4Ba can be proteolytically activated to a pore-forming structure *in vitro*, without cadherin receptors, and Cry1A can be engineered to oligomerize similarly (Soberón *et al.*, 2007). Furthermore, Cry proteins and the other group of (non-crystal) toxins, the Cyt proteins, are synergistic: mechanistically, Cyt1Ac has been shown to induce oligomerization of Cry11Aa (Pardo-López *et al.*, 2013).

Vegetative cells of *B. thuringiensis* strains, like *B. cereus*, can produce  $\beta$ -exotoxin (Sansinenea, 2012). This chemical analogue of adenine, a heat-stable neurotoxin, can interfere with RNA synthesis across species. In one study, five out of every six crystal-toxin producing strains also produced  $\beta$ -exotoxin (Perani *et al.*, 1998). For a strain to be commercially viable in North America and Europe, it must not produce  $\beta$ -exotoxin (Glare & O’Callaghan, 2000; via Palma *et al.*, 2014). Similarly, *B. thuringiensis* can produce enterotoxin and there have been reports of food poisoning in humans (Bishop *et al.*, 1999; Johler *et al.*, 2018). Many cases, thought to be caused by *B. cereus*, may have been thus misdiagnosed.

### High expression

Agaisse & Lereclus (1995) posed a question in the title of their paper: How does *Bacillus thuringiensis* produce so much insecticidal crystal protein? Crystal proteins make up to 20–30 wt% (dry basis) of some spore strains (Agaisse & Lereclus, 1996). The factors which encourage such high expression have utility beyond these species and these proteins. The high yields mean producing Cry proteins industrially, at scale, is relatively straightforward.

### Downstream processing

Following fermentation, the crude *B. thuringiensis* liquor is concentrated in an evaporator, disc-stack centrifuge or ultrafiltration unit. The resulting slurry is typically formulated as an SC (liquid suspension concentrate) e.g. Vectobac® 600L (Valent Biosciences Corporation) or, following spray-drying, as a WP (wetable powder) e.g. DiPel® WP (Valent), WG (wetable granule) e.g. DiPel® 2X DF (Valent) or OF (oil flowable) liquid/emulsion e.g. Thuricide® 48LV (Bonide) (Brar *et al.*, 2006; Bryant, 1994). Choice depends on delivery method: for aerial delivery high concentration OF formulations reduce evaporation; dry formulations reduce transport costs and have longer shelf lives; WG formulations are often easiest to process in the field. Recent advances include encapsulation, helpful for

aquatic use, and direct waste-water sludge formulation (Brar *et al.*, 2006). Industrial preparations of *B. thuringiensis* crystals usually contain spores too, partly as it is not cost effective to purify the mixtures and partly as there is a synergistic effect, possibly due to spores germinating during transit through the larval gut (Crickmore, 2006). One consequence is that though there are established, industrial scale processes for *B. thuringiensis* production, they do not extend to crystal purification.

★★

The crystalliferous strains of *B. thuringiensis* occupy a remarkable evolutionary niche, of which only farmers have so far taken advantage. The factors which make such spores a useful insecticide also make for capable expression systems. Not all of that utility is due to the crystals; the resistance of spores of *B. thuringiensis* to challenges in their environments is important, too.

#### 1.3.4 Spore survival

Clearly, spores do not give up their dormancy simply.

— Setlow (2014)

Bacterial spores, in their dormant state, resist: a) the denaturing effects of wet heat; b) DNA damage caused by dry heat, desiccation, freeze-drying, ionizing radiation and UV light; c) oxidation due to dry heat and chemical attack; d) physical disruption due to pressure (positive and vacuum) or shear; and e) other chemical and biochemical damage from acids, bases, ionophores, organic solvents, radicals and enzymes (Aronson, 2012; Pedraza-Reyes *et al.*, 2012).

The spore's remarkable properties are due to its unique structure (see figure 1.5). For many species the outer layer is the hydrophobic, flexible exosporium that provides an outer barrier (especially to ionophores) and can help the spore adhere to hydrophobic surfaces (Aronson, 2012; Xu Zhou *et al.*, 2017). In *B. anthracis* it is the exosporium which holds the superoxide dismutase and arginase needed for spores to survive inside macrophage lysosomes (Abel-Santos, 2012; Mock & Fouet, 2001). However, the exosporium structure is highly porous, and so for most resistance properties, the structural basis begins with the coat.

## A proteinaceous coat

The coat is a ‘reactive armour’ (Bassi *et al.*, 2012) comprising at least 70 proteins (McKenney & Eichenberger, 2012). Together, these provide structure, flexibility, strength and, critically, porosity to small molecules (in particular: water and germinants, including DPA, 2,6-dipicolinic acid). The variation in coat composition among (and even within) species is enormous, yet the main structural features — the distinct lamellar inner coat, and ability to change shape in response to water activity — are highly conserved (Aronson, 2012).

A few proteins, termed *morphogenetic*, are critical for structural integrity: SpoIVA (anchor), SafA (inner coat), CotE (outer coat), SpoVM and SpoVID (encasement, McKenney *et al.*, 2012). For example, Zheng *et al.* (1988) first investigated the effects of the  $\Delta cotE$  mutation on *B. subtilis*. Such spores are heat resistant, germination impaired and optically refractile, yet also lysozyme sensitive — lysozyme exposure leads to a >95% drop in viability. It is clear from TEMs (transmission electron micrographs) that indeed the outer structure does not form (figure 1.10). CotA–C are absent from such spores, too, though their genes *cotA–C* expressed normally. From this the authors inferred CotE anchors the outer coat to the inner, and subsequent work by Bauer *et al.* (2001) further elucidated the mechanism.

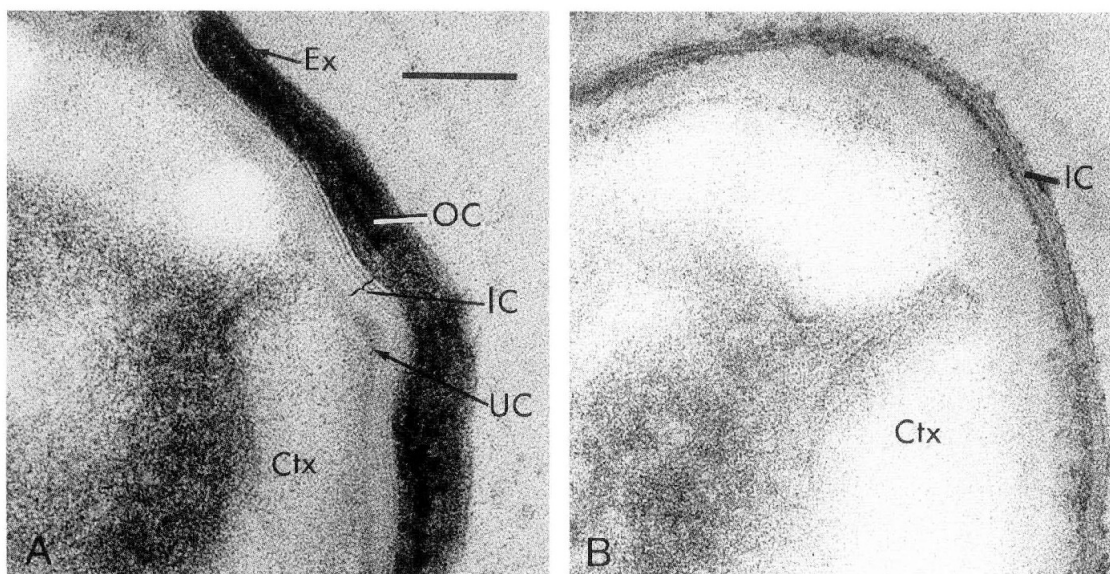


Figure 1.10: Transmission electron micrographs, comparing the outer layers of  $\Delta cotE$  mutant spores (right) derived from wild type *B. subtilis* PY-17 (left). The coat mutant lacks the (electron dense) outer coat and crust, and so its inner coat is exposed to the environment. Labels: Ex (exosporium), typically called the crust for *B. subtilis*; OC (outer coat); IC (inner coat); UC (undercoat); Ctx (cortex). The scale bar is 100 nm. (Source: Zheng *et al.*, 1988).

The coat electrically insulates the inner layers. This is particularly important for the stability of the core because of its interaction with the cortex.

## The cortex

The cortex is a crosslinked peptidoglycan wall, similar to the cell walls of vegetative cells, but 50% of what in peptidoglycan would be N-acetylmuramic acid is missing the pentapeptide side chain, and is therefore muramic acid  $\delta$ -lactam (Abel-Santos, 2012). During sporulation, the cortex grows at its inner surface, compressing the core (Algie, 1980). CLEs (cortex lytic enzymes), break down the cortex at germination, coinciding with the point at which germinating spores turn from phase bright to phase dark (Gould, 1969).

Peptidoglycan usually provides rigidity in bacteria, containing and constraining the membrane within, and in spores this constraining role is vital. The cortex peptidoglycan's negative charge attracts positive counter ions leading to an osmotic potential equivalent to 2 MPa (Bassi *et al.*, 2012), and this too is important for stability of the core, discussed below.

## The inner membrane

The IM (inner membrane), the layer just inside the cortex, is the main barrier to small molecules — in particular, DPA. Its lipid composition matches that of the plasma membrane, but its structure does not. At the end of sporulation, the volume contained by the IM halves and the membrane becomes a semi-solid gel. This volume then doubles by the start of cortex hydrolysis (during germination) and the membrane's physical properties revert to those of a plasma membrane (Setlow, 2014). There is no new membrane made as part of this process — indeed, ATP production does not start until later (Bassi *et al.*, 2012); this suggests the structure changes dynamically.

Vepachedu & Setlow (2007) proposed that some release of DPA was linked to the SpoVA proteins, with the rest due to the increase in IM permeability on germination. A step change in permeability of the membrane could surely not be due to the (admittedly large) changes in lipid arrangement; how would these small molecule concentrations reach such high levels on sporulation if the membrane were this permeable before the core dehydrates? More recent results, supporting the notion that SpoVA proteins form a mechanosensitive channel, imply the release associated with changes in the membrane is actually via the SpoVA channel itself (Velásquez *et al.*, 2014).

The IM is the final barrier to the spore core.



## The spore core

The core contains all the requirements for germination and the beginning of outgrowth of germinating spores. There has been some debate on whether it is in a glassy state (an amorphous near-solid) or that of a gel (e.g. Ablett *et al.*, 1999; Bradbury *et al.*, 1981). The preponderance of evidence leans towards the latter: that the core is a water permeable matrix, containing all the key macromolecules required by germinating spores (Sunde *et al.*, 2009).

Since the 1960s, researchers have known that most water in spores is mobile (97%, from D<sub>2</sub>O exchange, Bassi *et al.*, 2012), and more recently NMR studies have confirmed this (Kaieda *et al.*, 2013; Leuschner & Lillford, 2000; Sunde *et al.*, 2009). There have been conflicting results on the relative hydration of the cortex and core; the NMR study by Bradbury *et al.* (1981) found no difference, but later laser-diffractometry experiments by Ulanowski *et al.* (1987) found 0.6 g ml<sup>-1</sup> water in the cortex but just 0.3 g ml<sup>-1</sup> in the core. Not only is this water exchanged with the environment, the quantity of water in an individual spore will change depending on the environment's humidity (Westphal *et al.*, 2003). The true values will thus vary as governed by the osmotic potentials of the spore and cortex.

The composition of dry spores includes 5–15% w/w 2,6-DPA (Murrell, 1969); the dry cores comprise 20% w/w (Setlow *et al.*, 2006). Accounting for the water content in non-dried spores, this corresponds to 2 mol%, or 0.8 M (which is just lower than the limit of Ca-DPA solubility in a binary mixture with water, approximately 1 M). Colorimetric assays of spore extracts suggest DPA appears in a 1:1 stoichiometric relationship with Ca<sup>2+</sup> ions in the spore core (Murrell, 1969); calcium ions and DPA released from spores during germination maintain such a stoichiometry, too (Vepachedu & Setlow, 2007).

Indeed, lyophilized *B. cereus* showed Raman peaks corresponding to the symmetric breathing vibration of Ca<sup>2+</sup>-DPA (1021–1015 cm<sup>-1</sup>), rather than H<sub>2</sub>-DPA (1002–998 cm<sup>-1</sup>), suggesting the Ca<sup>2+</sup> salt is the dominant form *in vivo* (Shibata *et al.*, 1986). This does not rule out DPA in complex with other, non-Ca<sup>2+</sup> cations, as those other dipicolinate salts would show similar peaks. In particular, other divalent and monovalent metal ions, and free amino acids are prevalent, and likely complexed with DPA, in the core.

Based on work with *B. megaterium*, Murrell (1969) suggested the most prevalent free amino acids in *Bacilli* were arginine, histidine and glutamate. More recently, NMR (nuclear magnetic resonance) has confirmed this, indicating significant quantities of arginine,

glutamate and two other small molecules in the extracted cores of *Bacillus subtilis* (Magge *et al.*, 2008). Glutamate makes up 20–100  $\mu\text{mol}(\text{g dry spores})^{-1}$  (0.3–1.5% w/w) and Vepachedu & Setlow (2007) found 90% was released with the DPA on dodecylamine-induced germination (with most of the free arginine released in parallel). The formation of DPA–glutamate and DPA–arginine complexes *in vivo* is consistent with the parallel release hypothesis.

It is possible to estimate some values important to the physics of the core. Assuming  $\text{Ca}^{2+}$ -DPA is solvated but does not quite dissociate, for a 2 mol% ideal binary mixture of  $\text{Ca}^{2+}$ -DPA and water, the mole fraction of the latter is 0.98. The osmotic pressure of this greatly simplified system is given by the following equation, in which  $R$  is the molar gas constant in  $\text{kJ kmol}^{-1}\text{K}$ ,  $T$  is temperature in K,  $\underline{V}$  the molar volume of water in  $\text{m}^3\text{kmol}^{-1}$ ,  $\gamma$  the (dimensionless) activity coefficient and  $x$  the (dimensionless) molar fraction:

$$\Pi = -\frac{RT}{\underline{V}} \ln \left( \overbrace{\gamma_{\text{water}}}^{\text{Assume}=1} x_{\text{water}} \right) = -\frac{8314.5 \times 300}{0.018} \ln 0.98 = 2.8 \text{ MPa}$$

This rough calculation suggests the osmotic pressure of the core is of the order of 2–3 MPa, compared with reported values of 0.02–0.2 MPa for vegetative cells (Cayley *et al.*, 2000; Deng *et al.*, 2011). Indeed, Bassi *et al.* (2012) reported an osmotic pressure of 2 MPa, and the simplified calculation above is consistent with the proposition that the behaviour of DPA dominates that property. This means the cortex and core are in osmotic equilibrium, despite the core's far lower water content, and thus the cortex plays a vital role in the latter's stability. Furthermore, one can infer that the osmotic pressure is also a store of free energy, used to power the germinating cell.

Independently, Algie (1980) published a near-identical calculation, based on water activity rather than DPA concentration, which produced an identical result. This result was taken further, treating the cortex as a pressure vessel. The overall outcome is consistent with the core being dehydrated by reverse osmosis, as the pressure in the core increases with cortical growth. Further evidence comes from DSC (differential scanning calorimetry); Tiburski *et al.* (2014) showed that water in the spore core undergoes its vaporization transition at 200 °C, rather than 100 °C for surface water, indicating the high pressure state therein.

★★

The spore structure in this way creates (and maintains) the optimum environment in which to stabilize proteins. The core preserves the critical biological molecules at high osmotic pressure: genome, enzymes, ribosome system and an energy store. The cortex maintains the osmotic pressure, the coat protects the cortex from chemical attack, and an exosporium or crust protects the coat. Together, they keep the spore stable in a high energy state, so as soon as germination begins, the spore can become a vegetative cell as quickly as possible. It may be possible to mimic some of that state, without that full surrounding structure — and for this, DPA looks like a particularly interesting place to begin.

### 1.3.5 Protein stability in spore cores

Spores must stabilize their core proteins to resist wet heat (Pedraza-Reyes *et al.*, 2012). The magnitude of this resistance depends to a great extent on the water activity of the spores; manipulation of water activity suffices to overcome the  $10^4$  times difference in survival between different species (Murrell & Scott, 1966). The contraction of the spore, associated with a reduced water content, has been shown to correlate with resistance to wet heat (Algie, 1983). While DPA's role in heat resistance has been reported for 60 years (Church & Halvorson, 1959; Murrell, 1969), there is still no widely accepted mechanism for its action (Setlow, 2014). Both factors are related; water activity is a function of water and solute composition, and the solute is dominated (as described above) by DPA (Algie, 1984; Sunde *et al.*, 2009).

DPA is ubiquitous among spore-formers. Most possess the DPA synthetase enzyme to produce it by reducing DHDPA (dihydrodipicolinic acid); indeed, this enzyme is highly conserved across sporeformers. Taxonomic analyses (and both *in vivo* and *in vitro* experiment) suggest that before this enzyme evolved, ancestors of *Bacilli* and *Clostridia* co-opted the electron transfer flavoprotein EtfA in its place (Orsburn *et al.*, 2010).

#### **Heat resistance**

Heat is damaging to cells as it damages proteins: directly, through thermal denaturation, and indirectly, through acceleration of kinetics (Manning *et al.*, 2010). There are a number of mechanisms, through which DPA might increase spores' heat resistance; many stabilize the proteins against thermal denaturation.

One such mechanism is the role of DPA in the low water content of the spore core. In the core, water preferentially hydrates non-protein molecules, so proteins generally have only a single layer of water molecules around them. Low water content means fewer ROSs (reactive oxygen species), and less oxidative damage (Bassi *et al.*, 2012).

Bradbury *et al.* (1981) proposed a model in which dehydration alone is not enough to provide the resistance; Ca-DPA itself acts as a support. This support restricts the movement of macromolecules; restricting movement in this way is a reliable method of enhancing protein stability (Bhardwaj *et al.*, 2016). There is a mechanism by which DPA may form a support. Electron density is delocalized over the whole DPA molecule. Guanidinium and arginine show similar properties, and in low water environments they stack (Schneider *et al.*, 2011). It seems likely that DPA behaves similarly.

Another such mechanism is chelation of metal ions, preventing metal-catalysed oxidation. Calcium, potassium, magnesium and manganese species are the most prevalent ionic metal species in the spore core, followed by iron, aluminium, sodium, phosphorous and copper (Bassi *et al.*, 2012).

Finally, DPA may also interact more directly with proteins. Such behaviour has been demonstrated beyond spores. Tris(DPA)lanthanide, a DPA complex, has been shown to co-crystallize with proteins, acting as a crystallographic phasing agent (Pompidor *et al.*, 2008a). The carboxylate groups in the complex interacted specifically with arginine residues of hen egg white lysozyme, in both solid and liquid phases, producing a new crystal form (figure 1.11). Such specific interactions may help stabilize proteins in the spore core, in the manner described by Bhardwaj *et al.* (2016).

## UV resistance

When it comes to UV resistance, DPA too is an important component, along with SASPs (small acid-soluble proteins). UV damages spores mostly through damage to DNA.

UV radiation causes more DNA damage in spores containing DPA than mutants without (Paidhungat *et al.*, 2000). Nucleotides form 5-thymine-5,6-dihydrothymine (*i.e.* SP, spore photoproduct), rather than lactams. Unlike the latter, however, the former reaction product is reliably repaired on germination (Pedraza-Reyes *et al.*, 2012). As a consequence, UV damage is reversible. The gel structure of the core also restricts DNA motion so when the spore germinates, breaks are easier to repair.

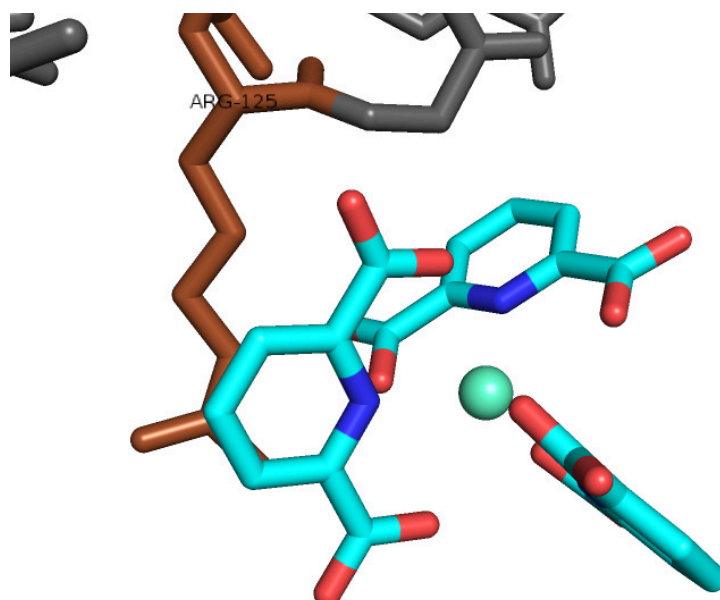


Figure 1.11: A DPA (2,6-dipicolinic acid)–lanthanide complex interacts specifically with arginine residues in hen egg white lysozyme. DPA chelates the lanthanide ions, keeping them from the surface of the protein in a way that might be relevant to the way proteins are stabilized in spores. Image produced using Pymol, from PDB entry 2PC2 (Pompidor et al., 2008b).

DNA extracted from spores differs in many properties from that of vegetative cells, mainly due to the presence of DPA. This has practical effects; Setlow *et al.* (2006) inferred from the change in DNA's UV photochemistry that DPA must be close enough to DNA for electron transfer to take place. Separately, and consistent with that hypothesis, DPA-derivatives have been shown to bind tightly to DNA. For example, a number of dipicolinate tris-arenes, such as methoxy-substituted 4,4'-dinitrodipicolinalinide have been shown to provide a hydrophobic DNA coat and thereby improve plasmid transformation efficiency in *E. coli* (Atkins *et al.*, 2012). In binding DNA in this manner, DPA may stabilize DNA like it might proteins: through specific interactions.

Finally, UV also creates DNA-damaging radicals such as superoxide. The reduced water content reduces the likelihood of superoxide-creation events occurring, and DPA in turn reduces such radical-associated damage when they do.

The UV protection mechanism *in vivo* may be a combination of all three effects: SP formation, direct binding to DNA and dehydration.

## Spores lacking DPA

From this correlation of DPA with reduced water content, one might infer there is a mechanism linking the two. Together, these spore resistance properties suggest DPA forms a water-solvated matrix, stabilizes proteins in an inactive but thermostable form, and excludes water from beyond proteins' first hydration shell. One way to test this hypothesis is to consider what happens when spores lack DPA.

DPA is produced via the DAP (diaminopimelic acid) pathway. DapA converts L-ASA (L-aspartate semi-aldehyde) and pyruvate to HTDA (4-hydroxy-tetrahydro-dipicolinic acid), which spontaneously dehydrates to DHDPA (dihydrodipicolinic acid). Then, in *Bacillus* and most *Clostridia*, the DPA synthetase enzyme SpoVF converts this to DPA (Orsburn *et al.*, 2010). The DPA is taken up into the spore via the SpoVA channel.

This provides two approaches to make spores that lack DPA via genetics, and physical methods lead to a third. Knocking out the *spoVF* operon in *B. subtilis* means the mother cell cannot produce DPA. Paidhungat *et al.* (2000) tried this (based on the work of Balassa *et al.*, 1979), but the spores produced were phase dark, indicating they had autogerminated; they lacked stability. The researchers then deleted the three main germinant receptors (with which a spore detects nutrients, if an environment is suitable for germination), leading to stable spores. Later, Magge *et al.* (2008) produced the  $\Delta spoVF \Delta sleB$  mutant, able to produce neither DPA nor the semi-redundant CLE SleB; these spores were also stable. Indeed, DPA was later shown to prevent SleB activation in an unknown way (Kaieda *et al.*, 2013). As expected, the mutants of Magge *et al.* (2008) showed reduced resistance to wet heat, indicating reduced protein stability. However, in these mutant strains, DPA channels still function, meaning any DPA in the mother cell would be taken into the forespore.

As described in section 1.3.2, SpoVA proteins form a gated channel, through which DPA is actively transported into the forespore during sporulation, and then, on germination, released (Velásquez *et al.*, 2014; Vepachedu & Setlow, 2007). Magge *et al.* (2008) produced *B. subtilis* mutants with a  $\Delta sleB \Delta spoVA$  genotype, which lack this gated channel. They could neither transport DPA against an enormous chemical potential gradient into the forespore, nor transport it with the chemical potential gradient out of the germinating spore. These spores were 'extremely stable' — evidence that the SpoVA channel is critical for ion or water release during germination, too. Paredes-Sabja *et al.* (2008) replicated this finding, that  $\Delta spoVA$  spores are stable, in *Clostridium perfringens*.

For the  $\Delta spoVF$  mutants of Magge *et al.* (2008), supplementing the sporulation medium with DPA led to *DPA replete* spores, which did contain DPA. The concentrations of DPA, and resistances to wet heat, oxidation and some ionophores followed the order: DPA-less spores < DPA-replete spores < WT spores. However, the water content of these spores varies; the level of dehydration followed the same order, and most of the wet heat resistance (and oxidation resistance) was probably due to varying water content.

It is also possible to physically remove DPA from spores. Margosch *et al.* (2004) exposed spores to up to 800 MPa in a 15 ml pressure vessel; 500 MPa will germinate spores in a way that bypasses their biological germination mechanism (Setlow, 2014) and which almost certainly activates the mechanosensitive (Velásquez *et al.*, 2014) SpoVA channel. After 2 min, the *B. subtilis* spores had lost almost all (96%) their DPA. They then heat shocked the spores, and for comparison a) heat shocked spores lacking DPA, and b) pressure and heat shocked DPA-replete spores. Spores missing DPA were significantly more sensitive to heat than those containing it, no matter why the spores contained or did not contain DPA. That said, the pressurised spores did not germinate on loss of DPA as the pressure damaged the CLEs, located outside the core (Margosch *et al.*, 2004).

Control of DPA must be very tight during uptake into the forespore, as the proteins in the IM must do a lot of work against the potential gradient inherent in building the 2 MPa osmotic pressure. Li *et al.* (2012) showed that in the *B. subtilis* SpoVA complex, the SpoVAD subunit specifically interacts with 2,6-DPA, but not the 2,3-, 2,5-, or 3,5- isomers. A highly conserved Cys-110 residue forms part of their suspected binding site, and based on docking simulations the authors suggested Asp-234 and Ser-277 recognise the acid groups at the 2 and 6 positions (see figure 1.12). However, one implication of DPA's interactions with proteins may be that standard *in silico* models do not correctly model it as a ligand. It would be interesting to see how the SpoVA channel differs in *B. megaterium*. The channel is made from fewer distinct subunits (six as opposed to seven), and the germinant receptor behaviour is more complex (Gupta *et al.*, 2013).

★★

This section has shown how spore-forming bacteria use their differentiated spore form as a means to survive harsh environments — at individual, and species levels. This can be a nuisance, when such bacteria are an undesirable presence. It is also a useful capability from a



*Figure 1.12: SpoVAD forms a gated DPA channel in *B. subtilis*. This channel is highly specific and is required for the forespore to fill with DPA at the end of sporulation. The crystal structure shown here, as a cutaway into the channel itself, is a single dimer subunit. The Cys-110 (magenta), Asp-234 and Ser-277 (orange) residues, which make the putative channel entrance, are highlighted. Image produced using Pymol, from PDB entry 3LM6 (Forouhar et al., 2010).*

biotechnological perspective. The very conditions which challenge spore survival also challenge many therapeutic protein products, and that similarity has informed the goals of the work reported here.



## 1.4 Spores as delivery vehicles

If spores have such remarkable protein-stabilizing properties, why not use spores themselves to deliver mAbs? Formulation scientists have a problem of proteins suffering irreversible damage; meanwhile, *Bacilli* and *Clostridia* — through the factors described in section 1.3.4 — package the proteins in their core, enabling them to resist the same challenges. Could mimicking the mechanisms of these spore-formers solve this formulation challenge?

As a delivery vehicle, spores are suitable for oral delivery, wherein therapeutic proteins they release are transported across the gut epithelium. Beyond that, *Bacillus* spores can travel around a body; the invasiveness of *B. anthracis* spores is certainly an extreme example, but the non-pathogenic *Bacilli* offer similar behaviour that might make them convenient hosts for delivering therapeutic proteins.

### 1.4.1 Spores protect their protein contents

Many of the protein damage mechanisms (discussed in section 1.2.3) require the protein to be in a hydrated local environment, whether in liquid solution or solid state. Even when the bulk environment is frozen, cold denaturation can happen if locally the protein is hydrated and below the thermodynamic cut-off temperature; for example, oxidation in freeze-dried formulations increases with increasing moisture content (Manning *et al.*, 2010).

Stabilizing proteins against the challenges of harsh or rapidly changing environmental conditions is a fundamental biological problem and organisms have independently evolved many solutions. Plants, seeds, pollen and fungal spores all stabilize their proteins against enormous changes in salt concentrations, fast temperature changes and radiation. In these systems, the local protein environment is a glass: an amorphous near-solid.

Spores are different, and hold proteins (and ions) immobilised in a water permeable matrix (Bassi *et al.*, 2012). Producing such a water-poor environment is tricky. Decreasing the water concentration increases salt concentrations, making salting in and chaotropic denaturation more likely. Spore cores avoid this. Not only would an understanding of the mechanisms involved be a valuable contribution to microbiology, it would also help those who design techniques to stabilize proteins in pharmaceutical formulations.

Despite preliminary results of Bradbury *et al.* (1981), showing DPA could stabilize proteins with respect to heat, it appears there has, until now, been no subsequent research. Arginine and glutamate, abundant in the spore core, show synergy in stabilizing proteins (Schneider *et al.*, 2011); it is only since the start of this project that anybody has investigated DPA, too, for this role *in vitro* (Batalha *et al.*, 2017).

#### 1.4.2 Spores can produce vast quantities of protein

Given the decades of research on Cry protein, why have so few researchers considered them for non-agricultural purposes? One factor must surely be the context in which much of this research has been conducted. Tautologically, the one thing all agriculture researchers have in common is that they are researching agriculture. Indeed, the work presented by Nair *et al.* (2015) was inspired by a serendipitous discovery (that fusions crystallized) while trying to improve imaging contrast to that end. Furthermore, and in contrast to much bacterial spore research, a good proportion of Cry research has been conducted in industry, rather than academia, and it may be the case that these ideas have been tested and reported within relevant companies, but not published. There has been work at this boundary between fields before (*e.g.* Pigott *et al.*, 2008), yet it has focused on improving specificity of the toxin rather than converting the protein for pharmaceutical use.

Crystallizing mAbs from commercial formulations leads to stable, bioactive samples, suitable for subcutaneous administration (Yang *et al.*, 2003). Volume restrictions mean that subcutaneous mAb formulations have a minimum concentration of 50 mg ml<sup>-1</sup>. However, this high concentration causes formulation problems (see section 1.2.3). Cry crystal suspensions can easily reach that minimum concentration limit.

Another somewhat novel proposition concerns yet another field of research. Cry fusions offer a novel screening method for crystallogenes. Much protein structural work relies on crystallization, yet many proteins of interest — in particular: membrane proteins, in general, or in the context of spores, coat proteins — have proved impervious to attempts to produce crystals. In a recent review, Giegé (2017) describes both the challenge of crystallogenes and its reward. For example, the author refers to work in which Ting *et al.* (2016) determine the crystal structure of a membrane anchored serine peptidase, using crystals of that protein as a fusion with MBP (maltose binding protein). Giegé (2017) does mention, in passing, the work of Nair *et al.* (2015) — yet only in the context of drug delivery. It is striking in a review on the future of crystallogenes the author does not propose the use of Cry fusions

for structural studies. While Cry crystals are not suitable for traditional X-ray crystallographic study, techniques such as Cryo-EM can produce structures. Indeed, there has been much interest in *in vivo* crystallization more generally (Adalat *et al.*, 2017; Koopmann *et al.*, 2012; Schönherr *et al.*, 2018), including work by Sawaya *et al.* (2014) on producing a 2.9 Å crystal structure by injecting Cry3A-producing vegetative *B. thuringiensis* cells into an X-ray free-electron laser beam.

### 1.4.3 Prior art

Given the above, what work has been done on using spores as delivery vehicles for therapeutic proteins? The prior art is sparse and not substantially developed, and covers coat fusions, forespore core expression, and Cry protein fusions; work has taken place on the former two in the Christie lab — see the theses of Lin (2017) and Mohamed (2015) respectively — though it is the latter two which are most relevant and shall be reviewed, briefly, below.

There has also been work on anaerobic spores, as a cancer treatment. *Clostridium* species have been used to deliver cytokines and enzymes to xenograft tumours in mice (Umer *et al.*, 2012). These bacteria are strict anaerobes, so only germinate and grow in the absence of oxygen. Tumours are hypoxic, so following ingestion, a) spores spread throughout the body, and b) germinate in tumours. c) The cells produce and secrete antibody fragments, which d) kill cancerous cells (strictly, all cells in the hypoxic zone), and then e) a short course of antibiotics kill the bacteria. For example, Groot *et al.* (2007) engineered *Clostridium novyi-NT* to produce a 15 kDa single chain camelid antibody raised against hypoxia inducible factor 1 $\alpha$ , which maintains tumour oxygen levels. The authors showed the purified antibodies bind their target, and their stated goal was a deliverable spore, but there has been no published progress from the research group, since.

Finally, there is some work on surface display that is especially relevant because of its relation to Cry proteins. Du *et al.* (2005) anchored GFP and an scFv to the coats of acrySTALLIFEROUS *B. thuringiensis* using N-terminal fusions of Cry1Ac.

#### **Cry fusions**

The academic literature contains very little on Cry protein fusions in a non-agricultural context. In the only real example, Nair *et al.* (2015) produced GFP and mCherry fusions of Cry3Aa and proposed they could be used to deliver therapeutics. Indeed, they showed

uptake by macrophages, conferment of gastric protection on fused luciferase, and migration through mouse lymph nodes. However, it is vegetative *B. thuringiensis*, not spores, that natively produces Cry3Aa, and the researchers used that vegetative machinery to produce their crystals.

There are a wide range of patents concerned with *B. thuringiensis* but few related to potential therapeutic use. It is instructive to consider differences between the applications for these patents and the remaining claims in the grants. Though the applications are often very broad, most of these claims do not survive review. For example, in granting Côté *et al.* (2008) for parasporin, an anti-cancer Cry variant (Mizuki *et al.*, 1999, first reports; and reviewed, Ohba *et al.*, 2009), the application was stripped of claims for all DNA sequences, the strain, all but two of the amino acid sequences, and their modulation method. The result is substantial freedom to operate, at the possible cost of difficulty in acquiring a patent on related work should that be desired.

The only directly relevant patent applications cover some of the work presented by Nair *et al.* (2015; these are Chan *et al.*, 2010; Chan & Nair, 2013). With the caveats of the above paragraph, the application by Chan *et al.* (2010) looks fairly unrestrictive. The claims cover “a protein crystal formed by a plurality of a fusion polypeptide, the fusion polypeptide comprising a Cry protein, or a crystal-forming fragment thereof, fused to a heterologous polypeptide” in various contexts, specifically: in a cell; as an isolated crystal; chemically crosslinked; as a fusion with “an immunogenic antigen” (i.e. a vaccine), “imageable agent”, “fluorescent protein”, “blood substitute”, or “therapeutic enzyme”; as DNA encoding a Cry fusion; and as a spore of a strain that contains such DNA. Not all combinations are represented. Bizarrely, they also claim for standard lab methods used to isolate such crystals. Claim 9 offers the restriction of Cry from “Cry1Aa, Cry1Ab, Cry2Aa, Cry3Aa, Cry4Aa, Cry4Ba, Cry11Aa, Cry11Ba, and Cry19Aa, their homologs [sic], or a crystal forming fragment thereof.” It is not clear why they do not explicitly reference Cry1Ac; from a patent search it doesn't appear to be covered under a similar patent, and there does not appear to be any Cry1Ac-specific prior art. There is still much room to operate, not least because many of the steps needed to produce a commercial formulation across the entire platform of Cry fusions have yet to be published, and, judging from the dearth of published preliminary requirements, are yet to be invented. Chan & Nair (2013) extended the earlier application to a worldwide patent and merged a few others; the above thoughts continue to apply. Furthermore it has now been over seven years since the first patent was filed; Google Patents reports that the application has been abandoned. Most importantly, though, there is no claim or reference made to therapeutic, non-enzyme proteins.

The final patent application to consider is that of Soto *et al.* (2014), on Cry proteins (not parasporin) that feature anti-cancer properties, similar to that of Aggarwal & Rodriguez-Padilla (1999), recently expired. These inventors too claim standard lab practices without refinement, and the remaining claims are notably vague.

### Expression of proteins in forespores

Work on expression of heterologous proteins by sporulating cells is less established, still. Following the work of Webb *et al.* (1995), Mohamed (2015) tested sporulation specific promoters  $P_{sspB}$  and  $P_{sspD}$ , demonstrating their relative levels of expression using a *lacZ* fusion ( $P_{sspB}$  expressed greater quantities of protein) and then using  $P_{sspB}$  to drive transcription of genes encoding human growth hormone, single chain insulin and an scFv against lysozyme.

From a densitometric analysis of a western blot, Mohamed (2015) inferred spores produced therapeutic proteins under  $P_{sspB}$  at yields from  $5 \mu\text{g} (\text{mg spores})^{-1}$  for GFP-fused single chain insulin, down to  $0.8 \mu\text{g} (\text{mg spores})^{-1}$  for a GFP-fused scFv. Quoting doses of  $1.4\text{--}2.1 \text{ mg day}^{-1}$  (from Walsh, 2005, for insulin), and for a human child of  $1.3 \text{ mg day}^{-1}$  human growth hormone — these correspond to  $0.3\text{--}0.4 \text{ g spores}$  and  $0.5 \text{ g}$  respectively — Mohamed (2015) deduced that “the level of protein production within the spore is high enough to allow for a reasonable amount of spores to constitute a dose.” ‘Reasonable’ in this context probably means a single tablet or capsule. However, this calculation did not account for the bioavailability of such a drug delivered orally, which for a protein therapeutic is often below 10% (Morishita *et al.*, 2006; Sarmiento *et al.*, 2007). The dose would have to increase by a factor of 5 to  $1.5\text{--}2 (\text{g spore}) \text{ day}^{-1}$  (assuming 50% bioavailability for the reported dose on which the calculation is based, Søbørg *et al.*, 2012). Beyond that, there is more to a pharmaceutical product than the active ingredient; even a minimal formulation which simply suspends the spores in fluid would contribute to an increased total dose size. Furthermore, as Walsh (2005) points out, insulin has acute and chronic dosage requirements; if  $1.5\text{--}2 (\text{g spore}) \text{ day}^{-1}$  does suffice for the chronic dose, acute doses are likely to be much higher. These problems are not insurmountable, but they do mean there is much work to do before a promising yield in the lab can become a commercial product.

What about the anti-hen egg white lysozyme scFv reported by Mohamed (2015)? For comparison, Durvalumab, the PD-L1 inhibitor recently indicated for bladder cancer, is delivered intravenously as  $10 \text{ mg kg}^{-1}$  once every two weeks, often for a year (Optum Inc., 2017). For a 70 kg patient, that means the equivalent of  $50 \text{ mg day}^{-1}$  — and that is just the

antibody. If the full antibody were produced to the same mass as the scFv fusion, that would correspond to 60 (g spore) day<sup>-1</sup> (i.e. a small drink). Add in the aforementioned potential for poor bioavailability and it becomes clear that the protein yields reported by Mohamed (2015) will not suffice.

Finally, this prior work has only involved *B. subtilis*. *B. megaterium* and *B. thuringiensis* express complex proteins at high yields and might provide a better option than *B. subtilis*.

### **Remaining milestones**

In attempting to design a bacterial spore-based biologic, a number of important milestones have not been reached. Nobody has yet produced fragments of a human or humanized antibody in sporulating cells. Nobody has yet produced whole antibodies in sporulating cells. It follows that nobody has demonstrated function or quality of these proteins; indeed, the formulation quality is absent from *any* related work in these organisms. These all form unanswered questions, some of which form the goals of this project.

## 1.5 This thesis

There is much scope to explore concerning production of heterologous proteins by sporulating bacteria, and this thesis will examine just a fraction of those possibilities. What follows is a feasibility study, asking the question ‘are sporulating bacteria capable of producing therapeutic proteins, in therapeutically useful quantities?’ There are three parts:

1. investigation of the mechanisms that enhance protein stability in spores,
2. design and optimisation of protein expression systems in spores, and
3. proof-of-principle production of a deliverable formulation which allows a controlled dose of proteins to be released in its environment.

How do spores stabilize the proteins in their cores? Much is known on the composition of the environment, but little on mechanisms — in particular, those involving DPA. Nobody has adequately controlled for water content of DPA-less spores when investigating their properties. Do chemical analogues provide an alternative mechanism by which to investigate this, and if so, what does such work reveal?

Building on previous work in the Christie group, is it possible to use established spore systems to produce novel, more complicated molecules? How does expression vary with different expression machinery, in different strains, or in different species? Is it then possible to evaluate such molecules using the tools of formulation science? How do they compare by these quality factors to antibodies produced in CHO cells?

What else might be needed as part of a deliverable formulation? This will certainly depend on the magnitude of expression; is a formulation even feasible? And if so, what is needed to progress from that to a finished product? Of particular interest is a mechanism by which proteins encapsulated within spores are released at the appropriate time and place.

The risk of this whole endeavour is high. Many standard techniques, in evaluating protein quality for therapeutic considerations, are yet to be established for spores. The very resilience of sporeformers that is so desirable also makes collaboration with pharmaceutical experts tricky; they will not allow spores near any of their equipment. Despite that, there is plenty of space in which to work; few researchers are currently investigating these questions, and answers to any of them will advance the understanding of these fascinating organisms and their biotechnological potential.

What follows is a report on the course of research, inspired by the context in this chapter. The long term goal — a spore-based pharmaceutical formulation — has been the driving force behind the research focus and direction. Following the descriptions of the methods used throughout this project in the next chapter, chapter 2, are a trio of chapters; each uses a separate route to investigate whether it is possible to develop biopharmaceutical products based on bacterial spores.

The first of these, chapter 3, describes an investigation of the role of DPA (dipicolinic acid) in the stability of spores, with a view to mimicking aspects of the environment in the spore core. The work of Magge *et al.* (2008) and Li *et al.* (2012) is extended to *B. megaterium*, showing similarities and differences, and is extended with a new selection of chemical analogues. This chapter presents a technique to investigate DPA-enhanced, in addition to DPA-depleted spores, by supplementing the sporulating medium. The work presented here has inspired one line of research from an industrial collaborator (published by Batalha *et al.*, 2017) and contributed to another publication from the Christie group (Xu Zhou *et al.*, 2017). Strains engineered as part of the work reported in chapter 3 have been sent to collaborators for further study.

Work on the opposite approach is reported in chapter 4; rather than designing a formulation that mimics the conditions within the spore core, this approach would see the *B. subtilis* spore core used itself, as a spore-based package. Specifically, the chapter reports the production of heterologous, therapeutic proteins in forespores. This chapter reports for the first time the production of a variety of humanized antibody fragments by sporulating cells, and the production of camelid antibody fragments in sporulating *B. subtilis*. A  $\Delta cotE$  mutant strain is reported; it can be disrupted using chemical, rather than mechanical means, and thus offers both a route to scale extraction of core contents and to release payloads *in vivo*.

The challenge of low protein yields is addressed in chapter 5. This chapter considers, as an alternative to production in the spore core, a novel way of producing therapeutic proteins in sporulating cells, using *B. thuringiensis* Cry proteins. A set of fluorescent Cry fusions have been created as a platform for subsequent engineering. The platform has been demonstrated to work, producing fusions to humanized antibody fragments. This work has been taken forward by a number of researchers: both within the Christie group and beyond.



Finally, in chapter 6 I review the achievements of this project, in the context of the academic literature and commercial opportunities. The chapter presents some direction for future work, both to directly answer some of the questions raised by the work reported here, and to take this project forwards towards the goal of a spore-based therapeutic product.



# Chapter 2

## Methods

## 2.1 Materials & Equipment

Sterile stock solutions were filtered using a 0.22  $\mu\text{m}$  Millex syringe filter (Merck Millipore).

Unless otherwise noted: chemicals were supplied by Sigma-Aldrich, enzymes by New England BioLabs, and dried, complex media by Melford.

### 2.1.1 Antibiotics

Antibiotics are listed in table 2.1, with the exception of 5-FU (fluorouracil). Cassettes were discussed by Guérout-Fleury *et al.* (1995). This was prepared as a 50 mM stock, for use (37.5  $\mu\text{M}$ ) as 3 in 4000 dilution (e.g. 75  $\mu\text{l}$  in 100 ml, or 300  $\mu\text{l}$  in 400 ml). This required 6.58  $\text{mg ml}^{-1}$  5-FU.

Table 2.1: Antibiotics, used in this project. Tetracycline was processed and stored in the dark, both as a stock and in broth/agar.

Antibiotic	Cassette	Stocks / $\text{mg ml}^{-1}$	Final <i>E. coli</i> / $\mu\text{g ml}^{-1}$	Final <i>Bacillus</i> / $\mu\text{g ml}^{-1}$	<i>Bacillus</i> stock to use / $\mu\text{l} \cdot (100 \text{ ml})^{-1}$
Carbenicillin	<i>bla</i>	100	50–100		
Kanamycin	<i>kan</i>	100	10–50	5	50
Tetracycline	<i>tet</i>	10	5–10	10	100
Chloramphenicol	<i>cat</i>	25	25–170	5	20
Erythromycin	<i>erm</i>	10	—	1	10
Lincomycin	<i>erm</i>	25	—	25	100
Spectinomycin	<i>spc</i>	50	50	100	200

For 25 mol% DMSO (dimethyl sulfoxide) in water (corresponding to 60% w/w and 57% v/v) a mix of (final) volume fraction 0.59 DMSO and 0.45 water was used. If the mix is prepared and then the 5-FU is added, dissolution is slow. Direct addition of the 5-FU to the DMSO, before slowly adding water, helped. Note the DMSO and water generate heat on mixing. If diluting 5-FU in DMSO, note also the latter has a specific gravity of 1.10.

## 2.1.2 Antibodies

The rabbit polyclonal Anti-6× His tag® antibody (HRP) ab1187 (AbCam), lot no. GR214185-2, was used at a 1 in 4000 dilution.

## 2.1.3 Ladders

DNA ladders were the Quick-Load 2-Log ladder (NEB) and Hyperladder 1kb (Bioline).

Protein ladders were Novex® Sharp Pre-stained Protein Standard (Thermo Scientific) MagicMark™ XP Western Protein standard (ThermoFisher).

## 2.1.4 Plasmids

### **pDBT\***

Plasmids in this thesis begin pDBT and the suffix is coded according to the following scheme.

- The first character of the code corresponds to the base vector (table 2.2).
- Subsequent characters correspond to variants of that base vector (such as those in table 2.3).
- Any plasmid ending in  $\emptyset$  is a vector designed to take an insert.
- A lower case character ends the code, and corresponds to a particular insert; there is typically a mnemonic.
- A question mark at any position corresponds to a series of plasmids sharing a common feature, where the plasmids differ at the single ? character.
- An asterisk at any position corresponds to a series of plasmids sharing common features or lineage, and differing in the \* position.

A full list of plasmids, constructed as part of this work, is in table 2.4.

## 2.1.5 Strains

### **Strains sourced from others**

Strains not constructed in this thesis are listed in table 2.5.

Table 2.2: Base plasmids, used in this project. Sources correspond to the original plasmid. BGSC, Bacillus Genetic Stock Centre.

Identifier	Purpose	Parent plasmid	Modifications in this work	Parent Source
1	Library	pGEM-3Z	Deletion of <i>BsaI</i> sites and introduction of Golden Gate donor sites	Mohamed (2015)
2	<i>B. megaterium</i>	pUCTV2	—	Wittchen & Meinhardt (1995)
3	<i>Bacilli</i> , mainly <i>B. thuringiensis</i>	pHT315	Deletion of <i>BsaI</i> sites and introduction of Golden Gate recipient sites	Lereclus <i>et al.</i> (1989)
6	<i>B. subtilis</i>	pDG1662	—	BGSC (Guérout-Fleury <i>et al.</i> , 1996)
7	<i>B. subtilis</i>	pSS	Deletion of <i>BsaI</i> sites	BGSC (Shi <i>et al.</i> , 2013)

### Strains engineered in this thesis

The strains constructed as a part of this project are named according to a similar schema to that presented in section 2.1.4. Strains are named for the base strain and the suffix of the plasmid used to transform them, separated by a ‘::’. Where there is no ambiguity, subsequent strains would keep only the final suffix of their parent strain.

For example, *B. subtilis* 168 transformed using pDBT611h would become 168::611h. By contrast, *B. subtilis* 168::690 transformed using pDBT71e would become 690::71e, as the preceding ‘168::’ may be elided without ambiguity.

The full lists of strains, which have been constructed as a part of this project, are presented in tables 2.6–2.8.

Table 2.3: Further plasmids used, but not designed, as part of this work.

Name here	Parent plasmid	Description	Source
pDBT6*	pDG1662-PsspB-SCI-GFP	pDG1662 with inserted coding sequences under control of P <sub>sspB</sub>	Mohamed (2015)
—	p7Z6	Source of <i>ble</i> cassette conferring zeocin resistance	Yan <i>et al.</i> (2008)
—	pDG1726	Source of <i>spc</i> cassette conferring spectinomycin resistance	Guérout-Fleury <i>et al.</i> (1996)
—	pEBS-cop1	Introduces <i>I-SceI</i> via the <i>i-SceI</i> for inducing recombination	Shi <i>et al.</i> (2013)
—	pMA-NIP109-Lc	Library vector containing the NIP109 light chain, codon optimised for <i>B. subtilis</i>	Medimmune
—	pMA-NIP109-Hc	Library vector containing the NIP109 heavy chain, codon optimised for <i>B. subtilis</i>	Medimmune

Table 2.6: *B. megaterium* strains, engineered to test behaviour of DPA. Genes *tet*, *spc* and *kan* confer tetracycline, spectinomycin and kanamycin resistance, respectively.

Strain	Genotype	Description
1551::21s+	<i>spoVF::tet::spc</i>	SXO (single crossover) DPA synthetase mutant
1462::21s	<i>sleB::kan spoVF::spc</i>	DXO (double crossover) double mutant

## 2.1.6 Equipment

Laboratory equipment is listed in table 2.9.

## 2.1.7 Buffers

Unless noted, buffers were autoclaved before storage.

### TE-1

TE-1 buffer is 10 mM Tris-HCl, 1 mM EDTA (ethylenediaminetetraacetic acid), at pH 8.

Table 2.4: Plasmids, constructed as part of this project and referenced in this thesis.

Plasmid pDBT...	Description
120	With kanamycin, not carbenecillin, cassette
12d	<i>cry1Ac</i> native operon
12u	<i>upp-spc</i> cassette
1510	BcII10 nanobody
1520	TEM02 nanobody
1530	TEM13 nanobody
1540	V <sub>H</sub> H GFm4 nanobody
21s	For indel mutation of <i>spoVF</i> locus in <i>B. megaterium</i>
310	Cry1Ac LTC
3110	Cry1Ac Lm
3120	Cry1Ac LmC
312h	Cry1Ac LmCh
312l	Cry1Ac LmCl
312s	Cry1Ac LmCs
3130	Cry1Ac LCm
313h	Cry1Ac LhCm
313l	Cry1Ac LlCm
313s	Cry1Ac LsCm
3140	Cry1Ac LTm
3150	Cry1Ac LTCm
3160	<i>cry1Ac</i> operon, with $\sigma^G$ recognition site in promoter
31610	mCherry, on <i>cry1Ac</i> operon with $\sigma^G$ recognition site in promoter
31710	<i>cry1Ac</i> m
31720	<i>cry1Ac</i> Cm
610	NIP109 plasmids; on P <sub>sspB</sub> , for expression in spore core during sporulation
6110	AL11-GFP-His fusion
611h	NIP109 Heavy chain
611l	NIP109 Light chain
611s	NIP109 scFv (L→H, 7-mer linker)
611t	NIP109 scFv (L→H, 18-mer linker)



...table cont'd

Table 2.4: Plasmids, constructed as part of this project and referenced in this thesis.

Plasmid pDBT...	Description
611u	NIP109 scFv (H→L, 7-mer linker)
6160	His fusion
616h	NIP109 Heavy chain
616l	NIP109 Light chain
616s	NIP109 scFv (L→H, 7-mer linker)
616t	NIP109 scFv (L→H, 18-mer linker)
616u	NIP109 scFv (H→L, 7-mer linker)
6510	BcII10 nanobody
651m	BcII10 chromobody
6520	TEM02 nanobody
6530	TEM13 nanobody
6540	V <sub>H</sub> H GFP4 nanobody
651m	V <sub>H</sub> H GFP4 chromobody
690	To (attempt to) generate supercompetent strain
69c	To generate 5-FU- and chloramphenicol-resistant strain
69d	To generate 5-FU- and chloramphenicol-resistant supercompetent strain
71e	Delete <i>cotE</i> , introduce spectinomycin resistance and 5-FU sensitivity
72e	Delete <i>cotE</i> , introduce chloramphenicol resistance and 5-FU sensitivity

### Disruption buffers

Cell disruption buffer	is 50 mM phosphate buffer (pH 7.5), 1 mM MgSO <sub>4</sub> , 10% w/v glycerol and 2 mM PMSF (phenylmethylsulfonyl fluoride).
Spore breakage buffer	is 50 mM Tris-HCl (pH 7.5), 0.5 mM EDTA and 1 mM PMSF.

Table 2.5: Background strains, used in this thesis.

Species	Name	Description	Source
<i>B. subtilis</i>	168	With fixed <i>trpC</i> locus	Prof. Peter Setlow (University of Connecticut Health Center, USA)
<i>B. megaterium</i>	QM B1551	Wild type	Prof. Patricia S. Vary (Northern Illinois University, USA)
<i>B. megaterium</i>	PS1462	$\Delta sleB::kan$ Km <sup>r</sup>	Prof. Peter Setlow (University of Connecticut Health Center, USA)
<i>B. thuringiensis</i>	HD-73	Wild type (produces Cry1Ac)	BGSC (strain 4D4)
<i>E. coli</i>	DH5 $\alpha$	Cloning strain	New England Biolabs
<i>E. coli</i>	Turbo	Cloning strain	New England Biolabs (C2984)
<i>B. cereus</i>	ATCC 14579	Wild type	Toril Lindbäck (Norwegian University of Life Science, Ås, )
<i>B. thuringiensis</i>	YBT-020	Wild type (spore crystal association)	BGSC (strain 4B4)

### His-tag buffers

His-binding buffer is phosphate buffered saline (20 mM phosphate buffer pH 7.4, 500 mM NaCl) with 20 mM imidazole.

His-elution buffer is phosphate buffered saline (20 mM phosphate buffer pH 7.4, 500 mM NaCl) with 500 mM imidazole.

Both were filter-sterilized and stored in the dark, at 4°C.

### Transforming buffer

Transforming buffer, for preparation of highly competent *E. coli*, is presented in table 2.10.

### T-base

T-base, used in preparation of chemically competent *B. subtilis* (see section 2.3.5) comprises the ingredients listed in table 2.11.

Table 2.7: *B. subtilis* strains, with coat mutation or for antibody expression. Genes *bla*, *spc* and *cat* are carbenicillin, spectinomycin and chloramphenicol antibiotic resistance cassettes, respectively.

Strain	Genotype	Description
168::616l	<i>amyE::cat</i>	NIP109 Light chain
168::616h	<i>amyE::cat</i>	NIP109 Heavy chain
168::616s	<i>amyE::cat</i>	NIP109 scFv
168::616t	<i>amyE::cat</i>	NIP109 scFv
168::616u	<i>amyE::cat</i>	NIP109 scFv
168::611l	<i>amyE::cat</i>	NIP109 Light chain (GFP)
168::611h	<i>amyE::cat</i>	NIP109 Heavy chain (GFP)
168::611s	<i>amyE::cat</i>	NIP109 scFv (GFP)
168::611t	<i>amyE::cat</i>	NIP109 scFv (GFP)
168::611u	<i>amyE::cat</i>	NIP109 scFv (GFP)
168::6510	<i>amyE::cat</i>	BcII10 nanobody
168::651m	<i>amyE::cat</i>	BcII10 chromobody
168::6520	<i>amyE::cat</i>	TEM02 nanobody
168::6530	<i>amyE::cat</i>	TEM13 nanobody
168::6540	<i>amyE::cat</i>	V <sub>H</sub> H GFP4 nanobody
168::654m	<i>amyE::cat</i>	V <sub>H</sub> H GFP4 chromobody
168::690	<i>upp::comK</i> (P <sub>ara</sub> )	Inducibly supercompetent counter-selectable strain
168::69c	<i>upp::cat</i>	5-FU validation strain
168::69d	+ <i>cat::comK</i> (P <sub>ara</sub> )	Progenitor of 168::690
690::71e	<i>upp::comK cotE::spc</i>	Coat deficient mutant
690::611h	<i>upp::comK</i> <i>amyE::cat</i>	NIP109 Light chain (GFP), WT coat
690::611l	<i>upp::comK</i> <i>amyE::cat</i>	NIP109 Heavy chain (GFP), WT coat
690::611s	<i>upp::comK</i> <i>amyE::cat</i>	NIP109 scFv (GFP), WT coat
71e::611h	<i>upp::comK cotE::spc</i> <i>amyE::cat</i>	NIP109 Light chain (GFP), coat deficient
71e::611l	<i>upp::comK cotE::spc</i> <i>amyE::cat</i>	NIP109 Heavy chain (GFP), coat deficient

...table cont'd

Table 2.7: *B. subtilis* strains, with coat mutation or for antibody expression. Genes *bla*, *spc* and *cat* are carbenicillin, spectinomycin and chloramphenicol antibiotic resistance cassettes, respectively.

Strain	Genotype	Description
71e::611s	<i>upp::comK cotE::spc amyE::cat</i>	NIP109 scFv (GFP), coat deficient

Table 2.10: Transforming buffer (*E. coli*). The first three ingredients were combined in water and adjusted to pH 6.7 with potassium hydroxide, KOH, before addition of the  $MnCl_2$ .

Component	Mass / $g L^{-1}$
PIPES	3.0
Calcium chloride ( $CaCl_2$ )	2.2
Potassium chloride (KCl)	18.6
Manganese chloride ( $MnCl_2$ )	10.9

Table 2.11: T-base buffer (*B. subtilis*). Ingredients were dissolved in water and autoclaved.

Ingredient	Final concentration / $g L^{-1}$
Ammonium sulphate ( $(NH_4)_2SO_4$ )	2.0
Potassium phosphate, dibasic ( $K_2HPO_4 \cdot 3H_2O$ )	18.3
Potassium phosphate, monobasic ( $KH_2PO_4$ )	6.0
Trisodium citrate ( $Na_3C_6H_5O_7 \cdot 2H_2O$ )	1.0

## Electroporation buffer

Solution A (electrocompetence variant) is a cell wall-weakening treatment used to prepare cells for electroporation. It comprises glycine (5 wt%) and sucrose (250 mM).

Electroporation buffer is described in table 2.12.

Table 2.8: Strains, for work with *cry1Ac* operon. Genes *bla* and *erm* are carbenicillin and erythromycin/lincomycin antibiotic resistance cassettes, respectively. The mnemonic is L, T, P, m for the leader, toxic core, protoxin and mCherry sequences, then 1 for light chain, h for heavy chain and s for scFv.

Strain	Species	Genotype	Description
Turbo::310	<i>E. coli</i>	+ <i>bla</i>	LTP assembly
Turbo::3110	<i>E. coli</i>	+ <i>bla</i>	Lm assembly
Turbo::3120	<i>E. coli</i>	+ <i>bla</i>	LmP assembly
Turbo::3130	<i>E. coli</i>	+ <i>bla</i>	LPm assembly
Turbo::3140	<i>E. coli</i>	+ <i>bla</i>	LTm assembly
Turbo::3150	<i>E. coli</i>	+ <i>bla</i>	LTPm assembly
Turbo::31710	<i>E. coli</i>	+ <i>bla</i>	m assembly
Turbo::31720	<i>E. coli</i>	+ <i>bla</i>	mP assembly
HD-73::30	<i>B. thuringiensis</i>	+ <i>erm</i>	Empty vector
HD-73::310	<i>B. thuringiensis</i>	+ <i>erm</i>	LTP
HD-73::3110	<i>B. thuringiensis</i>	+ <i>erm</i>	Lm
HD-73::3120	<i>B. thuringiensis</i>	+ <i>erm</i>	LmP
HD-73::312h	<i>B. thuringiensis</i>	+ <i>erm</i>	LmPh (NIP109)
HD-73::312s	<i>B. thuringiensis</i>	+ <i>erm</i>	LmPs (NIP109)
HD-73::3130	<i>B. thuringiensis</i>	+ <i>erm</i>	LPm
HD-73::313l	<i>B. thuringiensis</i>	+ <i>erm</i>	LPm1 (NIP109)
HD-73::313h	<i>B. thuringiensis</i>	+ <i>erm</i>	LPmh (NIP109)
HD-73::313s	<i>B. thuringiensis</i>	+ <i>erm</i>	LPms (NIP109)
HD-73::3140	<i>B. thuringiensis</i>	+ <i>erm</i>	LTm
HD-73::3150	<i>B. thuringiensis</i>	+ <i>erm</i>	LTPm
HD-73::31710	<i>B. thuringiensis</i>	+ <i>erm</i>	m
HD-73::31720	<i>B. thuringiensis</i>	+ <i>erm</i>	mP
690::3130	<i>B. subtilis</i>	+ <i>erm</i>	LPm
690::3140	<i>B. subtilis</i>	+ <i>erm</i>	LTm
690::3160	<i>B. subtilis</i>	+ <i>erm</i>	LTP
690::31610	<i>B. subtilis</i>	+ <i>erm</i>	m
14579::3130	<i>B. cereus</i>	+ <i>erm</i>	LPm
14579::3140	<i>B. cereus</i>	+ <i>erm</i>	LTm

...table cont'd

Table 2.8: Strains, for work with *cry1Ac* operon. Genes *bla* and *erm* are carbenicillin and erythromycin/lincomycin antibiotic resistance cassettes, respectively. The mnemonic is L, T, P, m for the leader, toxic core, protoxin and mCherry sequences, then 1 for light chain, h for heavy chain and s for scFv.

Strain	Species	Genotype	Description
YBT-020::3130	<i>B. thuringiensis</i>	+ <i>erm</i>	LPm
YBT-020::3140	<i>B. thuringiensis</i>	+ <i>erm</i>	LTm

Table 2.12: Electroporation buffer (*B. cereus* family). The ingredients were combined, adjusted to pH 7.0 and filter sterilized.

Component	Final Concentration / mM
Sucrose	250
HEPES (4-(2-hydroxyethyl)-1-piperazineethanesulphonic acid)	1
Magnesium chloride (MgCl <sub>2</sub> )	1
Glycerol	(10% v/v)

### Western blot buffers

TBS (Tris-buffered Saline)	is 20 mM Tris-HCl (pH 7.6) with 150 mM NaCl; the
TBST	variant also comprises 0.1% v/w Tween-20, and its
TBST-BSA	variant also contains 5% w/w BSA (bovine serum albumin).
Transfer buffer	is 10% v/v NuPAGE 20× Transfer buffer (Thermo Scientific), 0.1% v/v NuPAGE antioxidant (Thermo Scientific) and 10% v/v Methanol.

Table 2.9: Laboratory equipment. The original list was compiled by Mohamed (2015).

Instrument	Purpose	Supplier
FastGene blue light LED illuminator	Agarose gel electrophoresis	GeneFlow
Gel electrophoresis tanks	Agarose gel electrophoresis	BioRad
UVitec gel documentation system	Agarose gel electrophoresis	UVitec
Herasafe class II biological safety cabinet	Aseptic operation	Hereaus
Mars class II biological safety cabinet	Aseptic operation	Scanlaf
Microflow advanced biosafety cabinet Class-II	Aseptic operation	Bioquell
Incubators	Cell culture	New Brunswick Scientific
WhirliMixer vortex	Cell culture	Fisons
FastPrep F120-B10101	Cell disruption	Thermo Scientific
MC cell disruptor	Cell disruption	Constant Systems
5810R centrifuge, with A-4-62 swing rotor	Centrifugation	Eppendorf
Sorvall LYNX 400 super-speed centrifuge	Centrifugation	Thermo Scientific
ND-100 NanoDrop spectrophotometer	DNA quantification	Thermo Scientific
Gene Pulsar	Electroporation	BioRad
Biofuge pico table-top centrifuge	Microcentrifugation	Hereaus
Biophotometer	Optical density measurement	Eppendorf
Synergy HT Multi-Detection Microplate Reader	Optical measurements	Biotek
Wallac Envision 2104 Multiplate Reader	Optical measurements	Perkin-Elmer
BX51 microscope	Optical microscopy	Olympus
BX53 microscope (with UV source)	Optical microscopy	Olympus
Retiga 2000R cooled CCD	Optical microscopy	QImaging
DNA engine DYA thermal cycler	PCR	BioRad
Trans-Blot Semi Dry Transfer Cell	Western blot	BioRad

...table cont'd

Table 2.9: Laboratory equipment. The original list was compiled by Mohamed (2015).

Instrument	Purpose	Supplier
3D rocking platform	PAGE	Jencons Stuart Scientific
Bolt Mini Gel Tank	PAGE	Life technologies
G-Box gel documentation system	PAGE	Syngene
PowerPac 200 power supply	PAGE	BioRad
Xcell SureLock Mini-cell electrophoresis tanks	PAGE	Life technologies

### Qiagen kit buffers

- Buffer QG, used to dissolve agarose gels, comprises 5.5 M guanidine thiocyanate and 20 mM Tris-HCl, at pH 6.6.
- Buffer P1, the resuspension buffer for minipreps, comprises 50 mM Tris-HCl, 10 mM EDTA and 100 µg ml<sup>-1</sup> RNaseA, at pH 8.0.
- Buffer P2, the miniprep lysis buffer, comprises 200 mM NaOH and 1% w/v SDS (sodium dodecyl sulphate).
- Buffer N3, the miniprep neutralisation buffer, comprises 4.2 M guanidinium hydrochloride and 0.9 M potassium acetate, at pH 4.8.
- Buffer PB, the binding buffer for minipreps and PCR clean-ups, comprises 5 M guanidinium hydrochloride and 30% v/v isopropanol.
- Buffer AE is the elution buffer for gDNA (genomic DNA) extractions. It is composed of 10 mM Tris-HCl and 0.5 mM EDTA, at pH 9.0.
- Buffer PE is the elution buffer for miniprep and PCR clean-ups. It is composed of 10 mM Tris-HCl and 80% v/v ethanol, at pH 7.5.

### Proprietary buffers

Buffers AW1 and AW2 are proprietary Qiagen buffers. Buffer AW1 is a guanidinium hydrochloride based wash buffer; buffer AW2 is a wash buffer based on sodium azide (Himmelreich & Werner, 2014).



## 2.1.8 Media

Media were autoclaved at 121 °C for 15 min.

Difco nutrient broth comprises 3 parts by mass beef extract, to 5 parts peptone.

### Standard growth media

LB (Lysogeny Broth)	was prepared as described by Harwood & Cutting (1990). Composition: 10 gL <sup>-1</sup> tryptone, 10 gL <sup>-1</sup> NaCl, 5 gL <sup>-1</sup> yeast extract, pH 7.2.
SOB (Super Optimal Broth)	was prepared as described by Harwood & Cutting (1990). Composition: 20 gL <sup>-1</sup> tryptone, 0.5 gL <sup>-1</sup> NaCl, 5 gL <sup>-1</sup> yeast extract, magnesium sulphate (MgSO <sub>4</sub> ) 2.4 gL <sup>-1</sup> , potassium chloride (KCl) 0.186 gL <sup>-1</sup> , pH 7.0.
TSB (Tryptone Soy Broth)	was prepared using Tryptone Soy Broth CM0129 (Oxoid). Composition: 17.0 gL <sup>-1</sup> casein (pancreatic digest), 3.0 gL <sup>-1</sup> soy bean meal (papaic digest), 5.0 gL <sup>-1</sup> NaCl, potassium phosphate dibasic (K <sub>2</sub> HPO <sub>4</sub> ) 2.5 gL <sup>-1</sup> , glucose 2.5 gL <sup>-1</sup> , pH 7.3.
PDM (Plasmid DNA Medium)	was presented by Danquah & Forde (2007) as an effective and cost-effective medium for plasmid production. The optimized variant,
PDMR (PDM, ratio optimized),	uses a C/N ratio of 2.8. The recipe is provided in table 2.13 (base) and table 2.14 (supplement).

*Table 2.13: Base for PDMR (PDM, ratio optimized), with C:N ratio of 2.8:1. All listed ingredients were combined, then autoclaved.*

Component	Mass / gL <sup>-1</sup>
Water	910
Yeast extract Y1333 (Melford)	4.4
Tryptone LP0021 (Oxoid)	8.0
Ammonium chloride (NH <sub>4</sub> Cl)	5.5
Magnesium sulphate (MgSO <sub>4</sub> )	0.26

Table 2.14: Supplement for PDMR, added before use. Components were prepared as individual stocks, then combined into a master mix.

Component	Stock concentration	Volume / ml L <sup>-1</sup>
Glucose	50% w/v	20
Disodium phosphate (Na <sub>2</sub> HPO <sub>4</sub> )	1 M	48
Potassium phosphate, monobasic (KH <sub>2</sub> PO <sub>4</sub> )	1 M	22

### Transformation media

RHAF (Hadlaczky Alföldi Fodor) broth was prepared (table 2.15, as described by McCool & Cannon, 2001).

Table 2.15: Composition of RHAF (Hadlaczky Alföldi Fodor) broth (*B. megaterium*). The pH was adjusted to 7.5 using concentrated HCl before addition of magnesium chloride.

Ingredient	Concentration / mM	Mass / g L <sup>-1</sup>
Tris	100	12
Sucrose	200	68.46
Glucose	11	2
Ammonium chloride (NH <sub>4</sub> Cl)	19	1
Sodium sulphate (Na <sub>2</sub> SO <sub>4</sub> )	2	0.3
Mono-potassium phosphate (KH <sub>2</sub> PO <sub>4</sub> )	1.0	0.14
Sodium chloride (NaCl)	1.0	0.058
Potassium chloride (KCl)	0.50	0.035
Yeast Extract		5
Tryptone		5
Magnesium Chloride (MgCl <sub>2</sub> ·6H <sub>2</sub> O)	23.0	4.68

SpC & SpII are required for producing chemically competent *B. subtilis*. Table 2.16 describes the recipes. Media were made fresh from the listed stocks, on the day of use.

Electroporation recovery medium was prepared as a 2× stock in TSB, as described in table 2.17. To use, the stock was mixed with TSB in a 1:1 ratio

Table 2.16: Recipes for SpC and SpII media (*B. subtilis*). The individual ingredients were prepared as stocks (in 30 ml and 200 ml, respectively) of the given compositions.

Ingredient	Stock composition	Volume (SpC) / ml	Volume for (SpII) / ml
T-base		27.9	200
D-glucose	50% w/v	0.30	2
Yeast extract	10% w/v	0.60	2
Magnesium sulphate trihydrate (MgSO <sub>4</sub> ·3H <sub>2</sub> O)	1.2% w/v	0.45	14
Casamino acids	1.0% w/v	0.75	2
Calcium chloride (CaCl <sub>2</sub> )	0.1 M	–	1
Total		30.0	200

Table 2.17: Electroporation recovery medium.

Component	Stock Concentration / mM
Sucrose	250
Magnesium chloride (MgCl <sub>2</sub> )	5
Magnesium sulphate (MgSO <sub>4</sub> )	5

### Sporulation by nutrient exhaustion

SNB (Supplemented Nutrient Broth) was prepared (table 2.18, as described by Harwood & Cutting, 1990).

Table 2.18: Composition of SNB, supplemented nutrient broth (*B. megaterium*).

Component	Concentration / mM	Mass / gL <sup>-1</sup>
Difco nutrient broth		8.0
Glucose	5.55	1.0
Potassium chloride (KCl)	13.4	1.0
Manganese chloride (MnCl <sub>2</sub> )	0.02	0.004
Ferrous sulphate (FeSO <sub>4</sub> )	0.001	0.0003
Magnesium sulphate (MgSO <sub>4</sub> ·7H <sub>2</sub> O)	1.0	0.2465
Calcium chloride (CaCl <sub>2</sub> )	1.0	0.147

- 2×SG, the modified Schaeffer's media, was prepared according to Harwood & Cutting (1990). To 1 kg water were added 16.0 g Difco nutrient broth, 2.0 g KCl, 0.5 g MgSO<sub>4</sub>·7H<sub>2</sub>O, and 17.0 g technical agar (Melford). The pH was adjusted to 7.0 and the resulting medium (of specific gravity 1.04) autoclaved. Before use, this was supplemented with the volumes of the stock solutions listed in table 2.19.
- 2×SGR was prepared according to Warriner & Waites (1999), having demonstrated an increase in spore titre versus 2×SG (on switching half of the glucose for ribose).

Table 2.19: Supplements for 2×SG and 2×SGR medium (*B. subtilis*). Stocks were filter sterilized, then combined as a 5.0 ml L<sup>-1</sup> master mix.

Ingredient	Stock concentration	Volume (2×SG) / ml L <sup>-1</sup>	Volume (2×SGR) / ml L <sup>-1</sup>
Calcium nitrate (Ca(NO <sub>3</sub> ) <sub>2</sub> )	1.0 M	1.0	1.0
Manganese chloride (MnCl <sub>2</sub> )	0.1 M	1.0	1.0
Iron (II) sulphate (FeSO <sub>4</sub> )	1 mM	1.0	1.0
Glucose	50% w/v	2.0	1.0
Ribose	42% w/v	–	1.0

- CCY (casein casein yeast) medium (Stewart *et al.*, 1981) required the ingredients in table 2.20: combined, adjusted to pH ~ 7.5 with 1 M KOH (though this was often unnecessary) and autoclaved. The CCY salts master mix described in table 2.21 was added as a supplement at 0.1% v/v, before use.

Table 2.21: CCY salts, to supplement base medium. The master mix was stored at 4 °C.

Component	Stock concentration / mM
Magnesium chloride (MgCl <sub>2</sub> )	500
Manganese chloride (MnCl <sub>2</sub> )	10
Iron (III) chloride (FeCl <sub>3</sub> )	50
Zinc chloride (ZnCl <sub>2</sub> )	50
Calcium chloride (CaCl <sub>2</sub> )	200

Table 2.20: Base CCY (casein casein yeast) medium (*B. cereus* family).

Component	Final concentration / mM	Mass / gL <sup>-1</sup>
Water	–	1000
Enzymatic casein hydrolysate	–	1
Acid casein hydrolysate	–	1
Yeast extract	–	0.4
Potassium phosphate, monobasic (KH <sub>2</sub> PO <sub>4</sub> )	13	1.77
Potassium phosphate, dibasic (K <sub>2</sub> HPO <sub>4</sub> )	26	4.53
Glutamine	0.27	0.04
Glycerol		0.6

### SM medium for sporulation by resuspension

This recipe for SM (Sterlini–Mandelstam) medium was published as a technical resource, by Nicholson & Setlow (1990).

Growth medium was prepared fresh on the day of use, according to the recipe in table 2.22.

Resuspension medium was prepared fresh on the day of use, according to table 2.23.

Table 2.22: SM (Sterlini–Mandelstam) growth medium.

Component	Volume / ml (100 ml) <sup>-1</sup>
CH I + II	94.0
CH III	5.0
CH IV	0.2
CH V	1.0

CH I + II is described in table 2.24.

Table 2.23: SM (Sterlini-Mandelstam) resuspension medium.

Component	Volume / ml (100 ml) <sup>-1</sup>
Sporulation salts	91
Solution C	4.0
Solution D	1.0
Solution E	4.0

Table 2.24: CH I + II, for SM (Sterlini-Mandelstam) medium (*B. subtilis*). Glutamic acid was dissolved, using 10 M NaOH to adjust the pH to 7. The combined solution was autoclaved.

Component	Mass / g (940 ml) <sup>-1</sup>
Casein hydrolysate (Oxoid L41)	10.0
L-glutamic acid	3.68
L-alanine	1.25
L-asparagine	1.39
Potassium phosphate, monobasic (KH <sub>2</sub> PO <sub>4</sub> )	1.36
Ammonium chloride (NH <sub>4</sub> Cl)	1.34
Sodium sulphate (Na <sub>2</sub> SO <sub>4</sub> )	0.11
Ammonium nitrate (NH <sub>4</sub> NO <sub>3</sub> )	0.10
Iron (III) chloride (FeCl <sub>3</sub> ·6H <sub>2</sub> O)	0.0010

- CH III comprises magnesium sulphate (MgSO<sub>4</sub>·7H<sub>2</sub>O, 1.98 g L<sup>-1</sup>) and calcium chloride (CaCl<sub>2(aq)</sub> 10% w/v, 4 ml L<sup>-1</sup>): combined and autoclaved.
- CH IV is manganese sulphate (MnSO<sub>4</sub>·4H<sub>2</sub>O, 1.1 g ml<sup>-1</sup>), autoclaved.
- CH V is L-tryptophan (2 mg ml<sup>-1</sup>), filter-sterilized.
- Sporulation salts are Solution A (SM variant, 1 ml L<sup>-1</sup>) and Solution B (10 ml L<sup>-1</sup>), combined with 989 ml L<sup>-1</sup> water.

- Solution A (SM variant) comprises iron (III) chloride ( $\text{FeCl}_3 \cdot 6\text{H}_2\text{O}$ ,  $0.89 \text{ g L}^{-1}$ ), magnesium chloride ( $\text{MgCl}_2 \cdot 6\text{H}_2\text{O}$ ,  $8.30 \text{ g L}^{-1}$ ) and manganese chloride ( $\text{MnCl}_2 \cdot 4\text{H}_2\text{O}$ ,  $19.79 \text{ g L}^{-1}$ ): combined, autoclaved and stored at  $4^\circ\text{C}$ .
- Solution B comprises ammonium chloride ( $\text{NH}_4\text{Cl}$ ,  $53.5 \text{ g L}^{-1}$ ), sodium sulphate ( $\text{Na}_2\text{SO}_4$ ,  $10.6 \text{ g L}^{-1}$ ), potassium phosphate, monobasic ( $\text{KH}_2\text{PO}_4$ ,  $6.8 \text{ g L}^{-1}$ ) and ammonium nitrate ( $\text{NH}_4\text{NO}_3$ ,  $9.7 \text{ g L}^{-1}$ ): combined, balanced with 2 M NaOH to pH 7.0 and stored at  $4^\circ\text{C}$ .
- Solution C is L-glutamic acid, 5% w/v, adjusted to pH 7.0 with 10 M NaOH and autoclaved.
- Solution D is calcium chloride ( $\text{CaCl}_2$ ) 0.1 M, autoclaved.
- Solution E is magnesium sulphate ( $\text{MgSO}_4 \cdot 7\text{H}_2\text{O}$ ) 1 M, autoclaved.

## 2.2 Basic microbiology

### 2.2.1 Culture

Cells were routinely cultured in LB at 37°C (*E. coli*, *B. subtilis*, *B. thuringiensis* YBT-020) or 30°C (*B. megaterium*, *B. cereus*, *B. thuringiensis* HD-73), shaken in an orbital shaker at 225 rpm. Cells streaked on agar plates were incubated lid side down in static incubators at the same temperatures.

#### **Broth**

To measure growth, liquid cultures were tested for optical absorption at 600 nm. These data are reported here as OD<sub>600</sub> values, as is common in the literature on bacterial spores.

#### **Agar plates**

Solid media were set using High Gel strength technical agar (Melford). Broth containing agar was autoclaved (see section 2.1.8) and either stored in a 50°C water bath until use or, if allowed to cool to room temperature, melted in a microwave then cooled to 50°C in the same water bath. Antibiotics were added only once the agar bottle temperature had equilibrated.

Plates (90 mm) were filled with ~20 ml molten agar medium, swirled to displace bubbles, and allowed to set (~10 min).

### 2.2.2 Gradient plate analysis

Gradient plates were poured in two stages. Plates were set to rest with one edge on the horizontal surface and the diametrically opposite edge on the lid. Molten agar (10 ml) containing no antibiotic were added, with care taken to ensure wetting of the entire base of the plate. When set, the plates were placed horizontally, and agar containing the maximum antibiotic concentration poured atop the existing wedge.



### Validating 5-fluorouracil

With the positive control strain, 168::69c, and negative control WT strain, *B. subtilis* 168, LB cultures (10 ml) were inoculated and shaken at 37°C and 225 rpm for 5 h. Samples (100 µl) of each were spread on LB agar gradient plates, containing 5-fluorouracil from 0–50 µM (see section 2.2.1). The plates were incubated overnight at 37°C.

### 2.2.3 Promoter analysis

The NNPP (neural network promoter prediction) technique, as described by Reese (2001), was performed to identify potential promoters, using the NNPP ([http://www.fruitfly.org/seq\\_tools/promoter.html](http://www.fruitfly.org/seq_tools/promoter.html)) tool.

## 2.3 Cloning

### 2.3.1 *In silico* design

Sequences were designed with assistance of Snapgene (GSL Biotech LLC) or Benchling (Benchling, Inc.). Codon optimization was performed, where relevant, using the GeneArt® design tool (Thermo Scientific).

### 2.3.2 Producing DNA fragments

#### **Primers**

Primers were supplied by Sigma–Aldrich as dried  $\geq 25$  nmol pellets. Following resuspension to a 100  $\mu\text{M}$  stock in TE-1 buffer, and subsequent dilution with water to a working solution of 10  $\mu\text{M}$ , they were stored at  $-20^\circ\text{C}$ .

#### **High fidelity PCR**

All PCRs (polymerase chain reactions) performed to construct fragments for subsequent cloning or sequencing used Q5 polymerase (New England Biolabs UK), in the form of the 2×Master mix. Reactions proceeded consistent with the manufacturer's protocols, briefly: 30 s melt at  $98^\circ\text{C}$ ; 25–35 cycles of  $98^\circ\text{C}$  for 5 s, an optimized annealing temperature for 10 s, then a period, dependent on product size, at  $72^\circ\text{C}$ ; and a final extension for 2 min at  $72^\circ\text{C}$ .

Where possible, primers were designed to anneal to the template at  $60^\circ\text{C}$ . However, for overlap assemblies, primers were typically designed to anneal to PCR products at a higher temperature, often  $68^\circ\text{C}$  or  $72^\circ\text{C}$ , and the reaction proceeded with two stages of cycles; the first for 5 cycles annealing at  $60^\circ\text{C}$  and then a further 30 cycles at the higher temperature. Such a process was designed to reduce mispriming and encourage the formation of a single product band.

Templates for high fidelity PCR were plasmids: typically 1  $\mu\text{l}$  at concentration 1  $\text{ng}\mu\text{l}^{-1}$  was used per reaction; or gDNA: typically 1  $\mu\text{l}$  at  $\sim 100$   $\text{ng}\mu\text{l}^{-1}$  per reaction.

### **Genomic DNA extraction**

From various *Bacilli*, gDNA (genomic DNA) was extracted using a QIAamp DNA mini kit (QIAGEN) according to the manufacturer's protocol, modified by Mohamed (2015).

Overnight culture (600 µl) was mechanically disrupted, as per section 2.7.1 (but with 20 s pulses and no final dilution). Of the supernatant, 200 µl were combined with 20 µl proteinase K, pulsed on a vortex, briefly, incubated for 10 min at 37 °C, then mixed with 200 µl absolute ethanol and pulsed on a vortex for 15 s, until homogeneous. The sample was applied to the provided spin columns and centrifuged, each time in a clean collection tube: twice for 1 min at 6 000 *g*, then 3 min and 1 min at 20 000 *g*, and a final spin for 1 min at 6 000 *g*. Each was separated by addition of 500 µl AW1 buffer, 500 µl AW2 buffer, nothing, then 500 µl AE buffer, incubated for 3–4 minutes before the final spin.

### **GeneArt® Strings™**

DNA synthesized by Life Technologies/ThermoFisher was delivered dried, in centrifuge tubes. The pellet was resuspended to 50 ng µl<sup>-1</sup> with TE-1 and the resulting solution used as (cleaned-up) PCR product in subsequent assembly reactions.

While the GeneArt® gene synthesis service guarantees that their product is monoclonal and correct, their Strings™ service offers no such guarantee; however the latter is both 10% of the cost and has a quicker turnaround (5–7 days, versus a fortnight).

### **PCR clean-up**

PCR products were purified using the QIAquick Gel Extraction Kit (Qiagen), according to the manufacturer's protocol for either the gel extraction or the PCR clean-up.

### **Klenow extension**

Where necessary, DNA was extended (with random bases) using the large (Klenow) fragment of DNA Polymerase I (NEB). Gel extracted oligomers were combined with 1 µl dNTPs (deoxy-nucleoside triphosphate) and 1 µl Klenow polymerase for 30 min at 37 °C. The product was purified using gel extraction or PCR clean-up.

### 2.3.3 Assembly

DNA fragments were assembled into whole plasmids using Gibson assembly (Gibson *et al.*, 2010, 2009) or, later, the simpler and less expensive KAM (Klenow Assembly Method), developed in-house by David Bailey (Bailey & Mohamed, 2018). The former was performed with 2×Gibson assembly master mix (New England Biolabs) following the manufacturer's protocol.

KAM is similar to Gibson assembly, but dispenses with the polymerase and ligase, while swapping the 5'→3' exonuclease for a 3'→5' variant: the Klenow fragment of *E. coli* DNA polymerase I. Linear double-stranded DNA is digested from the 3' ends, exposing 5' overhangs. Homologous sequences anneal reversibly and, following transformation of chemically competent cells (typically *E. coli*), the native DNA repair mechanisms complete the plasmid assembly. Fragments designed for Gibson assembly are also compatible with KAM. KAM was used routinely for five- or six-fragment assemblies, and even showed success with assemblies of eight fragments.

Golden gate cloning, using standard (eukaryotic) parts, offered an alternative (Engler *et al.*, 2008; Patron *et al.*, 2015). A 9× golden gate buffer was prepared with 1 volume ATP (adenosine triphosphate) solution (100 mM, pH 7 with KOH; optionally stored at -80°C) and 9 volumes of Cutsmart buffer (NEB). A 2× master mix was prepared with 22% v/v 9× golden gate buffer, 10% v/v *Bsa*I (NEB), 10% v/v T7 ligase (NEB) and 58% v/v water, and stored in 20 µl aliquots at -20°C. Reactions (5 µl) used 2.5 µl master mix with 200 ng of each plasmid.

### 2.3.4 Verification of constructs

Assemblies were verified by colony PCR, restriction digest, and Sanger sequencing.

#### Colony PCR

For simple constructs, direct colony PCR is an effective screening method. A PCR reaction was set up, using, as template, 1 µl of:

- a bacterial colony diluted in 20–50 µl water (for *B. subtilis*, *B. cereus*, *B. thuringiensis* and *E. coli*), or
- a 50 µl sample of liquid culture, boiled for 10 min (*B. megaterium*).

Primers were chosen such that the correct genotype would produce a band of known size, typically shorter than 1.5 kb. It was often possible to multiplex the reaction, such that an incorrect genotype would also produce a band, but at a different size, thereby indicating that the reaction had worked but the template was incorrect; where that was the case, this has been done.

The reactions used the *taq* enzyme, either as a) Reddymix (Thermo Scientific), b) OneTaq 2× master mix (New England Biolabs), c) 2×Taq master mix (New England Biolabs), supplemented with 1 part in 80 160× (4%) Orange G dye (Sigma-Aldrich), or d) a in-house produced *taq* master mix of the same composition, and reactions followed the manufacturers' protocols, where available.

For the home-made *taq* the protocol was as per Reddymix: a 2 min melt at 95 °C; 30–35 cycles of 25 s at 95 °C, 35 s at 50 °C, 1 min kb<sup>-1</sup> at 72 °C; 5 min extension at 72 °C; and storage at 4 °C. Master mixes contained loading dye and glycerol, for subsequent agarose gel electrophoresis.

Reaction products were loaded (typically 7 µl) on a 1 wt% TAE (tris acetate EDTA)–agarose gel containing 0.05% v/v ethidium bromide (Sigma Aldrich). Electrophoresis was conducted at 5–10 V cm<sup>-1</sup> for 35–75 min. A CCD (charge-coupled device) collected light from the gel under UV transillumination, and KY-Link (JVC) recorded images (table 2.9).

Agarose gel images were routinely processed using the linear functions of GraphicsMagick (GraphicsMagick Group); they were typically inverted for printing.

### Restriction digest

Restriction digests have utility when screening constructed plasmids, as they give a reliable indication of whether a construct has assembled correctly.

Typically, 500 µg of plasmid DNA would be digested in a 5 µl reaction containing 0.5 µl 10×buffer, ≤0.5 µl enzyme, topped up to 5 µl with deionized water. Where this was not possible, due to a low miniprep yield for example, the digest would be designed to ensure maximum DNA, a total volume as close to 5 µl as possible, and no more than 10% v/v of the restriction enzyme.

The other routine use of restriction digest follows a high-fidelity PCR from a plasmid template. The 4 bp cutter *DpnI* (New England Biolabs; GA\*|TC — the star indicates methylation) digests adeno-methylated DNA. Added to crude PCR product, with the aim of

reducing false positives following subsequent cloning, it digests only the template.

Typically, a 40 µl PCR product would be incubated at 37 °C: either with 1.0 µl of enzyme for 2 h, or overnight with 0.5 µl.

### Sanger sequencing

Sanger sequencing was ordered as a service from either

- Department of Biochemistry, University of Cambridge; or
- Genewiz (formerly Beckmann-Coulter genomics).

## 2.3.5 Transformation

### *E. coli*

Chemically competent cells were produced using a protocol, reported by D. M. D. Bailey (personal communications, 2013–2019). *E. coli* were streaked on LB-agar and incubated at 37 °C overnight. Large colonies (3–12) were transferred into 250 ml SOB (super optimal broth) and incubated at room temperature and 225 rpm, until the culture reached OD<sub>600</sub> 0.6–0.75. For *E. coli* DH5α, this took up to five days; *E. coli* Turbo cultures attained this optical density with growth overnight. The culture was cooled on ice for 10 min, then pelleted twice in a pre-chilled centrifuge at 2 500 g, for 10 min: respectively 1) resuspending in 80 ml ice cold transforming buffer and incubating on ice) for 10 min, then 2) resuspending in 20 ml ice cold transforming buffer. After addition of DMSO to 7% v/v and incubation for 10 min on ice, aliquots of 50 µl were flash frozen in liquid nitrogen and stored at -80 °C.

Transformation of *E. coli* was via the protocol provided by New England Biolabs. Aliquots (50 µl) were thawed on ice, mixed with a 5 µl assembly mix or 1 µl 100 ng µl<sup>-1</sup> plasmid and iced for 30 min. Following a 30 s heat shock at 42 °C and 5 min recovery on ice, 200 µl warm SOB were added and cells were shaken at 37 °C for ½–1½ h (more than 1 h, if not subsequently selecting on carbenicillin).

### *B. subtilis*

Chemically competent *B. subtilis* subsp. *subtilis* 168 were prepared and transformed using the procedure from Harwood & Cutting (1990), as modified by Mohamed (2015).

Pre-warmed SpC medium (20 ml) was inoculated from an overnight culture in LB to an OD<sub>600</sub> of 0.5, then shaken at 37°C and 225 rpm, until stationary phase (identified as no change in OD<sub>600</sub> over 30 min), usually 3½ h. Pre-warmed SpII (200 ml) was then inoculated with 2 ml of this culture, and shaken at 37°C and 120 rpm, for 90 min. The sample was pelleted at 8 000 *g* for 5 min, then resuspended in 18 ml of the supernatant. After addition of 2 ml sterile glycerol, the suspension was divided into 200 µl aliquots (or multiples thereof), flash frozen, in liquid nitrogen, and stored at -80°C.

### Supercompetent strains (*B. subtilis* 168::690-derived)

Shi *et al.* (2013) generated a *B. subtilis* 168-derived supercompetent strain, which they claimed transforms efficiently, is suitable for counter-selection, and can quickly recycle markers. Strain *B. subtilis* 168::690, and its derivatives, were handled in a similar manner to that of Shi *et al.* (2013).

Overnight cultures of *B. subtilis* in LB were diluted 10×, grown to OD<sub>600</sub> ~ 1, then shaken with 0.4% w/v arabinose for 2 h. Of the resulting mixture, 100 µl were incubated with ~150 ng plasmid DNA, followed by 90 min shaking at 37°C. The whole mixture was spread on LB plates containing appropriate antibiotic, before incubation at 37°C overnight. Colonies were selected the following morning.

Induced competent cells could be frozen for later use. After shaking with arabinose, DMSO was added as a cryoprotectant, to 7% v/v. Aliquots were flash frozen in liquid nitrogen.

For a negative control, water would be added to the competent cells, at the same volume as that of plasmid solution in the experimental samples.

### *B. megaterium*

Transformation was via the PEG-mediated protoplast protocol of McCool & Cannon (2001).

A confluent *B. megaterium* lawn on an LB-agar plate was suspended in 3 ml RHAF. A 25 ml RHAF culture, in a 250 ml bottom-baffled flask, was inoculated with 200 µl of the suspension, then incubated (37°C, 225 rpm) until the OD<sub>600</sub> reached 0.6, not exceeding 0.7 (typically 2 h). The culture was pelleted, four times, at 1 250 *g* and 4°C for 7 min: respectively 1) resuspending in 2 ml RHAF broth; 2) resuspending in 1.8 ml RHAF broth and 200 µl

lysozyme (12 mg ml<sup>-1</sup> in RHAF), then mixing gently and incubating at room temperature for 10 min; 3) resuspending in 2 ml RHAF broth; and 4) resuspending in 1 ml RHAF broth. Protoplasts were stored on ice immediately.

Protoplasts (200 µl) were transferred to a 50 ml centrifuge tube, with 10 µl plasmid (1 µg) and gently mixed. A 30% w/v PEG/RHAF solution (200 µl) was aspirated around the side of the tube, without mixing. The tube was gently mixed, then immediately incubated in a 37°C water bath, for 4–5 min. At this point 3 ml RHAF was added, and the culture immediately pelleted at 1 250 g and 4°C for 7 min. The supernatant was fully discarded (with the tube tipped upside down and lid changed) before the pellet was resuspended, gently, in 1 ml RHAF. The tube was incubated at 30°C and 175 rpm for 3 h, after which samples (200 µl) were spread on selective RHAF plates. Plates were incubated at 30°C overnight.

### *B. thuringiensis*

Electrocompetent *B. thuringiensis* subsp. *kurstaki* HD-73 and *B. thuringiensis* subsp. *finitimus* YBT-020 were prepared and transformed according to Lereclus *et al.* (1989).

Electrocompetent cells were prepared from an overnight culture, in LB. A 100 ml culture of TSB was inoculated with 1 ml of this overnight sample, then incubated at 37°C and 225 rpm until the OD<sub>600</sub> reached 0.5. (Note, 0.65 was acceptable, 0.8 was not.) The culture was split in two and pelleted at 3 000 g, for 7 min, four times: 1) resuspending in 35 ml Solution A (electrocompetence variant), 2) resuspending in 35 ml said Solution A and resting on ice for 15 min, 3) resuspending in 35 ml electroporation buffer, and 4) resuspending in 1 ml electroporation buffer. This volume was split among 50 µl aliquots, flash frozen in liquid nitrogen, then stored at -80°C.

For electroporation, 500 ng of plasmid were added to a thawed 50 µl aliquot of electrocompetent cells. The mixture was tapped to mix, incubated on ice for at least 5 min, then transferred to an electroporation cuvette, which had itself been rinsed with water, dried, and cooled on ice. A 2 kV electric field was applied, at 200 Ω and 25 µF, and the cells were immediately diluted with 1 ml of recovery medium. This culture was incubated at 30°C and 225 rpm for 2–3 h, before being spread (200 µl) on LB plates containing selective antibiotics.

### *B. cereus*

The transformation protocol for *B. cereus* ATCC 14579 was as for *B. thuringiensis*.



### 2.3.6 Isolation of desired recombinant *B. megaterium*

Plasmid pUCTV2 (and the derived pDBT2\* plasmids) carry a *Bacillus* origin of replication that is temperature sensitive: *ori<sup>T</sup>*. Strains transformed with such a plasmid will maintain the plasmid at 30°C or 37°C, but find it cured after growth at 42°C. Incubating such strains at the latter temperature on LB containing an antibiotic, the resistance marker to which is borne by the pDBT2\* plasmid, will select for strains which integrate the plasmid into the genome via a SXO (single crossover) event (see figure 2.1). Colonies were thus propagated, to generate such a Campbell-type insertion mutation.

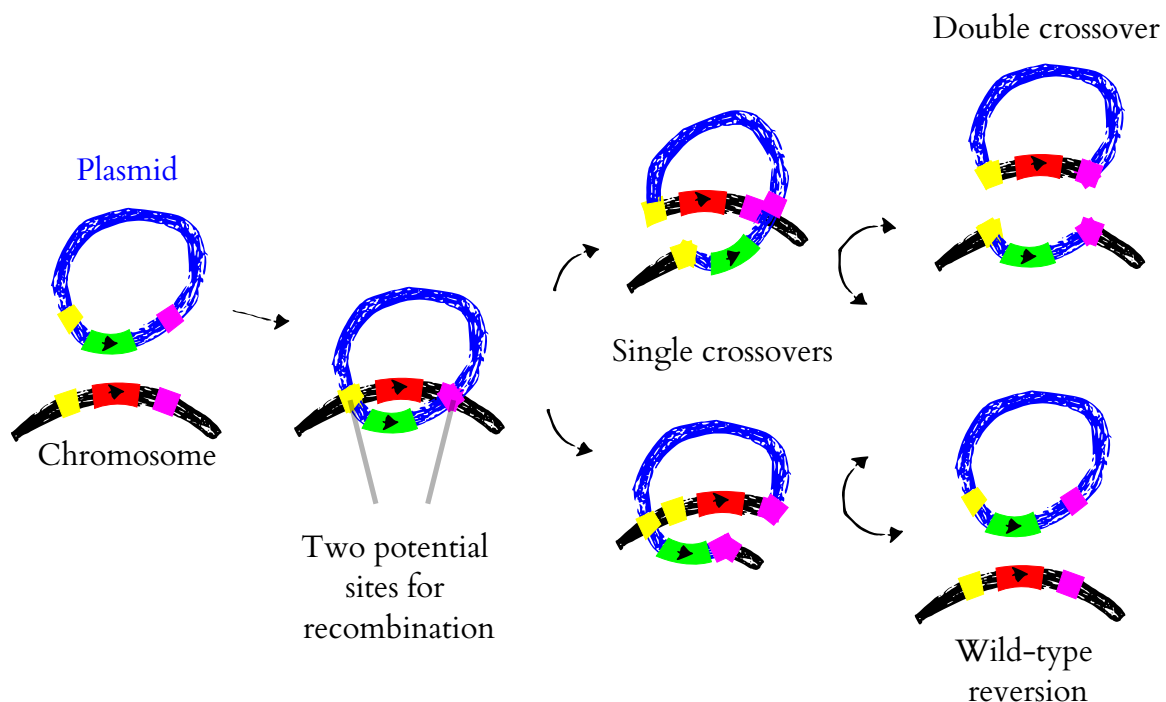


Figure 2.1: Allelic exchange via Campbell-type homologous crossover between the vector and target genome. The plasmid matches a region upstream of the target with a region upstream of its replacement, and vice versa for the downstream region. The first crossover event is the SXO (single crossover), known as a Campbell type insertion, which can happen at one of two sites: producing one of two genotypes, as indicated. The upper path shows the desired variants; this crosses over at the upstream region of homology. The single DNA strand that results can cross over itself at either region of homology; the desired event is a crossover at the downstream region.

To isolate a DXO (double crossover) strain, the SXO colonies were re-plated on LB (without antibiotic) twice per day, five days per week over a three week period, and incubated for this time at 42°C. The pDBT2\* plasmids bear two antibiotic resistance cassettes: one on the backbone, one in the insert. Following every evening plating, each colony was

subcultured on a trio of LB agar plates: one without antibiotic (the propagation plate), the others containing respectively antibiotics corresponding to the insert marker and the backbone. Strains which grew on the insert plate, yet did not grow on the backbone plate, were selected from the propagation plate. Candidate DXO strains were grown in 5 ml liquid LB, with antibiotic, overnight at 30 °C and shaken at 225 rpm. These overnight cultures were used for colony PCR verification.

### 2.3.7 Plasmid extraction

Plasmids were extracted from 3–10 ml liquid cultures using the QIAprep Spin Miniprep Kit (QIAGEN) according to its manufacturer's protocol, from either overnight or (for *E. coli* Turbo strains) day cultures. Options within the protocol were chosen to maximize yield and correctness, specifically: incubating for the maximum time with wash buffers, and eluting with elution buffer, warmed to 70 °C.

### 2.3.8 *I-SceI* digestion

The restriction enzyme *I-SceI* (New England Biolabs) cuts at the 18 bp recognition sequence TAGGG|ATAA\_CAGGGTAAT leaving the 4 bp ATAA overhang. This sequence is not present within the *B. subtilis* 168 genome.

The plasmid pBKJ223 features the *i-SceI* gene coding for the enzyme, and has been used with success in the Christie lab for markerless cloning in association with the pMAD vector in *B. cereus* ATCC 14579 (Ghosh *et al.*, 2018). Janes & Stibitz (2006) constructed the former from *B. amyloliquefaciens* genomic DNA and the *i-SceI* sequence obtained from plasmid pUC19RP12 (Pósfai *et al.*, 1999).

Shi *et al.* (2013) produced pEBS-cop1 containing the *i-SceI* gene and a temperature sensitive *Bacillus ori*, meaning the plasmid is cured by growth at 37 °C. Here, double strand breaks were induced in the *B. subtilis* genome using this plasmid.

A 2–10 ml LB culture of *B. subtilis*, transformed to erythromycin/lincomycin<sup>r</sup> with pEBS-cop1, was grown overnight at 30 °C (or 37 °C) and 225 rpm, then diluted 10× in (typically 10 ml) fresh LB. These day cultures were shaken at 30 °C (or 37 °C) and 225 rpm until the OD<sub>600</sub> reached 1.0, at which point they were induced with 10% w/v D-xylose (Sigma Aldrich), to a final concentration of 1% w/v xylose. Shaking was continued at 30 °C and 225 rpm for a minimum of 6 h.

Of this mixture, 100 µl were spread on 5-FU plates and incubated at 37°C for 24 h. Colonies were checked for chloramphenicol sensitivity on LB-chloramphenicol plates at 37°C, then verified by colony PCR across the excised region. Correct clones were cured of pEBS-cop1 by growing on LB plates, without antibiotic, overnight at 50°C: as per the protocol of Shi *et al.* (2013).

## 2.4 Strain construction

### 2.4.1 *B. megaterium*

#### Plasmid pDBT21s

Two fragments of the *B. megaterium* QM B1551 genome (corresponding to sections of *spoVFA* and *spoVFB*) and one from the p7Z6 plasmid (corresponding to the zeocin resistance gene *ble*) were amplified by PCR using primers in table 2.25. These fragments were assembled into pUCTV2, which had been digested with *EcoRI*-HF (NEB UK), using Gibson assembly. To avoid excision of the *ble* gene due to recombination at *lox* sites during cloning with *E. coli* DH5 $\alpha$ , this antibiotic resistance cassette was switched for *spc* (spectinomycin resistance) from *HindIII*-HF (NEB UK)-cut, Klenow-extended pDG1726. Inverse PCR was used to create a backbone free of the remaining *ble* operon, into which the *spc* fragment was ligated (figure 3.1). Competent *E. coli* DH5 $\alpha$  transformed this plasmid; colonies which grew on LB-spectinomycin plates were cultured for miniprep.

Table 2.25: PCR primers, to construct plasmid pDBT21s.

Label	Template	Sequence
y001	<i>spoVFA</i> 5'	cagctatgaccatgattacgaattcGCGACGAAATATCAGATAGAGGAGC
y004	<i>spoVFA</i> 3'	tccaatggaaaagggttggaattcCTGTTTATCTTCAAGCGCTGCG
y007	p7Z6	GGGTTTGCAACCTTTCTATCTTTCTtctcgagctcggtacccgggg
y008	<i>spoVFA</i> 3'	cggtagaatcgctgcacctgcaggTAATTTGGGAGCAGAAGTGTTACCG
y009	p7Z6	CGGTAACACTTCTGCTCCCAAATTAcctgcaggctcgacgattctaccg
y010	<i>spoVFA</i> 5'	ccccgggtaccgagctcgaaAGAAAGATAGAAAGTTGCAAACCC

#### Strains 1551::21s+ and 1462::21s

*B. megaterium* QM B1551 and *B. megaterium* PS1462 were transformed to dual tetracycline-spectinomycin resistance, via PEG-mediated protoplast transformation. Transformants were subsequently incubated on LB-spectinomycin at 42°C to induce a SXO (single crossover) mutation (see section 2.3.6). The location of integration into the chromosome was verified by PCR. The amplified region was from 100 bp upstream (in the genome) of the upstream homology in pDBT21s, to a region only present in the vector; the

PCR was designed to produce defined bands only if a SXO had occurred. Single crossover strains were named for the final, DXO strain, but with a suffix: + for integration at the upstream region of homology, - for downstream.

The SXO strains were subsequently cultured to isolate DXO (double crossover) mutants, as described in section 2.3.6. Vegetative strains based on the PS1462 background differ from those based on QM B1551 only in having a kanamycin<sup>r</sup> phenotype. Candidate DXO strains were screened by PCR for loss of QM B1551 plasmid 7, pBM700 (Manetsberger, 2015).

## 2.4.2 *B. thuringiensis*

Table 2.8 includes all *B. thuringiensis* strains constructed in this work.

Plasmid pDBT30 (figure 2.2) was assembled using KAM from pHT315 using the primers listed in table 2.26.

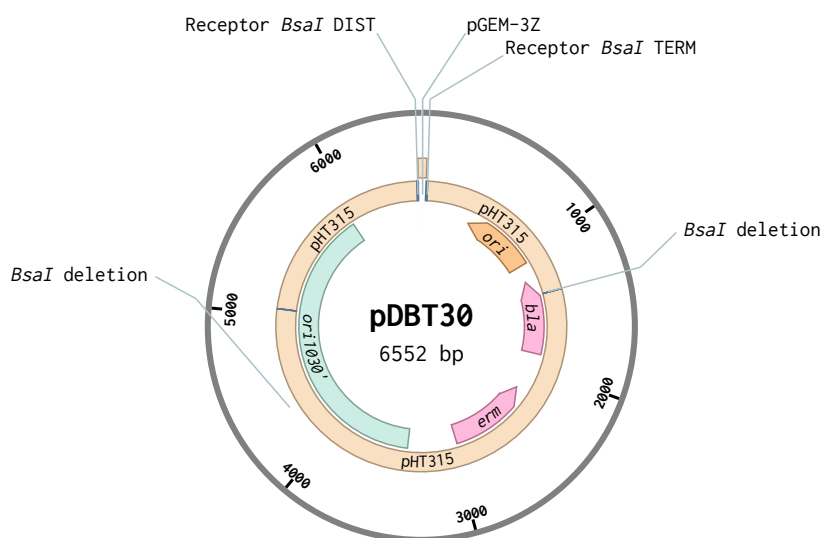


Figure 2.2: Map of plasmid pDBT30, based on pHT315. The *BsaI* deletions and added Receptor elements enable Golden Gate cloning with standard parts. Antibiotic cassettes are *erm* (erythromycin) and *bla* (carbenicillin); the *E. coli* and *Bacillus* origins are *ori* and *ori1030'* respectively.

### Cry1Ac sub-unit fusions

Library plasmid pDBT12d was constructed using KAM from plasmid pDBT10 (pGEM-3Z) and *B. thuringiensis* subsp. *kurstaki* HD-73 gDNA. Sequences, corresponding to *cry1Ac* variants detailed in table 5.1, were subsequently amplified from pDBT12d, assembled using KAM, and

Table 2.26: PCR primers, to construct plasmid pDBT30. Primers  $\gamma$ 149 and  $\gamma$ 150 were used to delete the *BsaI* site from *bla* in other plasmids, too.

Label	Template	Sequence
y149	pHT315 <i>bla</i> - <i>BsaI</i>	gtgagcgtggttctcgcggtatcattgcag
y150	pHT315 <i>bla</i> - <i>BsaI</i>	accgcgagaaccacgctcaccggc
y151	pHT315 <i>ori3010</i> - <i>BsaI</i>	caatctcaattcgagtcctcggcatctaagccag
y152	pHT315 <i>ori3010</i> - <i>BsaI</i>	gatgccgaggactcgaattgagattggttgcatt
y156	pHT315 + <i>BsaI</i>	attcgggtctcactccactggccgctcgttttaca
y157	pHT315 + <i>BsaI</i>	ggccagtgaggatgagaccgaattcgagctcggtagcc
y158	pGEM-3Z	tacgccagcgtgagaccaagcttgcattgcctgca
y159	pGEM-3Z	ttggtctcacgctggcgtaatacatggtagct

used to transform *E. coli* Turbo cells to carbenicillin resistance. PDMR-carbenicillin cultures (10 ml) were inoculated with individual colonies, resulting from each transformation. Primers are listed in Table 2.27.

The various pDBT31\* plasmids were used to transform electrocompetent *B. thuringiensis* HD-73 to erythromycin/lincomycin resistance, with successful transformants subsequently induced to sporulate in 5 ml CCY medium. The resulting cultures were pelleted and resuspended in sterile deionized water to 500  $\mu$ l total volume, for microscopy.

Additionally, with pDBT3130 and pDBT3140, *B. thuringiensis* subsp. *finitimus* YBT-020 were transformed to erythromycin/lincomycin resistance and subsequently induced to sporulate in 5 ml CCY (*B. cereus* group).

### Antibody fusions

Table 2.28 lists primers used to construct plasmids for antibody triple fusions. The plasmids in table 5.3 were assembled as the sub-unit fusions. *E. coli* cloning strains were checked for the red hue, associated with mCherry on the *cry1Ac* expression system. *B. thuringiensis* subsp. *kurstaki* HD-73 were transformed and selected as before, with spores produced as 5 ml CCY cultures, then concentrated to 500  $\mu$ l for microscopy.

Table 2.27: PCR primers, to construct *cry1Ac-mCherry* plasmids. The *mCherry* fragments were amplified from pDBT654m.

Label	Template	Sequence
y073	pDBT10, pDBT30	tctagagtcgacctgcaggc
y074	pDBT10, pDBT30	ggatccccgggtaccgagctcgaat
y177	<i>cry1Ac</i> operon	tccggctctcaggagagaacgtgagggctgg
y178	<i>cry1Ac</i> operon	ctctagaggtctctagcgcagaaccttttctacatactttctagg
y252	pDBT30	aggttctgcgctggcgtaatcatgg
y253	pDBT30	gttctctccactggccgctgttttaca
y254	<i>cry1Ac</i> 5'	ggccagtgagagaacgtgagggc
y255	<i>cry1Ac</i> 3'	gccagcgcagaaccttttctacatactttctagg
y256	<i>cry1Ac</i> 6×His	ccaccatcattagctctcatgcaaactcaggt
y257	<i>cry1Ac</i> 6×His	atgagactaatgatgggtgatgatgttctccataaggagtaattcca
y258	<i>mCherry</i>	ggaggaacggggtgtgagcaagg
y259	<i>mCherry</i>	tgagactaatgatgggtgatgatgcttgtagcagctcg
y260	<i>cry1Ac</i> protoxin	caccccgttctccataaggagtaattcca
y261	<i>cry1Ac</i> leader	tcacaccccgtgggtgtaaccagtttct
y262	<i>mCherry</i>	ttacaccccacggggtgtgagcaagg
y263	<i>mCherry</i>	ttgcagtcttgtagcagctcgtccatg
y264	<i>cry1Ac</i> protoxin	tgtacaagactgcaaacactcgagg
y265	<i>cry1Ac</i> 5'	acaccccgcataagttacctccatctcttttattaaga
y266	<i>mCherry</i>	aacttatgccccgtgtgagcaagg
y268	<i>cry1Ac</i> protoxin	cacccaactgcaaacactcgagg
y269	<i>cry1Ac</i> leader	gtgttgagcttgggtgtaaccagtttct
y280	<i>cry1Ac</i> toxic core	acaccccgaactggaataaattcaaactctgtctattatc
y281	<i>mCherry</i>	ttccagttcggggtgtgagcaagg
y289	P <sub><i>cry1Ac</i></sub>	tttccggccattttaacataataactaaattgtagtaatgaaaaacagtat
y290	P <sub><i>cry1Ac</i></sub>	atgttaaaatggccggaatcatgctgctaaatatcaatttttgaccag

Table 2.28: PCR primers, to construct *cry1Ac-NIP109* plasmids.

Label	Template	Sequence
y333	NIP109 light chain	aactggttacaccccagatattcaaatgacacaatcaccg
y334	NIP109 light chain	cctcgagtggtgcagtgcatcgcctctattaaatgatttt
y335	NIP109 light chain	tactccttatggaggaagatattcaaatgacacaatcaccg
y336	NIP109 light chain	tgagactaatgatggtggtgatgatggcattcgcctctattaaatgattt
y337	NIP109 heavy chain	actggttacaccccacaagttaactctgagagaatcaggg
y338	NIP109 heavy chain	gcctcgagtggtgcagttttgccagggctcagtg
y339	NIP109 heavy chain	actccttatggaggaacaagttaactctgagagaatcaggg
y340	NIP109 heavy chain	gcatgagactaatgatggtggtgatgatggttgccagg
y341	NIP109 scFv	gcctcgagtggtgcagttgatgaaactgtaaccagtgatgaacc
y342	NIP109 scFv	tgagactaatgatggtggtgatgatgtgatgaaactgt

### 2.4.3 *B. cereus*

Table 2.8 lists the *B. cereus* strains constructed in this work. With pDBT3130 and pDBT3140, *B. cereus* ATCC 14579 were transformed to erythromycin/lincomycin resistance and subsequently induced to sporulate in 5 ml CCY medium.

### 2.4.4 *B. subtilis*

Tables 2.7, 2.8 list the strains engineered for chapter 4 and chapter 5 respectively.

#### Antibodies

MedImmune (Cambridge, UK) generously provided coding sequences for the NIP109 antibody as a pair of plasmids, codon optimized for expression by *Bacillus subtilis*. One of the pair (pMA-NIP109-Lc) bears the light chain; the heavy chain is within the other (pMA-NIP109-Hc). Listing A1.1 lists the peptide sequences used for antibody fusions.

Fragments as GeneArt® Strings™ (ThermoFisher), with and without GFP fusions, were inserted into the vector pDBT60. This plasmid contains the SASP promoter, P<sub>sspB</sub>, which features a  $\sigma^G$  binding site (Connors *et al.*, 1986; Mohamed, 2015). The vector backbone was



amplified as two fragments (see table 2.29 for primers), and assembled with the Strings™ using KAM. Competent *E. coli* DH5 $\alpha$  were transformed to carbenicillin resistance with the ligation mix.

Table 2.29: PCR primers, to construct pDBT6\* plasmids.

Label	Template	Sequence
y049	pDBT60	CCATACTAAATAAAAAGGAGATTTTACACatggatattcaaatgacacaa
y050	pDBT60	TAAGAATTCTCATGTTTGACAGCTTATCATC
y124	pDBT60	gcatatgatcagatccttaaggcctagg
y125	pDBT60	ttaagatctgatcatatgcatccgc

Each vector was used to transform transform chemically competent *B. subtilis* subsp. *subtilis* 168 to chloramphenicol resistance, and clones, selected on LB–chloramphenicol plates, were isolated for subsequent study. The strains were named in the same manner as previously: e.g. the strain transformed with plasmid pDBT611s became 168::611s. Figure 4.1 shows a sample plasmids.

## Nanobodies

DNA sequences corresponding to the nanobodies in table 4.2 were designed, codon optimized for *B. subtilis*, and subsequently synthesized as GeneArt® Strings™ (ThermoFisher). Fragments were assembled, using KAM, into pGEM-3Z for the library plasmids pDBT15\*. The presence of coding sequences for anti- $\beta$ -lactamase nanobodies had no effect on carbenicillin selection, for *E. coli* DH5 $\alpha$  used for assembly. This nanobody work was performed by undergraduate research students Joshua Cozens and Luke Vinter. Primers are in table 2.30.

Nanobody coding sequences were assembled similarly into pDBT60–derived vectors for expression during sporulation, on the  $P_{sspB}$  promoter. This includes the  $V_{\text{H}}\text{H GFP4}$  chromobody (pDBT654m). With these plasmids, aliquots of chemically competent *B. subtilis* 168 were transformed to chloramphenicol resistance. Strains 168::6520, confirmed by colony PCR to contain the correct insertion at the *amyE* locus, were cultured and induced to sporulate. This nanobody work was performed by undergraduate research students Joshua Cozens and Luke Vinter, and masters student Tayla Gordon.

Additionally, Tayla Gordon cloned a chromobody with *bcII10* and *mCherry*, to make pDBT651m (and *B. subtilis* strain 168::651m).

Table 2.30: PCR primers, to construct nanobody plasmids. Primers *tg\_02* and *tg\_03* were designed by Tayla Gordon.

Label	Template	Sequence
y073	pDBT10, pDBT30	tctagagtcgacctgcaggc
y074	pDBT10, pDBT30	ggatccccgggtaccgagctcgaat
y108	nanobody 5'	taaaggaggaaggatccatgACCAAGTTCAACTGGTTG
y109	nanobody 5'	ggggacgttaatgatggtggtgatgatgTGATGAACTGTAACCTGTGTG
y110	nanobody 5'	ttgaatttctTGATGAACTGTAACCTGTGTG
y111	chromobody linker	agtttcatcaAGAAATTCATCAGCTCACTG
y112	chromobody linker	tcacacccccgATCAACAGGCGGATCTCTTG
y113	<i>mCherry</i>	gcctgttgatCGGGGTGTGAGCAAGGGC
y117	<i>vhgfp4</i>	aaggagattttacacatgACCAAGTTCAACTGGTTG
y119	<i>mCherry</i>	tcaaacatgagaattcttaatgatggtggtgatgatgCTTGTACAGCTCG
y120	chromobody linker	GTCAACAGTTCCGAGAGCAAGAGATCCG
y121	chromobody linker	TTGCTCTCGGAACTGTTGACGGAATTGAC
y122	pDBT60 (with His-tag)	catcatcaccaccatcatTAAGAATTCTCATG
y123	nanobody 3'	AGAATTCTTAatgatggtggtgatgatgtgatgaaactgtaacttgtgtg
y133	nanobody 5'	ataaaaaggagattttacacATGCAAGTTCAACTGGTTG
y134	nanobody 3'	GAGAATTCTTAATGATGGTGGTATGATGTGATGAACTG
tg_02	chromobody 3'	GCCACCTCCGCCTGAACCGCCTCCACctgatgaaactgtaacttgtgtgc
tg_03	<i>mCherry</i>	GGAGGTGGCTCTGGCGGTGGCGGATCGcgggggtgtgagcaagggcg

### Inducibly (super-)competent *B. subtilis*

Table 2.31 lists primers used to construct inducibly supercompetent *B. subtilis*.

Plasmid pDBT69c was assembled using KAM and checked by restriction digest with *Pst*I. Following transformation of chemically competent *B. subtilis* 168, three candidate 168::69c colonies showed the correct band.

For plasmid pDBT69d, fragments were assembled using KAM (see section 2.3.3); transformed colonies of *E. coli* Turbo cells were selected on LB-carbenicillin plates. Plasmids were verified with *Ssp*I *Sac*I double digest and Sanger sequencing of the indel region. Chemically competent *B. subtilis* 168 were transformed to chloramphenicol<sup>r</sup> with pDBT69d, and selected on LB plates containing chloramphenicol.

Table 2.31: PCR primers, to construct pDBT69? plasmids.

Label	Template	Sequence
y180	pDBT60	TCTTGACACTCCTTATTTGATTTTTGAAGACT
y181	<i>upp</i> 5'	TAAGGAGTGTCAAGAgcgcttacttcatggtggat
y182	<i>upp</i> 5'	tagaaaaataggaagtgtcccatcaacaattacacact
y183	<i>comK</i>	attgttgatgggacacttctatTTTTtctaataccgttccc
y184	<i>comK</i>	cgggagggcagggaaatgagtcagaaaacagacgca
y185	<i>araR</i>	tgttttctgactcatttccctgccctccc
y186	<i>araR</i>	tccacagaatgttcattattcattcagttttcgtgcg
y187	<i>upp</i> 3'	aaactgaatgaataatgaacattctgtggagacgt
y188	<i>upp</i> 3'	CGTCTAGCCTTGCCCttcacctctcttccattgatga
y196	pDBT60	GGGCAAGGCTAGACGGGA
y198	<i>cat</i>	TATCAAGATAAGAAAGAAAAGGATTTTTCG
y199	<i>cat</i>	ATGCGTCCGGCGTAGA
y200	pDBT690	CTACGCCGGACGCATtgaacattctgtggagacgt
y201	pDBT690	TTTTCTTTCTTATCTTGATAtgtcccatcaacaattacacac
y204	<i>upp</i>	TTTCTTATCTTGATAttttttgacgatgttcttgaaactc
y205	<i>upp</i>	CGTCTAGCCTTGCCCcattttcacctataattgtatacagattcac
y210	<i>comK</i>	cttatgcccggcgggCTCGAGcttctatTTTTtctaataccg
y211	<i>upp</i> 5'	cccgccgggcataagc

Candidate supercompetent strains were transformed with pEBS-cop1 to erythromycin/lincomycin<sup>r</sup> via induced competence, and colonies were cultured at 30°C. Markers were then excised by activating the xylose-inducible *i-sceI* gene, as described in section 2.3.8. Strains were selected on LB agar plates (selection plates) containing 38 µM 5-FU. Colonies were propagated on LB-5-FU at 37°C (propagation plates) and cured (cure plates) at 50°C, on LB agar. At the same time, the same colonies were challenged on agar plates containing chloramphenicol or erythromycin/lincomycin, at 37°C, for the desired phenotype (chloramphenicol<sup>s</sup> 5-FU<sup>r</sup> erythromycin/lincomycin<sup>s</sup>). Candidate strains were challenged with antibiotic both before and after a sporulation-germination cycle. The resulting strain was labelled 168::690.

### $\Delta cotE$ mutants

Plasmids pDBT72e, pDBT12u and pDBT71e, were designed to introduce the  $\Delta cotE$  mutation into *B. subtilis* (see figure 2.3). Table 2.32 lists the primers. First, pDBT72e was assembled, from pSS and *B. subtilis* gDNA (genomic DNA). The template for amplification of the spectinomycin resistance cassette, *spc*, was pDG1662. Library plasmid pDBT12u, with an improved cassette, was assembled with *spc*, *upp* from *B. subtilis* gDNA and pDBT130. This cassette was then used, with *B. subtilis* gDNA and pSS, to assemble pDBT71e. *E. coli* Turbo transformants of pDBT71e were selected on carbenicillin, then patched onto LB medium containing spectinomycin.

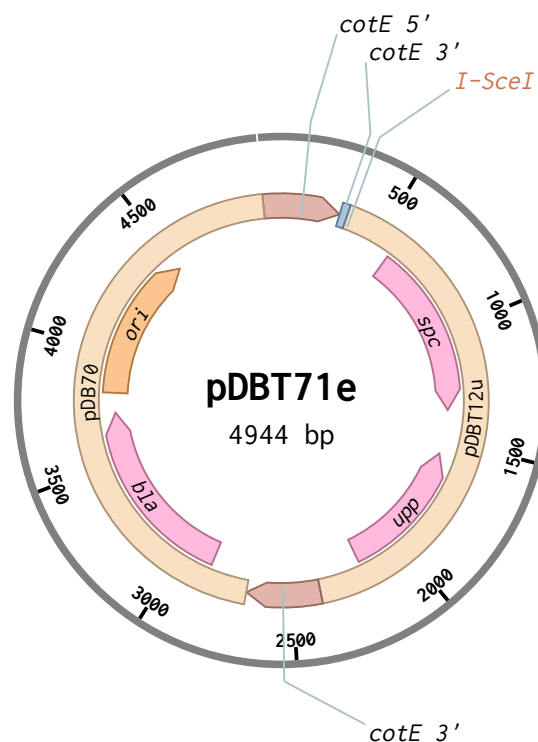


Figure 2.3: Plasmid pDBT71e, constructed to delete *cotE* from *B. subtilis*. The two regions flanking the *spc-upp* cassette match those flanking the *cotE* sequence in the genome. On recombination, by double crossover, these two regions of homology would excise the native gene, replacing it with the paired selection-counter-selection cassette, and thereby introducing the twin spectinomycin<sup>r</sup> 5-FU<sup>s</sup> phenotype. The *I-SceI* site lies between two regions of homology from the 3' end of *cotE*; following digestion, recombination at these loci will excise the selection and counter-selection cassettes.

Plasmid pDBT71e was used to transform *B. subtilis* 168::690 to spectinomycin resistance, via arabinose-induced chemical competence. The resulting strain was transformed using pEBS-cop1 as part of the marker excision process previously described.

Table 2.32: PCR primers, to construct pDBT12u and pDBT71e? plasmids.

Label	Template	Sequence
y212	pDBT72e	gcgtgtagctgctctgac
y230	pDBT70	ACTTAAGAGATCTACTAGTCATATGTGA
y231	pDBT70	Gcatgcctgcaggctcg
y232	<i>cotE</i> 5'	acctgcaggcatgCgcttgaagagattcctgttatcc
y233	<i>cotE</i> 5'	aaaagtgataaaagaatgatatgataaagtttatacgcggtga
y234	pDBT70 cassette	cattcttttatcactttttgtttatgTCGAACTCGAGCCATGG
y235	pDBT70 cassette	ATTACCCTGTTATCCCTAACTTTAC
y236	<i>cotE</i> 3'	TAGGGATAACAGGGTAATatatacattcttttatcactttttgtttatgt
y237	<i>cotE</i> 3'	GTAGATCTCTTAAGTcggctttcggatcttcc
y247	pDBT130	agagcagctacacgcGGTAagagacctctagagtcgacct
y248	pDBT130	ATTACCCTGTTATCCCTAAAGCtgagaccggatccccg
y250	<i>spc</i> (pDG1662)	GACGTAAAGTaagcttgagatggcactaataactaagt
y251	pDBT72e	aagcttACTTTACGTCTCCACAGAATGt
y267	<i>spc</i> (pDG1662)	TAGGGATAACAGGGTAATGCATATGATCAGATCTTAAGGCC
y270	pDBT70	ggtgaagcttCCGTAAGAGATCTACTAGTCATATGTGA
y271	pDBT70	aagcCTCCgcctgcaggctcgact
y272	<i>cotE</i> 5'	gcaggcGGAGgcttgaagagattcctgttatcc
y275	<i>cotE</i> 3'	cgcGGTAaaaaaagggactaggggagac
y276	<i>cotE</i> 3'	GTACGGAagcttcaccgccgtctctgc

## Cry1Ac

With pDBT3130 and pDBT3140, *B. subtilis* subsp. *subtilis* 168::690 were transformed to erythromycin/lincomycin resistance and subsequently induced to sporulate on 2×SG plates.

Plasmids pDBT316\* were constructed, containing the full length *cry1Ac* gene (pDBT3160, *cf.* pDBT310) and just *mCherry* (pDBT31610, *cf.* pDBT31710) respectively. These plasmids substituted the *B. subtilis*  $\sigma^G$  promoter for the *B. thuringiensis cry1Ac* sequence table 2.33. They were used to transform *B. subtilis* 168::690 to erythromycin/lincomycin resistance. Clones were induced to sporulate by nutrient exhaustion (see section 2.5.1), before examination by phase contrast and fluorescence microscopy. Table 2.33 shows the promoters native to *cry1Ac*, versus the  $\sigma^G$  alternative, from *B. subtilis*.

*Table 2.33: Promoters switched, in constructing pDBT316\* plasmids.*

Promoter	Nucleotide sequence
P <sub>cry1Ac</sub>	taaaattagttgcactttgtgcattttttcataagatgagtcatatgttt
P <sub>sspB</sub>	cgcatgattttccggccattttaacataatac

## 2.5 Spore-specific microbiology

### 2.5.1 Sporulation

For *B. subtilis*, two methods were used (Nicholson & Setlow, 1990).

1. Sporulation by resuspension, a synchronized approach, yields a small quantity of spores with moderate work.
2. Sporulation by nutrient exhaustion on 140 mm plates with 2×SG media induces unsynchronized sporulation, with minimal work.

*B. megaterium* and *B. cereus/B. thuringiensis* were induced to sporulate by nutrient exhaustion in SNB (supplemented nutrient broth) and CCY (casein casein yeast) medium, respectively (Nicholson & Setlow, 1990). After ~12 h, these cells depleted the broth of nutrients, and start to sporulate. After a further ~24 h, the broth contained almost all spores, with few to no vegetative cells.

Sporulation media contained no antibiotic.

#### **Sporulation by resuspension (*B. subtilis*)**

SM growth media (5 ml) were inoculated and incubated at 37 °C and 225 rpm overnight. The cultures were diluted with warm growth medium to OD<sub>600</sub> of ~0.1, then incubated at the same conditions until the OD<sub>600</sub> had reached 0.5–0.8. After pelleting at 8 000 g and room temperature, for 5 min, cells were resuspended with warm resuspension medium, to the same volumes (and in the same vessels) as the previous growth phase; the time of resuspension was recorded as time  $t_0$ . Samples were incubated as before, and sampled at various times.

#### **Sporulation by nutrient exhaustion (*B. subtilis*)**

Overnight culture in LB (600 µl) were spread on a 140 mm 2×SG, or 2×SGR, plate. Plates were wrapped loosely in polythene and incubated at 37 °C for 5 days.

### Sporulation by nutrient exhaustion (*B. megaterium*)

Cultures were inoculated in liquid volumes 400 ml in a 2 L bottom baffled volumetric flask (of true volume 2.5 L), or 2 ml in a 50 ml conical-bottomed centrifuge tube (true volume 55 ml), and shaken at 30°C and 225 rpm, for up to two days; true volumes indicate the gas volumes in each vessel, important for aeration.

Media, supplemented with DPA (dipicolinic acid), were prepared by adding DPA and NaOH in a 2:1 molar ratio, *i.e.* a mass of 0.48 (g NaOH) (g DPA)<sup>-1</sup>.

### 2.5.2 Spore washing

For most analyses, spores must be washed free of nutrients, cell debris (sporangia) and any remaining vegetative cells. Typically in the Christie laboratory this is done with water (as per Church *et al.*, 1954). A more effective approach uses an aqueous two-phase system to split the washing into two phases:

1. separating spores from vegetative cells and sporangia, and
2. diluting any remaining soluble components of the sporulation medium.

#### *B. subtilis*

Spores were recovered from 2×SG plates with a sterile spreader and ~22.5 ml water, and transferred to a 50 ml Nalgene® centrifuge tube.

System W (PEG-1000 and 3 M buffered potassium phosphate: Sacks, 1969) separated *B. subtilis* spore suspensions from plates into a PEG rich upper phase containing spores, and a salt-rich lower phase; cells migrated to the interface. Progressive decanting, pelleting and recycling of the upper phase (Delafield *et al.*, 1968) was used to extract spores until that phase became relatively transparent (typically two cycles). The spores were then washed once with water, before transfer to centrifuge tubes for storage. The yield was noticeably greater than for the traditional water washing technique (this has not been tested quantitatively, here).

Note that with PEG-6000, the upper phase of the System W master mix solidified at room temperature, complicating processing. The spore preparations had huge variation in ratio between the two phases. This was avoided by switching to PEG-1000.



Finally, ball milling was occasionally used to diminish clumps, where it was not desirable to add a surfactant. Glass beads, of 1 mm diameter, were added to a 15 ml centrifuge tube containing the spore sample. The tube was pulsed on a vortex until clumps were sufficiently diminished, as measured with phase contrast microscopy.

### *B. megaterium*

*B. megaterium* spores were washed with water to >99% spores, as measured by phase contrast microscopy (Gupta *et al.*, 2013).

## 2.6 Microscopy

All optical microscopy was performed on a BX53 Upright Microscope (Olympus) fitted with a 10× eyepiece and one of the objective lenses listed in table 2.34. This microscope was fitted with a Retiga 2000R CCD (QImaging) and operated using the software suite QCapture Pro (QImaging).

*Table 2.34: Lenses and corresponding magnifications, for optical microscopy. Lenses supplied by Nikon Instruments, Inc.*

Objective magnification	Overall magnification	Interface
10×	100×	Air
40×	400×	Air
100×	1000×	Type F immersion oil

Transmission electron microscopy was performed on samples prepared by Sina Schack; images were taken by her at CAIC (Cambridge Advanced Imaging Centre) with assistance of Dr. Katrin Mueller and Lyn Carter.

### 2.6.1 Slide preparation

Samples (2 µl) of culture were transferred by micropipette to a ground glass slide (VWR) and covered with a coverslip. For one or two samples per slide, 22 mm × 22 mm coverslips would be used; with three samples each had a smaller coverslip (18 mm × 18 mm) instead. Spores or cells on agar plates were scraped with a micropipette tip loaded with 2 µl water, then rinsed with that water onto the slide.

#### **Agar pad**

Spores were fixed using an agar pad: 600 µl of 2% w/w agarose, aspirated quickly onto a slide and immediately sandwiched with another slide, to set.

### 2.6.2 Phase contrast

Phase images paired with fluorescence images were typically taken with the same filter as the fluorescent images, to avoid the stage shifting on changing filter.

### 2.6.3 Fluorescence

Samples were illuminated with a mercury lamp, through blue or green filters (see table 2.35).

*Table 2.35: Fluorophores, used in fluorescence microscopy.*

Fluorophor	Excitation / nm	Emission / nm	Filter
GFP (green fluorescent protein)	488	510	Blue
mCherry	587	610	Green

Whereas for GFP fluorescence the filters were adjusted from phase contrast to collect more light, this was not done for mCherry fluorescence. Sets of GFP micrographs were normalized.

### 2.6.4 Image processing

Images were prepared with Fiji (ImageJ), GraphicsMagick (GraphicsMagick Group) and Inkscape (Software Freedom Conservancy).

Many micrographs are presented here as triples of phase contrast image on the left, fluorescence on the right, and an overlay in the middle. The overlays were created using the `composite -compose Over` function of GraphicsMagick. The fluorescence micrographs are all presented as negatives, with dark regions corresponding to greater intensity.

Polyacrylamide gels were recorded as monochromatic images, and are presented in false colour.

## 2.7 Protein processing

### 2.7.1 Spore disruption

Spores were mechanically disrupted using a FastPrep FP120 Cell Disrupter (Thermo Scientific) based on the protocol established by Mohamed (2015). A spore pellet of equivalent OD<sub>600</sub> 5 (*i.e.* if resuspended in 5 ml it would have had an OD<sub>600</sub> of 1) was resuspended in 400 µl disruption buffer and supplemented with 2 µl ml<sup>-1</sup> 1 M PMSF<sub>EtOH</sub>. The suspension was transferred to lysing tubes: either a) Lysing Matrix B 2 ml tubes (MP Biomedicals), or b) those same tubes containing 0.1 µm zirconia (*i.e.* the in-house version); and beaten in the disrupter 2–3 times at speed 6 for 30 s, separated by 5 min coolings on ice. The disruption was confirmed with phase contrast microscopy. The supernatant, typically 650 µl after dilution with 500 µl buffer and pulses on a vortex, was recovered to a microcentrifuge tube.

### 2.7.2 Isolation of soluble protein fraction

The extracts from cell or spore disruption contained the total protein content of the cell or spore core. To isolate the soluble fraction, a portion of the liquid recovered from disruption was pelleted at top speed in a microcentrifuge. The resulting supernatant contained the soluble protein fraction.

### 2.7.3 SDS-PAGE

Polyacrylamide gel electrophoresis was performed using NuPAGE reagents and either NuPAGE 4% Bis-Tris Mini protein gels or RunBlue SDS Protein Gels 4–12%, per the manufacturers' instructions. Either 20× MES, 2-(N-morpholino)ethanesulphonic acid (Thermo Scientific) or 20× MOPS, 3-(N-morpholino)propanesulphonic acid (Thermo Scientific) buffer was diluted to either 800 ml or 400 ml for the Xcell SureLock™ Mini-cell electrophoresis tanks (Thermo Scientific) or Bolt™ Mini gel tank (Thermo Scientific), respectively. NuPAGE antioxidant (Thermo Scientific) was added (500 µl) to the 200 ml of buffer at the well side of the gel, with the remaining buffer in the other compartment of the chamber. Of each sample buffer-containing sample, 90% v/v (typically 18 µl) were mixed with 10% v/v (2 µl) NuPAGE sample reducing agent and loaded into each well. Novex® Sharp Pre-stained Protein Standard (Thermo Scientific) (5 µl) were loaded as a ladder for

subsequent Coomassie staining, and 2 µl MagickMark™ XP Western Protein standard (Thermo Scientific) were used if the gel were destined for western blot. Sample buffer was loaded into any empty wells to reduce smiling.

Electrophoresis was conducted with a PowerPac 200 power supply (Bio-Rad) for 35 min at 200 V (MES) or 50 min at 200 V (MOPS).

### **Sample denaturation for PAGE**

Samples of total or soluble protein were mixed in a 13:5 volumetric ratio of protein sample, to 4× NuPAGE LDS (lithium dodecyl sulphate) sample buffer, typically 52 µl protein sample with 20 µl sample buffer. Mixtures were incubated at 70 °C for 10 min (standard conditions). The resulting samples were either placed on ice and used immediately for PAGE, stored for up to a week at 4 °C, or stored long term at -20 °C.

In the modified conditions, after addition of LDS (lithium dodecyl sulphate) sample buffer, samples were boiled for 5 min rather than incubated for 10 min at 70 °C (Thomas & Ellar, 1983).

### **Coomassie stain visualisation**

Gels were released from their frames, rinsed with sterile water, then shaken for 2 h in a 140 mm Petri dish containing 50 ml Quick Coomassie stain (Generon). The Coomassie was then recovered, while the stained gels were rinsed again in sterile water, then returned to the Petri dish and shaken in 50 ml sterile water for at least 4 h, typically overnight. Gels were stored for up to a week in 20% v/v ethanol.

Images were taken using either the G-Box gel documentation system (Syngene) or the main camera of a OnePlus One (OnePlus) with an Exmor IMX214 CMOS (Sony Semiconductor).

### **Western blot**

Blots were performed as Mohamed (2015), with the only difference being use of Amersham Hybond LFP 0.2 PVDF (polyvinylidene difluoride) membranes (GE Healthcare). Membranes were wetted in methanol (30 s), rinsed in water and then soaked in transfer buffer (5 min). A semi-dry blotting stack was built with the membrane and transfer buffer-equilibrated polyacrylamide gel sandwiched between two sets of equilibrated blotting paper. The blotter was operated at 15 V for 20 min, and the membrane blocked

with TBST-BSA (either for 2 h at room temperature on a 3D rocking platform, or at 4 °C overnight). Membranes were labelled with 2.5–10 µl antibody in 10 ml TBST-BSA for an hour; if not using a conjugate, secondary labelling took 30 min. Gels were sometimes fixed with TMB (3,3',5,5'-tetramethylbenzidine), using Pierce 1-Step™ Ultra TMB-Blotting Solution (ThermoFisher)

Blots images were taken using either the *enhanced chemiluminescence* option on the G-Box gel documentation system (Syngene) or (where fixed with TMB) the main camera of a OnePlus One (OnePlus) with an Exmor IMX214 CMOS (Sony Semiconductor).

#### 2.7.4 Purification

Proteins were purified, either using an ÄKTA Pure (General Electric), with the supplied UNICONV software and protocols optimized by Al Riyami (2017), or using Ni-NTA Spin columns (Qiagen), according to the manufacturer's protocols. On the ÄKTA, the HisTrap™ HP (GE Life Sciences) and HisTrap™ FF crude (GE Life Sciences) columns were used.

#### 2.7.5 Buffer exchange

Buffer exchange was conducted by repeated concentration and dilution using Amicon® Centrifugal Filter Units (Merck Millipore), based on the protocol optimized by Al Riyami (2017). Columns were washed with water, then equilibrated and centrifuged with room temperature buffer for 15 min. All centrifugation steps were performed at 3 220 g and room temperature. Up to 4 ml of sample were then transferred to the membrane, before centrifugation for (initially) 20 min and until the solution was at the desired concentration. New buffers were added to the columns, and the centrifugation repeated as necessary. The samples were then diluted with the new buffers, and these retentates recovered by aspiration.

## 2.8 Spore assays

### 2.8.1 DPA assay

Spores' DPA concentrations were measured by colorimetric assay (Janssen *et al.*, 1958; Nicholson & Setlow, 1990; Rotman & Fields, 1968). Spores grown in 2 ml culture were centrifuged, resuspended in 1 ml water, boiled for 20 min, then iced for 15 min. Samples (400  $\mu$ l) were diluted in equal volumes of water, to which 200  $\mu$ l assay reagent (L-cysteine, FeSO<sub>4</sub> and (NH<sub>4</sub>)<sub>2</sub>SO<sub>4</sub> in pH 4.6 acetate buffer) were added. These samples and assays of known DPA concentration (for a calibration curve) were measured for absorption at 440 nm in a Lambda 19 photospectrometer (PerkinElmer) with a 1 cm path length (Nicholson & Setlow, 1990), or measures of 100  $\mu$ l were analysed in 96-well plates using a Wallac Envision 2104 Multiplate Reader (PerkinElmer).

Concentrations were calculated based on standard curves, taken contemporaneously with the readings. The standard curves were consistent among the runs of the experiments (figure A1.1). Results were normalized to the levels of DPA measured for the WT strain, within each batch.

### 2.8.2 Lysozyme susceptibility

Spores were washed with 1 M NaCl and water, then 1 ml of spores with OD<sub>600</sub> of 1 were pelleted and resuspended in 1 ml 50 mM Tris-HCl (pH 7.2). Experimental samples contained 50  $\mu$ g ml<sup>-1</sup> lysozyme. Samples were placed on a rolling platform overnight at 4 °C.

### 2.8.3 Wet heat susceptibility

A protocol based on that of Church & Halvorson (1959) was followed. Spores at OD<sub>600</sub> of 1 were incubated at various temperatures for 20 min, then plated on LB to estimate the loss of viability.

## 2.8.4 Spore viability count

Spores were serially diluted, by a factor of ten each time, over six orders of magnitude, before plating on LB agar (Nicholson & Setlow, 1990). The plating arrangement of Miles *et al.* (1938) was followed: 10 µl drops of each dilutions were plated, in triplicate. The plates were incubated at 30 °C for 12 h, after which the number of colonies were counted.

Counts were analysed using Bayesian inference techniques (Clough *et al.*, 2005; Comoglio *et al.*, 2013; Hedges, 2002; Niemelä, 2003). In particular, the R library presented by Comoglio *et al.* (2013) was used to process the serial dilution counts. The relative viability of the spores is directly proportional to the dilution-adjusted number of colonies (for example, 3 colonies at  $10^4$  dilution is the same viability as 30 colonies at  $10^3$  dilution, but with less statistical power). Viabilities are presented as the maximum likelihood estimators for the population count, with errors corresponding to the 95% credible intervals.

Judgements as to whether samples could be said to be drawn from different populations were informed by BEST (Bayesian estimation [that] supersedes the  $t^*$ -test); strictly this should be modified for Poisson experiments such as colony counts, but as probability distributions from samples are adequately described by the  $t$ -distribution, the existing framework suffices (Kruschke, 2013).



## Chapter 3

# The effects of dipicolinic acid on spores

## 3.1 Introduction

Although DPA (2,6-dipicolinic acid) is known to contribute to spores' heat resistance, the precise mechanism by which it does this is unknown (Setlow, 2014). Given that wet heat damages proteins, in preventing that damage, DPA must be protecting the proteins in the spore core. If it does so in the spore core, why not in a pharmaceutical formulation?

An important factor in protein damage is water. At a molecular level, proteins in water are free to alter their configurations; given excessive kinetic energy, they are free to alter their configurations irreversibly, and thereby denature. In addition, water can be ionized, producing superoxide radicals, which directly degrade proteins. Water is thus critical to the heat susceptibility, and therefore heat resistance, of spores. It is possible that the sole effect of DPA on this heat resistance is through stabilization of low water environments; it is also possible that DPA protects proteins through direct interaction. One might expect that spores lacking DPA would suffer more damage than WT (wild type) spores, when challenged with heat. Indeed, this is almost always the case (Balassa *et al.*, 1979; Magge *et al.*, 2008; Paidhungat *et al.*, 2000). However, nobody has yet produced spores, modified to have no DPA, yet with no change in their water content. Most experiments in spores therefore cannot differentiate between absence of DPA and presence of water.

DPA has proved capable of improving such products' stability (Batalha *et al.*, 2017), but without elucidating the mechanism, constraints of formulation robustness and intellectual property preclude its use. DPA does not act in isolation, and there are likely to be other spore components which prove useful to formulation scientists.

To separate the effects of DPA from those of water, one must remove or replace the DPA at a fixed water composition, This in turn requires spores for which the DPA composition of the core can be controlled, and either chemical or physical ways to control water content. Assays of wet-heat sensitivity conflict with the latter, so the need here is for spores which can be doped to contain chemical replacements for DPA in their cores.

There is precedent for this. In *B. subtilis*, Magge *et al.* (2008) demonstrated that inactivating the *spoVF* operon results in spores lacking DPA. This operon encodes a pair of DPA synthetases: *spoVFA* and *spoVFB*. Sporulating cells of strains which lack this operon will scavenge DPA from their environment, and the resulting spores, termed DPA-replete,

behave much like WT variants. Is this behaviour is seen in other *Bacilli*, too? *B. megaterium*'s genome includes homologues of the aforementioned genes from *B. subtilis*, and this chapter demonstrates that the operon operates similarly.

As for doping spores, Li *et al.* (2012) repeated the uptake experiments using position isomers of DPA instead, finding none of those chemical analogues present in the core. Importantly, the authors reported that SpoVA, the DPA uptake channel in *B. subtilis*, relies on specific residues at the channel entrance. With this additional knowledge, they might have chosen the chemical analogues based on interactions with these residues, rather than similarity of chemical formula. The work presented here does just that.

Finally, while prior work on changing DPA composition has sought to deplete or restore DPA, and alternative is to *enhance* its level. One might expect such to offer a different relationship between DPA and water content and thereby help identify any DPA-specific effects.

The outcome of the work presented in this chapter is an extension of understanding of DPA uptake, and a platform for further investigation of DPA uptake behaviour in *B. megaterium*.

## 3.2 Results & discussion

### 3.2.1 Spores lacking the putative DPA synthetase

The bicistronic WT putative–DPA synthetase operon comprises the upstream *spoVFA* and downstream *spoVFB* genes, named for their homologues in *B. subtilis*. Mutant *B. megaterium* strains were constructed, for which this operon had been disrupted, using the plasmid pDBT21s (figure 3.1). Table 3.1 lists all the *B. megaterium* strains; section 2.4.1 describes the construction of mutants.

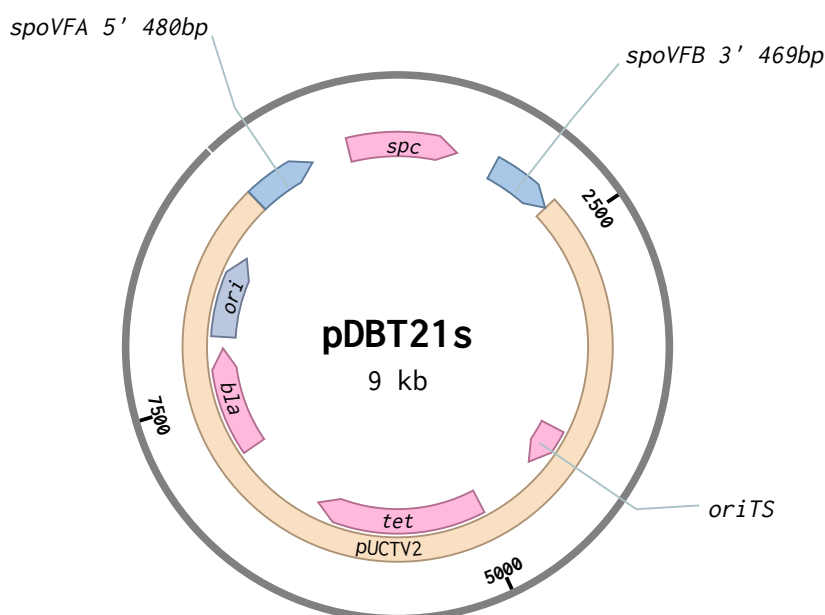


Figure 3.1: Map of the pDBT21s plasmid, used to disrupt the *spoVF* operon in *B. megaterium* by allelic exchange. The insert contains the two homologous regions for the *spoVF* operon, and the following antibiotic resistance cassettes: *bla* for carbenicillin<sup>r</sup>; *tet* for tetracycline<sup>r</sup>; *spc* for spectinomycin<sup>r</sup>. The temperature sensitive origin of replication, *oriT*, functions at 30 °C but not at 42 °C, so at that latter temperature only a cell which integrates the plasmid into its chromosome will survive on media containing spectinomycin or tetracycline. The length of the insert (~1800 bp) is known from the verification PCR.

The pDBT21s plasmid could integrate into the chromosome via a Campbell-type mechanism at one of two points, and so produce one of two SXOs.

1. If the plasmid were to integrate at *spoVFA*, the cassette would displace the last 1/3 of *spoVFA* and all of *spoVFB*.
2. A crossover at *spoVFB* would disrupt the last 16 of 202 residues.

Table 3.1: *B. megaterium* strains, used in this chapter. Genes *tet*, *spc* and *kan* confer tetracycline, spectinomycin and kanamycin resistance, respectively. Abbreviations: WT (wild type), SXO (single crossover), DXO (double crossover).

Strain	Genotype	Description
QM B1551	WT	WT
1551::21s+	<i>spoVFA::tet::spc</i>	SXO DPA synthetase mutant
PS1462	<i>sleB::kan</i>	SleB CLE (cortex lytic enzyme) mutant
1462::21s	<i>sleB::kan spoVFA::spc</i>	DXO double mutant

The crossover event at *spoVFA* would knock out the whole operon (which is termed *spoVF*, after its *B. subtilis* homologue).

Figure 3.2 shows how these mutants (thus termed  $\Delta spoVF$ ) sporulated, in standard SNB (supplemented nutrient broth) or SNB containing 1.1 mM DPA. The bright phase signal from WT spores in figure 3.2a indicates the high refractive index of the core, associated with the reduced water content. WT spores turn phase dark in a 30s transformation shortly after commitment to germination (figure 3.2b). Within a WT sample, some spores spontaneously turn phase dark; this is termed *autogermination*. Such WT spores immediately proceed with germination.

Strains, for which pDBT21s had integrated at *spoVFA*, produced phase dark spores. Whereas in standard medium QM B1551 (WT) spores appeared phase bright, 1551::21s+ spores appeared phase dark. The latter had thus autogerminated, yet the next germination phase, outgrowth, did not begin. The 1551::21s+ spores in figure 3.2c were viable, and germinated readily on rich medium. By contrast, strains for which pDBT21s had integrated at *spoVFB* produced phase bright spores. The mutant strain 1551:21s-, containing an insertion of pDBT21s at the downstream region of homology, produced spores which appeared no different from wild type (images not shown).

In standard medium,  $\Delta sleB \Delta spoVFA$  double mutant 1462::21s spores appeared phase grey (figure 3.2d). Additionally, with brighter illumination, these could appear phase bright, just as WT spores.

The spores shown in figures 3.2e, 3.2f were grown in media supplemented with DPA. These spores, termed DPA-replete, were mostly phase bright. This indicates (as per Balassa *et al.*, 1979) that the sporulating cells scavenged the DPA from the sporulation medium and

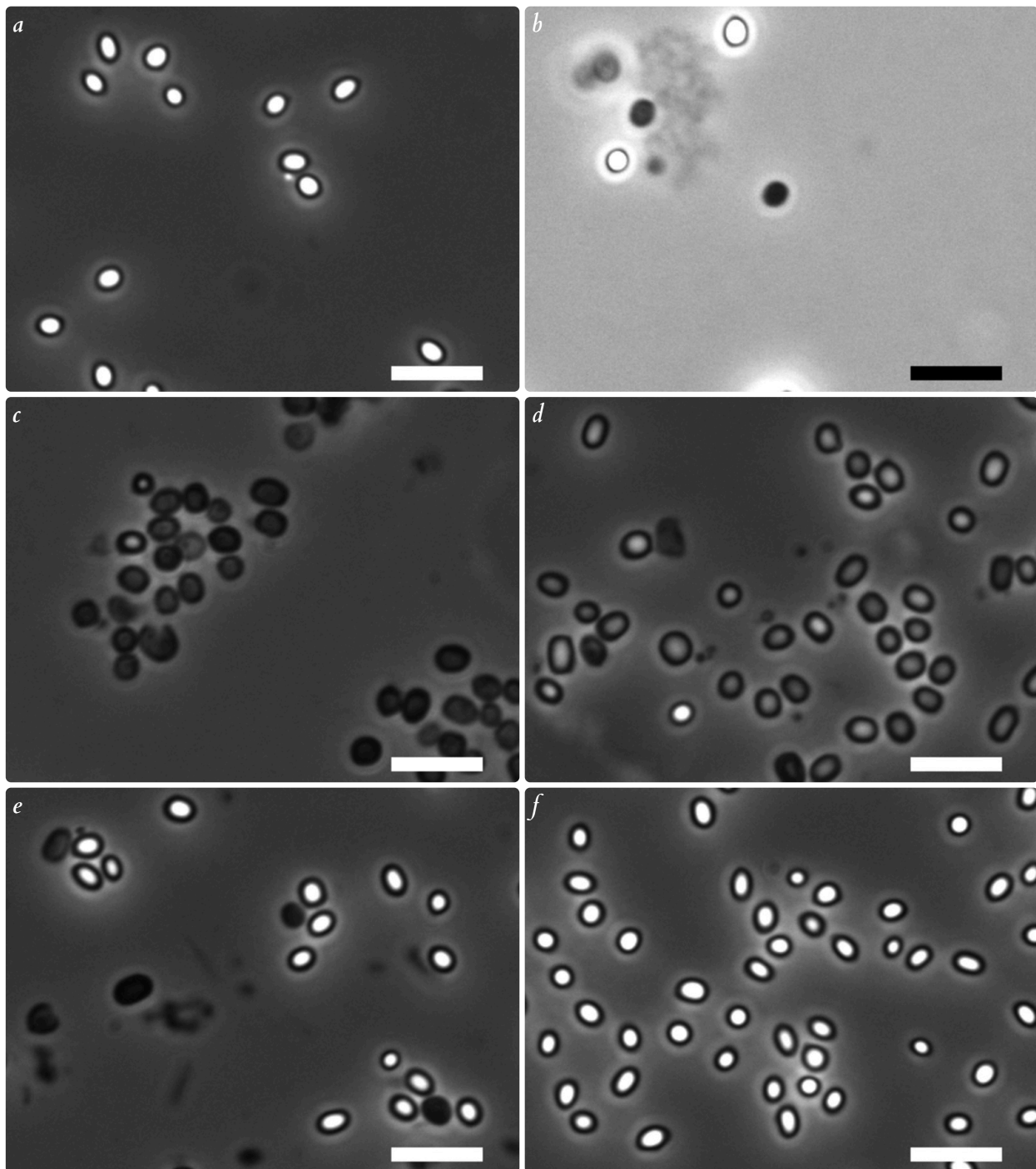


Figure 3.2: Phase contrast micrographs of *B. megaterium* spores, from strains with *spoVF* deletions. (a) shows phase bright WT spores; (b) shows germinated spores (phase dark, even with the bright illumination); (c) shows  $\Delta spoVF$  mutants 1551::21s+, grown in SNB (phase dark); (d) shows  $\Delta sleB \Delta spoVF$  double mutants 1462::21s grown in SNB (phase grey); (e) shows 1551::21s+ spores grown with DPA in the medium (mostly phase bright — with some phase dark); (f) shows 1462::21s spores grown with DPA in the medium (phase bright). Results are categorical: the intensity values of phase contrast images do not correspond straightforwardly to any measurable parameter of objects in the field. Spores were produced via nutrient exhaustion. Exogenous DPA was present at 1.1 mM. Scale bars are  $5 \mu\text{m} \times 1 \mu\text{m}$ .

sequestered it in the forespore. The behaviour was bimodal, as reported for *B. subtilis*, in that spores either showed phase bright or phase dark spores, corresponding respectively to WT core hydration, or hydration like that in germinated spores.

Many of the observations recorded for *B. megaterium* DPA mutants matched those reported for *B. subtilis* (Balassa *et al.*, 1979; Magge *et al.*, 2008). The behaviour of the 1462::21s double mutants, though, departed slightly. When grown with no exogenous DPA, these spores were not phase white but phase grey (figure 3.2d); they were noticeably different from WT spores. (Magge *et al.*, 2008, describe the equivalent *B. subtilis* mutants as “phase bright”.) This indicates a higher water content of the core compared with spores containing DPA, and supports the model in which DPA is required for spores to maximally exclude water. The DPA-replete variant did still look like WT spores (figure 3.2f).

The DPA mutants may be useful in probing the missing details of mechanisms through which CLEs operate. Without SleB, the  $\Delta spoVF$  spores do not autogerminate. It would appear that this enzyme has a key role in such autogermination. It is likely that DPA prevents it from degrading the cortex, thereby in the absence of SleB the high osmotic pressure, and thus reduced core water content, is maintained. Researchers interested in the dormancy of SleB may therefore have use for these  $\Delta spoVF$  spores; if one could produce a strain bearing a  $\Delta spoVF$  mutation and a functioning SleB, yet which results in stable spores, it may be possible to infer the factors preventing SleB activation.

### DPA assay

The colorimetric DPA assay (section 2.8.1) confirmed that *B. megaterium* spores with the  $\Delta spoVF$  mutation were DPA-deficient (figure 3.3). The strains bearing WT *spoVF* genes, QM B1551 and PS1462, contained more DPA than their respective  $\Delta spoVF$  mutant progeny: 1551::21s+ and 1462::21s. A paired comparisons test (table A1.1), using the method of unweighted means (Montgomery, 2012), estimated that the differences between the strains with *spoVF* ( $86 \pm 13\%$  of QM B1551) and those with the  $\Delta spoVF$  mutation ( $12 \pm 9\%$ ) were statistically significant ( $t = 20.4$ ,  $p = 0.016$ ).

Strains 1551::21s+ and 1462::21s differ in more than just their background; the former includes the whole pDBT21s vector as an insertion, disrupting the original operon (i.e. it's an SXO, single crossover). For the latter, a DXO (double crossover), the vector has re-ligated, deleting the original operon. Section 2.3.6 describes the mechanism; the relevant aspect is that only the latter 1462::21s lacks the *spoVF* genes fully. The SXO strain (and other SXOs such as 1462::21s+ — results not shown) showed non-zero DPA concentrations for spores

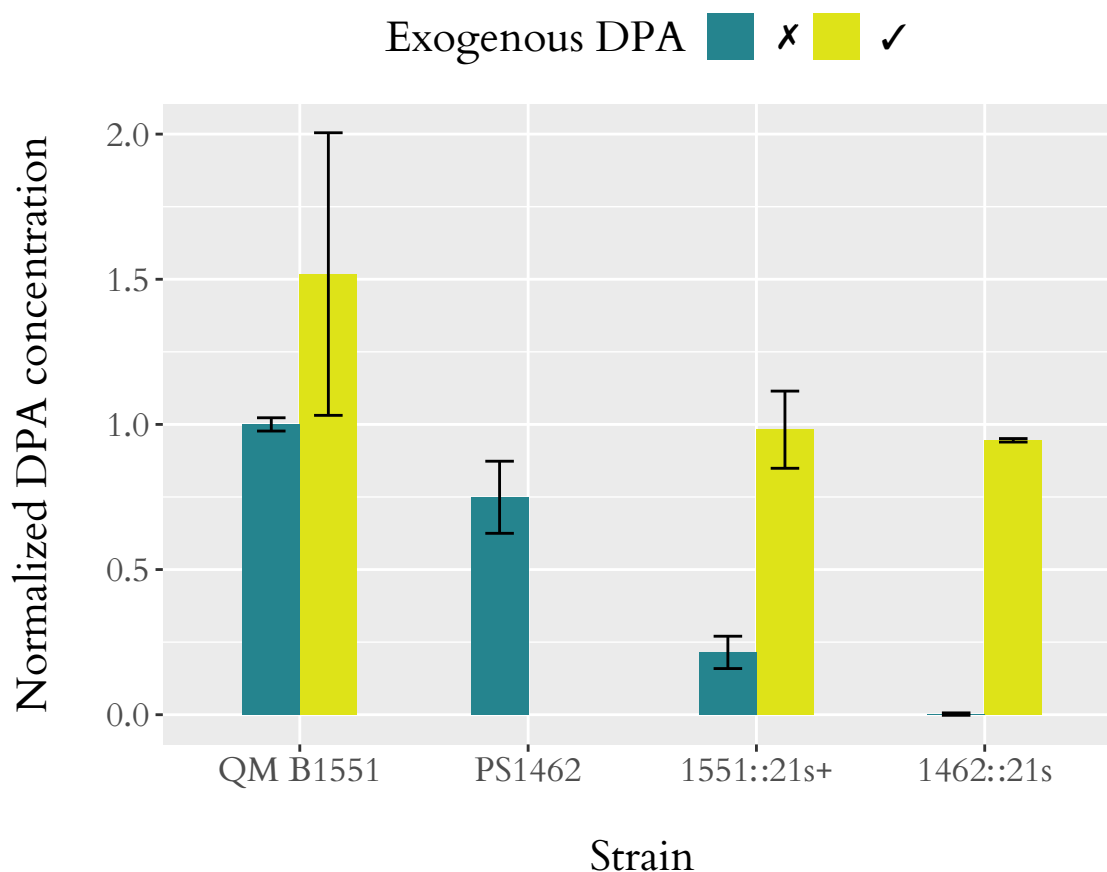


Figure 3.3: Results of the DPA assays, for *B. megaterium* spores. These show the effects of the  $\Delta spoVF$  mutation and sporulation in exogenous DPA. Strains with WT *spoVF* gave higher absorption readings at 440 nm than those without, corresponding to higher DPA concentrations (QM B1551 and PS1462 versus 1551::21s+ and 1462::21s). Spores grown with 1 mM exogenous DPA read higher for absorption at 440 nm, thus containing more DPA (the three within-strain comparisons). The PS1462 reading with exogenous DPA is not presented. Results have been combined across multiple batches (see table A1.3). Concentration values are normalized to the level of WT (QM B1551) spores within each batch. Errors correspond to standard deviations from multiple batches. Spores were produced via nutrient exhaustion in SNB; media contained no or 1 mM DPA.

grown without exogenous DPA; the DXO gave a repeatable zero result. This zero error does not affect the outcome. The DPA assay results showed that *B. megaterium* strains with *spoVF* deletions did not produce DPA.

The assay was subsequently used to compare levels of DPA among spores grown in different media. Spores of  $\Delta spoVF$  mutants, grown in the presence of DPA, recovered the WT DPA level (figure 3.3). A paired comparisons test (table A1.2) showed that the differences between the strains grown in standard SNB ( $40 \pm 20\%$  of QM B1551 grown in standard SNB) and those grown in DPA-supplemented medium ( $115 \pm 15\%$ ) were statistically significant ( $t = 5.95$ ,  $p = 9.6 \times 10^{-4}$ ). Again, this matched behaviour seen in *B. subtilis* (Magge *et al.*, 2008).



### 3.2.2 Scavenging of DPA during sporulation

Balassa *et al.* (1979) reported that the increase in DPA levels shown by spores produced in DPA-supplemented medium was not seen for WT spores. (None of Li *et al.*, 2012; Magge *et al.*, 2008; Paidhungat *et al.*, 2000 commented on this). By contrast, results here show that supplementing the sporulation media of a WT strain too leads to spores with elevated DPA levels.

Spores with WT *spoVF*, grown in the presence of DPA, showed elevated DPA levels, compared with that of spores in standard SNB (figure 3.3). Confirmation of this result itself in subsequent experiments was precluded by the failure to sporulate at 1 mM exogenous DPA (section 3.2.3), though other researchers have used the techniques to probe spores' magnetic abilities (for example Xu Zhou *et al.*, 2018). The finding presents opportunities for a novel way to investigate the role of DPA in spores, by considering its elevation rather than its absence. It is not clear to what extent an enhancement of DPA level within the core is possible.

The increase in measurements is almost certainly due to differences in the quantity of DPA extracted from cores, as the washing steps remove any DPA from the sporulation medium (as confirmed by the low readings for DPA-depleted spores). The cause is also more likely due to differences in the mass of DPA per spore than the extraction efficiency — *i.e.* a real difference in spore behaviour.

From an evolutionary perspective, one might expect that spores selected for their resistance to wet heat might already produce sufficient DPA to reach the upper limit within the forespore — but this does not seem to be the case. It raises a question: why don't spores saturate their cores with DPA? Perhaps higher levels of DPA confer marginal or no advantage and so were not positively selected; perhaps they confer a disadvantage — such as reduced flexibility due to DPA being present near its solubility limit — and so were negatively selected. For the former, it may be relevant here that spore populations across the genera do demonstrate heterogeneity of dormancy as a collective survival strategy; perhaps flexibility in DPA level is a part of that. It is possible that higher concentrations might be difficult for cells to process, and thus cause sporulation to arrest.

### 3.2.3 Inhibition of sporulation by DPA

Exogenous DPA at 1.4 mM prevented sporulation in *B. megaterium* (figure 3.4). By contrast, at 1.1 mM, spores looked phase bright. In a separate laboratory, however, this limit could not be reproduced: spores grown at 1.0 mM did not sporulate (and appeared like the aforementioned 1.4 mM sample), yet with 0.5 mM DPA cultures sporulated without impediment.

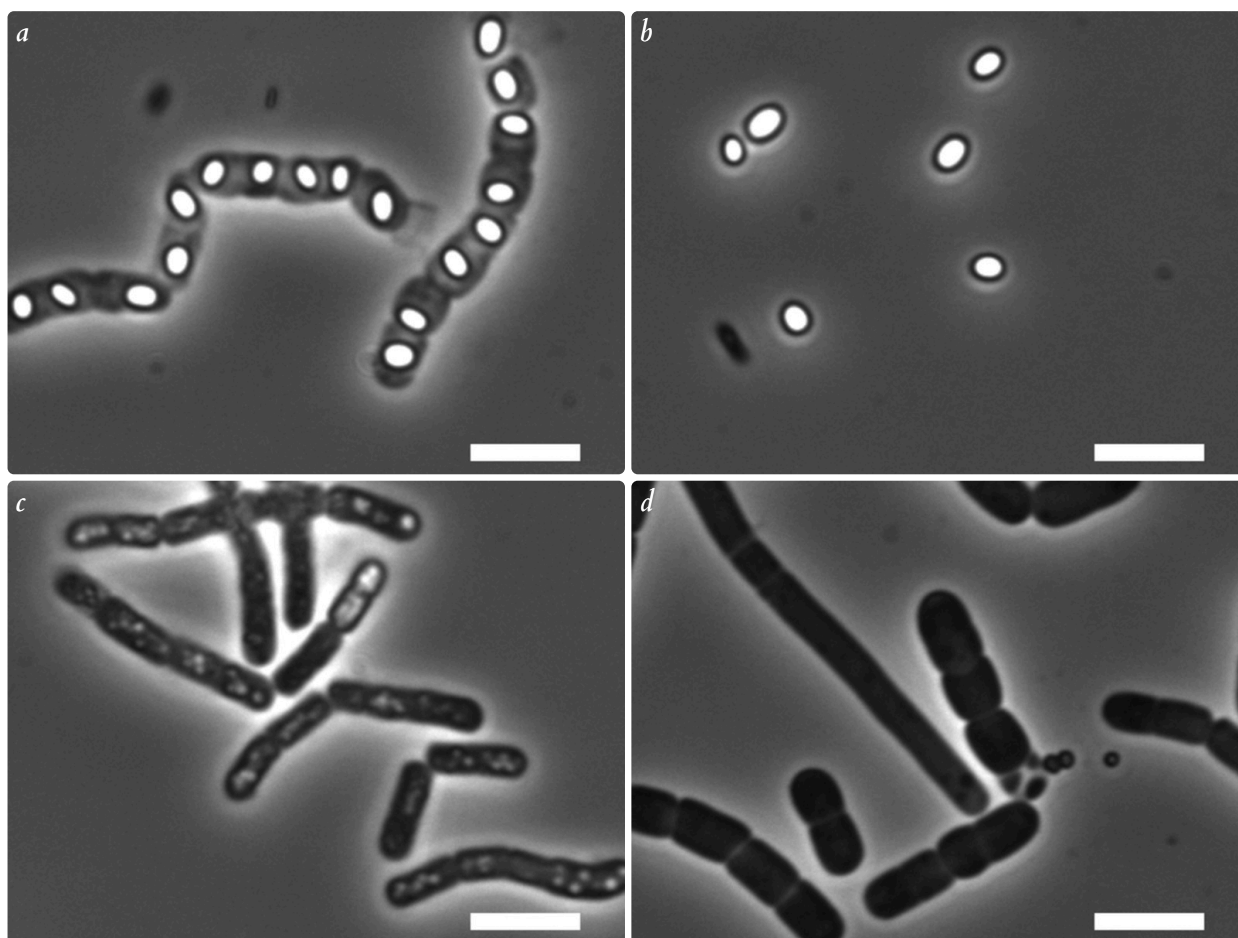


Figure 3.4: Micrographs of (WT) *B. megaterium* QM B1551, sporulated in SNB with exogenous DPA. (a) shows sporulating cells after 18 h with 1.1 mM DPA; (b) shows spores, fully released from sporangia, after 40 h with 1.1 mM DPA; (c) shows (not quite) sporulating cells after 18 h with 1.4 mM DPA; (d) shows cells that appeared to have stopped growing, after 40 h with 1.4 mM DPA. Over time (left to right) cells above the DPA concentration threshold (bottom row, versus top) began to sporulate, produced a variety of small phase bright structures (but no forespores) and then arrested. Spores were grown using nutrient exhaustion; a time of 0h corresponds to inoculation. Scale bars are  $5\ \mu\text{m} \times 1\ \mu\text{m}$ .

There has been no toxic concentration reported for *B. subtilis* in the relevant literature, where concentrations up to 2 mM have been used with success (Magge *et al.*, 2008, for example). In *B. megaterium*, here, such a threshold was seen. Researchers with access to the corresponding strain of *B. subtilis* may wish to investigate this.

It has been suggested that the fault here is pH: that the added DPA is lowering the initial pH such that the culture pH drops too low for the cells to survive, too soon for them to sporulate. However, this effect is seen when media are pH adjusted back to pH 7.2. In addition, no other acid analogue inhibited sporulation in the concentrations used in these experiments. It is possible that there is an interaction with SNB not seen with the sporulation medium used for *B. subtilis*, though given that this effect is not seen with chemical analogues it seems unlikely. Finally, Balassa *et al.* (1979) added exogenous DPA after initiation of sporulation (Magge *et al.*, 2008 were somewhat ambiguous on this); it could be that supplementing at this point in the sporulation cycle results in viable spores.

Given DPA activates CLEs (cortex lytic enzymess), one might suspect this process is at fault — though it would be surprising as sporulation arrests before forespores are produced. Perhaps DPA then inhibits sporulation? DPA may reach sufficient concentration in the mother cell to stop the sporulation machinery (through reaching solubility limits or otherwise), and thereby kill the cells.

Most concerning, though, is the lack of reproducibility of the threshold, and this merits further investigation. Whilst cells grown in one laboratory sporulated reproducibly at  $\lesssim 1.4$  mM exogenous DPA, in a second laboratory cells arrested reproducibly with exogenous DPA concentrations of just 1.0 mM. Such behaviour has already forestalled further work, which would otherwise directly follow the experiments presented here: specifically, a rigorous analysis of wet heat resistance of DPA-enhanced spores.

### 3.2.4 Wet heat susceptibility

Spores of the following strains were challenged at 70 °C, 80 °C or 90 °C for 20 min, using the method described in section 2.8.3:

- PS1462 ( $\Delta sleB +kan$ , a negative control);
- 1462::21s, grown in standard SNB ( $\Delta sleB \Delta spoVF +kan +spc$ );
- 1462::21s, grown in medium, doped with DPA; and
- 1551::21s+, in doped medium ( $\Delta spoVF +spc$ ).

Viabilities of samples were estimated using the Miles *et al.* (1938) plating technique, and the Comoglio *et al.* (2013) analysis (section 2.8.4). Such colony counts were also used to test the variation among spores, without heat challenge.

Strains of *B. megaterium*, cultured with or without exogenous DPA, produced spores with the viabilities presented in figure 3.5. The experiment for strain 1551::21s+ without exogenous DPA was not included, as this combination resulted in autogerminated spores. The inferred colony count for QM B1551,  $(1.11 \pm 0.10) \times 10^8$  cfu ml<sup>-1</sup>, matches the guideline spore wet density for that strain, for which an OD<sub>600</sub> of 1 is considered to correspond to 10<sup>8</sup> spore ml<sup>-1</sup>. The corresponding value for the  $\Delta sleB$  mutant, of  $(3.3 \pm 0.4) \times 10^7$  cfu ml<sup>-1</sup>, was lower, broadly matching published behaviour (Setlow *et al.*, 2009). The spores of strain 1462::21s, grown in DPA-supplemented media, showed greater viable counts than matching samples without the supplement:  $(2.8 \pm 0.4) \times 10^7$  cfu ml<sup>-1</sup> and  $(1.6 \pm 0.3) \times 10^6$  cfu ml<sup>-1</sup> respectively. This agrees with reported behaviour in *B. subtilis* (Balassa *et al.*, 1979). Strain 1552::21s (grown with the supplement) resulted in a count of  $(5.5 \pm 0.8) \times 10^7$  cfu ml<sup>-1</sup>: roughly half that of WT. Overall, DPA-depleted spores produced fewer colonies than DPA-producing variants, with  $\Delta sleB$  mutants showing diminished germination efficiency.

DPA-replete spores showed greatest viability after heat challenge. Figure 3.6 shows preliminary outcomes (single replicate) of the wet heat susceptibility assay for strains PS1462 and 1462::21s grown with or without 1 mM exogenous DPA. The 1462::21s spores grown with exogenous DPA consistently showed higher viable counts than those grown without.

Results of the assays for 1551::21s+ are shown too, in figure 3.6. *B. megaterium* spores, subject to heat challenge, typically show heat activation at 70 °C, resulting in increased measurements of the viable spore count. At higher temperatures, the heat challenge causes a decline in measurements, as spores are killed. This has been demonstrated with the presented results. At moderate heat shock (80 °C), the differences between strains, as seen with no heat shock, had disappeared.

Further heat susceptibility assays were precluded by the inability to reproduce spores with 1 mM exogenous DPA. Likewise, the inability to isolate a DXO variant of 1551::21s+ precluded experiments in the WT background. Notwithstanding this, the preliminary results regarding heat resistance concur with the behaviour reported for *B. subtilis*.

The germinated viabilities measured without heat activation for PS1462 were lower than those for QM B1551; the difference disappeared when spores of PS1462 were heat activated. Though *sleB* is semi-redundant, its deletion may change the dynamics of germination sufficiently that a colony count experiment will underestimate the number of spores present in the original sample. Indeed, the  $\Delta sleB$  mutation in *B. megaterium* has been shown to reduce viability of spores by up to 50% (Setlow *et al.*, 2009). On heat activation, the PS1462

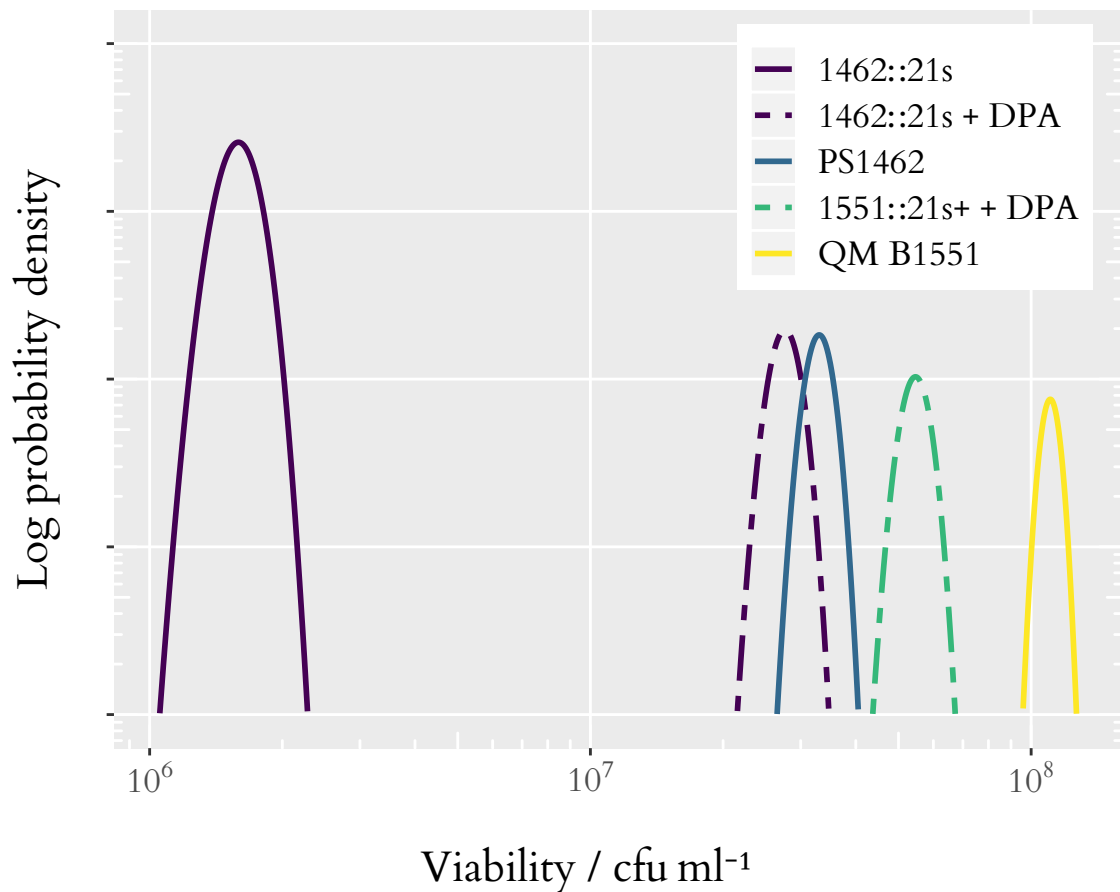


Figure 3.5: Probability density plot of viable colony counts for germinated *B. megaterium* spores, grown with (+ DPA) or without (no suffix) exogenous DPA. Strains with WT *sleB* produced higher viable counts than the deletion mutants. Samples grown with exogenous DPA had higher viable counts than the same strains in standard medium. The curves show >95% highest density intervals, and peaks indicate the maximum likelihood estimators; the heights are confounded with width, hence the labels on the abscissa have not been shown. Cultures were induced to sporulate using nutrient exhaustion in either standard SNB or SNB supplemented with 1.1 mM DPA. Spores were induced to germinate on LB agar.

strain with *cwlJ*, alone of the germination receptors, recovered the count of non-heat activated WT spores; one might hypothesize that the (poorly-understood) heat activation process somehow activates *CwlJ*.

★★

The microscopy, DPA assay and preliminary heat susceptibility results confirm that the  $\Delta spoVF$  mutation works in *B. megaterium* just as in *B. subtilis*, in both the WT and  $\Delta sleB$  backgrounds.

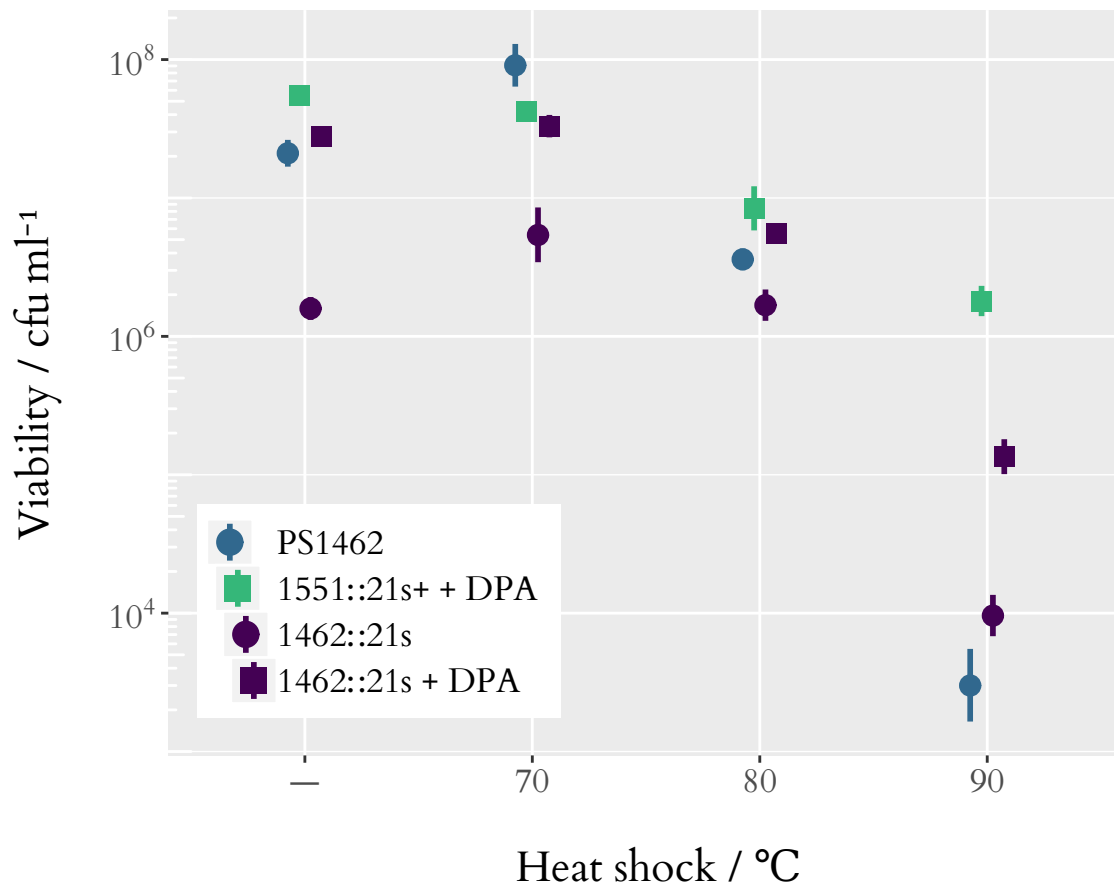


Figure 3.6: Survival plots for *B. megaterium* spores, grown in standard (circles) or DPA-supplemented (squares) medium. Spores were subjected to no shock (-) or shocked for 20 min at the temperatures on the ordinate. These temperatures are categorical; points within each category are horizontally displaced, for clarity (as in the legend). Strains showed either no change or an increase in the measured viability, after challenge at 70 °C; for 80 °C and 90 °C, viability measurements decreased. This decrease was greater for the strains sporulated without exogenous DPA. Error bars indicate the 95% credible intervals. These data show a single replicate.

### 3.2.5 Spores grown in DPA analogue-doped media

The DPA-depleted strains were induced to sporulate in analogue-doped SNB (section 2.5.1). The analogues replicate specific properties of DPA, differing in single, specific ways (figure 3.7).

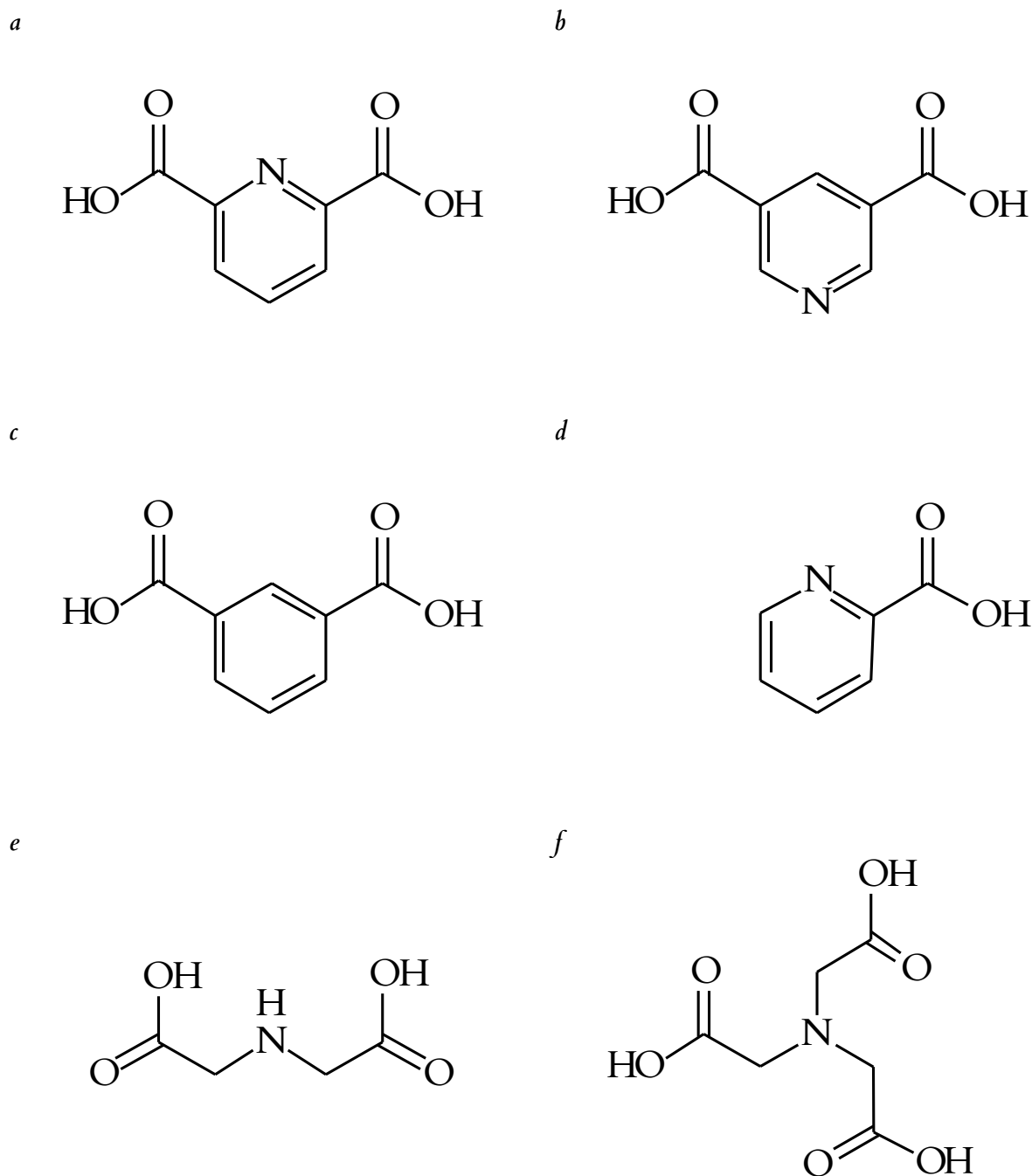


Figure 3.7: Chemical structures of DPA (2,6-dipicolinic acid) and some chemical analogues. (a) shows DPA; (b) the structural isomer 3,5-pyridinedicarboxylic acid, a.k.a. dinicotinic acid: not tested in this work; (c) the weaker acid IPA (isophthalic acid); (d) the chelation-incompetent PA (picolinic acid); (e) the amine (not pyridine) IDA (iminodiacetic acid); (f) the sterically bulkier tertiary amine NTA (nitrilotriacetic acid).

Li *et al.* (2012) probed the *B. subtilis* SpoVA channel's specificity to DPA compared with its position isomers. They found the gate very specific, but the details of the channel mechanism remained unclear. Analogues were chosen based on these findings.

- Unless the back end of the pyridine ring is sufficient for interactions within the spore, the interactions with IPA (isophthalic acid) should be the same as for 3,5-pyridinedicarboxylic acid, found not to interact specifically with the channel (Li *et al.*, 2012).
- PA (picolinic acid) does still possess the groups, which Li *et al.* (2012) suggested would allow it to interact with SpoVAD, though it has different charge delocalization.
- In addition to lacking the aromatic ring, the IDA (iminodiacetic acid) and NTA (nitrilotriacetic acid) bond angles are different (as is the delocalization of charge over the structure) so specific interactions would suggest that only the functional groups or chelation are important.

Sporulation was evaluated in the first instance with phase contrast microscopy: the brightness of a phase structure gives a qualitative guide to level of hydration. Additionally, chemicals may have concentrations above which cells do not sporulate. Therefore spores were produced in various concentrations of the DPA analogues, in a 96-well plate. Samples, of volume 20  $\mu$ l per 200  $\mu$ l well, were incubated, without shaking, at 30 °C.

This screen showed that exogenous analogues present in the medium had no effect on sporulation (figure 3.8). WT strains produced spores in the same manner as in the standard medium; likewise strains with the  $\Delta spoVF$  mutation produced phase dark spores. For the 1551::21s+ strain, only medium supplemented with DPA led to production of phase bright spores; only DPA led to the sporulation failure seen in figure 3.4d. Spores grown in larger volumes of supplemented medium showed the same result. IPA (isophthalic acid) was tested separately from the screen; the results were equivalent.

Additionally, spores of WT strain QM B1551, grown in media supplemented with these DPA analogues, did not differ from those grown in native SNB (data not shown).

Spores grew successfully in the 20  $\mu$ l screening samples. However, the samples dried out, whereas 40  $\mu$ l samples did not. The 40  $\mu$ l samples also showed a higher sporulation efficiency. Given the uniform physics of the wells, it is likely that the mass of water evaporated was similar in each case. Therefore the concentrations of analogues in the medium increased with time — quite significantly so for the 20  $\mu$ l samples. The reported concentrations might therefore be considered as initial concentrations, and the resulting data points as





Figure 3.8: Outcome of sporulation screening, in analogue-supplemented SNB. Cells either failed to sporulate (×), or produced phase bright (○) or phase dark (●) spores. Results with DPA match those reported already (with a slightly different sporulation arrest threshold); those with analogues matched the behaviour of the strains with no analogue. Sporulation media were supplemented with one of DPA (dipicolinic acid), PA (picolinic acid), NTA (nitrilotriacetic acid) and IDA (iminodiacetic acid). Medium supplemented with 0 mM DPA was standard SNB. Cultures of volume 20 µl were induced to sporulate via nutrient exhaustion in a 96-well plate.

underestimates of the true concentrations. However, the DPA threshold, above which sporulation did not occur, was reproducible between the 20 µl screen and larger volume samples.

Screening these spores by phase contrast gives a direct, albeit qualitative, measure of the hydration of the spore core. There are severe limitations to this screening technique, though — most importantly that it cannot demonstrate that the specific chemical has been taken into the spore, and that it gives little information in the case of a negative result. Demonstrating spores have taken up the relevant chemical is non-trivial, especially as there are few *in situ* methods to detect what is in the spore core. Raman microspectroscopy is the most suitable option (Ichimura *et al.*, 2014; Setlow *et al.*, 2012), and was indeed used by Li *et al.* (2012) to test the DPA analogues; NMR (nuclear magnetic resonance) spectroscopy of spore extracts would be the gold standard for characterising the contents of the spores core. However, it is

also possible that the DPA assay is unable to discriminate between these analogues, and may result in formation of the  $\text{Fe}(\text{NH}_4)_2(\text{SO}_4)_2$ -analogue complex; this may be worth investigating.

The best way to ensure spores take up DPA analogues would be engineering the proteins in the SpoVA channel. Given that a crystal structure has been solved for only one sub-unit of seven, belonging to one species of about 50, such an endeavour has a low chance of success. More promising would be to try to supplement a species of *Clostridium*, which has a simpler, three sub-unit SpoVA operon (C–E). It may even be possible to replace the A–F operon in a *Bacillus* with the simpler *Clostridium* variant. The combination of a simpler operon and a convenient species would greatly simplify future attempts to elucidate the channel's mechanism.

The microscopy evidence presented here suggests sporulating *B. megaterium* do not scavenge these molecules from the medium. Spores grown with up to 4 mM of the analogues looked the same as those without. These results are weakly negative, and pursuit of stronger evidence is less valuable than investigating the reproducibility issues with exogenous DPA.

### 3.2.6 Experimental design

Experimental designs for the work, reported in this chapter, failed to differentiate a number of factors. Replicating the *B. subtilis* work in *B. megaterium* offered a good comparison, but given differences it would be good to repeat experiments with the relevant *B. subtilis* strains. Likewise, work with the analogues would be significantly more valuable in both strains, as the current results confound the behaviour in the presence of analogues with the behaviour of the different species.

Separately, two factors arose, during the experimental work, that caused difficulties with this project: reproducing the toxic DPA threshold, discussed in section 3.2.3; and, discussed here, isolating a DXO strain. A number of further improvements could be made to the experimental design.

## Isolation of DXO strains

The DXO isolation procedure, with strains 1551::21s+ and 1462::21s+, resulted in strain 1462::21s ( $\Delta sleB \Delta spoVF$ ). A DXO strain with the  $\Delta spoVF$  genotype was isolated, but it had been cured of plasmid pBM700 ( $\Delta p7$ ). Indeed, no strain 1551::21s ( $\Delta spoVF$  DXO), which had not lost its plasmid 7, was isolated, despite four three-week rounds of attempts (~600 total events).

The protocol to isolate a DXO strain thereby resulted in a single candidate for strain 1462::21s, and no candidate strain for 1551::21s. As a result, the experiments planned for 1551::21s were only possible with the SXO strain, 1551::21s+. Early results with the SXO strains were disquieting. The DPA assays for the SXO strains grown without exogenous DPA were close to 25% of the WT levels. By contrast, the DXO gave readings close to zero (and with low variance, too).

Is it possible that cells revert to WT in the sporulation medium, and thereby the resulting spore crop is actually a polyclonal sample? Cells with SXOs are genetically unstable: there is a small probability that each cell will revert to WT (see figure 2.1); strains with a DXO are genetically stable in this regard.

It is possible to estimate the expected number of revertants in a spore crop. Fabret *et al.* (2002) reported an elevated pop-out frequency in *B. subtilis* of  $10^{-6}$  (an overestimate, but sufficient here). Neglecting cell death, and assuming all cells become spores, this would give a reversion rate of  $10^{-6}$  — well below the sensitivity of the DPA assay. However, the timing of the event matters; at one extreme, if the initial inoculum contained only one cell — and that cell reverted — the whole sample would be of the revertant. Assuming a small initial inoculum (perhaps  $10^3$  cells) and a final culture at sporulation of  $10^{11}$  cells ( $10^8\times$ ), this gives 27 generations. Even factoring in cell death, and slightly less than doubling each generation, the generation number is unlikely to reach triple figures. With 50 generations, and a pop-out frequency of  $10^{-6}$ , that gives an expected pop-out proportion of their product:  $5\times 10^{-5}$  (see section A1.4 for the model here). This overestimate is well below the proportion of the wild type value seen for SXOs in the DPA assays.

There are other possible explanations. *B. megaterium* may co-opt *etfA* (BMQ\_4730), which *Clostridium perfringens* uses instead of *spoVF* (Orsburn *et al.*, 2010). Such spores would contain DPA, and a colorimetric assay may be sufficiently sensitive to detect this. There is

currently no evidence that gene is expressed. However, even if there were, it would still not explain the differences seen between the SXO and DXO strains. It is possible too that the results are due to chance.

The corollary of the instability of SXOs is that in order to isolate a DXO, one must rely on that same stochastic process. What is the probability of isolating a DXO strain? This three week isolation procedure was performed four times for the 1551::21s+ SXO mutant, still with no positive result (and as plating events have errors, there were many false positives). The overestimate above gives a guide. If independent, the 600 plating events (12 colonies, 4 week-nights, 3 weeks, 4 times, 576 total) would result in an expected 3% probability to isolate a DXO. In this case the pop-out frequency is slightly underestimated (it is higher at 42°C). Whatever the outcome of such a probability model, the low frequency of events alone destroys the predictability of the technique.

Overall, it is hard to recommend the allelic exchange approach of pUCTV2. There are many reported counter-selection techniques, which improve the chances of identifying a pop-out, and it is worth establishing those before continuing, or attempting to replicate, this work (Biedendieck *et al.*, 2011).

The inability to isolate a DXO strain (1551::21s) thereby precluded further research into the true behaviour of the  $\Delta spoVF$  mutation, in isolation.

### Limitations of protocols

In addition to the above challenges, there are limitations to some published protocols. The most serious of these concerns the DPA assay. The protocol confounds a number of factors: growth rate, spore size, spore number and spore dipicolinic acid content. In addition, in its published laboratory manual form (Nicholson & Setlow, 1990) it mentions nothing about sporulation times. It would be improved were samples normalized to the same optical density, rather than taking a fixed volume sample, as these factors could then be separated.

When initially compared with the standard curve, a number of spore extract readings evaluated to negative concentrations. This is most likely a zero error. Spore extract is a more complex mixture than the water used for the blank, and may inhibit formation of the  $\text{Fe}(\text{NH}_4)_2(\text{SO}_4)_2$ -DPA complex of the assay. Despite the published protocol, it may be better to produce the standard curve with cell extract or extract of DPA-depleted spores, rather than water.

Another difficulty with analysis of extracted DPA is batch-to-batch variation. Different batches have different ranges of DPA level, such that the readings are not directly comparable. To compare, one must normalize the readings based on matched samples; ideally this should be done with two endpoints (e.g. WT and DPA-less spore samples). Like the zero error, this is mentioned in neither the reporting publications nor the published protocol.

Colony counts proved reproducible and benefited from efficient experimental design. Time, temperature, strain, growth conditions and batch are all important factors which contribute to the measured counts. It is feasible to run complementary fractional factorial experiments to efficiently cover the state space of the experimental design. Indeed, such a design was undertaken, but the inability to reproduce spores with 1 mM exogenous DPA forestalled the experiment itself.

Finally, given the inference model for colony counts (Clough *et al.*, 2005; Comoglio *et al.*, 2013), it ought to be possible to identify the optimal number of cells to count in order to give sufficient confidence that two samples are drawn from different populations. This may require an initial Miles *et al.* (1938) plating, followed by biological replicates of full plate counts. It would then be possible to modify BEST (Bayesian estimation [that] supersedes the  $t^*$ -test) such that the Monte-Carlo model generates gamma distributed test data (Kruschke, 2013). This would ensure that the statistical foundations for discrimination of spore populations can be justified — in a way that no published research has been able to do.

### 3.3 Conclusion

The ubiquity of DPA among known sporeformers implies that it confers a selective advantage. Demonstrating, as here, that different *Bacilli* lacking DPA behave similarly, implies that the processing of DPA too is evolutionarily conserved.

Here, the putative *spoVF* operon in *B. megaterium* is confirmed, and the behaviour of *B. megaterium* strains with the  $\Delta spoVF$  mutation is shown mostly to match that of *B. subtilis*, reported by Magge *et al.* (2008). Such spores do not contain DPA, as the forming spore cannot produce it, yet spores of such strains grown in the presence of DPA show near WT levels.

Unlike as reported for *B. subtilis*, however, too much DPA in the sporulation medium caused sporulation to arrest. This arrestation was reproducible, though the associated exogenous DPA concentration was not, and this precluded confirmatory studies of other effects and behaviour.

For example, results here reproduce the finding that DPA-deficient spores show diminished resistance to wet heat (and demonstrate this behaviour for the first time in *B. megaterium*). It appears, too, that DPA-replete spores, incapable of producing DPA themselves, do not scavenge sufficient quantities from their environment to replace all the DPA that is lost, and consequently appear to have a higher water content and lower resistance to wet heat.

By contrast, it is possible to produce *B. megaterium* spores with *elevated* levels of DPA — a feat others have failed to show for *B. subtilis*. Such spores have assisted in probing other spore characteristics (*e.g.* paramagnetism, Xu Zhou *et al.*, 2018) and could in future help elucidate the interaction between DPA, water and proteins in the spore core.

From supplementation with DPA analogues, the specificity of the DPA *B. megaterium* uptake mechanism appears to match that of *B. subtilis*. The SpoVA channel interactions reported in *B. subtilis* focus on the positive requirement for the two carboxylate groups of DPA (Li *et al.*, 2012). Results here agree with this, and support the assertion that while these groups may be necessary, they are not sufficient.

Despite the co-incident work of Batalha *et al.* (2017), while one might consider DPA a candidate pharmaceutical excipient, it is not yet known *how* it protects proteins. As repeatedly pointed out in comprehensive reviews by Peter Setlow (2006, 2014), nobody knows how the forespore is able to reduce its water content to such a degree during sporulation. The strains, techniques and results presented here may help solve this mystery.

However important for spore microbiology, the results presented here not contributed directly to the overall goal of producing an improved pharmaceutical formulation. With guidance from those with such expertise, the second approach was investigated, and the results are presented in the next chapter. That chapter reports work that, rather than investigating the behaviour of the spore core in order to mimic it, instead engineers spores themselves to become the delivery vehicles.





## Chapter 4

# Therapeutic proteins in sporulating

## *Bacillus subtilis*

## 4.1 Introduction

Bacterial endospores possess many desirable qualities for stable pharmaceutical products. *Bacillus* species form spores which protect their crucial components in a shielded core: most critically, their genomes and proteins. One way to mimic that behaviour would be to replicate the conditions in the core, perhaps using DPA (2,6-dipicolinic acid) as a stabilizer (as in chapter 3). An alternative, presented in this chapter, uses spores themselves as the delivery vehicle. In practice, this means engineering sporeformers to express therapeutic proteins during sporulation.

Unfortunately, some of the features that protect endospores from environmental challenge are undesirable in other ways. Spores' robustness has limited the development of spores bearing therapeutic proteins.

This chapter presents the first investigation of *B. subtilis* spores as a platform for delivering humanized mAbs (monoclonal antibodies). It is not, however, the first research to implement this approach. In previous work in the Christie laboratory, Mohamed (2015) established the SASP (small acid-soluble protein) promoter  $P_{sspB}$  for production of heterologous proteins in the core of *B. subtilis* spores. The work was successful with human growth hormone and single chain insulin, but required heavy strain engineering to produce just a single antibody fragment (scFv, single chain variable fragment).

Much of the research presented here involves the mAb (monoclonal antibody) NIP109: a humanized monoclonal IgG (immunoglobulin G), which binds the hapten, NIP (4-hydroxy-3-iodo-5-nitrophenylacetic acid). In addition to whole IgGs, various other configurations of domains are therapeutically useful, notably the scFv: a fusion of light and heavy chain, comprising only their variable fragments ( $F_V$ , see figure 1.3).

Antibodies are not limited to conventional IgGs, though; for example, the *nanobody*, a fragment comprising the variable domain of a camelid heavy-chain antibody, can be considered an alternative to an scFv. Nanobodies might be used in the form of a single protein domain, or conjugated to a fluorescent protein to form a chromobody (useful for imaging as they are small enough to clear the kidneys, Panza *et al.*, 2015). The platform developed here is tested with a small range of nanobodies:  $V_{HH}$  GFP4, which binds GFP (green fluorescent protein); BcII10, which binds the *B. cereus* metallo- $\beta$ -lactamase; and two further nanobodies which bind other  $\beta$ -lactamases. The  $\alpha$ -GFP nanobodies serve laboratory

purposes; the  $\alpha$ - $\beta$ -lactamase nanobodies might be candidates to combat antibiotic resistance. Using nanobodies avoids the technical bottleneck of having to demonstrate assembly of a full IgG — a challenge due to spores' robustness.

Such robustness poses challenges both for product design and research. Laboratory techniques to investigate the contents of the spore core fall well short of the standards required for initial formulation characterization, never mind product approval or cGMP (current good manufacturing practice). Additionally, no method has yet been established to ensure the protein payload is released appropriately from the spores. What is needed is a fast, minimally intensive technique to break spores for the purposes of laboratory measurements, and a reliable method to ensure spores release their contents correctly *in vivo*. The challenge is to disrupt the cortex, without allowing the spore to germinate and potentially degrade the contents of its core.

In earlier work, Mohamed (2015) engineered a release system, in which the PBSX prophage caused germinating spores to lyse during outgrowth. Though reasonably successful, the need for germination causes issues with this approach: specifically, the lag time between germination and release, and the requirement that the spore is *capable* of germinating. Additionally, this mechanism does not address the need to disrupt spores, for laboratory measurement.

The novel alternative, presented in this chapter, uses a single deletion mutation to achieve both goals. Spores lacking their outer coats retain most environmental resistance, yet the cortex becomes susceptible to enzymatic degradation (as described in section 1.3.4). Deleting *cotE* results in a lysozyme sensitivity, useful for disruption of spores in the laboratory. It might also provide a novel, simple way to release encapsulated proteins from the spore *in vivo*.

This chapter therefore seeks to evaluate whether bacterial spores are viable carriers for therapeutic antibodies. The work presented here demonstrates that sporulating cells can produce these pharmaceutically relevant therapeutic proteins, and shows it is possible to engineer spores to release such protein in a controlled, scalable manner.


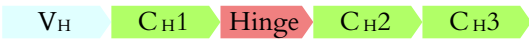
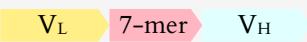
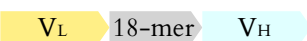
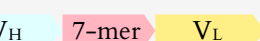
Two undergraduate research students, and one masters student, performed a number of the experiments in this chapter; these contributions are indicated in descriptions of the methods and results.

## 4.2 Results & discussion

### 4.2.1 Antibody expression by sporulating *B. subtilis*

In addition to the light and heavy NIP109 chains, three scFvs (single chain variable fragments) were constructed. One uses an 18-mer amino acid linker, of peptide sequence G<sub>2</sub>S<sub>2</sub>RS<sub>4</sub>G<sub>4</sub>SG<sub>4</sub>; the other two use the 7-mer GGSSRSS (see Andris-Widhopf *et al.*, 2011). All constructs are detailed in table 4.1 (see listing A1.1 for the primary amino acid sequences of the fusion domains). For production during sporulation of each fragment there were two variants: the fragment with a C-terminal 6×His tag (0.8 kDa), and the fragment with a C-terminal GFP (green fluorescent protein) fusion (28.8 kDa — the AL11 linker, Robinson & Sauer (1998); GFP; and a 6×His tag). A representative ectopic plasmid for integration at the *amyE* locus is in figure 4.1.

Table 4.1: Fragments of the NIP109 antibody. Of the scFvs, two have the light chain first, then heavy; one vice versa. The domains are labelled as V, for variable, or C, for constant, with suffixes L for light chain and H for heavy, and numerals according to their position in the chain. 18-mer linker G<sub>2</sub>S<sub>2</sub>RS<sub>4</sub>G<sub>4</sub>SG<sub>4</sub>; 7-mer GGSSRSS (G ~ glycine; R ~ arginine; S ~ serine; subscript suffixes indicate the chain length of identical repeats). The mass is that of the protein with a 6×His tag. ThermoFisher produced these ten fragments as GeneArt® Strings™, suitable for overlap assembly.

Code	Fragment	Domains	Mass / kDa
l	Light chain		24.0
h	Heavy chain		50.0
s	scFv		26.0
t	scFv		26.7
u	scFv		26.0

#### WT *B. subtilis* strains

Aliquots of *B. subtilis* subsp. *subtilis* 168 were transformed to Chloramphenicol resistance, with single pDBT61\* plasmids, to give the 168::61\* strains, and then induced to sporulate. Micrographs of the concentrated spore slurry can be seen in figure 4.2. Spores in the left column of triples, the non-GFP strains (168::616?), show some diffuse background fluorescence. Spores in the right column, the GFP strains (168::611?), additionally show strong, localized fluorescence. For most strains, the vegetative cells do not appear in the

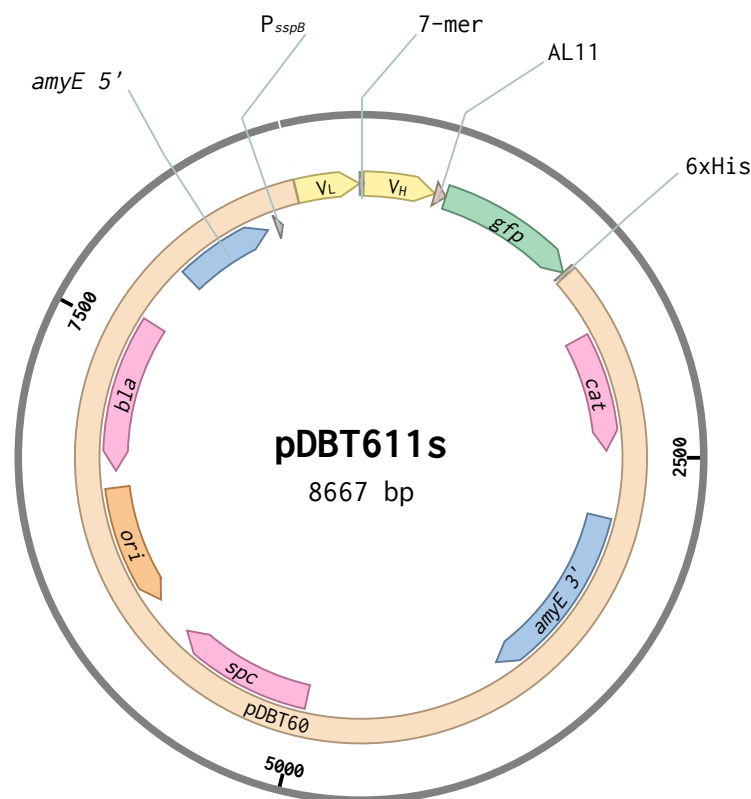


Figure 4.1: Representative *pDBT61\** plasmid for expressing NIP109 fragments under control of promoter  $P_{sspB}$ . Plasmid *pDBT611s* carries an ORF (open reading frame) encoding an scFv ( $V_H \rightarrow V_L$ ) with a C-terminal AL11-GFP-6xHis fusion. (Bold type indicates the mnemonic; the *pDBT616\** plasmids have just the C-terminal 6xHis tag.) Other features are antibiotic cassettes: *cat*, *bla*, and *spc* (conferring resistance to Chloramphenicol, Carbenicillin and Spectinomycin respectively); the *E. coli* origin of replication, *ori*; and two regions of homology matching upstream and downstream of *amyE*. KAM (Klenow assembly method) was used for assembly.

fluorescence micrographs; where they do, the corresponding cells in the phase contrast images appear much as strains which have arrested during sporulation back in chapter 3 (figure 3.4d).

These micrographs offer promising results. In contrast to the experience of Mohamed (2015), there is evidence that scFvs were produced, in the WT background. From the localized fluorescence for strains bearing C-terminal GFP fusions, one can infer that GFP was being produced. In turn, from the presence of a fully formed, functional, C-terminal GFP fusion, one can infer that the full protein was expressed correctly. Typically, antibodies are produced in mammalian cells; such cells feature complex protein production mechanisms, from introns and variant exon splicing, to post-translational modifications. Transcription is far simpler in bacteria, so many of the techniques that demonstrate the resulting amino acid sequences are correct (*e.g.* peptide mapping) are not needed for bacterial protein production.

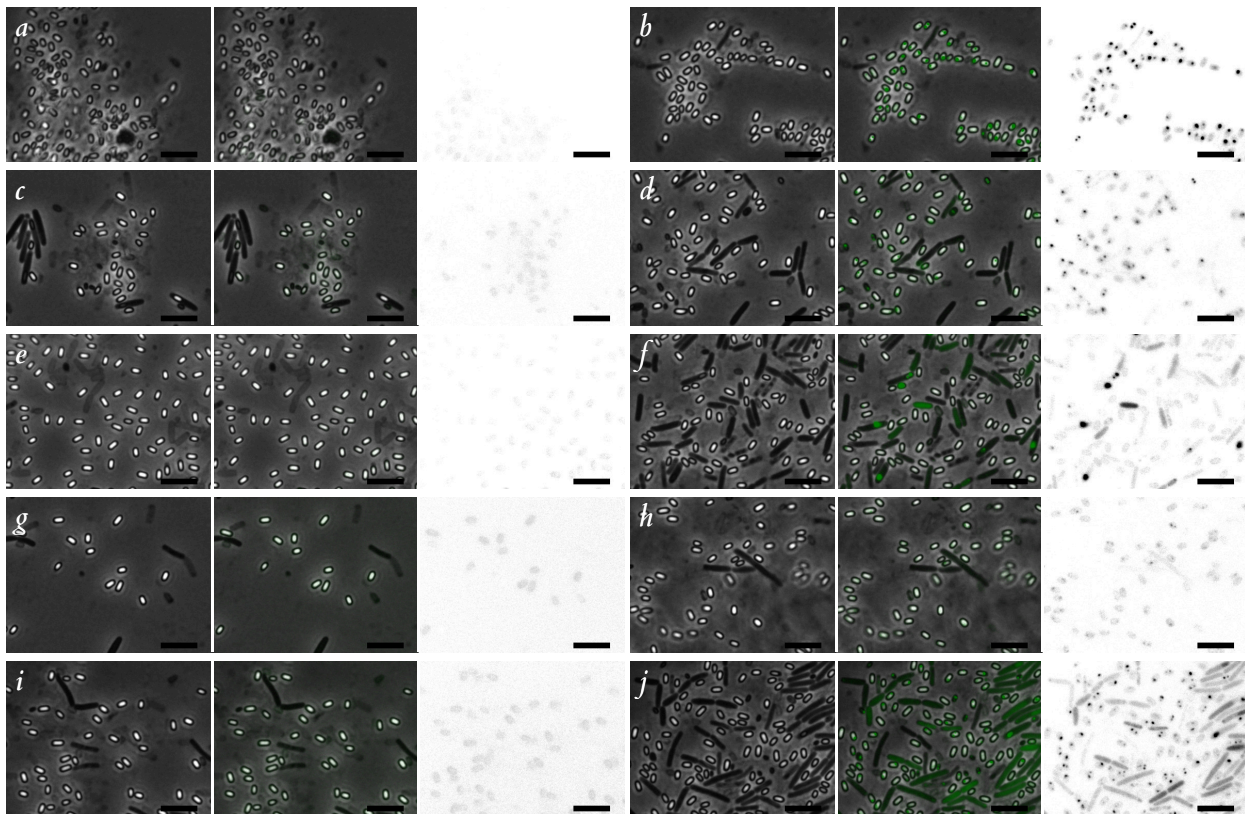


Figure 4.2: Triples of phase contrast (left), composite (centre) and fluorescent (right) micrographs of *B. subtilis* 168::61\* crude spore crops, aligned such that rows share a NIP109 fragment and columns share a C-terminal fusion (the GFP fusion is on the right). (a) shows light chain strain 6l; (b) 1l; (c) shows heavy chain strain 6h; (d) 1h; (e) shows scFv L→H (7-mer) strain 6s; (f) 1s; (g) shows scFv L→H (18-mer) strain 6t; (h) 1t; (i) shows scFv H→L (7-mer) strain 6u; (j) 1u; The identifiers refer to the codes which take the place of the asterisk in the strain names. The bright structures in the phase images are the highly (refractile) spores. Dark signal in the (inverted) fluorescence images corresponds to fluorescence; the distinct structures, present for the GFP strains only, indicate localized fluorescence. Strains were induced to sporulate by nutrient exhaustion. Where possible, images were selected to include both cells and spores. Scale bars are  $5\mu\text{m} \times 1\mu\text{m}$ .

Considering the micrographs in detail, one might notice that there is localized fluorescence within the spore outlines, for samples 1l, 1h and 1t, corresponding to GFP fusions of the light chain, heavy chain and scFv (with 18-mer linker) respectively. For the other GFP fusions, both scFvs with the 7-mer linker, there are many vegetative cells showing intense fluorescence. Given that  $P_{\text{sspB}}$  is active in the forespore, it is likely that these cells had produced fluorescent protein, and subsequently arrested during sporulation. This effect is probably due to metabolic load; the forespore has a finite incoming energy flux from the mother cell, and by producing heterologous rather than native proteins it may result in intense fluorescence rather than a viable spore. Those continuing to research production of heterologous proteins in the spore core would do well to monitor sporulation yields, to

investigate this. Comparing single cells would be valuable; it may identify an upper threshold on the mass of protein per spore. Such a threshold would put a hard limit on the dose of a therapeutic protein, using this delivery method.

The western blot, figure 4.3, confirms correct expression. All lanes show bands of the predicted masses; for all but one (6l) there is no band more intense. For 6l, the band at 24kDa is very faint, and there is an intense band at 27 kDa; subsequent blots, though, show the 24kDa band, with similar intensity to predicted bands of other strains. A number of lanes (6l, 6h, all 1?) show bands at approximately integer multiples of the predicted masses. The 6h lane shows many additional bands, at smaller masses than the predicted band; at greater masses, the background intensity is relatively high.

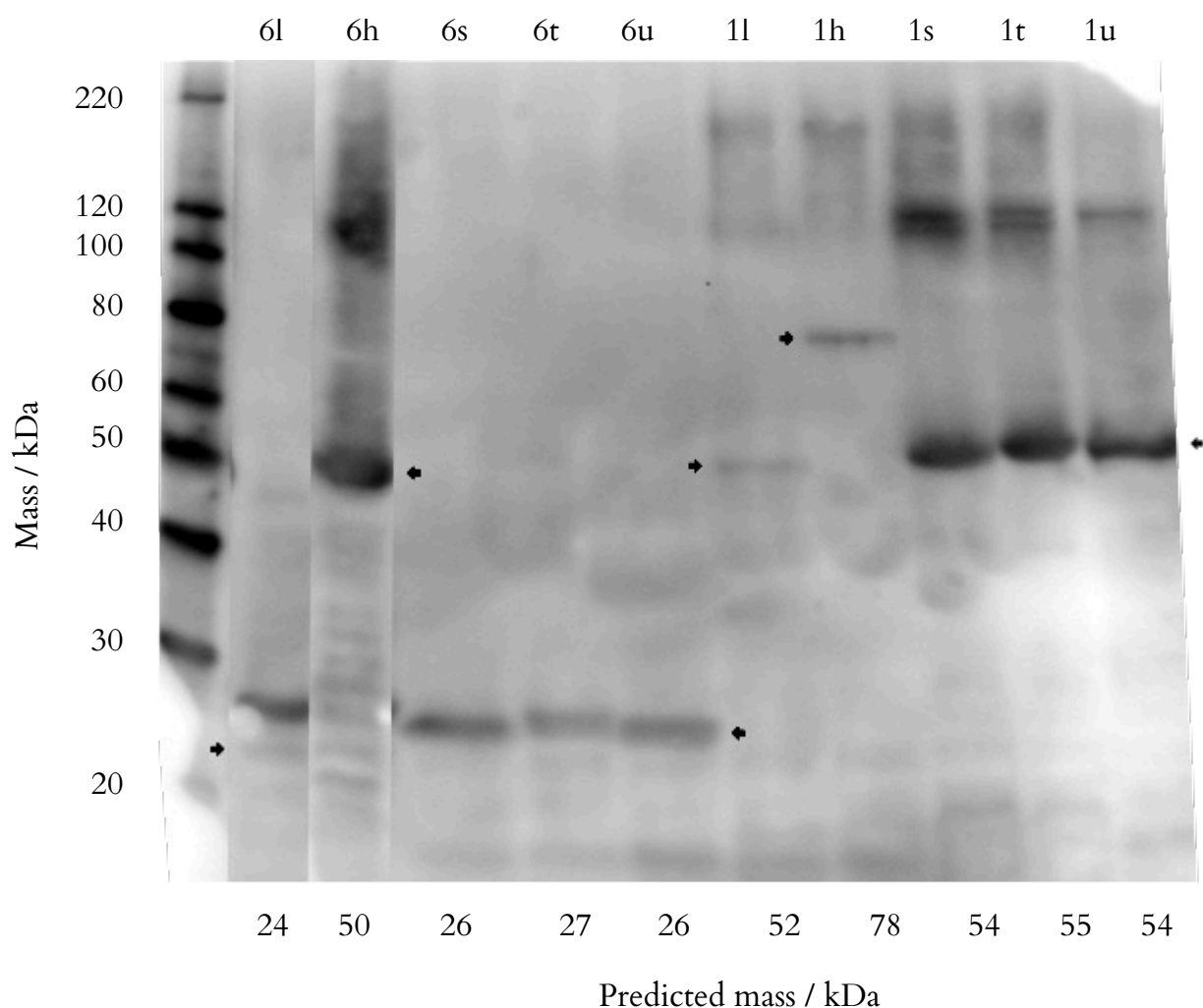


Figure 4.3: Western blot of NIP109 fragments, extracted from *B. subtilis* 168::61\* spores. Lanes are labelled for the fusion (6×His tag, AL11-GFP) and variant (letters). All lanes show predicted bands, indicated with arrows (and the s, t and u bands share an arrow). The left-most lane is the MagicMark™ XP Western Protein standard ladder. Spores were mechanically disrupted. The total protein fraction was fractionated with SDS-PAGE and transferred to a PVDF membrane, for single antibody western blot analysis.

The blot indicates that not only were the antibody fragments produced, they could be extracted from the spore cores. It is hard to judge the extent to which the differences in intensity among the lanes correspond to differences in production level, extraction efficiency and probe affinity. The first seems unlikely, as the pattern of fluorescence intensities in micrographs does not match the intensities of the bands. Given the relatively low intensities of the 11 and 1h bands at 120 kDa and 180 kDa, it is unlikely the difference is due to the His tag affinity (the latter two factors). That leaves the extraction efficiency; the extraction is not only a bottleneck in throughput for protein analysis, but may well damage the proteins in the resulting extract, too. Research into superior methods to disrupt the spores would offer immense value, here.

Figure 4.3 shows bands with masses that are integer multiples of the predicted bands; these are most likely aggregates. From the bands at integer multiples of the predicted masses, one might infer that there is some association between proteins, despite the reducing, denaturing environment. This is typically seen when the standard SDS-PAGE conditions are not optimized for the samples in use, or the chemical components have degraded. One might consider adding DTT (dithiothreitol) to samples, or heating at lower temperature. Size exclusion chromatography might help here, too. As these aggregates have multiple His tags, they may bind multiple western probes, thereby giving a more intense signal than one would expect for a single protein of the same prevalence.

### **$\Delta cotE$ strains**

The coat-deficient strain of Zheng *et al.* (1988) carries a *cotE::cat* mutation (indicating the chloramphenicol acetyltransferase gene, *cat*, has replaced the *cotE*). Unfortunately, this is the same antibiotic resistance cassette as the various pDBT61\* plasmids, which had already been constructed and shown to result in expression of various heterologous proteins in the spore core (see figures 4.1, 4.3). Furthermore, the progenitor strain was *B. subtilis* PY-17, rather than *B. subtilis* 168. It was therefore preferable to generate a new mutant with the  $\Delta cotE$  genotype, but in a background suitable for comparison, and with a different marker. Furthermore, as subsequent strain engineering would be required, that mutation could be introduced in a strain suitable for marker cycling and counter-selection. The most suitable strain is that reported by Shi *et al.* (2013), *B. subtilis* BUK, derived from *B. subtilis* 168. It is both inducibly supercompetent and a suitable host for 5-FU counter-selection, the ideal combination for the repeated strain engineering processes required. Though some of the plasmids of Shi *et al.* (2013) were available from the *Bacillus* Genetic Stock Centre, this strain



itself was not. The strain engineering required to replicate those authors' work, and generate the isogenic *B. subtilis* 168::690, is described in sections 2.4.4, A1.7. This strain was then transformed to give the chloramphenicol-sensitive  $\Delta cotE$  strain: *B. subtilis* 690::71e.

The *B. subtilis* 168::690 and 690::71e strains were each transformed to Chloramphenicol resistance with pDBT6111, pDBT611h and pDBT611s. All sporulated successfully. Clumps were successfully diminished by ball milling; for example, 71e::611l spores were not damaged fluoresced as expected.

The PAGE and western blot data in figure 4.4 show that the 168::690-derived (inducibly supercompetent) and 690::71e ( $\Delta cotE$ ) strains can express NIP109 fragments, just as WT *B. subtilis* 168. The extracts showed predicted bands, by western blot, with some intense bands on the matching Coomassie stained polyacrylamide gel. The predicted bands are only present in their corresponding lanes; this is clearer for the 168::690-derived samples on the gel, and clearest on the blot, where only the 611? strains show intense bands. The blot itself shows the predicted bands, bands at integer multiples, and, for the light chain samples, a band at around 35 kDa. On the polyacrylamide gel, the 168::690-derived strains display more intense bands than the 690::71e-derived strains, with the exception of bands at approximately 32 and 41 kDa.

It is illustrative to compare the intensities of the bands in figure 4.4. The predicted bands for the 168::690-derived strains are more intense than the equivalent 690::71e bands. This indicates that the protein concentration in the 690::71e lysate was lower than that for 168::690. A number of factors would lead to such an occurrence; differences in extraction efficiency and errors in normalizing the optical density of the clumped spores are the most likely culprits, here. A surfactant would improve this latter factor.

Other bands on the blots merit some discussion. The considerations regarding bands at integer multiples of predicted lengths match figure 4.3, and shall not be repeated. The bands at 35 kDa on the light chain samples are most likely C-terminal fragments of the NIP109 light chain AL11-GFP fusion, with the break in the middle of the C<sub>H</sub> domain. Very faint bands at this length can be seen on other blots featuring this light chain. It is not clear why the bands should be so strong on the blot, here. The additional bands seen on the gel from 690::71e-derived strains may well be coat proteins that, in the absence of CotE, loosely associate during spore washing, but dissociate during mechanical disruption. Peptide mapping would be required to identify the constituents of these bands.

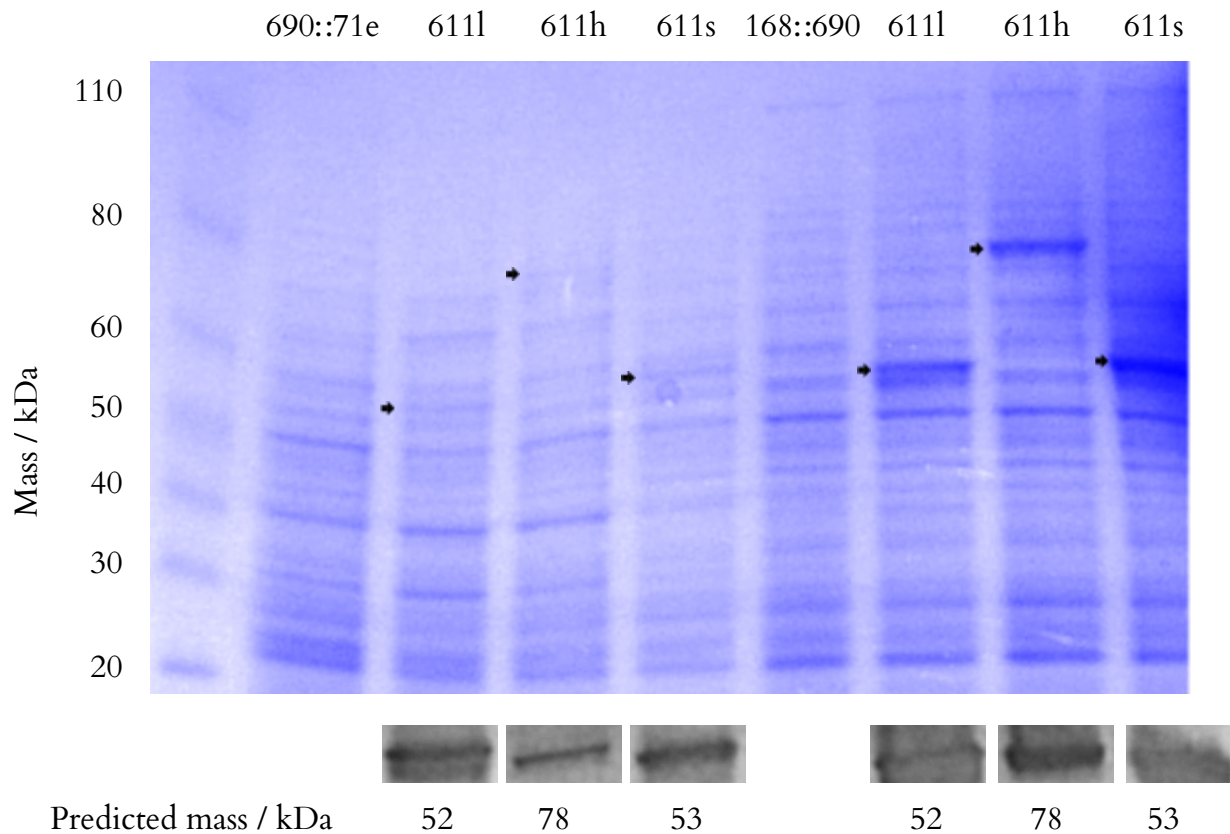


Figure 4.4: Fractionated crude lysates from WT coat and  $\Delta cotE$  *B. subtilis* spores containing antibody fragments. Predicted bands on the SDS-PAGE are indicated with arrows; the corresponding bands are all present on the blot (inset below each lane). The experimental lanes are grouped by progenitor strain, with fragment labels; the ladder at the left is the Novex® Sharp Pre-stained protein ladder. Spores were processed and samples treated as previously described. The right-most lane on this photograph has been truncated to minimize display of interference from its neighbouring lane.

These proteins were extracted through mechanical disruption; this may well be a cause of the variation in extraction efficiency and the main cause of fragmentation. It is likely that lysozyme disruption, with its gentler conditions, would cause less variation and fragmentation, and therefore analysis of spore core extracts would more closely represent the state of the core.

#### 4.2.2 Behaviour of the $\Delta cotE$ strain

*B. subtilis* spores, with either viable outer coats or coat disruptions (based on 168::690 and 690::71e strains, respectively), were assayed using the lysozyme susceptibility test (see section 2.8.2). The specific strains chosen had been transformed, using pDBT6111, and spores were verified by fluorescence microscopy and western blot to contain NIP109 with C-terminal GFP fusions (e.g. figure 4.4).

When viewed with phase contrast, only the coat-deficient strain (71e::611l), and only when challenged with lysozyme, showed lysed spores (figure 4.5); for all other conditions the spores were structurally intact, as can be seen in the other panels. For the  $\Delta cotE$  strain, challenged with lysozyme, the localized spots of fluorescence correspond only to spores which, in phase contrast, remained phase bright — *i.e.* spores which had not been disrupted.

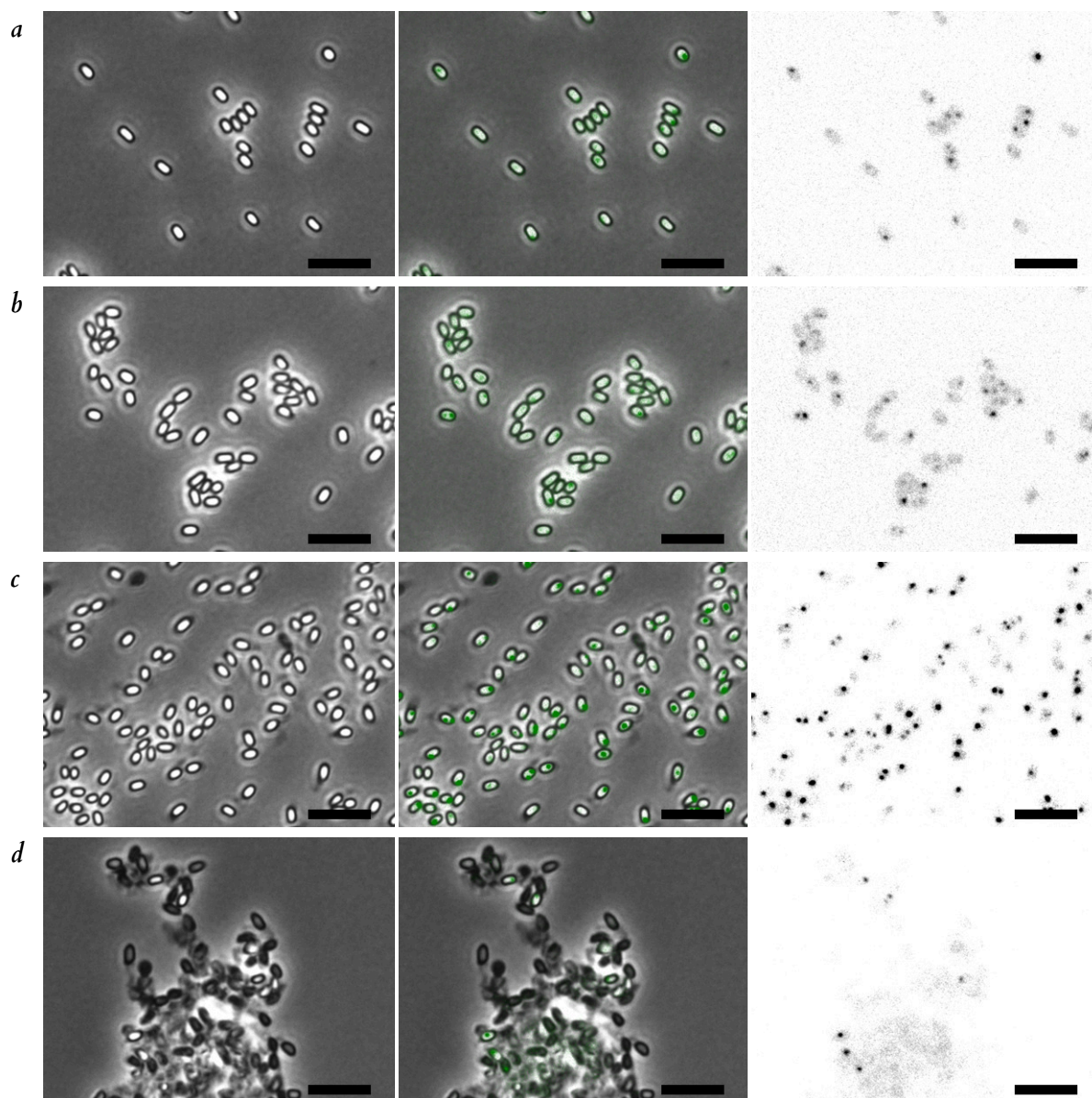


Figure 4.5: Micrographs (phase contrast, composite, fluorescence) of *B. subtilis* spores containing fluorescent antibody fusions, challenged with lysozyme. (a) shows spores with WT coat in buffer; (b) and challenged with lysozyme; (c) shows coat deficient spores in buffer; (d) and challenged with lysozyme. Only the  $\Delta cotE$  strain, and only when challenged with lysozyme, showed disrupted spores (phase dark and lacking distinct fluorescence). Strains are negative control 690::611l, with intact *cotE*, and  $\Delta cotE$  strain 71e::611l: transformed from their base strains using pDBT6111. Spores were produced using nutrient exhaustion and challenged on a rolling platform with  $50 \mu\text{g ml}^{-1}$  lysozyme overnight at  $4^\circ\text{C}$ . Scale bars are  $5 \mu\text{m} \times 1 \mu\text{m}$ .

One should infer from this assay that  $\Delta cotE$  spores, challenged with lysozyme, released their contents; this matches the behaviour described by Zheng *et al.* (1988). The fluorescence micrographs show that non-disrupted spores contained the fluorescent, antibody-fusion proteins. These two properties of  $\Delta cotE$  spores make them suitable as a platform with which researchers might produce sufficient heterologous spore core protein for analysis of protein quality, using the techniques of formulation science (section 1.2.5).

From a laboratory perspective, the ability to operate the spore extraction process at larger scale, thanks to lysozyme sensitivity, would certainly be valuable. It may be valuable, too, for release of a therapeutic payload from the spore core, in a pharmaceutical formulation. Even if the coat-disrupted spores were susceptible to gastric fluid, it may be possible to protect them during transit through the stomach. Perhaps a lyophilized pellet of lysozyme and spores could be covered in an enteric coating; the pellet would hydrate on reaching the intestine and lysozyme would disrupt the spores, releasing their payload. There are options to further engineer the outer layers of the spore to induce sensitivity to antagonists, present at delivery locations *in vivo*. One option might be to harness a CLE (cortex lytic enzyme) stored natively as a zymogen, such as SleC from *Clostridium*, present as ProSleC in dormant spores. A formulation could be designed such that these spores lyse at the correct part of the gut.

A more straightforward option would be available were intestinal fluid shown to disrupt  $\Delta cotE$  spores — wherein lysozyme would be redundant. Ideally,  $\Delta cotE$  mutant spores would lose their (intestinal) pepsinogen resistance but retain their resistance to the stomach enzyme, pepsin; this is indeed possible. There is value in ascertaining whether this hypothesis is correct. The spores shown in figure 4.5 would make for a suitable test strain; indeed other than the test fluids (gastric and intestinal), the experiment would look much the same as that shown here. In addition to the microscopy tests, one could track the change in OD<sub>600</sub> over time, for spores exposed to such challenges, for both lysozyme and simulated gastric and intestinal fluids. Preliminary work, here, did not reach a stage at which it could produce results; indeed, the kinetics of the disruption are important for detailed design of a suitable laboratory protocol.

One must have confidence that coat-deficient spores retain the aforementioned desirable properties for a pharmaceutical formulation. The *B. subtilis* 168::690 spores produced here were indistinguishable from wild type *B. subtilis* 168 under microscopy. The sporulation efficiency and yield appeared unchanged — there was no noticeable difference between plates of either strain. Spores germinated to produce vegetative cells, which themselves

sporulated and responded to arabinose just as cells which had not undertaken such a sporulation–germination cycle. Resistance to wet heat remains to be tested, both for the supercompetent strain and its  $\Delta cotE$  derivative; this is an important proxy measurement for ensuring the protection of proteins in the spore core.

During washing, water formed beads on the *B. subtilis* 690::71e spore-covered plate's surface. These spores, unlike their parent strain with a full copy of *cotE*, clumped during subsequent processing. They floated on the top of the System W mixture used to isolate them from vegetative cells. Despite this, neither cells nor sporangia were carried over into the final, washed spore suspension. Ball milling diminished the clumps such that optical density measurements could be taken.

From the high surface tension of water on  $\Delta cotE$ , one might infer that clumping of the washed spores is due to hydrophobicity. The high hydrophobicity of the *B. subtilis*  $\Delta cotE$  mutants is consistent with the loss of their hydrophilic outer coat and crusts. Surfactants, such as Tween-20, are typically used in cleaning hydrophobic strains such as *B. cereus*. It is likely that such surfactants would reduce clumping for this strain. However, when testing the spores' resistance to enzymatic challenge, it would be good to find a non-chemical methods to reduce aggregation; otherwise one ought to investigate interference of surfactants with the enzyme behaviour. In the long term, it may be worth engineering the  $\Delta cotE$  strains to display a more hydrophilic surface, not least to simplify industrial processing.

Sporulation yields were informed by the visual thickness of the growth on plates and the size of the recovered pellet. An approximate estimate of relative yields was calculated from equivalent optical densities ( $OD_{600}$ ) of resuspended pellets. These were analysed using a paired comparisons model (Montgomery, 2012). Base strains were paired; strains transformed with the same plasmid were paired, too.

The  $\Delta cotE$  variant showed a mean  $59 \pm 7\%$  decrease in the resulting optical density measurements, quoted as equivalent  $OD_{600}$  per millilitre (*i.e.* the volume in millilitres if the sample were diluted to an  $OD_{600}$  of 1). The paired comparison test (table A1.5) showed that the differences between the 168::690-derived strains ( $630 \pm 50 OD ml^{-1}$ ) and the 690::71e-derived strains ( $270 \pm 60 OD ml^{-1}$ ) were statistically significant ( $t = -15.4$ ,  $p = 5.9 \times 10^{-4}$ ).

From these optical density measurements, one can infer a  $\frac{3}{5}$  drop in sporulation yield. The paired comparisons test suggests that this measurement is reliable across batches, for given sporulation conditions. It is likely that much of this effect was due to differences in the

number of spores produced, and a little was due to the aggregation. Spores with a  $\Delta cotE$  mutation fail to produce a complete coat; mother cells are more likely to stop the process, as a result. However, the spore samples did not show excessive vegetative cells, as would be expected in that scenario. It is possible that the 690::71e-derived strains sporulated at a lower cell density. Some of the difference in optical density will be due to aggregation, though while the aggregates were larger than individual spores, they remained in the same scattering regime. This difference could be resolved by measuring the viable colony count, but that assumes there is no difference in germination efficiency due to the  $\Delta cotE$  mutation — which would run counter to the evidence of Zheng *et al.* (1988).

While this  $\Delta cotE$  mutant strain enables the rigorous analysis of heterologous proteins, there remain other laboratory challenges. For example, the first candidate  $\Delta cotE$  strain (spectinomycin<sup>r</sup> 5-FU<sup>s</sup> ::  $\Delta cotE$  +*spc* +*upp*) was notably slow growing, compared with *B. subtilis* 168::690. While there are anecdotal reports of  $\Delta cotE$  mutant strains growing slowly (G. Christie, personal communications, 2013–2019), it was not clear why this should be so. It was only when this first candidate displayed other undesirable behaviour (a visibly poor sporulation yield, close to 50% of the 168::690 strain, and loss of the inducible competence phenotype) that it became evident that the strain had a problem. None of these behaviours was seen for the second candidate; it is therefore likely that there had been a genome rearrangement, of some description. Despite that, the *B. subtilis* genome is usually stable, in that allelic exchange will usually cause genome changes at only the one locus. As whole genome sequencing becomes routine, any genome loss, or rearrangements, will be apparent during colony screening. Meanwhile, before characterization of proteins produced at scale by  $\Delta cotE$  strains, it would be worth sequencing the full 690::71e strain genome, to identify any such changes. It would also be valuable to complement the strain with a functional *cotE* to confirm that the WT phenotype results.

The  $\Delta cotE$  strains here were based on inducibly competent *B. subtilis*, designed for marker cycling with counter-selection. Improvements to cloning velocity were invaluable, despite some technical issues.

### 4.2.3 Inducible competence and counter-selection

Inducibly competent cells proved to be as useful as suspected, and made simultaneous transformation of multiple candidate strains feasible. However, there are a number of ambiguities in the transformation protocol of Shi *et al.* (2013); in attempting to replicate their work many were identified and resolved.

The gene *upp*, commonly used in Gram-negative bacteria, confers sensitivity to 5-FU (fluorouracil). *B. subtilis* contains such a gene, natively; Fabret *et al.* (2002) reported how knocking out *upp* allows use of 5-FU as a counter-selection marker. When the authors flanked the cassette with 30 bp repeats, they saw spontaneous pop-out of the cassette at an elevated frequency of 1 in  $10^6$ ; homologous recombination with the chromosome more generally requires repeats of 400–500 bp. Taken together, this allows for marker cycling with an efficient marker regeneration step. This research was further developed into the protocol of Shi *et al.* (2013).

This protocol states that the culture is induced to competence at  $OD_{600}$  1, yet gives no idea of precision. In the standard arabinose induction protocols,  $P_{ara}$  is only induced during linear growth. In the standard chemical competence protocols, *B. subtilis* cells are only incubated with CaCl once they reach stationary phase. Presumably, the authors' intention here was that cells should be at the end of exponential growth, and are in their linear growth phase when induction takes place. Attempts to induce overnight cultures, which had passed into stationary phase, did result in some colonies, though far fewer than those induced at the suggested point of growth, and only visible after 24 h rather than 16 h. In all other cases, cultures were induced when  $OD_{600}$  were measured to be between 0.8 and 1.2, and there was no evidence of a relationship between  $OD_{600}$  and transformation success.

Induced competent cells also lack the immediacy of a stock stored in a  $-80^\circ\text{C}$  freezer. In order to freeze bacterial cells in this manner, they typically require a cryoprotectant. Shi *et al.* (2013) did not report details of such treatment for their strain. Freshly prepared competent cells could in fact be supplemented to 7% v/v DMSO, then flash frozen and stored at  $-80^\circ\text{C}$ ; these cells retained their competence, and could be transformed just as their freshly prepared counterparts.

Attempts to delete the native *upp* from *B. subtilis* 168 in the manner of Shi *et al.* (2013) failed, with all colonies showing the wild type locus. Transformation of *B. subtilis* 168 with the 4527 bp linear fragment, corresponding to the replacement *upp* operon, resulted in ~600

colonies, none of the 2% screened had the desired mutation: indeed, all were false positives. This trade-off is as described by You *et al.* (2012). A transformation protocol producing fewer false positives is more desirable; this is the case even though there are fewer true positives. Even for the supercompetent strains, transformation using plasmids offers exactly that trade-off, and so plasmids were used for all subsequent cloning in this chapter. Eventually, a more conventional transformation with pDBT69d, selecting on Chloramphenicol, was successful (see sections 2.4.4, A1.7).

Counter-selection with 5-FU proved disappointing. From the gradient plate analysis (figure 4.6), selection with 5-FU appeared to be somewhat reliable, in that there were lawns for the strain with the resistant genotype, yet that with the sensitive variant showed only sporadic colonies. However, those sporadic colonies appeared across the entire plates. A concentration of  $\sim 40 \mu\text{M}$  retarded growth of the 5-FU<sup>s</sup> lawn, but permitted growth of the resistant strain, and so a concentration of  $37.5 \mu\text{M}$  (corresponding to 0.075% v/v) was picked for subsequent selection. The sporadic, 5-FU-sensitive colonies were more prevalent on sample  $10 \mu\text{M}$  plates, matching the Fabret *et al.* (2002) and Shi *et al.* (2013) protocols, than on the  $37.5 \mu\text{M}$  plates. Even with selection at a variety of 5-FU concentrations, it was not possible to isolate a 5-FU<sup>s</sup> strain from transformation with pDBT690: a plasmid equivalent to pSS (that used by Shi *et al.*, 2013). Given that a strain with the desired genotype was eventually isolated, this appears to be a consequence of transformation efficiency — specifically, selection on 5-FU. It was the ability to validate the selection process, using the chloramphenicol<sup>r</sup> 5-FU<sup>s</sup> strain 168::69c, that proved invaluable; perhaps Shi *et al.* (2013) had other strains suitable for this, though they gave no mention in their publication. As a consequence, marker cycling for *B. subtilis* 690::71e was unsuccessful.

The value of 5-FU was not diminished by the initial failure of direct selection. Rather, its critical deficiency was failure to select strains following digestion with *I-SceI*, i.e. a) stationary phase recombinant strains (rather than recovered chemically competent cells), b) following a single homologous recombination event (more probable than a double crossover), for which c) there is a double strand break in the genome (enhancing the chance of homologous recombination). These factors make viable colony formation far more likely; failure here thus greatly reduced the value of the technique.

Perhaps *upp* counter-selection is not such a great idea after all, though some form of counter-selection would still be useful in this system. Based on this experience with *upp* and 5-FU, the most promising alternative might be the *pheS* system, selecting on *para*-chlorophenylalanine. In that system, the presence of the mutant *pheS* cassette confers



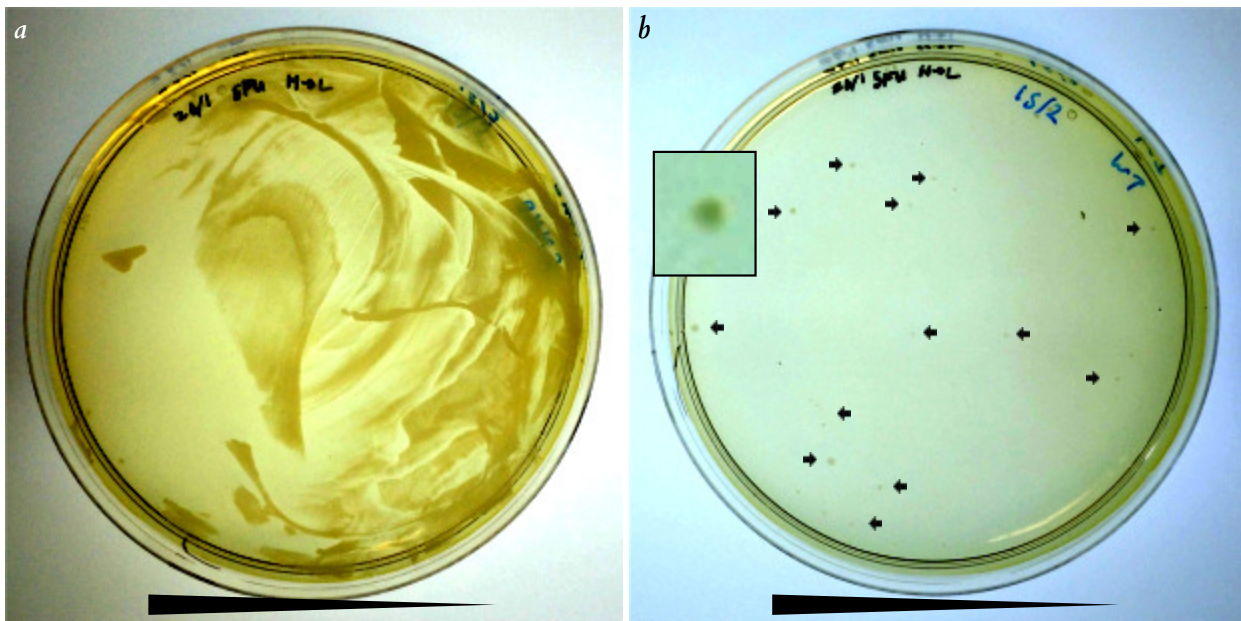


Figure 4.6: Gradient plates ( $\varnothing$  90 mm) of 5-FU (fluorouracil), spread with *B. subtilis*. (a) shows  $\Delta upp$  strain 168::69c; (b) shows WT. A smooth, near-confluent lawn of growth can be seen for the nominally 5-FU-resistant strain (168::69c) at concentrations  $\lesssim 40 \mu\text{M}$ . By contrast, the WT strain (168) produced sporadic colonies, some of which are indicated on the image with arrows; the inset is a magnified region including the colony just to its right. Concentration gradients were linear, increasing 0–50  $\mu\text{M}$  from right to left, as indicated by the triangular bars; the regions of the plate beyond these bars were at the minimum or maximum concentration.

sensitivity, even in the presence of native *pheS*. This dominant phenotype means that unlike with *upp*, counter-selection is feasible in strains with an existing copy of *pheS* (which includes all strains reported here). Furthermore it should be straightforward to determine whether *B. subtilis* strains without the mutant *pheS* allele are reliably resistant as on chloramphenicol, and as opposed to their behaviour on 5-FU. Finally, Carr *et al.* (2015) reported two tips for generating a suitable *pheS* for a strain: that the cassette works better (at least in *T. thermophilus*) when the protein is native but the nucleotide sequence shares minimal homology with the native DNA, and *para*-chlorophenylalanine can be added to agar before autoclaving (and in fact it was necessary as its water solubility is poor). The former tip may have precluded use of such a system, until the recently widened availability of gene synthesis; the latter indicates another advantage of *para*-chlorophenylalanine over 5-FU, in preparing working solutions.

Difficulties, experienced with 5-FU, themselves demonstrate the benefits of counter-selection. Such benefits will be invaluable as use of a spore platform becomes routine, and the research focus shifts to functionality of the therapeutic proteins.

#### 4.2.4 Nanobodies expressed by sporulating *B. subtilis*

There is a major obstacle in verifying the functionality of NIP109 fragments, produced in the forespore core. Conventionally-produced NIP109 is only available in its full IgG form. Given  $\Delta cotE$  strains can produce heterologous proteins and be disrupted by lysozyme, it may now be possible to verify assembly, within the spore core, of full IgGs. This is not yet possible; the failure of 5-FU counter-selection impeded the relevant experiments. Thankfully it is also not necessary for testing functionality; an alternative without a complex quaternary structure, such as a nanobody, might be more amenable to a functional assay.

*B. subtilis* subsp. *subtilis* 168 aliquots were transformed to Chloramphenicol resistance with pDBT65\* plasmids, containing coding sequences for the nanobodies in table 4.2 (see listing A1.2 for the sequences). The resulting strains 168::65\* were induced to sporulate and examined in a similar manner to section 4.2.1. Most microbiological work with nanobodies was performed by undergraduate research students Joshua Cozens and Luke Vinter, or by masters student Tayla Gordon.

*Table 4.2: Nanobodies, used in this chapter. In all cases the authors of the nanobody sequence demonstrated binding of the nanobodies to their target. The code is the plasmid/strain suffix; the masses include the nanobody and C-terminal 6×His tag. The  $\beta$ -lactamase sequences were located by undergraduate research students Luke Vinter and Joshua Cozens.*

Code	Nanobody	Target	Source	Mass / kDa
1	BcII10	<i>Bacillus</i> metallo- $\beta$ -lactamase	Conrath <i>et al.</i> (2001)	14.7
2	TEM02	TEM-1 $\beta$ -lactamase	Conrath <i>et al.</i> (2001)	14.2
3	TEM13	TEM-1 $\beta$ -lactamase	Conrath <i>et al.</i> (2001)	14.0
4	V <sub>H</sub> H GFP4	eGFP (enhanced green fluorescent protein)	Kirchhofer <i>et al.</i> (2010)	12.8

Just as for antibody fragments, sporulating cells deposited nanobodies in their cores. Both the BcII10 and V<sub>H</sub>H GFP4 nanobodies were produced (strains 168::6510 and 168::6540 respectively), and shown to migrate to the predicted bands under PAGE (figure 4.7 shows a

corresponding western blot). The only discernible bands were at the predicted masses for each protein. In addition, masters research student Tayla Gordon was able to demonstrate that sporulating cells of strain 168::651m can produce chromobodies (see figure 4.8).

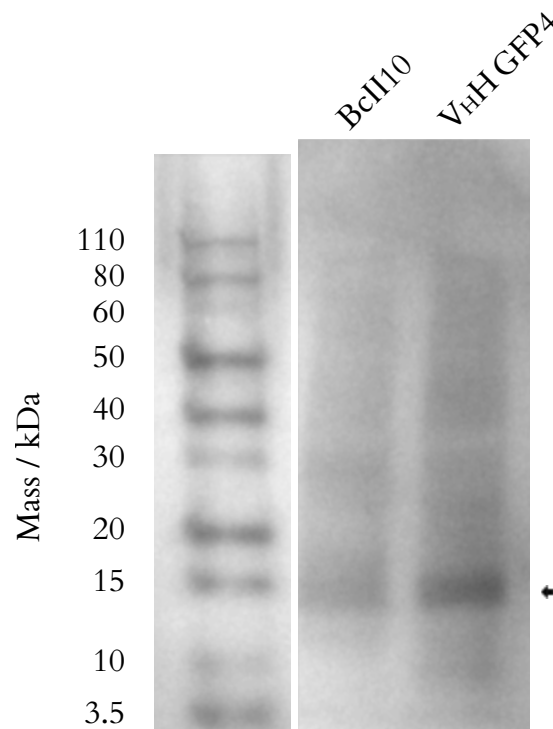


Figure 4.7: Western blot of *B. subtilis* 168::6510 (BcII10, 12.8 kDa) and 168::6540 (V<sub>H</sub>HGFP4, 14.7 kDa) spore core extracts. Bands are present at the predicted sizes. Spores extracts were fractionated and blotted as previously described.

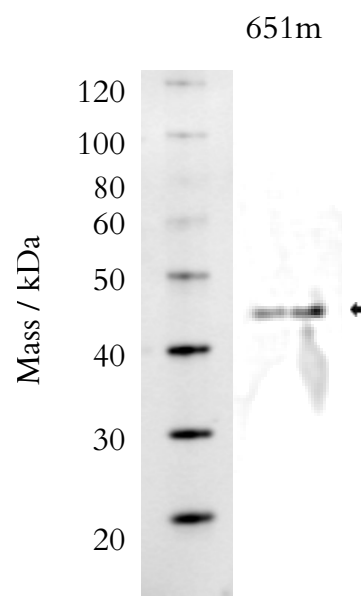


Figure 4.8: Western blot of extract from strain 168::651m (BcII10-mCherry chromobody). The predicted band at 42.5 kDa, indicated with the arrow, is present. Spores extracts were fractionated and blotted as previously described. The blot was produced by masters student Tayla Gordon.

Fractionated, purified, extracted cores of strain 168::6510 (engineered to express BcII10 nanobodies) showed predicted bands on a polyacrylamide gel (figure 4.9). The HisTrap-purified extract shows a band at the predicted mass of the BcII10 nanobody (14.8 kDa, see table 4.2). There is also a band at 60 kDa, and a faint band around 48 kDa, which most likely correspond to aggregates. The His tag would still be present on aggregates, which would then bind along with the desired monomer and elute into the purified sample. Insufficient quantities of TEM02 and TEM13 were isolated to detect.

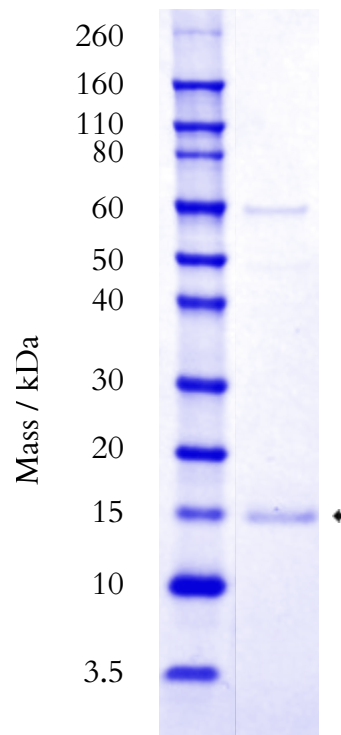


Figure 4.9: Fractionated, purified extracts of *B. subtilis* 168::6510 spores (BcII10 nanobodies). The band at the predicted mass, 14.8 kDa, is indicated by the arrow. The crude extract was purified using a HisTrap column. Eluents were concentrated from 5 ml to 500  $\mu$ l using 3 kDa columns. Samples were otherwise extracted and fractionated as described previously, alongside a Novex® Sharp ladder. All this nanobody work was performed by undergraduate research students Joshua Cozens and Luke Vinter.

Compared with the antibody results, those for the nanobodies were a little more mixed. While the V<sub>H</sub>H GFP4 and BcII10 nanobodies were produced, the same could not be said for the TEM02 and TEM13 variants. Indeed, as the extraction and purification protocol gave a positive result for the BcII10 nanobodies, it is likely these TEM variants were not expressed. It is not clear at which point the process failed; it could have been poor codon optimization, instability of the final protein (perhaps related to missing disulphide bridges) or problem inherent to the sequences. More positively, despite sporulation failures seen with the V<sub>H</sub>H GFP4-mCherry chromobody, the BcII10-mCherry chromobody was successfully expressed. Taken together, this is good evidence that sporulating *B. subtilis* are capable of producing a range of nanobodies.

## 4.2.5 Path to a commercially viable product

### Do expressed proteins function?

While these results demonstrate that antibody fragments and nanobodies can be produced by sporulating cells, they provide no further evidence that those proteins function correctly. Assaying function is tricky; in previous, related work, Mohamed (2015) performed a binding assay on the anti-lysozyme scFv produced in his optimized strain, though the assay, using spore lysate, was difficult to validate (and gave slightly nonsensical results: no signal for some positive controls). The proteins chosen for use in this chapter offer the promise of robust functional assays, in the future.

While useful as a model IgG and therapeutically relevant humanized antibody, NIP109 is at a disadvantage when it comes to a functional assay. NIP109 is a hapten binder; that means it binds the small hapten molecule, NIP (4-hydroxy-3-iodo-5-nitrophenylacetic acid), for which it is named. The resulting antibody-hapten complex will generate a measurable immune response. For the NIP109 functional assay, one must measure this response. There are two difficulties with this approach: the antibody configuration, and isolating sufficient quantities.

MedImmune use NIP109 in the form of a whole IgG, and do not even have standard scFv constructs (C. F. van der Walle, personal communications, 2016). There is neither specific evidence that these particular antibody fusions demonstrate hapten-binding, nor that the resulting complexes generate an immune response. One may therefore wish to use this spore expression system to produce full IgGs rather than individual chains, or fusion fragments; indeed there was some progress made in developing plasmids to construct such strains. However, this is far from straightforward. One must match expression ratios of the light chain and heavy chain; work by Guiziou *et al.* (2016) indicated potential promoter mutations to help with this challenge.

There is also no established technique (such as BiFC, bimolecular fluorescence complementation) for assessing protein interactions *in vivo* in the spore core. It would be worth validating BiFC (bimolecular fluorescence complementation) within the spore core; this would then help indicate the nature of interactions within the spore core itself, both in the context of therapeutic proteins and basic microbiology of spores — in particular, how proteins are stably maintained. Without such a technique, assessing IgG assembly would

involve native PAGE, which would enable direct comparison of spore and CHO sourced antibodies. However, with mechanical disruption one cannot be confident that the condition of antibodies in the lysate reflects their state in the spore core.

That last point touches on the second difficulty: that of isolating sufficient quantities of protein for an immunoassay. A rigorous set of assays requires reliable production of milligram levels of protein. Scaling up the spore batches to produce such quantities is relatively straightforward; growth of spores on plates scales linearly in the number of spores required, using a CSTR (continuous stirred tank reactor) would make this growth sublinear and much of the subsequent processing benefits from economies of scale. However, mechanical disruption is a major bottleneck. A new technique to disrupt spores in the laboratory is a requirement for producing protein of sufficient quantity, never mind quality.

To this end, the nanobodies may prove useful. They do not require inter-domain association to effect their functions, though the issues of spore disruption remain. For the anti-GFP nanobody V<sub>H</sub>H GFP4, a binding assay would test the nanobodies' ability to attach specifically to GFP and a functional assay that such complexes show diminished fluorescence. In a binding assay, the anti- $\beta$ -lactamase nanobodies would need to demonstrate that they form complexes with their corresponding  $\beta$ -lactamase. In a functional assay, working nanobodies would re-sensitize  $\beta$ -lactam resistant bacteria. There is another functional assay, which measures  $\beta$ -lactamase activity via colour change of the cephalosporin *nitrocephin*. Though nitrocephin degradation is only one example of  $\beta$ -lactamase degradation, and that itself is only a proxy for antibiotic resistance, the mechanisms are generally well understood and the colour change makes for a robust screening assay. Indeed, preliminary work on the nitrocephin assay, by masters student Tayla Gordon, suggests that the BcII10 nanobodies can inhibit the  $\beta$ -lactamase induced colour change, meaning it is a promising avenue for the future.

Finally, in producing spores which carry a therapeutic protein payload, it does not matter whether these proteins are functional in the core; it only matters that they do not degrade there, and are functional when released. Characterising this must be a goal of future research.

### Expression levels

It is not enough that spores bear functional therapeutic proteins; if the level within a spore is too low, the spore dose would be infeasible — as would research into protein quality. The *B. subtilis* spore preparations on 90 mm 2×SG plates typically yield a quantity of spores which

if suspended at  $OD_{600}$  of 1 would take a volume of 150 ml; this is hereafter described as equivalent to an  $OD_{600}$  of 150, even though the linear relationship between  $OD_{600}$  and particle density is only valid for  $OD_{600} \lesssim 1$ . Mohamed (2015) supplies the figures for yield in terms of this equivalent  $OD_{600}$  of a spore suspension, based on  $OD_{600}$  1 corresponding to 0.1 mg spores. According to this conversion rate, one 90 mm plate yields 150 times this, *i.e.* 15 mg spores. At least 10 plates of spores would be needed to produce a single, daily dose of single chain insulin, and the daily dose of full IgG would need perhaps 40 000. In practice, producing such quantities is far beyond the scope of this project. However, the full battery of protein characterisation tests used by formulation scientists requires 250 mg protein *per variant* (see section 1.2.5). With the productivity presented by Mohamed (2015), this corresponds to 300 g spores, *i.e.* 20 000 plates.

One might no doubt propose changing the method by which spores are grown, and harvested, perhaps taking advantage of the recent developments in cGMP (current good manufacturing practice) manufacture of spores. Unfortunately, there is one step for which such an improved process does not exist, and that is extraction of the contents of spores. The use of  $\Delta cotE$  mutants, as explored in this chapter, may help, here.

### **Analysing the spore core *in vivo***

Indeed it is problematic that the core proteins must be extracted, for analysis. The properties of proteins within the spore core are important, and the dearth of techniques for probing such a location is problematic. The standard biophysical techniques for *ex vivo* analysis of proteins are impossible here; one could not, for example, perform dynamic light scattering on a spore core. What remains are inference techniques, relying on extensively controlled interaction experiments; none has yet been implemented for the spore core.

The most immediately implementable of these is BiFC (bimolecular fluorescence complementation), in which a pair of non-fluorescent, weakly interacting domains of YFP (yellow fluorescent protein) are fused to the target proteins; if the target proteins interact, only the correctly paired fusions will fluoresce. (One might consider the system of Trauth & Bischofs, 2014, to reduce background noise.) BiFC requires positive controls with two proteins known to interact (Kudla & Bock, 2016), and given the state of the dormant spore core it is not clear which proteins do interact there. It is possible that IgG chains turn out to be suitable here, as positive controls.

A compromise approach may be hydrogen–deuterium–exchanged mass spectrometry (Dobson *et al.*, 2016). The spore core does exchange ions with its environment. The hydrogen atoms on these proteins could therefore be exchanged with deuterium. Minuscule quantities of these protein would be required for subsequent analysis. Protected proteins within the core are likely to resist the hydrogen–deuterium exchange; a comparison with exchange beyond the core, perhaps in other pharmaceutical formulations, would give a good indication of the relative degree of protection the spore affords.

With such techniques, one would have a suitable platform for screening protein interactions within the spore core, without needing to produce large spore batches. This would be a useful addition to a spore formulation tool-kit, and could well lead to an improved understanding of the spore core.

Many of these remain an open research problems: both in order to develop a potential formulation, and as a prerequisite for conducting the necessary plethora of formulation experiments on spore proteins, before spores bearing therapeutic proteins can become a viable commercial offering.



### 4.3 Conclusions

The research presented in this chapter seeks to evaluate whether bacterial spores are viable carriers for therapeutic antibodies. Results demonstrate that sporulating *B. subtilis* cells can produce a variety of therapeutic proteins. These proteins — IgG fragments (NIP109) and nanobodies — have the correct masses, and are highly likely to have folded correctly, too. Spores bearing the *cotE* mutation demonstrated sensitivity to lysozyme, and the same capability to produce heterologous proteins WT backgrounds. These spores form a proof-of-principle bacterial spore formulation.

The nanobodies show mixed results; both the V<sub>H</sub>H GFP4 and BcII10 nanobodies were produced successfully, though corresponding chromobodies followed only in the latter case. Though these fragments have been produced in the core, it may also be possible to use these configurable binding proteins to decorate the spore (Lin, 2017), perhaps as sensors, or for environmental clean-up. There is a straightforward functional assay for  $\beta$ -lactamase activity, and when the strains of spores which produce the relevant nanobodies can themselves be produced and disrupted at scale, it will be possible to evaluate whether these nanobodies do indeed function.

There is a different story for NIP109, the IgG from MedImmune. A variety of fragments — individual chains and scFvs — were produced. The next steps would be to produce both chains in the same spore, and attempt to assemble a full IgG. However, the necessary technology does not yet exist, to allow for satisfactory evaluation of the result. There is neither technology to characterize interactions between the chains, within the core, nor to disrupt the spores at scale and in a minimally damaging manner so that proteins can be analysed *in vitro*. Although NIP109 is a standard model antibody, its scFv is not; it is best evaluated in its full IgG form. With work on such techniques in future, *B. subtilis* spores might become useful for delivering therapeutic proteins. The benefits of such a protein platform might be greatest for non-IgG therapeutic proteins, however.

The single, simple  $\Delta$ *cotE* mutation may resolve both the laboratory and formulation core-release problems. It appears that spores bearing this coat deficiency correctly produce heterologous proteins in their cores, too. These spores must, however, retain their other resistances: the properties which make them desirable as a pharmaceutical formulation. In particular, it is highly desirable that these spores maintain their resistance to wet heat, as it is this challenge which primarily damages spore core proteins. Were the stability conferred on

proteins packaged in the core found to suffer, formulating with such spores would no longer be a viable approach. This is unlikely; the coat deficiency was first reported thirty years ago, with no reported loss of heat resistance since. It is the use, here, that is novel.

It remains to be seen what sensitivity these spores have to gastric and intestinal fluid, and to that end, experiments in which these spores were challenged with those fluids will be worthwhile. This system might yet provide a novel, simple way to release encapsulated proteins from the spore *in vivo*.

Despite the advances presented here, many challenges with packaging therapeutic proteins in the spore core remain. It may be possible to use a completely different sporulation system to produce therapeutic proteins, thereby obviating the requirement to disrupt spores to release the active ingredient; this forms the topic of the next chapter.

## Chapter 5

# Cry protein fusions

## 5.1 Introduction

One difficulty with producing therapeutic proteins in the sporulating *B. subtilis* forespore is described in detail in section 1.4.3: heterologous protein comprises a low proportion of the resulting spore. By contrast, there is one sporulation system notable for the scale of its protein production: the Cry machinery of *B. thuringiensis*. In a review, Agaisse & Lereclus (1995) asked “How does *Bacillus thuringiensis* produce so much insecticidal crystal protein?” — and mercifully they answered, too (see section 1.3.3). Can this system be engineered to produce heterologous fusions of therapeutic proteins?

Despite a great deal of research into Cry proteins over the past century, focus has fallen mostly on the toxins, which form but one part. Few publications considered affordances of a robust crystallization process, already operating at scale (Nair *et al.*, 2015; Roh *et al.*, 2004; Sawaya *et al.*, 2014). Others have considered these same proteins for surface display instead (Du *et al.*, 2005; Shao *et al.*, 2009). These researchers all produced single fusions to full length Cry proteins, or single subdomains (for Cry1Ac). This chapter presents a systematic approach.

Cry1Ac, native to *B. thuringiensis* subsp. *kurstaki* HD-73, is fused in combinations of its subdomains, the fluorescent protein mCherry, and antibody fragments. The expression operons are tested in *B. thuringiensis*, *B. cereus* and *B. subtilis*. *B. thuringiensis* HD-73 produces native Cry1Ac crystals; the other strains do not. Triple fusions of a Cry domain, mCherry fluorophore and antibody fragment are a prerequisite for a Cry-protein antibody platform.

The TEMs (transmission electron micrographs) in this chapter were prepared by fellow PhD candidate Sina Schack, whose own project builds on this work.

## 5.2 Results & discussion

### 5.2.1 Cry1Ac subdomain fusions

The region which confers on the full Cry1Ac protein the ability to form crystals, corresponding to domains IV–VII at the C-terminus, is known as the *protoxin* domain, and the three N-terminal domains, I–III, as the *toxic core* (see figures 1.9, 5.1).

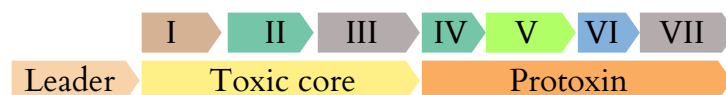


Figure 5.1: The domains of the Cry1Ac protein (arranged as primary structure). The native operon comprises (from N- to C-terminus) the leader, the toxic core, and the protoxin domains. The seven subunits of the protein make up the toxic core (I–III) and protoxin (IV–VII) domains.

By breaking the *cry1Ac* coding sequence into leader, protoxin and toxic core, there are 21 different mCherry fusions it is possible to make.

- Each of the three native regions can be present or absent.
- Each of these ( $2^3 = 8$ ) can take an N-terminal, C-terminal or no mCherry ( $\times 3 = 24$ ).
- However, there is only one option with none of the three native elements ( $-2 = 22$ ).
- Additionally, both N- and C-terminal fusions are identical when only the leader and mCherry are present ( $-1 = 21$ ).

Of those 21 fusions, eight are indicated in table 5.1. Coding sequences were assembled into pDBT30 (see table 2.2, figure 2.2), a general purpose vector for *B. thuringiensis* derived from the high copy number *E. coli*–*Bacillus* shuttle vector, pHT315, for expression, in *Bacillus* species, of the Cry fusions. The coding sequences are flanked by the *B. thuringiensis* HD-73 native *cry1Ac* promoter and terminator regions. Plasmid pDBT310 is shown in figure 5.2. Further vectors in the pDBT31\* family feature the domains listed in table 5.1, in place of the native *cry1Ac*.

Aliquots of *B. thuringiensis* HD-73 were transformed to Erythromycin resistance with one of these pDBT31\* plasmids to give the corresponding HD-73::31\* strains, induced to sporulate and pelleted to concentrate the resulting spore-crystal slurries. Slurries were analyzed by microscopy and PAGE.

Table 5.1: Schematic representation of mutant *cry1Ac* fusion operons. The element names give rise to the mnemonic for identifying the variants. For example, the construct LTPm comprises the leader, toxic core, protoxin and mCherry sequences: in that order when tracing the primary amino acid structure from N- to C-terminus. The 6×His tag allows simpler downstream processing of the proteins.

Code	pDBT31...	Domains				Mass / kDa
LTP	0	Leader	Toxic core	Protoxin	6×His	133.6
Lm	10	Leader	mCherry		6×His	31.5
LmP	20	Leader	mCherry	Protoxin	6×His	96.6
LPm	30	Leader		Protoxin	mCherry 6×His	96.6
LTm	40	Leader	Toxic core		mCherry 6×His	95.8
LTPm	50	Leader	Toxic core	Protoxin	mCherry 6×His	160.9
m	710		mCherry		6×His	27.7
mP	720		mCherry	Protoxin	6×His	92.9

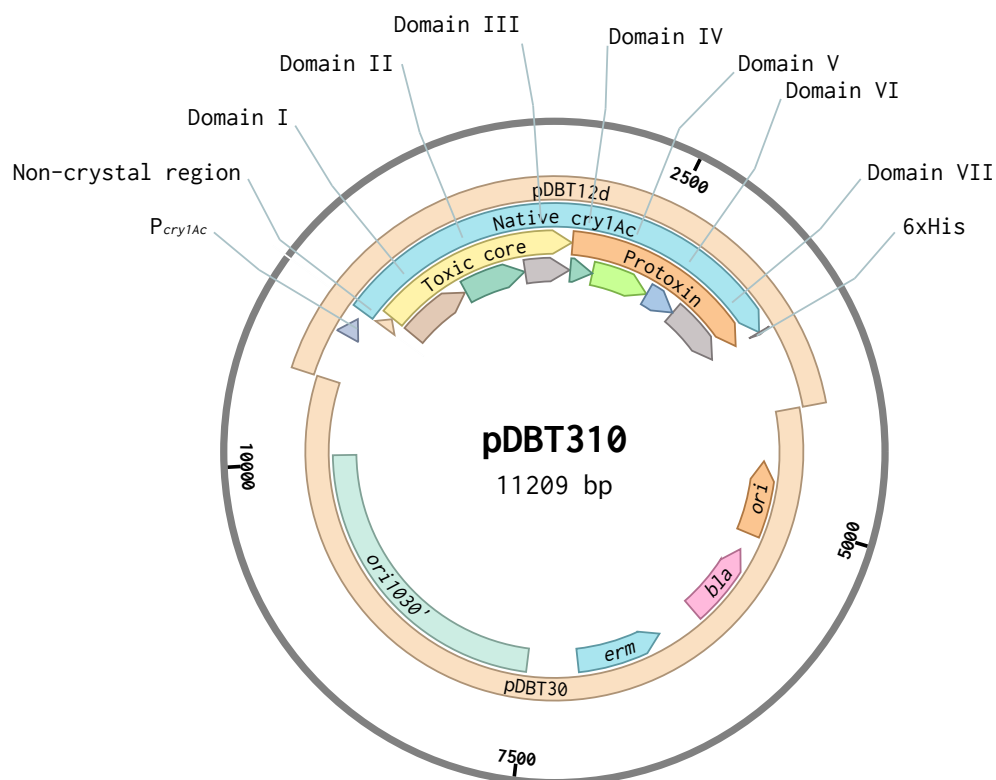


Figure 5.2: Plasmid pDBT310, for expression of (His-tagged) *Cry1Ac*, from its native operon. Antibiotic cassettes are *erm* (erythromycin) and *bla* (carbenicillin); the *E. coli* and *Bacillus* origins are *ori* and *ori1030'* respectively.

Figure 5.3 shows the outcome of fractionating the solubilized spore-crystal slurries, using PAGE. The Coomassie-stained gel shows bands of varying intensity present at all of the predicted positions, and at many other positions, too. Likewise, the western blots shows bands with a variety of intensities at all the predicted positions; there were also distinct bands present at various other positions, notably at 20 kDa for the LTPm and LPm variants (less intense bands can be seen at that position on the m and LTm lanes). The constructs in these lanes all feature C-terminal mCherry fusions. These bands are not seen on any lane without a C-terminal mCherry fusion. They are most likely C-terminal fragments of mCherry and its His-tag. (The His-tagged mCherry itself produced neither fluorescent bodies nor a convincing band.) From the gel and blot bands, it is clear that the solubilization protocol needs refinement.

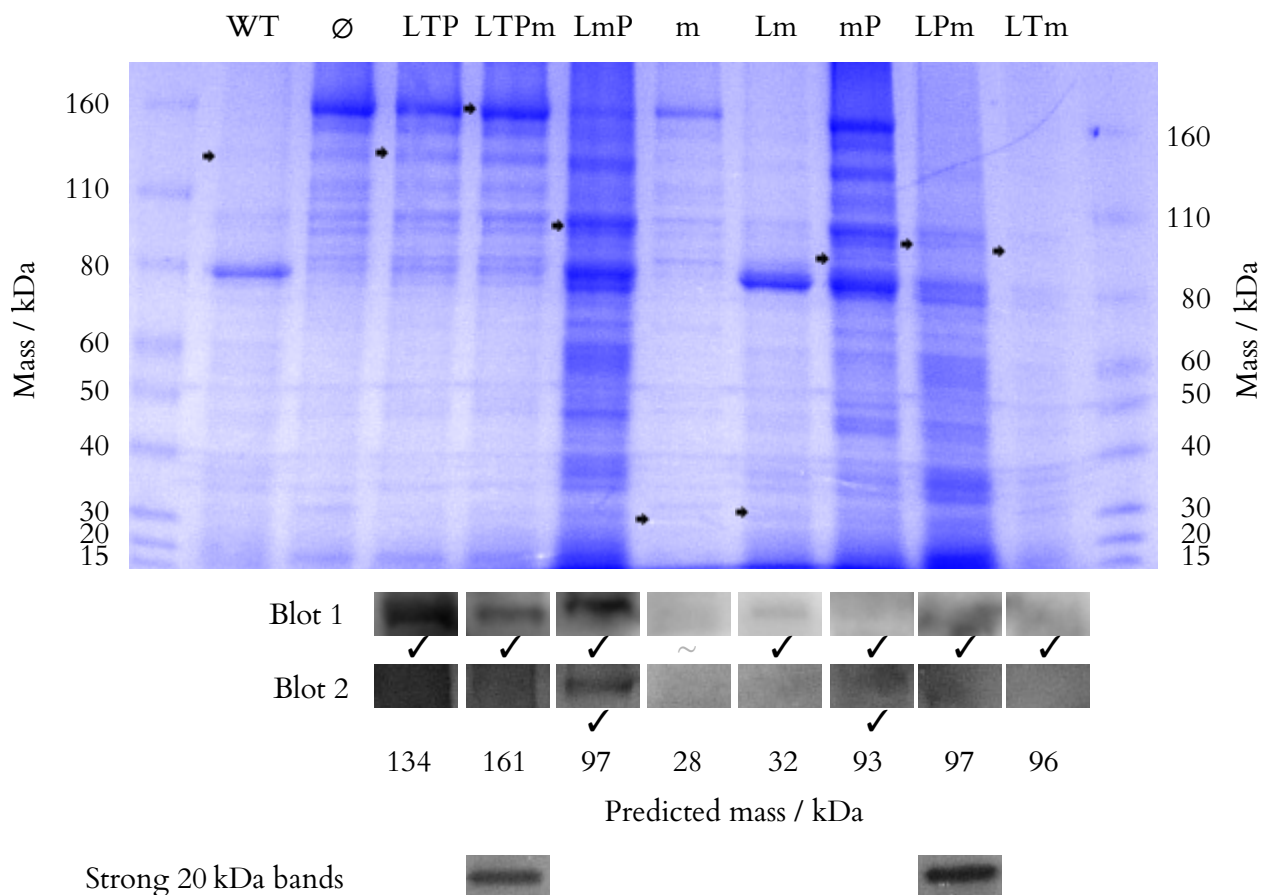


Figure 5.3: Analysis by PAGE of spore slurries for *B. thuringiensis* subsp. *kurstaki* HD-73-derived strains expressing Cry1Ac-mCherry fusions. All strains with Cry1Ac fusion (L, T, P) showed bands at predicted sizes on the associated blots (lower); bands are also visible on the (upper) gel. Arrows on the Coomassie-stained polyacrylamide gel indicate positions of the predicted bands (using the Novex® Sharp Pre-stained protein ladders). Snippets below cover the predicted band positions (and two 20 kDa regions) from corresponding western blots; ticks indicate presence of a detectable band, the tilde indicates possible presence, and no symbol indicates no band. Lane labels: WT (wild type), empty vector (∅) pDBT30 strain, HD-73::3\* strains. Spore slurries were produced by nutrient exhaustion, pelleted and resuspended in water at 10× concentration, and solubilized in LDS at the modified conditions.

The fluorescence phenotypes of the *B. thuringiensis* HD-73::31\* slurries are summarized in table 5.2; micrographs follow. The WT strain, the background strain for all the transformations, produces the native Cry1Ac protein. All strains produced crystals; these are the phase dark, (typically) diamond-shaped structures in the phase contrast micrographs. Some micrographs show sporulating cells, bearing both forespore and crystal. All strains bearing mCherry fusions fluoresced distinctly; none did without. This was as expected, and all fluorescence can be attributed to mCherry.

*Table 5.2: Fluorescence phenotypes of B. thuringiensis HD-73 strains bearing cry1Ac fusion operons. All strains with an mCherry (m) fusion showed distinct fluorescence. This was associated with the crystals for all strains with the protoxin (P) too. The ∅ variant indicates the strain transformed with the empty vector. The columns indicate the quality (distinct) or location (crystal, spore, shells) of the fluorescence. Missing entries indicate unsatisfied dependencies (e.g. no distinct fluorescence means no location would be meaningful).*

Variant	Strain	Distinct	Crystal	Spore	Shells
WT	HD-73	—			
∅	HD-73::30	—			
LTP	HD-73::310	—			
m	HD-73::31710	—			
LTPm	HD-73::3150	✓	✓	—	
LmP	HD-73::3120	✓	✓	—	
LPm	HD-73::3130	✓	✓	—	
mP	HD-73::31720	✓	✓	—	
Lm	HD-73::3110	✓	—	✓	—
LTm	HD-73::3140	✓	—	✓	✓

Micrographs of strains which lack fluorescent fusions are displayed in figure 5.4. Strains shown in figures 5.4a, 5.4b, 5.4c do not bear plasmids encoding fluorescent fusions; the negative control strain for fluorescent structures in figure 5.4d bears the gene for a His-tagged mCherry only. There is only limited, diffuse background fluorescence for these strains.

By contrast, the remaining strains have been transformed with plasmids encoding fluorescent fusions; all showed distinct (and often very bright) fluorescence. For the strains in figure 5.5, bright fluorescence associated with the crystals and vegetative cells, not spores.



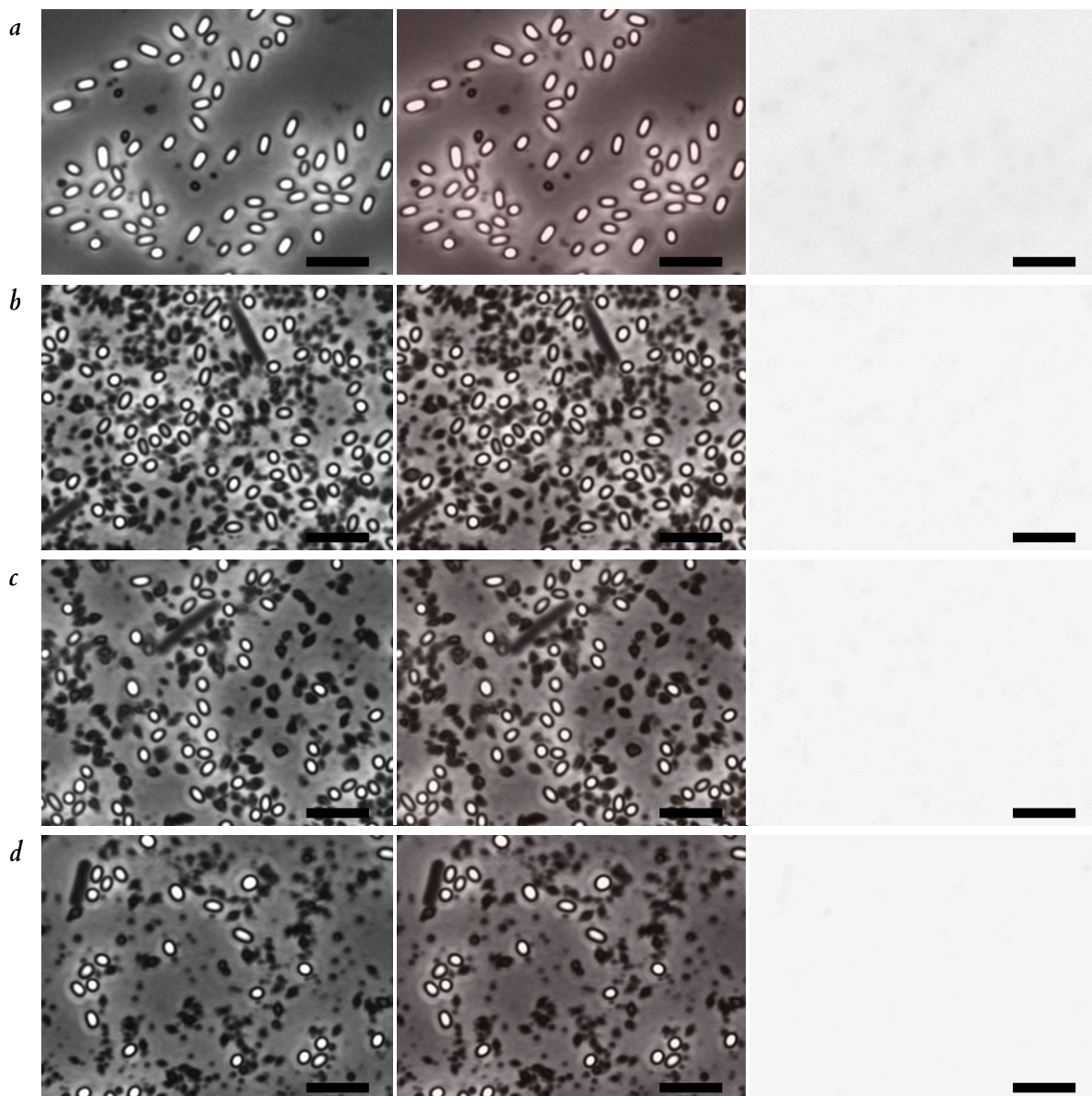


Figure 5.4: Micrographs (phase, composite, fluorescence) of *B. thuringiensis* HD-73 negative control spores, i.e. not engineered to encode fluorescent fusions of Cry1Ac. (a) shows WT HD-73; (b) shows HD-73::30, the empty vector strain ( $\emptyset$ ); (c) shows LTP strain HD-73::310; (d) shows m strain HD-73::31710. Cells, spores and crystals do not differ from WT; differences in relative proportion are an artefact. There is only limited, diffuse background fluorescence. Spore slurries were produced as previously described. Scale bars are  $5\mu\text{m} \times 1\mu\text{m}$ .

The largest construct fluoresced (160.9 kDa, in the crystal-positive control strain HD-73::13150, see figure 5.5a), indicating that the Cry1Ac expression pathway is not unduly taxed by the extra fluorophore. No variation in fluorescence was seen with age, over a two month period. Indeed, samples stored at  $4^\circ\text{C}$  still fluoresced after twelve months.

The brightest and most uniformly distributed fluorescence was seen in samples of HD-73::3120 and HD-73::3130 (LmP and LPM respectively, in figures 5.5c, 5.5b). These variants lack the toxic core, having an mCherry fusion (respectively in its place, and

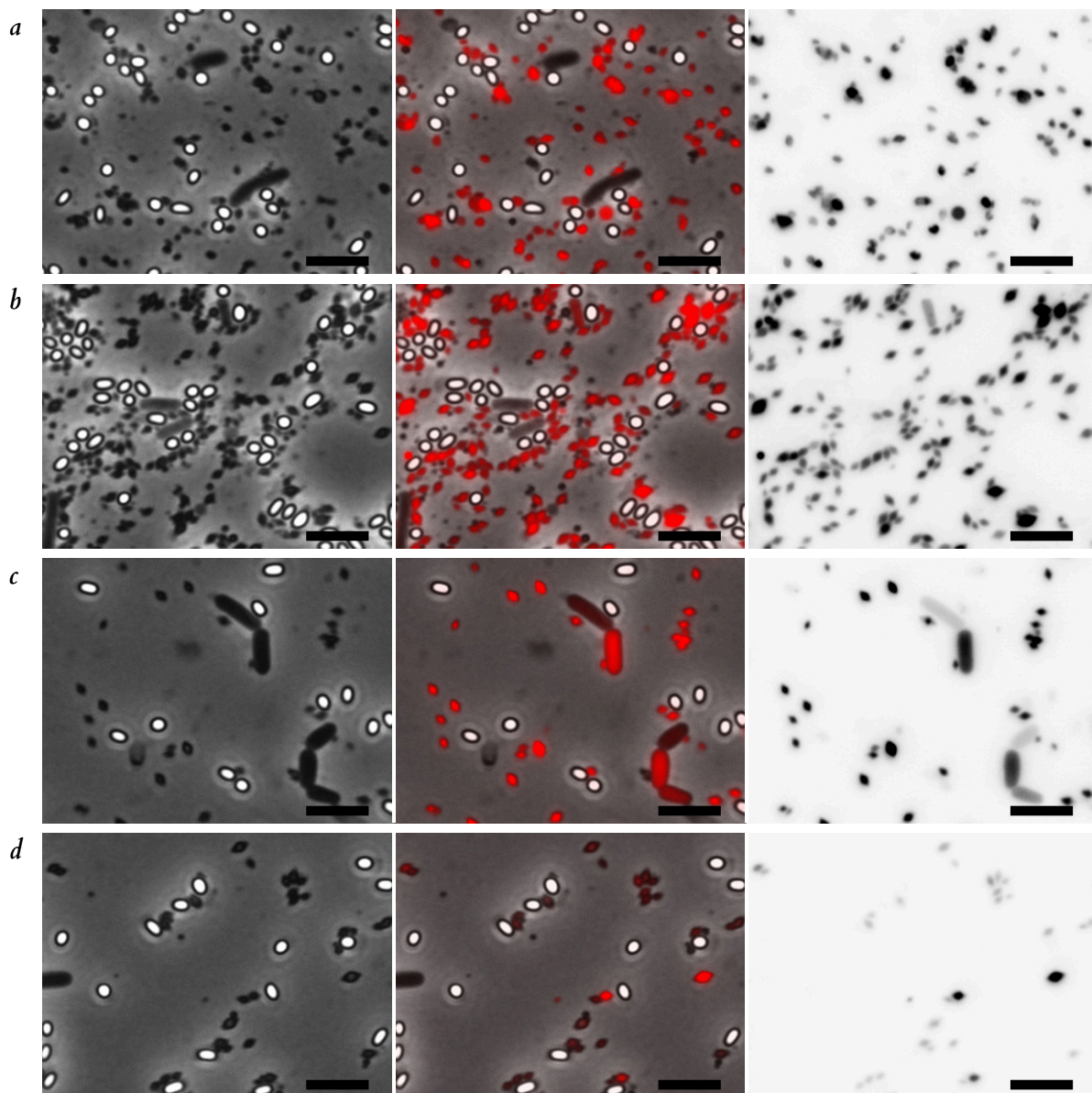


Figure 5.5: Micrographs (phase, composite, fluorescence) of *B. thuringiensis* HD-73 spores bearing pDBT31\* vectors encoding fluorescent fusions of Cry1Ac. (a) shows LTPm strain HD-73::3150; (b) shows LPM strain HD-73::3130; (c) shows LmP strain HD-73::3120; (d) shows mP strain HD-73::31720. Almost all crystals fluoresced, with near-uniform high intensity for the L variants. Spores did not fluoresce; some cells did. In phase contrast, cells, spores and crystals do not differ from WT. Spore slurries were produced as previously described. Scale bars are  $5\mu\text{m} \times 1\mu\text{m}$ .

between the protoxin domain and C-terminal 6×His tag). This fluorescence was localized to the crystals, not spores (though some cells fluoresce brightly, too). These are minimal fusions, to which additional sub-units of interest might be added, and are thus candidates for the base of a therapeutic protein platform.

The transformed strains contain both the native and the heterologous operons. Where any crystals fluoresced, nearly all did; it is most likely the crystals were heterogeneous: well documented behaviour for these crystal proteins. It is possible that the heterologous gene

was reducing or preventing transcription or translation of the native *cry1Ac*, perhaps due to copy number effects. However the plasmid, from which pDBT31\* were derived, has been shown to display saturation kinetics with *B. thuringiensis cry1Ac* (Agaisse & Lereclus, 1995), making this unlikely.

Since the completion of the bulk of the work presented here, PhD student Sina Schack has used the techniques and results to design and construct further fusions. Transmission electron microscopy of a number of fluorescent fusions of Cry1Ac revealed no differences from native crystals. Micrographs of the native Cry1Ac and a fusion with mCherry and the exosporium basal protein ExsFA (Stewart, 2015), are in figure 5.6. Crystals showed the same bipyramidal structure, with some patches of low electron density, and edges with regular order at the 500 nm scale, but great irregularity at the 50 nm scale.

Whereas HD-73::3120 (LmP) showed near uniform, distinct, bright fluorescence across all crystals, the leaderless mP variant (HD-73::31720) showed greater variation (figure 5.5d). A more extreme version of this leader effect can be seen comparing the negative control strain HD-73::31710 (m) to the Lm variant (HD-73::3110, in figure 5.7), *i.e.* with the leader. In the former case one can see no fluorescence; for the latter, cells and spores, but not crystals, fluoresce.

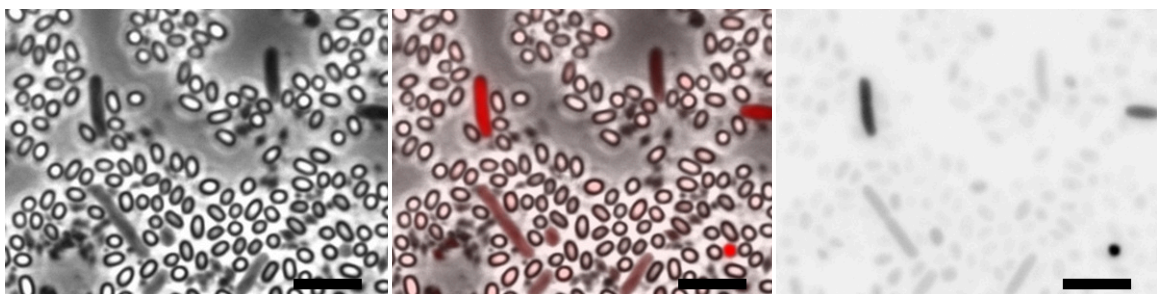


Figure 5.7: Micrographs (phase, composite, fluorescence) of *B. thuringiensis* Lm variant (HD-73::3110). The bipyramidal structures did not fluoresce, whereas cells and spores did. Spore slurries were produced as previously described. Scale bars are  $5\mu\text{m} \times 1\mu\text{m}$ .

Comparing outcomes for all four (LmP, mP, Lm, m), one can infer that the protoxin domain is necessary for the fusion protein to embed into the heterogeneous crystals. One might hypothesize that the leader is involved in crystallisation, despite not appearing in diffraction patterns (Evdokimov *et al.*, 2014, not that an amorphous sequence would appear). This does not explain why the Lm variant's fluorescence demarcates spores, but not crystals.

A more likely explanation is that the leader prevents export of the associated peptide from the mother cell, or perhaps prevents its degradation during sporulation, and thus the LmP variant can embed in the crystal, and the Lm associate with the spore. This by itself would

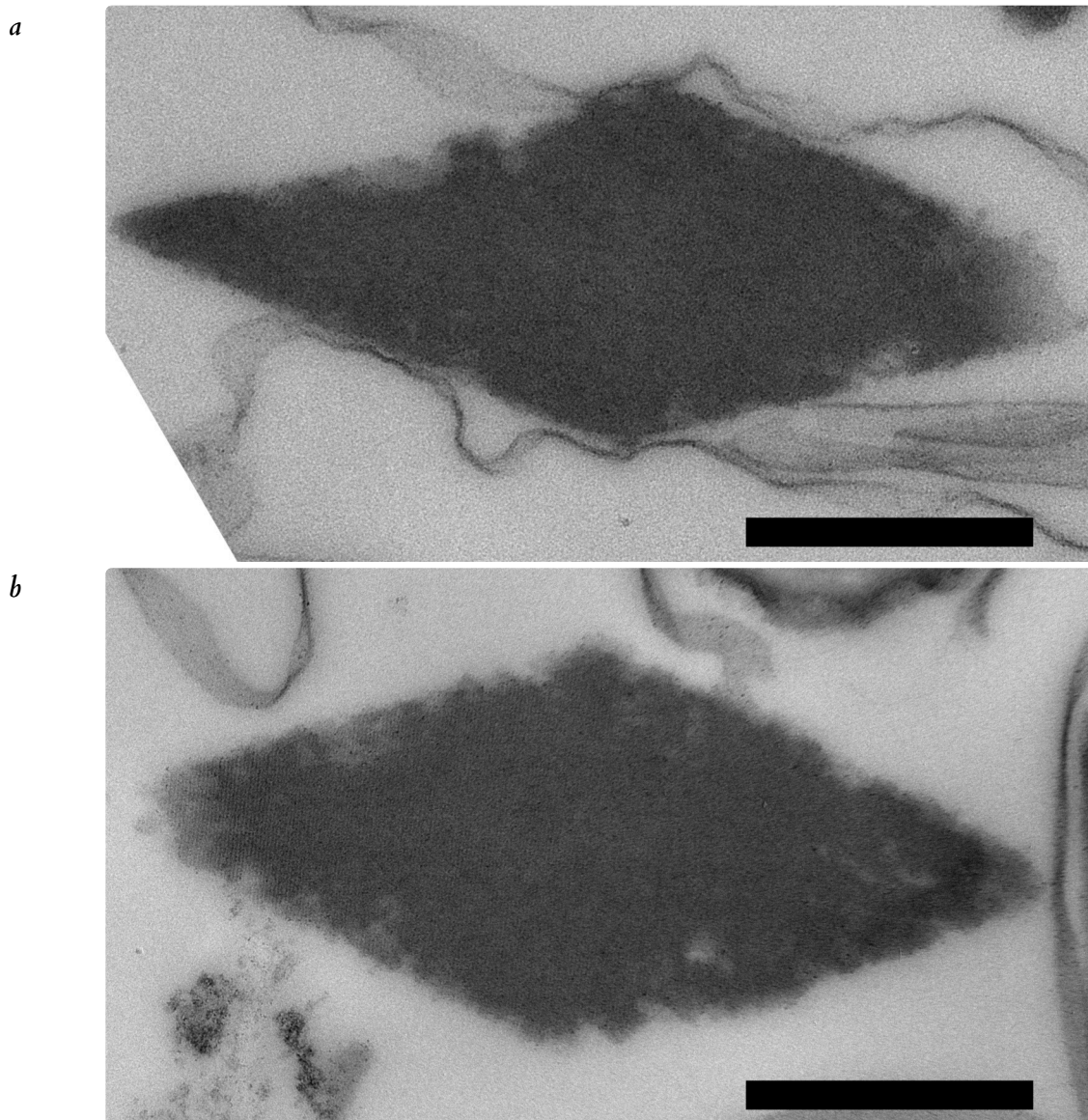


Figure 5.6: TEMs of Cry1Ac crystals. (a) shows the native crystal; (b) shows the fluorescent fusion with ExsFA and mCherry. Both variants form typical crystals (the large, electron dense structures); on 5.6b, near-vertical lines can be seen. The thin strands are fragments of exosporium. The objects at the top right and right of 5.6b are spores. It is not clear what the electron density at the lower left of 5.6b represents. Samples were prepared by Sina Schack; images were taken at CAIC (Cambridge Advanced Imaging Centre) with assistance of Dr. Katrin Mueller and Lyn Carter. Scale bars are  $500 \times 50 \text{ nm}$ .

not explain why no spore of the LPm variant showed more than background fluorescence; there are however two factors that can explain this. Firstly, unlike for the LPm fusion none of the Lm protein is incorporated into crystals, meaning there is more available to attach to the spores. Secondly, this experiment could not control for total protein expression: if the total protein expressed in each sample had the same mass, the mass of mCherry produced would be greater in the Lm than the LPm variant, and thus there would be more fluorophore and more leader in the former case, leading to a greater fluorescence signal. The total protein

expressed is likely to be similar, given similar conditions. These two factors would explain the difference in background fluorescence, supporting the model that the leader prevents protein export or degradation.

The most surprising result corresponds to strain HD-73::3140 (LTm, figure 5.8). Distinct rings are visible at locations corresponding to the spores' outer layers. The rings are not uniform; they appear thickest at the spore equator. There is some diffuse fluorescence corresponding to the vegetative cells, too. However, the vast majority of the crystals, seen on phase contrast, did not fluoresce. Some structures, faint on phase contrast, fluoresced brightly; indeed in phase contrast there is no signal at the corresponding locations. This evidence strongly suggests the heterologous protein is not integrating into the crystal; rather it is deposited into one of the outer layers of the spore: the coat, interspace, or exosporium.

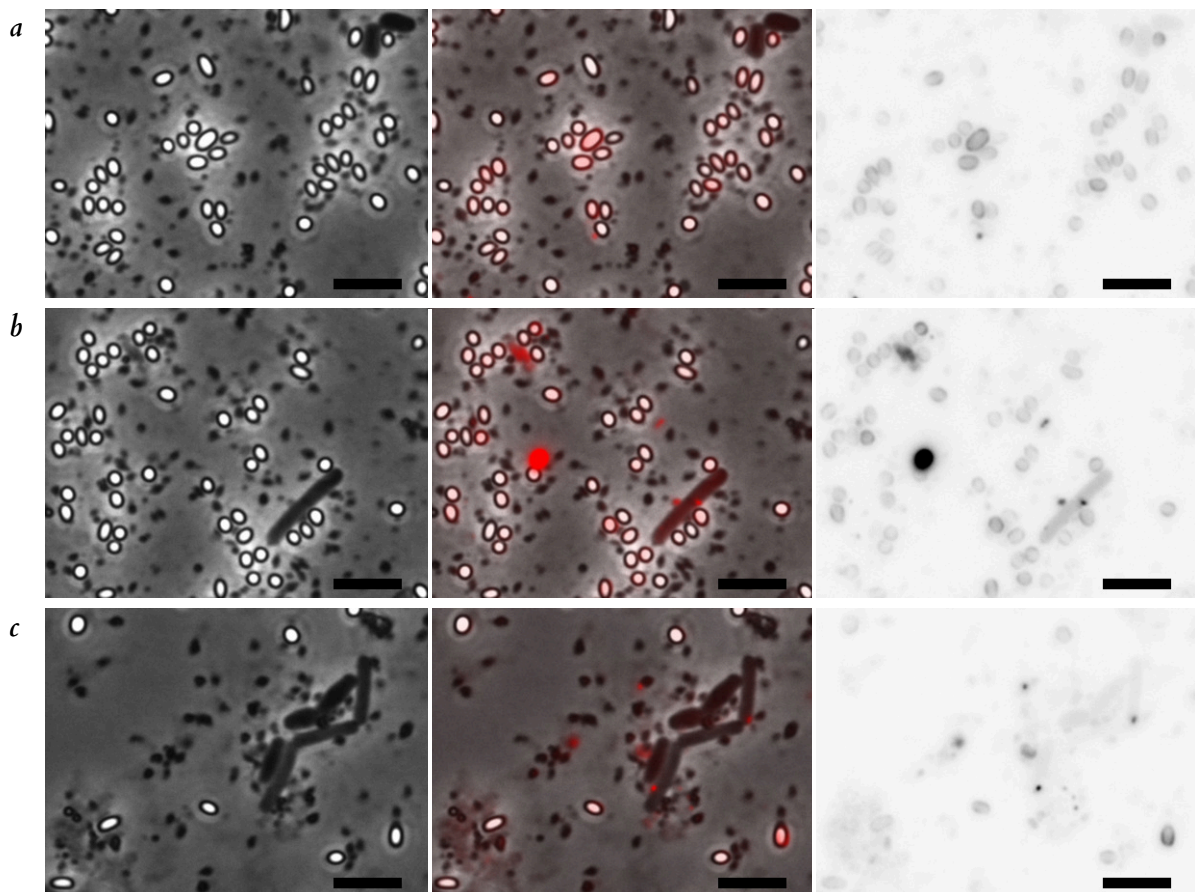


Figure 5.8: Micrographs (phase, composite, fluorescence) of *B. thuringiensis* HD-73::3140 spores, bearing the LTm fusion variant. Most of the fluorescent objects are spores, for which the shells show distinct fluorescence. Spore slurries were produced as previously described. Scale bars are  $5\mu\text{m} \times 1\mu\text{m}$ .

It is unusual that fluorescence appears to concentrate at the spore equator. More typical is pooling at the poles, as that is where the coat is normally thickest (Manetsberger *et al.*, 2015). The effect here might be seen were the protein to embed in the coat, where the coat is already otherwise thinnest. Considering Cry1Ac, Du & Nickerson (1996) postulated that

“the N-terminal ‘business end’ of the protoxin is exposed on the spore surface and the C-terminal region anchors the protoxin inside the spore coat”. The result demonstrated here is perhaps inconsistent with this model, as here the entire C-terminus of the protein has been replaced. It is still possible that wild-type Cry1Ac is embedding in the coat and the heterologous protein is attaching through complementary interactions; such an occurrence would be quite surprising as the toxic cores are not thought to interact until the protoxin is cleaved, and crystallographic studies demonstrate minimal interaction between toxic cores (Evdokimov *et al.*, 2014). The postulated model is most likely wrong, and in fact Cry1Ac embeds in the coat in some other way. This plausibly relates to the leader sequence itself, as discussed above. ELM (Ellipsoid Localization Microscopy) may help identify what is happening here, though it has yet to be tested in *B. thuringiensis* (Ghosh *et al.*, 2018; Manetsberger *et al.*, 2015).

Whether or not some of the heterologous protein is embedded in the spore coat, it is likely that some is located in the interspace. Even if every molecule partially embedded in the coat, the rest of the structure would be in the interspace. From the non-uniform distribution of fluorescence around the shell of the spore, it is likely that there would still be a specific interaction with the coat.

One might note that it is only strain HD-73::3140, for which the micrographs show these fluorescent shells. This suggests that it is the absence of an inhibitory factor (the protoxin domain) rather than the presence of the leader, 6×His tag, or mCherry, causing the protein to deposit in this manner — though the earlier comments on mass of protein produced apply here (albeit as a lesser consideration).

There was also fluorescence beyond the shells. Careful inspection of slides revealed some localised fluorescence at positions corresponding to some crystals and mother cells in phase contrast. It is not clear to what these spots correspond. From their brightness on the fluorescence micrographs, it is likely that these are aggregates of fluorescent protein. These perhaps comprise the native domain, with which the toxic cores of the fluorescent fusion interact, though there is not enough information in these images to be certain. The larger objects could be partially crystalline aggregates of Cry1Ac, with fusions embedded therein.

☆☆

The Cry1Ac subdomain fusions display the desired properties: most importantly, expression of heterologous protein at high yield. Thus these proteins might therefore serve as a platform, in which the gene for a protein of interest is cloned into the mutant *cry1Ac* genes in pDBT3120 or pDBT3130, following (C-terminal to) and preceding (N-terminal) the protoxin domain, respectively.

## 5.2.2 Cry1Ac–antibody fusions

What if an antibody fragment were cloned into these Cry1Ac fusions?

Table 5.3 lists the *B. thuringiensis* vectors, for expression of Cry1Ac–NIP109 fusions. The source plasmid for the entries with an N-terminal antibody fragment and C-terminal mCherry is pDBT3130; pDBT3120 provides for an N-terminal mCherry and C-terminal antibody fragment (see table 5.1).

Table 5.3: Schematic representation of Cry1Ac–NIP109 fusion operons. The extended mnemonic includes *l* for light chain, *h* for heavy chain and *s* for scFv. For example, pDBT312s comprises (in order from the N-terminus) the leader, mCherry and protoxin, before, at the C-terminus, the NIP109 scFv.

Code	pDBT31...	Domains					Mass / kDa
L1Pm	3l	Leader	light	Protoxin	mCherry	6×His	119.8
LhPm	3h	Leader	heavy	Protoxin	mCherry	6×His	145.8
LsPm	3s	Leader	scFv	Protoxin	mCherry	6×His	121.8
LmPh	2h	Leader	mCherry	Protoxin	heavy	6×His	145.8
LmPs	2s	Leader	mCherry	Protoxin	scFv	6×His	121.8

Phase contrast and fluorescence micrographs of spore–crystal mixtures, for *B. thuringiensis* HD-73, engineered to produce Cry–antibody fusions, are shown in figure 5.9. Fluorescent, bipyramidal crystals can be seen for all samples, though there is visible heterogeneity. The signal is strongest for L1Pm (HD-73::313l) and LmPs (HD-73::312s). The latter is uniformly strong; by itself it is not clear whether the full protein has been expressed, as the fluorescent fusion is near the C-terminus. The phase contrast and fluorescence micrographs clearly show that something fluorescent was being produced, which mostly aligned with the positions of crystals visible under phase contrast.

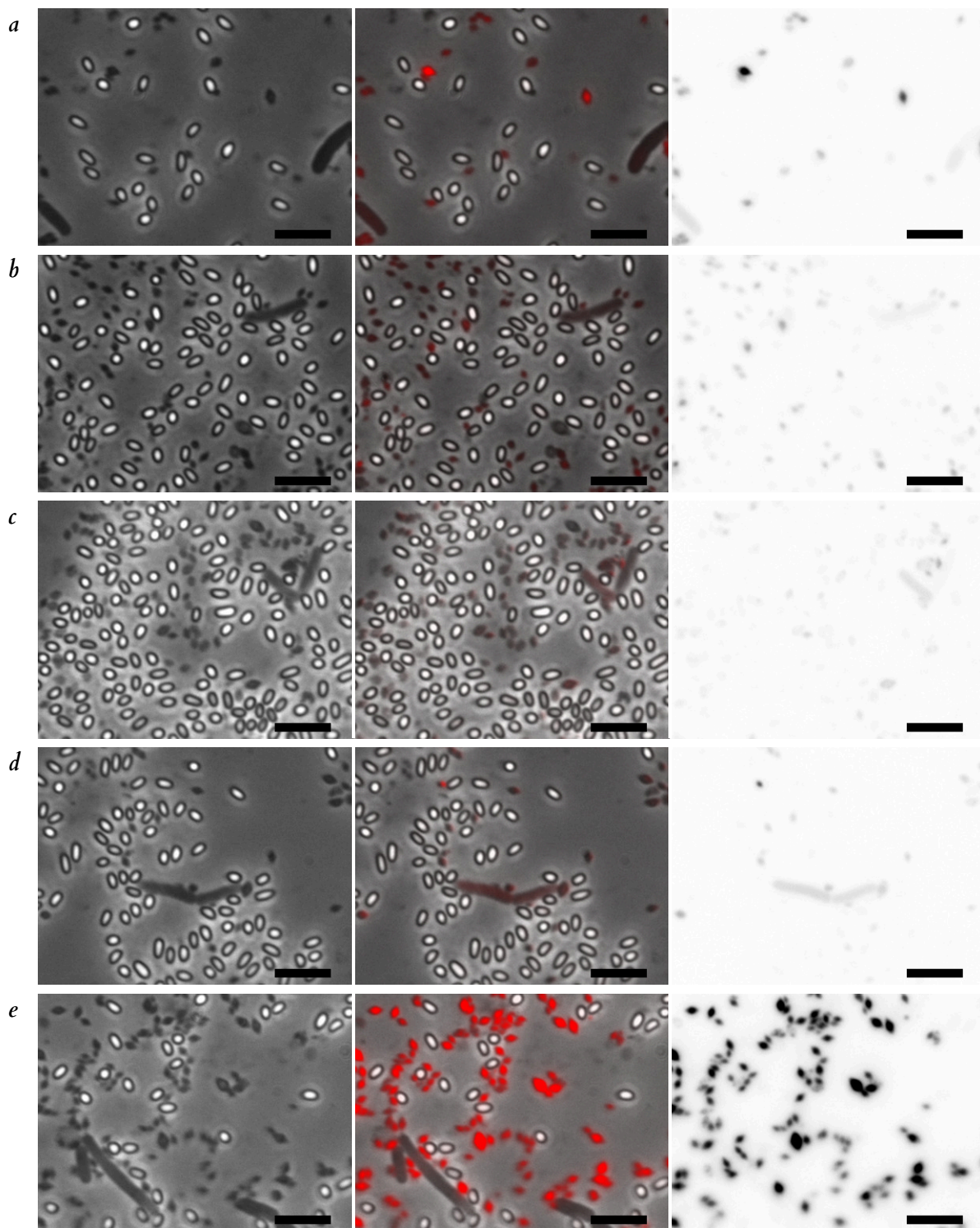


Figure 5.9: Micrographs (phase, composite, fluorescence) of cells, spores and NIP109 fusion crystals in *B. thuringiensis* HD-73 spore cultures. (a) shows L1Pm strain (HD-73::313l); (b) shows LhPm strain (HD-73::313h); (c) shows LmPh strain (HD-73::312h); (d) shows LsPm strain (HD-73::313s); (e) shows LmPs strain (HD-73::312s). All strains showed fluorescence corresponding to the locations of crystals on phase contrast; the fluorescence is particularly distinct for the C-terminal scFv LmPs. Spore slurries were produced as described previously. Scale bars are  $5\mu\text{m} \times 1\mu\text{m}$ .



A representative outcome of fractionating solubilized slurries of the Cry1Ac-NIP109 fusions can be seen in figure 5.10. As for the Cry1Ac-mCherry fusions in figure 5.3, from figure 5.10 it appears these triple fusion crystals had not been solubilized correctly, and there are few distinct bands. No western blot band corresponded to the predicted mass of a NIP109 fusion, nor did any band correspond to a C-terminal domain fragment (*i.e.* a fragment bearing the His tag). On the gel, predicted bands are visible for the LsPm, LmPh and LmPs variants. This result was seen across multiple gels and blots.

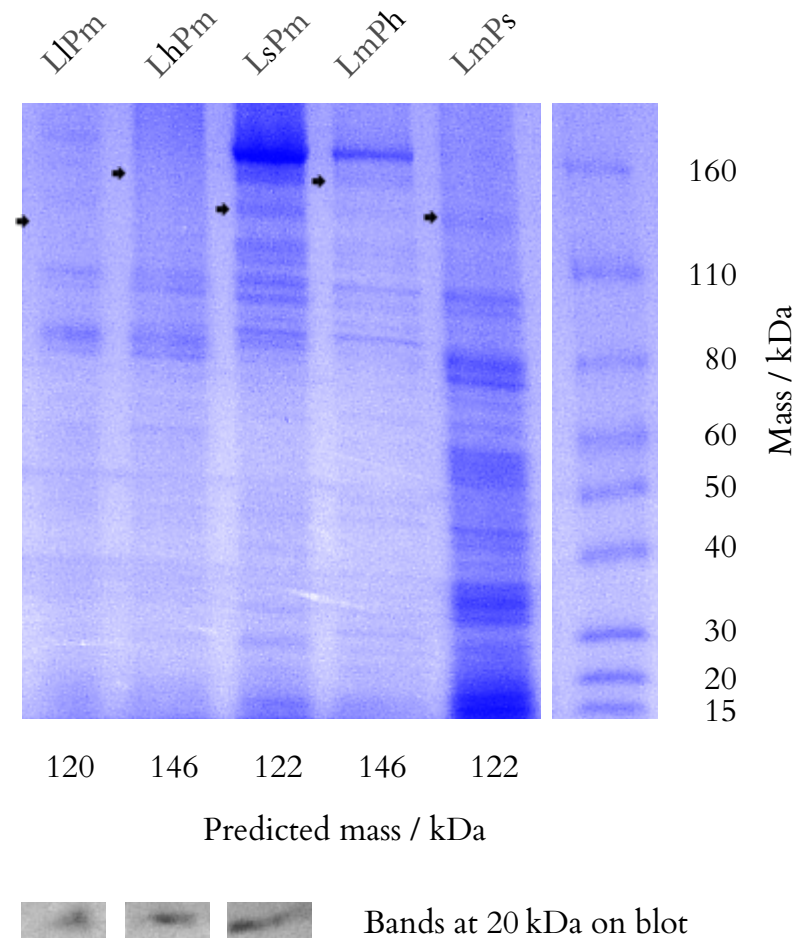


Figure 5.10: Analysis by PAGE of spore slurries, for strains expressing Cry1Ac-mCherry-NIP109 fusions. No strain showed bands at predicted sizes on the associated blots, but the C-terminal mCherry fusions showed bands at 20 kDa. On the gel, bands are visible at predicted positions for LsPm, LmPh and LmPs variants (at arrows, inferred from the Novex® Sharp Pre-stained protein ladder). Lane labels are for HD-73::3\* strains. The spore slurries were solubilized in LDS at the modified conditions.

For the strains with C-terminal mCherry fusions (figures 5.9a, 5.9b, 5.9d), one can be almost certain that the correct primary sequence was expressed, and that the mCherry folded correctly; for the C-terminal mCherry fusions to express, cells must translate the whole protein (the unlikely possibility of internal ribosomal entry sites notwithstanding). Further supporting evidence is provided by the appearance of the 20 kDa mCherry degradation bands on lanes corresponding to the variants with C-terminal mCherry.

It is possible that for the variants with the N-terminal mCherry fusion (figures 5.9c, 5.9e), expression arrested after producing the fluorophore but before the antibody fragment. Direct analysis of the relevant proteins ought to help eliminate that possibility; the lack of bands on the western blots provide weak evidence in favour of elimination. One should infer that the successful expression of the C-terminal mCherry fusions makes it unlikely that the N-terminal variants failed to express. However, current evidence cannot confirm the contrary.

These triple antibody fusions form heterogeneous crystals, in the presence of the WT Cry1Ac. Is it possible to produce crystals of these fusions in the absence of the native protein? This could be answered by transforming an acrySTALLIFEROUS strain of *B. thuringiensis*, using the pDBT31\* plasmids.

### 5.2.3 Expression in other *Bacilli*

Phase contrast and fluorescence micrographs of various strains, transformed with the pDBT3130 and pDBT3140, are displayed in figures 5.11–5.13. These plasmids feature variants LPm and LTm of the *cry1Ac* operon with *mCherry* at the 5' end, which lack the toxic core and protoxin domain coding sequences, respectively. No sample showed fluorescent crystals.

Surely another species of *B. thuringiensis* would produce protein crystals? *B. thuringiensis* subsp. *finitimus* YBT-020 produces Cry4A crystals within its exosporium (*i.e.* spore-crystal association). Micrographs of that strain, transformed with the aforementioned plasmids, showed background fluorescence only (figure 5.11). Indeed, while the YBT-020–native Cry4A crystals were present, there seemed to be no production, or no interaction, with the Cry1Ac fusions. It is strange that the promoter from one *B. thuringiensis* would not appear to be active in another; it seems likely that there are other factors, present in *B. thuringiensis* HD-73 alone. For comparison, one might clone the *cry1Ac* fusions into vectors driven by  $\sigma^K$  from *B. thuringiensis* YBT-020, or clone both the native *cry1Ac* variant and a fusion into that strain.

The difference between *B. thuringiensis* and *B. cereus* is the former's *cry*- or *cyt*-bearing plasmids (Agaisse *et al.*, 1999). One might expect expression in *B. cereus* to be similar to that in *B. thuringiensis*; however, this was not the case. Figure 5.12 shows *B. cereus* transformed as *B. thuringiensis* YBT-020, above.

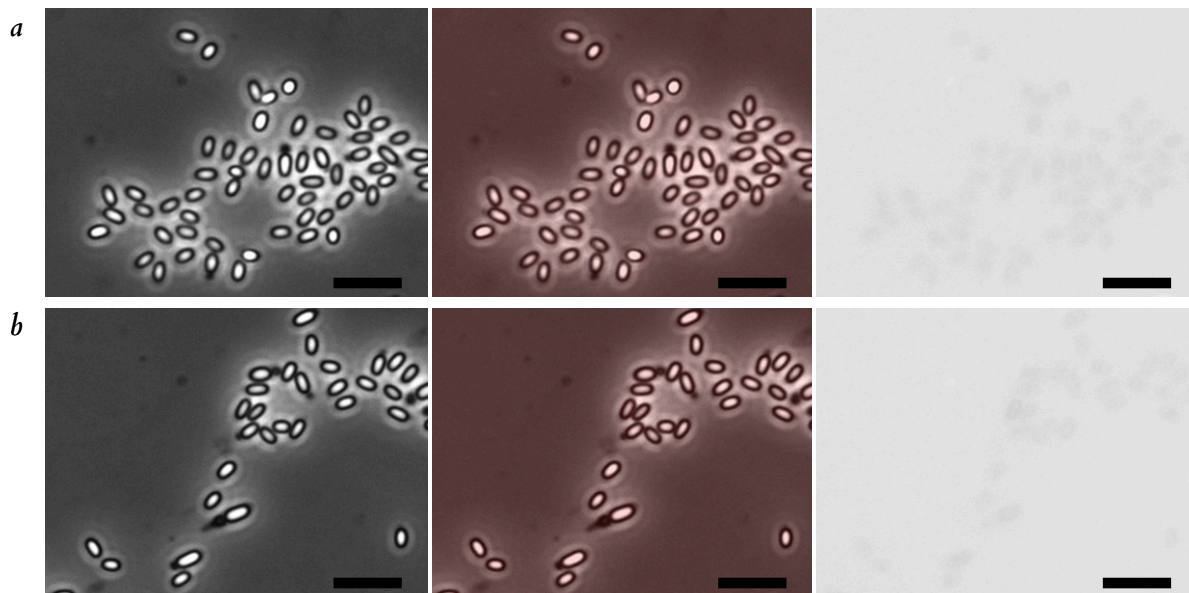


Figure 5.11: Micrographs (phase, composite, fluorescence) of *B. thuringiensis* subsp. *finitimus* YBT-020 spore slurries. (a) shows LPm strain YBT-020::3130; (b) shows LTm strain YBT-020::3140. The resulting cultures appeared like WT (not shown): crystals were exclusively associated with the spores, and no structure fluoresced distinctly. Spore slurries were produced as described previously for *B. thuringiensis* HD-73 strains. Scale bars are  $5\mu\text{m} \times 1\mu\text{m}$ .

The spores of strains bearing the LPm variant showed fluorescent inclusions within cells, but no other fluorescence of cells nor spores beyond that seen for the WT strain. The fluorescent shape at the top of figure 5.12b appears like neither cell nor spore. By contrast, the LTm variant showed a mixture of fluorescent inclusions and fluorescent shells around some spores (figure 5.12d). As seen in that figure, the fluorescence was most intense at the poles.

For *B. cereus* ATCC 14579, at least, there was discernible fluorescence corresponding to both fusions, and possibly crystals, seen in figure 5.12b, whereas the other LPm image (more representative of that strain) and that for LTm both show fluorescent inclusions of some kind. The LTm strain showed shells very similar to that for *B. thuringiensis* HD-73. However, the level of production of what might be crystals was nowhere near that seen in *B. thuringiensis*; the Cry fusions alone thus appear unable to form extracellular crystals.

It would seem unlikely that *B. subtilis* spore crops would fluoresce. Within the *Bacilli*, *B. thuringiensis* and *B. subtilis* share a relatively distant phylogenetic relationship. In addition, as *B. subtilis* does not feature an exosporium there can be no interspace. Despite this, figure 5.13 shows faint shells of fluorescence for both the LPm and LTm variants. For the LTm variant fluorescence was greatest at the poles. This seems like evidence for the various cry fusions embedding in the coat.

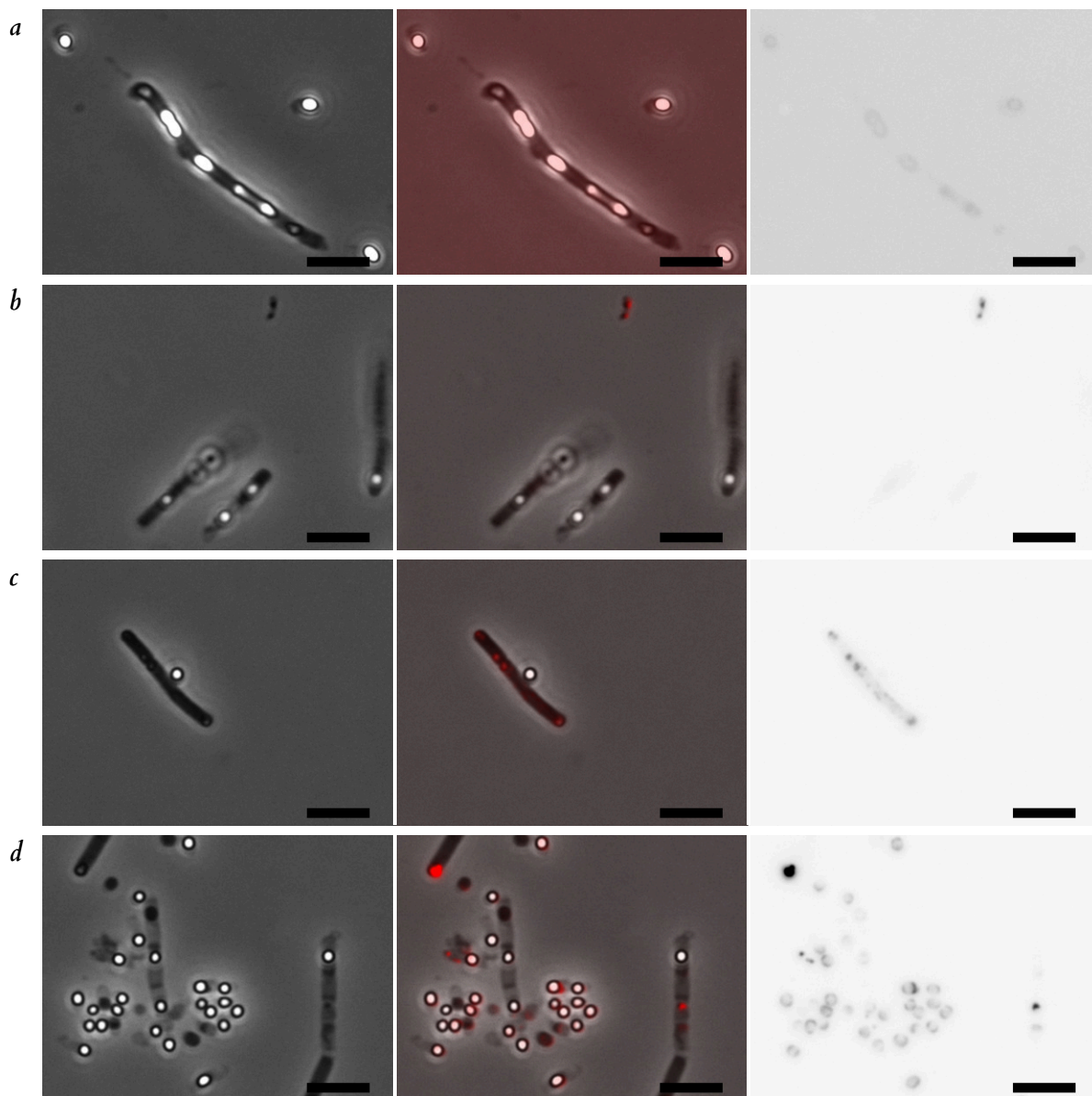


Figure 5.12: Micrographs (phase, composite, fluorescence) of *B. cereus* ATCC 14579 spore slurries. (a) shows WT *B. cereus*; (b) shows LPM strain 14579::3130; (c) likewise; (d) shows LTM strain 14579::3140. There were no bipyramidal structures, though small fluorescent inclusions can be seen — in both experimental strains. For LTM variant, shells fluoresced with very bright poles (compared with the distinct but less bright fluorescence for the WT strain). Spore slurries were produced using nutrient exhaustion, then processed as described previously. Scale bars are  $5\mu\text{m} \times 1\mu\text{m}$ .

Finally, the work in chapter 4 considered expression in the forespore of sporulating *B. subtilis*. Such expression relied on the  $P_{sspB}$  promoter, under control of  $\sigma^G$ , which drives transcription in the late forespore. As it is desirable to increase this protein expression, the *cry1Ac* machinery appeals: a *cry1Ac* operon, for which the aforementioned promoter  $P_{sspB}$  would replace  $P_{cry1Ac}$ , might be a useful tool. With it, one could investigate the extent to which this *B. thuringiensis* *cry1Ac* machinery can boost protein expression in the *B. subtilis* forespore.

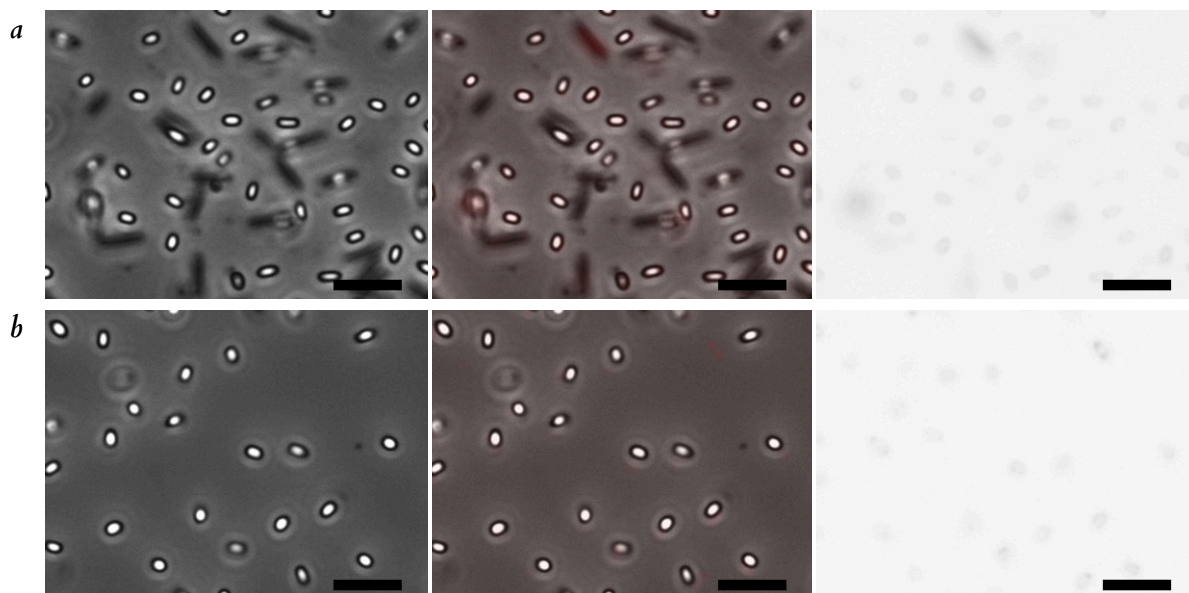


Figure 5.13: Micrographs (phase, composite, fluorescence) of *B. subtilis* 168::690 progeny, for expression of the modified *cry1Ac* operon. (a) shows LPM strain 690::3130; (b) shows LTm strain 690::3140. There were no bipyramidal structures, although shells showed distinct fluorescence, in particular at poles. Spore slurries were produced using nutrient exhaustion, then processed as described previously. Scale bars are  $5\ \mu\text{m} \times 1\ \mu\text{m}$ .

Micrographs of such a *B. subtilis* strain 690::31610, engineered to express 6×His-tagged mCherry in the forespore, can be seen in figure 5.14. Fluorescence can be seen over the whole of each spore, though intensity is greater at the shell (especially at the poles), indicating that *mCherry* is indeed produced from such an operon. It is possible that this corresponds to diffuse *mCherry*, over the whole spore core; ELM would help clarify this. A variant based on the mother cell promoter, such as one driven by  $\sigma^K$ , might make a worthwhile comparison.

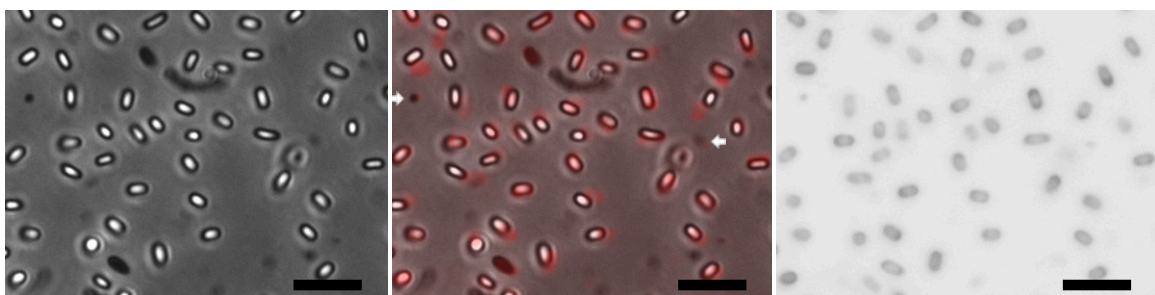


Figure 5.14: Micrographs (phase, composite, fluorescence) of *B. subtilis* 690::31610 progeny, for expression of His-tagged mCherry. Shells showed distinct fluorescence, particularly at poles. There are also small, faint, phase dark structures, which also appear in the fluorescence micrograph; These are indicated on the composite with white arrows. Spore slurries were produced as described previously. Scale bars are  $5\ \mu\text{m} \times 1\ \mu\text{m}$ .

\*\*

It does appear that none of these strains produces crystals. It is plausible that there are additional factors required for crystallization of these fusions. It may be worth investigating the capacity of these strains to produce the native crystal or (fluorescent) LTPm variant. Likewise, testing with an acrySTALLIFEROUS variant of *B. thuringiensis* subsp. *kurstaki* HD-73 would be worthwhile — however, it should ideally lack only the native *cry1Ac* operon.

Despite this, some strains did produce fluorescent protein. As it turns out, such strains were not limited to *Bacilli*.

#### 5.2.4 Expression of the *cry1Ac* operon in *E. coli*

During cloning of *E. coli* bearing the desired plasmids, a number of strains showed fluorescence. Samples of these cultures, when examined under optical microscopy, were found to fluoresce. Some LmP (pDBT3120) cells contained large, phase-bright inclusions, which fluoresced with great intensity under UV illumination: indeed, an intensity often visible even while the sample was illuminated for phase contrast. Representative micrographs can be seen in figure 5.15.

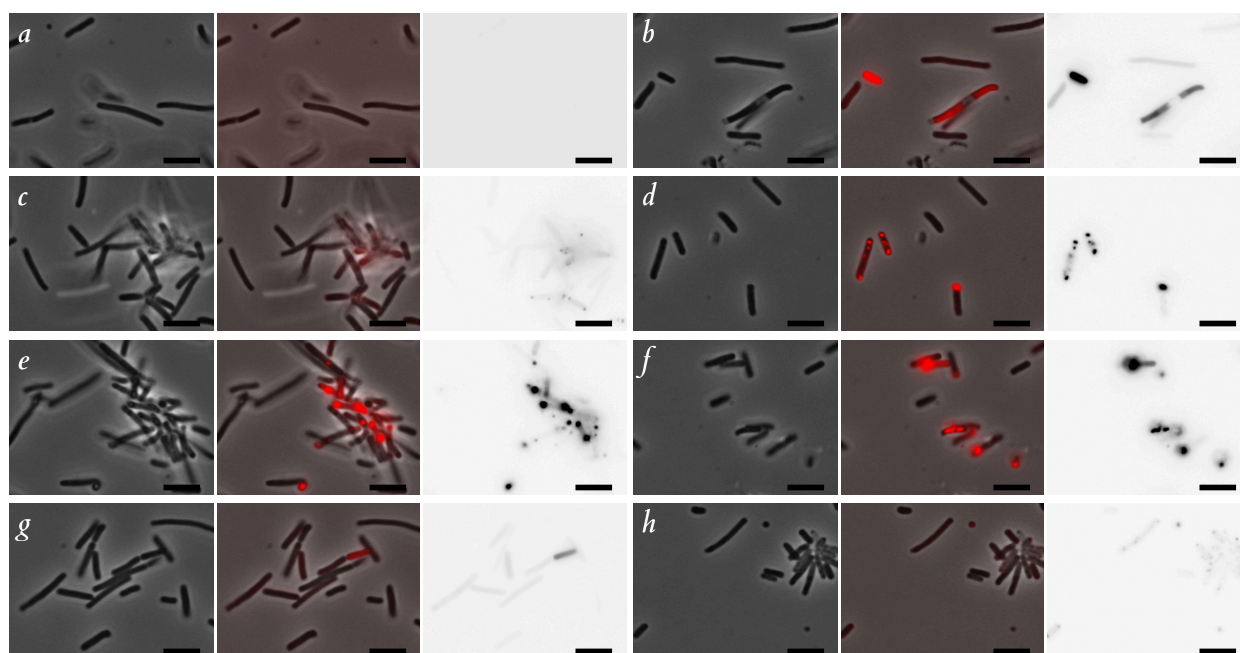


Figure 5.15: Micrographs (phase, composite, fluorescence) of *E. coli* Turbo cells used to assemble pDBT31\* vectors. (a) shows LTP variant ( $\theta$  suffix); (b) shows *m* (710); (c) shows LTPm (50); (d) shows LmP (20); (e) shows LmP (30); (f) shows mP (720); (g) shows Lm (10); (h) shows LTm (40). All strains bearing mCherry-encoding plasmids showed fluorescence. Samples were taken from cultures grown for Miniprep. Scale bars are  $5\mu\text{m} \times 1\mu\text{m}$ .

All strains but that in figure 5.15a contained plasmids encoding fluorescent fusions; all samples but that in figure 5.15a fluoresced. Unlike for *B. thuringiensis* spores (in figure 5.4d) the m variant fluoresced, too (figure 5.15b). The localization and heterogeneity of the fluorescence varied. While strains showed diffuse fluorescence if and only if they carried the *mCherry* variants, some strains showed highly localized fluorescence, within the structures of the cells. The plasmids in these latter strains all contained the protoxin domain; indeed only the strains with a protoxin domain and mCherry fusion showed such localized fluorescence figures 5.15c, 5.15d, 5.15e, 5.15f. Within the micrographs of strains which fluoresced, one can also see cells which do not — there was heterogeneity of fluorescence. Older cultures showed more uniform fluorescence.

Phase contrast microscopy of samples revealed what appeared to be large inclusions within the *E. coli* cells. These are not as clearly visible on images, recorded by the CCD, as they were through the eyepiece of the microscope. The inclusions were also present in samples of the strain containing pDBT310, encoding the LTP variant.

Fluorescence was not limited to microscopy. Routinely, cultures were pelleted for miniprep after 8 h growth; for three of these cultures (LPM: Turbo::3110, Lm: Turbo::3120 and m: Turbo::31710) the pellets would appear red. Indeed, old liquid culture turned red, too. This red colour could be seen on plates. Day old colonies on plates would turn red, even if refrigerated. The change in colour began at the centre of the colony and spread from there. Figure 5.16 shows an example of this. N-terminal mCherry fusions in particular showed a striking red colour, with the greatest intensity corresponding to *mCherry* (with or without the leader sequence). This latter detail supports the hypothesis that more mCherry was present for the Lm than LmP variant in *B. thuringiensis* (postulated in section 5.2.1).

To identify a cause of such protein expression, NNPP was performed, as described in section 2.2.3, with the region of the *cry1Ac* operon just upstream of the RBS. The target: the *E. coli*  $\sigma^s$  (aka  $\sigma^{38}$ ) consensus sequence, is TTGACA N<sub>15</sub> KC TATACT TWWWW R (Becker & Hengge-Aronis, 2001). This revealed four matches for the *E. coli*  $\sigma^s$  promoter with scores  $\geq 0.99$  just upstream of the *cry1Ac* RBS (ribosome binding site). This sigma factor is not only the main stationary phase transcription factor, it is also involved in stress response (Becker & Hengge-Aronis, 2001). The presence of these matches suggests transcription of the crystal proteins is likely during stationary phase growth; this is what was seen experimentally. The diffuse fluorescence seen from all the samples whose plasmids encode fluorescent proteins supports this  $\sigma^s$  hypothesis. Beyond that, the variation in localized fluorescence seen among

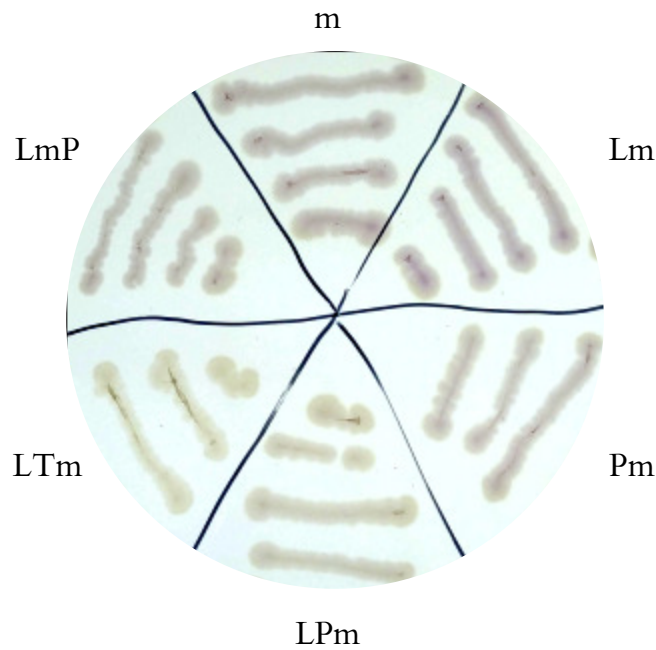


Figure 5.16: Streaks of *E. coli* Turbo cells, bearing pDBT31\* plasmids for expression, in *Bacillus*, of Cry fusions, from their native promoter. The top half and lower right sector showed a red colour, which on the agar plate itself (as opposed to a photograph) was quite distinctive and clearly visible to the naked eye. The colour saturation was strongest for the top and top-right sectors, corresponding to mCherry (alone or with the leader). This red hue was quite stable; it was still visible after storage for two months at 4°C. Cultures were streaked onto a 90 mm LB-agar plate.

the fusions matches what has been shown for expression in *B. thuringiensis*: that the protoxin domains enhance stability. However, the causes of the heterogeneity within each sample are less clear. The  $\sigma^s$  story is not complete, though it would explain some cloning difficulties.

Isolation of gDNA corresponding to the *cry1Ac* operon was straightforward, as was cloning into library vectors. This was also the case for *cry4A*, from *B. thuringiensis* YBT-020.

However, cloning the full *cry1Ac* gene (or any of the operons from YBT-020) into pHT315 proved challenging; often transformations would result in single digits of transformants, and colony PCRs indicated the resulting constructs had mis-assembled, sometimes in interesting and unpredictable ways. Overlap assembly methods have their limitations, and so plasmid pDBT30 was designed and constructed as a Golden Gate recipient vector, using standard parts (Patron *et al.*, 2015). Golden gate cloning, too, proved unsuccessful; colony PCR of transformants identified either religations or no PCR product. Plasmid pDBT30 proved as susceptible to these issues as pHT315.



Eventually, using a batch of freshly prepared *E. coli* Turbo competent cells, a correct clone containing pDBT310 was produced (from the single colony to result from the transformation). By contrast, transformations with the fusions produced numbers of colonies (20–100 per 90 mm plate) more typical of successful ligations. Having successfully identified a clone containing pDBT310, it became most likely that these difficulties related to the operon sequence itself. From the low number of colonies (and low likelihood that they comprised correct clones) one should infer that the correct ligation is a toxic sequence and only incorrect ligations resulted in viable colonies. Transcription from the backbone vector, and concomitant leaky translation, seemed unlikely; whilst there was a *lac* operon present, from the lack of reports of cloning difficulties with pHT315, one might infer this is not the fault of the vector.

Unintended expression from the *cry1Ac* operon explains the difficulties in cloning the full length *cry1Ac* gene. Protein expression causes metabolic load which can greatly reduce growth rates (Glick, 1995). It is possible that during cloning, expression of Cry proteins shortly after the start of recovery reduced growth rates to such an extent that visible colonies were not formed. By contrast, transformants with mis-assembled *cry1Ac* operons would grow at the expected rate. Researchers working with this operon should bear this in mind for future work, and consider mutating these consensus sequences.

There is precedent for production of Cry proteins in *E. coli*. Of note here, *E. coli* has been engineered to express Cry proteins from the *tac* promoter before, and the resulting inclusion bodies were found to be amorphous if grown at 37 °C, yet crystalline if grown at 30 °C (Oeda *et al.*, 1989). One might grow these strains at 30 °C to test whether that observation holds in this case, too.

While this operon has presented cloning difficulties, this autoinduced expression of fluorescent proteins presents an opportunity. Given that cells assembling a coding sequence featuring *mCherry* turn red, one might identify correct clones with high likelihood before colony PCR, digest or sequencing. Whilst the coding sequences of all picked colonies that turned red were subsequently verified successfully by Sanger sequencing, the numbers sequenced were too small to judge the sensitivity or specificity of this test.

Cloning was not the only process to show unexpected fluorescence; crystals in denaturing conditions maintained their fluorescence, too.

## 5.2.5 Solubilization of crystal proteins

Many researchers have analysed crystal proteins, and there are a number of methods used to solubilize them for different purposes (Bulla *et al.*, 1977; Huber *et al.*, 1981; Pearson & Ward, 1987; Schnepf & Whiteley, 1981; Thomas & Ellar, 1983). For the work here, the approach of Thomas & Ellar (1983) was selected, as it involved minimal modification to the existing PAGE protocol. Importantly, this protocol can be used without needing to purify the crystals, making it suitable for screening.

It was tested on *B. thuringiensis* subsp. *kurstaki* HD-73 bearing pDBT3130 (with the standard PAGE technique as a negative control), and then performed on all strains (including the antibody fusions).

Phase contrast and fluorescence micrographs of spore-crystal slurries following the solubilization process can be seen in figure 5.17. The direct solubilization process of Thomas & Ellar (1983) resulted in complete loss of fluorescence, and no phase-dark bipyramidal structures could be seen on the phase contrast micrographs (figure 5.17b)

Thus boiling the slurry dissolved the crystals, as there was no longer visible fluorescence. However, the PAGE and western blot results show that the process also resulted in significant degradation of the proteins. The crystal proteins — which from microscopy were clearly present as a major component — barely appeared on gels (though they did on blots). Many lanes showed strong bands at 20 kDa; all these lanes corresponded to fusion variants with the Pm C-terminus: the protoxin domain, mCherry, then the His-tag. There were 20 kDa bands, though fainter, for other variants with just a C-terminal mCherry (and His-tag). This must surely indicate that the fusion, specifically the mCherry tag, had been degraded (as seen, for example, in Beilharz *et al.*, 2015). In addition to confirming that the whole protein was produced, this may explain some of the other bands that could be seen on the gels and blots. It is worth optimizing the solubilization protocol, for further work on these proteins.

Under standard PAGE conditions, however, the crystals appeared to grow. The crystals were barely visible when viewed using phase contrast; indeed, at first glance it had appeared they had dissolved. When illuminated with UV, however, fluorescent bodies were clearly visible (figure 5.17c). These structures featured the distinctive, bipyramidal shape of Cry1A crystals. They were, however significantly larger than those in untreated samples (see figure 5.17a).

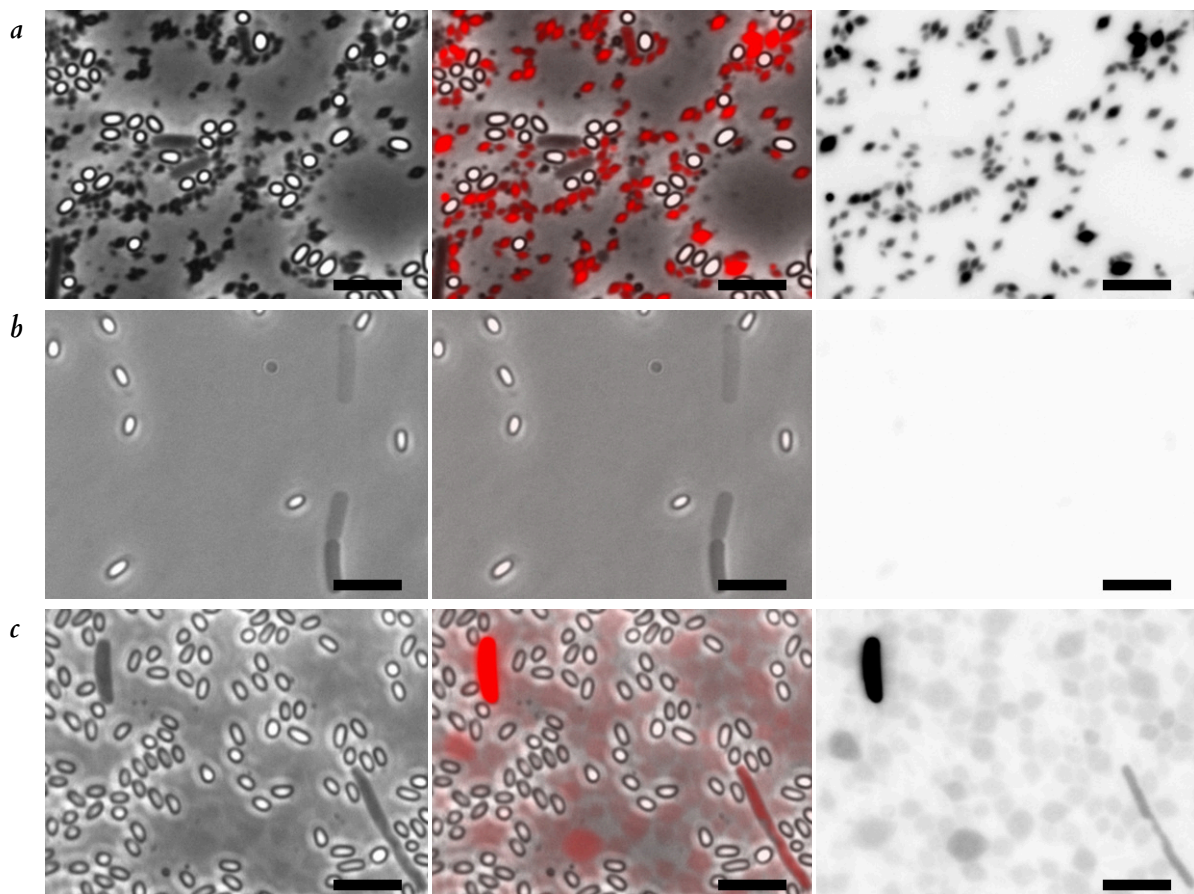


Figure 5.17: Micrographs (phase, composite, fluorescence) of *B. thuringiensis* HD-73, following attempts to dissolve crystal proteins. (a) shows LPM strain (HD-73:3130) without treatment; (b) shows the modified treatment; (c) shows standard PAGE conditions. After application of the modified protocol (boiling for 5 min), no crystal remained; furthermore boiling can destroy spores, meaning the smaller number of spores is most likely not an artefact. Following the modified protocol (incubation at 70 °C for 10 min), the fluorescent structures appeared larger and more diffuse: the matching objects in the phase contrast micrographs likewise. Spore slurries were produced as described previously, then solubilized with the selected treatment. Scale bars are 5 μm × 1 μm.

There are a number of possible explanations. It is unlikely that this was an example of selection bias: that there was no difference between the samples but smaller crystals appeared in the untreated slurries and larger in those treated. Likewise, it is unlikely to have been an artefact: the fluorescence of the larger crystals was significant when compared with the spores in the same field.

The most likely reason is also the most interesting: that the crystals begin to dissolve, yet not fully, and when cooled the remaining crystals act as seeds around which the protein in solution aggregates (and possibly crystallizes). Further evidence for this mechanism is that there were still cells in the sample, which fluoresced with the same magnitude of brightness as the untreated samples; these proteins had not been dissolved and can be treated as a control. It is not clear whether the resulting bodies were crystalline, although the shape

suggests this may have been the case. Likewise it is not clear whether the resulting bodies were the same material as the originals. The original crystals were heterogeneous: composed of native and fluorescent protein. It is clear these extended crystals all contained the latter, and they are likely to have contained the former too. There may also have been lithium ions or dodecyl sulphate present within the crystals, though. A protocol for analysis of such structures would require careful design, though to start it would be worthwhile to screen a variety of similar conditions for this crystal growth phenomenon.

This effect may provide a way to combine separately produced subdomains into a single, heterogeneous crystal, which could greatly simplify the challenge of producing antibody-fused Cry crystals.

## 5.3 Conclusions

The research presented in this chapter confirms the utility of Cry as a fusion protein platform for antibody fragments. Triple fusions of a Cry domain, mCherry fluorophore and antibody fragment have been produced. For most of these fragments, results confirm they have been produced at the correct sizes; the same limitations as chapter 4 apply, concerning function. Such fusion crystals may indeed prove suitable for oral or subcutaneous formulation, subject to acceptable release profile or bioavailability. Additionally, a variant of the *cry1Ac* operon, adjusted to use the late forespore promoter  $\sigma^G$ , may help increase the mass of protein produced per spore using the *B. subtilis* spore core expression system of chapter 4.

This result for triple-fusions builds on the systematic approach taken to analysing Cry1Ac-mCherry fusions. It extends results presented in the academic and patent literature, demonstrating for example that the *in vitro* work of Nair *et al.* (2015) is applicable to Cry1Ac (a variant missing from the list of Cry proteins in the patent application of Chan *et al.*, 2010). The fluorescence demonstrated by mCherry fusions was bright and resisted photobleaching, meaning such crystals could provide suitable labels for samples at risk of that damage. This is consistent with understanding of the native crystals (Agaisse & Lereclus, 1995). Other results were surprising: from the operation of the native *B. thuringiensis* promoter in *E. coli* to the apparent recrystallization in lithium dodecyl sulphate. Results contradict the model in which Cry1Ac embeds in the spore coat (Du & Nickerson, 1996), as the phenotype is shown in the absence of the apparently necessary domain.

While Cry protein research will continue to focus on the toxic core, and the use of *B. thuringiensis* spores as a pesticide, it is likely that researchers will be drawn to the novel applications in crystallogenesis. New imaging techniques increase the value of these crystals: still simple to produce, no longer computationally intractable to analyse. A platform comprising a fluorescent reporter protein and crystallizable domain may have value in screening candidate crystals.

Crystallogenesis notwithstanding, the main outcome here concerns formulation of therapeutic proteins. This chapter reports — for the first time — production during sporulation of antibody fragment fusions to a Cry protein. It contains the first report of triple fusions of target protein, crystallization domain and fluorescent protein, too. Together, these provide the ground onto which it may be possible to build a novel platform for antibody delivery.



## Chapter 6

# Bacterial spores as a commercially viable therapeutic product

The introduction to this dissertation listed a trio of goals for this project:

1. an investigation of the mechanisms that enhance protein stability in spores,
2. the design and optimisation of protein expression systems in spores, and
3. the production, as a proof-of-principle, of a deliverable formulation which allows a controlled dose of proteins to be released in its environment.

These are intended to help answer the question: is it possible to use bacterial spores as vehicles for drug delivery? The answer is certainly yes. It is possible to produce large quantities of spore protein (chapter 5), including various antibody fragments, and it is possible to release antibody fragments from the spore core (chapter 4). For the goal (beyond this thesis) of actually producing such a product, many significant challenges remain — both for the biology and the process engineering. This chapter shall review the progress made in evaluating these new technologies.

The work reported here improves the prospects for spores as a means to formulate therapeutic proteins. Many challenges around commercial viability remain: choice of biologic and delivery location, fabrication and validation concerns (including scale-up and cGMP, current good manufacturing practice), environmental and commercial proliferation requirements, and the organizational difficulties of adding an entirely new product line. As a result of the work in this dissertation, these challenges have become worthwhile topics for future research.

## 6.1 The effects of DPA

Chapter 3 reported a somewhat standalone investigation of the role of DPA (dipicolinic acid) in the stability of spores. Previous research has been unable to separate the absence of DPA from presence of water, and therefore has struggled to investigate whether DPA plays a role by itself or whether it simply allows the spore to maintain or generate a low water content. Here the work in *B. subtilis* of Paidhungat *et al.* (2000) and Magge *et al.* (2008) on spores that cannot produce DPA was successfully replicated in *B. megaterium*, a species with more complicated germination machinery. Like Li *et al.* (2012), attempts to replace DPA with other, similar chemicals, were not successful. However, in doing so chapter 3 demonstrated a new tool, with which to investigate the effects of DPA alone: spores with an enhanced DPA level. The research proved sufficiently promising that a new research project was begun, resulting in a publication by Batalha *et al.* (2017) (and an unsuccessful patent application) on DPA as a pharmaceutical excipient.

However, from the perspective of the goals of this thesis, the work on the effects of DPA proved disappointing. The screening of DPA analogues revealed no suitable candidate. The protocol of analysis of spores by phase contrast was appropriate for screening, but would have been unsuitable for confirming a positive result. It may have been possible to adapt the DPA assay to work with these analogues, but this was beyond the scope of the investigation. Likewise, the use of Raman microscopy and NMR (nuclear magnetic resonance) were deemed not worthwhile, given the negative result in the screen. With such guidance from collaborators, with expertise in formulating biopharmaceuticals, the focus shifted to the second approach: investigating the protein-producing capabilities of sporulating bacteria themselves.



## 6.2 Therapeutic proteins in the spore core

The question of whether sporulating cells can produce therapeutic proteins, such as antibodies, inspired the remainder of this thesis. Building on the work of Mohamed (2015), the work in chapter 4 demonstrated that *B. subtilis* can produce a variety of antibody fragments; the specific fragments were the light chain, heavy chain and three different scFvs (single chain variable fragments) of an IgG (immunoglobulin G), and camelid V<sub>HH</sub> nanobodies. The strain that was engineered to produce these fragments had not been optimized for protein production; indeed, this work demonstrated for the first time that sporulating *B. subtilis* subsp. *subtilis* 168 is capable of producing an scFv in the spore core, without such optimizations.

The antibody fragments were demonstrated to run at their predicted masses on SDS-PAGE, and fluorescent fusions shown to fluoresce. However, it has not been demonstrated whether such antibodies are functional. The lack of a simple assay for NIP109 means that optimization cycles take far longer than they might otherwise do. The work with the camelid antibody fragments was designed to make such a functional assay feasible; this is now the case. The BcII10 nanobodies, targeting *B. cereus* metallo- $\beta$ -lactamase, may be used in the colorimetric nitrocephin assay as an indirect test. Directly testing the effect on antibiotic resistance in culture would then be valuable.

The challenge of producing a full, assembled IgG inside the spore core remains. There is a straightforward route to producing both chains in the core, using a two-promoter system. However, there exists no suitable technique to analyse such co-expression *in vivo*, in the spore core. Analysis *ex vivo* presents another form of the challenge addressed by the following chapter.

In chapter 4, production of antibody fragments has only been demonstrated in *B. subtilis* subsp. *subtilis* 168. Other sporeformers — notably the large *B. megaterium* or a strain like *B. thuringiensis* subsp. *finitimus* YBT-020, for which there is a crystal and spore core together within the exosporium — may prove a far better host, based on their size. It is not yet clear which location (core, coat or interspace) in a spore may prove the best. It may be possible to use multiple locations to combine targeting and payload functionality.

Finally, the total mass of protein in each spore is relatively low, as seen in earlier work by Mohamed (2015). The work in chapter 5 showed some success in adapting the *cry1Ac* operon to function in the late forespore; such work may in future help to increase this low limit.

One bottleneck in much work with spore cores has been extraction of the expressed protein — leading to an inability to scale the production process. Part of the original aim of this project was to analyse the structural properties of these proteins from a formulation perspective. However, having successfully, and for the first time, produced various antibody fragments, it became clear that there existed no process capable of producing and extracting enough protein from the cores to perform such analysis.

A potential solution to the bottleneck in extraction of protein from spores, investigated in chapter 4, is to use spores bearing a  $\Delta cotE$  mutation. This manifests as a missing outer coat (and damaged inner coat), thereby rendering the spores sensitive to lysozyme. Though such a mutation has been known for three decades, it has never been proposed as a technique to facilitate such analysis of the spore core. Such chemical disruption scales in a way mechanical disruption does not. With such spores it will now be possible to produce sufficient protein to run a full set of formulation experiments: work which has never before been reported for a therapeutic protein produced by sporulating cells.

The chapter reported successful development of a strain with the  $\Delta cotE$  mutation in a supercompetent background; it also demonstrated the ease of working with such a strain by replicating earlier transformations. Coat deficient spores, containing fluorescent antibody fusions, were disrupted by exposure to lysozyme. This released the fluorescent contents of the spores.

The spores of these strains, containing a model therapeutic protein that can be released by a specific chemical mechanism, are a proof-of-principle bacterial spore formulation.

This research ought to move forward in two directions. Firstly, the lysozyme disruption protocol should be optimized for use in the laboratory; this would enable further experiments on the proteins produced in the spore cores. Secondly, the spores should be tested in simulated gastric and intestinal fluids, to investigate whether the coat deficiency alone will help ensure that a protein payload is released at the GALT (gut associated lymphatic tissue). Indeed, it may now be possible to produce spores which lyse in the duodenum, thereby providing one solution to the delivery challenge around commercial viability.

Such a solution may be considered an *engineering* solution to the aforementioned problem. An alternative way to solve problems is to revisit assumptions and completely revise the approach. In this case, the problem is the inherently limited productivity of forespores; the core is already fairly well packed and so there may well be a relatively low upper limit to the mass fraction of heterologous protein the spore can contain. The assumption to revisit is that, in order to benefit from spores' ability to stabilize proteins, the protein must be in the spore core.

### 6.3 Crystal protein fusions

*B. thuringiensis* is well known for its large crystalline inclusions, which typically reach the same size as the spore. Chapter 5 demonstrated the successful production of various fluorescent fusions of Cry1Ac as inclusions in *E. coli* and as heterologous crystals with native Cry1Ac in the mother cells of sporulating *B. thuringiensis* subsp. *kurstaki* HD-73. Furthermore, it demonstrated that sporulating *B. thuringiensis* subsp. *kurstaki* HD-73 can produce fluorescent Cry1Ac fusions of antibody fragments: light-chain, heavy-chain and scFv.

There were difficulties in analysing such crystals, however. Attempts to solubilize crystal fusions for SDS-PAGE resulted in widespread fragmentation. In a few cases, this has made it difficult to be certain whether the full length crystal has been produced; in others, by contrast, it helped confirm it.

The fabrication system developed here offers the possibility to produce robust therapeutic crystals, suitable for delivery to patients in crystalline form. Even conventional formulations may benefit from such a bacterial production system. The productivity improvements of a greater titre are an advantage over CHO (Chinese hamster ovary)-produced antibodies; that and the reduced requirements for downstream processing offer an advantage over *E. coli*. If encapsulated within the spore exosporium, in the same manner as *B. thuringiensis* YBT-020, crystal protein fusions offer an alternative to the core protein model presented in chapter 4 — another fully self-contained delivery system.

Perhaps the most significant unexpected outcome, with its own promising line of further research, concerns the utility of Cry fusion proteins in enabling structural studies of proteins that have proved impervious to crystallization, and one can hope there are opportunities to

investigate such possibilities. At the time of this work, nobody had yet proposed Cry fusions as a tool with which to produce crystals from recalcitrant proteins; indeed, the use of fusions in crystallogenesis is itself very recent.

The crystals produced by *B. thuringiensis* are too small for conventional X-ray diffraction and though they may suit Cryo-EM, it may also be possible to recrystallize these fusions. For recrystallization, Evdokimov *et al.* (2014) claimed it was necessary to substitute fourteen cysteine residues within the protoxin domain of native Cry1Ac. Here, for the first time, it has been demonstrated that heating crystals to 70 °C for 10 min in LDS sample buffer (for PAGE analysis) resulted in crystals that did not appear on phase contrast, yet still fluoresced, and were measurably larger than the source culture, or those not heated. While it is not yet fully clear what mechanism lies behind such a serendipitous observation, nor the factors affecting such behaviour, it may offer an alternative method of growing crystals to a size suitable for structural studies.

The work on Cry1Ac protein fusions has resulted in a platform for producing fusion crystals, at scale. There is now a project investigating such a possibility. Additionally, while inclusions have previously been reported in *E. coli*, this dissertation has demonstrated for the first time that in *E. coli* the  $P_{cry1Ac}$  from the aforementioned *B. thuringiensis* strain appears to be constitutively active. Such constructs might be used when assembling plasmids encoding crystal fusions, so that colonies can be screened for correct DNA assembly and protein folding.

## 6.4 Final conclusions

In sum, this dissertation reports a number of novel findings concerning the heterologous production capabilities of sporulating cells, and highlights significant leads for future research.

The investigation of the mechanism by which DPA acts in spores has led directly to others demonstrating that DPA enhances protein stability *in vitro*. It is not clear how relevant this is to *in vivo* stabilization of proteins; however thanks to the work presented here, a new technique — that of producing DPA-enhanced spores — is now available to researchers.

The engineering of *B. subtilis* to produce therapeutic proteins, while sporulating, was a success. However the spore is able to keep proteins in its core stable, it may be possible to confer that stability on heterologous proteins, too. The antibody chains and scFvs have been produced with the predicted masses, and fluorescent fusions gave a positive signal (and *vice versa* for non-fluorescent variants). Likewise, various nanobodies and nanobody fusions produced correct outputs. Furthermore, by genetically removing the spore outer coat (and perturbing the inner coat), this work has resulted in a proof-of-principle *B. subtilis* strain capable of releasing antibody fragments on demand.

There is an alternative model, too, using the Cry1Ac production mechanism of *B. thuringiensis*, to produce antibody fusions. The resulting crystals may be useful as part of pharmaceutical formulations, and beyond, in crystallogenesi for structural study.

Taken together, the core and crystal expression systems show, as proof of principle, that bacterial spores are feasible vehicles for delivery of therapeutic proteins. There is, however, much work needed to develop that possibility into a commercial product.

The great variety of healthcare challenges demands a variety of formulation approaches. Bacterial endospores offer a new possibility.



# References

- ABEL-SANTOS, E. (ED.) (2012) *Bacterial Spores: Current Research and Applications*. Norfolk, UK: Caister Academic Press. ISBN: 978-1-908230-00-3
- ABLETT, S., DARKE, A. H., LILLFORD, P. J., & MARTIN, D. R. (1999) Glass formation and dormancy in bacterial spores. *International Journal of Food Science and Technology*, **34**(1), 59–69. DOI: 10.1046/j.1365-2621.1999.00240.x
- ADALAT, R., SALEEM, F., CRICKMORE, N., NAZ, S., & SHAKOORI, A. R. (2017) *In vivo* crystallization of three-domain cry toxins. *Toxins*, **9**, 80. DOI: 10.3390/toxins9030080
- ADAMS, L. F., BROWN, K. L., & WHITELEY, H. R. (1991) Molecular cloning and characterization of two genes encoding sigma factors that direct transcription from a *Bacillus thuringiensis* crystal protein gene promoter. *Journal of Bacteriology*, **173**(12), 3846–54. PMID: 1904859
- AGAISSE, H., GOMLNET, M., ØKSTAD, O. A., KOLSTØ, A. B., & LERECLUS, D. (1999) PlcR is a pleiotropic regulator of extracellular virulence factor gene expression in *Bacillus thuringiensis*. *Molecular Microbiology*, **32**(5), 1043–1053. DOI: 10.1046/j.1365-2958.1999.01419.x
- AGAISSE, H., & LERECLUS, D. (1995) How does *Bacillus thuringiensis* produce so much insecticidal crystal protein? *Journal of Bacteriology*, **177**(21), 6027–32. DOI: 10.1128/jb.177.21.6027-6032.1995
- AGAISSE, H., & LERECLUS, D. (1996) STAB-SD: a Shine-Dalgarno sequence in the 5' untranslated region is a determinant of mRNA stability. *Molecular Microbiology*, **20**(3), 633–43. DOI: 10.1046/j.1365-2958.1996.5401046.x
- AGGARWAL, B. B., & RODRIGUEZ-PADILLA, C. (1999) Antiproliferative protein from *Bacillus thuringiensis* var. *thuringiensis*. United States Patent Office: US 5977058 A. FROM [HTTPS://PATENTS.GOOGLE.COM/PATENT/US5977058A](https://patents.google.com/patent/US5977058A)
- ALGIE, J. E. (1980) The heat resistance of bacterial spores due to their partial dehydration by reverse osmosis. *Current Microbiology*, **3**(5), 287–290. DOI: 10.1007/BF02601807
- ALGIE, J. E. (1983) The heat resistance of bacterial spores and its relationship to the contraction of the forespore protoplasm during sporulation. *Current Microbiology*, **9**(4), 173–175. DOI: 10.1007/BF01567577
- ALGIE, J. E. (1984) Effect of the internal water activity of bacterial spores on their heat resistance in water. *Current Microbiology*, **11**(5), 293–295. DOI: 10.1007/BF01567389

- AL RIYAMI, B. Z. R. (2017) *Molecular and structural analysis of proteins involved in bacterial spore germination* (PhD thesis). University of Cambridge
- ANDRIS-WIDHOPF, J., STEINBERGER, P., FULLER, R., RADER, C., & BARBAS, C. F. (2011) Generation of human scFv antibody libraries: PCR amplification and assembly of light- and heavy-chain coding sequences. *Cold Spring Harbor Protocols*, **2011**(9), 1139–1151. DOI: [10.1101/pdb.prot065573](https://doi.org/10.1101/pdb.prot065573)
- ARONSON, A. I. (2012) The structure and composition of the outer layers of the bacterial spore. In: E. Abel-Santos (ED.), *Bacterial spores: Current research and applications* (pp. 57–72). Norfolk, UK: Caister Academic Press
- ARZENŠEK, D., KUZMAN, D., & PODGORNIK, R. (2012) Colloidal interactions between monoclonal antibodies in aqueous solutions. *Journal of Colloid and Interface Science*, **384**(1), 207–16. DOI: [10.1016/j.jcis.2012.06.055](https://doi.org/10.1016/j.jcis.2012.06.055)
- ATKINS, J. L., PATEL, M. B., DASCHBACH, M. M., MEISEL, J. W., & GOKEL, G. W. (2012) Anion complexation and transport by isophthalamide and dipicolinamide derivatives: DNA plasmid transformation in *E. coli*. *Journal of the American Chemical Society*, **134**(33), 13546–9. DOI: [10.1021/ja304816e](https://doi.org/10.1021/ja304816e)
- BAILEY, D. M. D. (2013–2019) Personal communications. [dmdb1@cam.ac.uk](mailto:dmdb1@cam.ac.uk)
- BAILEY, D. M. D., & MOHAMED, M. Y. H. (2018) Klenow Assembly Method: Seamless cloning. RETRIEVED APRIL 1, 2019, FROM [HTTPS://OPENWETWARE.ORG/WIKI/KLENOW\\_ASSEMBLY\\_METHOD:\\_SEAMLESS\\_CLONING](https://openwetware.org/wiki/Klenow_Assembly_Method:_Seamless_Cloning)
- BALASSA, G., MILHAUD, P., RAULET, E., SILVA, M. T., & SOUSA, J. C. F. (1979) A *Bacillus subtilis* mutant requiring dipicolinic acid for the development of heat-resistant spores. *Microbiology*, **110**(2), 365–379
- BASSI, D., CAPPÀ, F., & COCCONCELLI, P. S. (2012) Water and cations flux during sporulation and germination. In: E. Abel-Santos (ED.), *Bacterial spores: Current research and applications* (pp. 143–168). Norfolk, UK: Caister Academic Press
- BATALHA, I. L., KE, P., TEJEDA-MONTES, E., UDDIN, S., WALLE, C. F. VAN DER, & CHRISTIE, G. (2017) Dipicolinic acid as a novel spore-inspired excipient for antibody formulation. *International Journal of Pharmaceutics*, **526**(1–2), 332–338. DOI: [10.1016/j.ijpharm.2017.05.012](https://doi.org/10.1016/j.ijpharm.2017.05.012)
- BAUER, T., LITTLE, S., STÖVER, A. G., & DRIKS, A. (2001) Functional analysis of the *Bacillus subtilis* morphogenetic spore coat protein CotE. *Molecular Microbiology*, **42**(4), 1107–1120. DOI: [10.1046/j.1365-2958.2001.02708.x](https://doi.org/10.1046/j.1365-2958.2001.02708.x)
- BECHTEL, D. B., & BULLA, L. A. (1976) Electron microscope study of sporulation and parasporal crystal formation in *Bacillus thuringiensis*. *Journal of Bacteriology*, **127**(3), 1472–1481



- BECKER, G., & HENGGE-ARONIS, R. (2001) What makes an *Escherichia coli* promoter  $\sigma^S$  dependent? Role of the -13/-14 nucleotide promoter positions and region 2.5 of  $\sigma^S$ . *Molecular Microbiology*, **39**(5), 1153–1165. DOI: [10.1046/j.1365-2958.2001.02313.x](https://doi.org/10.1046/j.1365-2958.2001.02313.x)
- BEILHARZ, K., RAAPHORST, R. VAN, KJOS, M., & VEENING, J.-W. (2015) Red fluorescent proteins for gene expression and protein localization studies in *Streptococcus pneumoniae* and efficient transformation with DNA assembled via the Gibson assembly method. *Applied and Environmental Microbiology*, **81**(20), 7244–7252. DOI: [10.1128/AEM.02033-15](https://doi.org/10.1128/AEM.02033-15)
- BHARDWAJ, G., MULLIGAN, V. K., BAHL, C. D., GILMORE, J. M., HARVEY, P. J., CHENEVAL, O., ... BAKER, D. (2016) Accurate *de novo* design of hyperstable constrained peptides. *Nature*, **538**(7625), 329–335. DOI: [10.1038/nature19791](https://doi.org/10.1038/nature19791)
- BIEDENDIECK, R., BORGMEIER, C., BUNK, B., STAMMEN, S., SCHERLING, C., MEINHARDT, F., ... JAHN, D. (2011) *Systems biology of recombinant protein production using Bacillus megaterium* (1st ed., Vol. 500, pp. 165–195). Elsevier Inc. ISBN: 9780123851185
- BISHOP, A. H., JOHNSON, C., & PERANI, M. (1999) The safety of *Bacillus thuringiensis* to mammals investigated by oral and subcutaneous dosage. *World Journal of Microbiology and Biotechnology*, **15**(3), 375–380. DOI: [10.1023/A:1008983818692](https://doi.org/10.1023/A:1008983818692)
- BOSTRÖM, M., TAVARES, F. W., FINET, S., SKOURI-PANET, F., TARDIEU, A., & NINHAM, B. W. (2005) Why forces between proteins follow different Hofmeister series for pH above and below pI. *Biophysical Chemistry*, **117**(3), 217–24. DOI: [10.1016/j.bpc.2005.05.010](https://doi.org/10.1016/j.bpc.2005.05.010)
- BRADBURY, J. H., FOSTER, J. R., HAMMER, B., LINDSAY, J., & MURRELL, W. G. (1981) The source of the heat resistance of bacterial spores. *Biochimica et Biophysica Acta (BBA) - General Subjects*, **678**(2), 157–164. DOI: [10.1016/0304-4165\(81\)90201-4](https://doi.org/10.1016/0304-4165(81)90201-4)
- BRAR, S. K., VERMA, M., TYAGI, R. D., & VALÉRO, J. R. (2006) Recent advances in downstream processing and formulations of *Bacillus thuringiensis* based biopesticides. *Process Biochemistry*, **41**(2), 323–342. DOI: [10.1016/j.procbio.2005.07.015](https://doi.org/10.1016/j.procbio.2005.07.015)
- BRYANT, J. E. (1994) Commercial production and formulation of *Bacillus thuringiensis*. *Agriculture, Ecosystems & Environment*, **49**, 31–35. DOI: [10.1016/0167-8809\(94\)90018-3](https://doi.org/10.1016/0167-8809(94)90018-3)
- BULLA, L. A., KRAMER, K. J., & DAVIDSON, L. I. (1977) Characterization of the entomocidal parasporal crystal of *Bacillus thuringiensis*. *Journal of Bacteriology*, **130**(1), 375–383. PMID: 853031
- CAMP, A. H., & LOSICK, R. (2009) A feeding tube model for activation of a cell-specific transcription factor during sporulation in *Bacillus subtilis*. *Genes & Development*, **23**(8), 1014–1024. DOI: [10.1101/gad.1781709](https://doi.org/10.1101/gad.1781709)
- CAMP, A. H., WANG, A. F., & LOSICK, R. (2011) A small protein required for the switch from  $\sigma^F$  to  $\sigma^G$  during sporulation in *Bacillus subtilis*. *Journal of Bacteriology*, **193**(1), 116–124. DOI: [10.1128/JB.00949-10](https://doi.org/10.1128/JB.00949-10)

- CARLSON, C. J., GETZ, W. M., KAUSRUD, K. L., CIZAUSKAS, C. A., BLACKBURN, J. K., BUSTOS CARRILLO, F. A., ... STENSETH, N. C. (2018) Spores and soil from six sides: interdisciplinarity and the environmental biology of anthrax *Bacillus anthracis*. *Biological Reviews*, **93**(4), 1813–1831. DOI: [10.1111/brv.12420](https://doi.org/10.1111/brv.12420)
- CARR, J. F., DANZIGER, M. E., HUANG, A. L., DAHLBERG, A. E., & GREGORY, S. T. (2015) Engineering the genome of *Thermus thermophilus* using a counterselectable marker. *Journal of Bacteriology*, **197**(6), 1135–1144. DOI: [10.1128/JB.02384-14](https://doi.org/10.1128/JB.02384-14)
- CAYLEY, D. S., GUTTMAN, H. J., & RECORD, M. T. (2000) Biophysical characterization of changes in amounts and activity of *Escherichia coli* cell and compartment water and turgor pressure in response to osmotic stress. *Biophysical Journal*, **78**(4), 1748–1764. DOI: [10.1016/S0006-3495\(00\)76726-9](https://doi.org/10.1016/S0006-3495(00)76726-9)
- CHAN, M. K., & NAIR, M. S. (2013) Cry crystals for the production of antimicrobial proteins. United States Patent Office: WO 2013085540 A2. FROM [HTTPS://PATENTS.GOOGLE.COM/PATENT/WO2013085540A2](https://patents.google.com/patent/WO2013085540A2)
- CHAN, M. K., NAIR, M. S., & LEE, M. M. (2010) Biomaterials, compositions, and methods. United States Patent Office: US 2010/0322977 A1. FROM [HTTPS://PATENTS.GOOGLE.COM/PATENT/US20100322977](https://patents.google.com/patent/US20100322977)
- CHRISTIE, G. (2013–2019) Personal communications. [gc301@cam.ac.uk](mailto:gc301@cam.ac.uk)
- CHURCH, B. D., & HALVORSON, H. (1959) Dependence of the heat resistance of bacterial endospores on their dipicolinic acid content. *Nature*, **183**(4654), 124–125. DOI: [10.1038/183124a0](https://doi.org/10.1038/183124a0)
- CHURCH, B. D., HALVORSON, H., & HALVORSON, H. O. (1954) Studies on spore germination: its independence from alanine racemase activity. *Journal of Bacteriology*, **68**(4), 393–399. PMID: [13201542](https://pubmed.ncbi.nlm.nih.gov/13201542/)
- CLOUGH, H. E., CLANCY, D., O'NEILL, P. D., ROBINSON, S. E., & FRENCH, N. P. (2005) Quantifying uncertainty associated with microbial count data: a Bayesian approach. *Biometrics*, **61**(2), 610–6. DOI: [10.1111/j.1541-0420.2005.030903.x](https://doi.org/10.1111/j.1541-0420.2005.030903.x)
- COMOGLIO, F., FRACCHIA, L., & RINALDI, M. (2013) Bayesian inference from count data using discrete uniform priors. *PloS One*, **8**(10), e74388. DOI: [10.1371/journal.pone.0074388](https://doi.org/10.1371/journal.pone.0074388)
- CONNORS, M. J., MASON, J. M., & SETLOW, P. (1986) Cloning and nucleotide sequencing of genes for three small, acid-soluble proteins from *Bacillus subtilis* spores. *J. Bacteriol.*, **166**(2), 417–425
- CONRATH, K. E., LAUWEREYS, M., GALLEN, M., MATAGNE, A., FRÈRE, J.-M., KINNE, J., ... MUYLDERMANS, S. (2001)  $\beta$ -Lactamase inhibitors derived from single-domain antibody fragments elicited in the *Camelidae*. *Antimicrobial Agents and Chemotherapy*, **45**(10), 2807–2812. DOI: [10.1128/AAC.45.10.2807-2812.2001](https://doi.org/10.1128/AAC.45.10.2807-2812.2001)

- CORDOBA, A. J., SHYONG, B.-J., BREEN, D., & HARRIS, R. J. (2005) Non-enzymatic hinge region fragmentation of antibodies in solution. *Journal of Chromatography. B, Analytical Technologies in the Biomedical and Life Sciences*, **818**(2), 115–21. DOI: [10.1016/j.jchromb.2004.12.033](https://doi.org/10.1016/j.jchromb.2004.12.033)
- CÔTÉ, J.-C., JUNG, Y.-C., MIZUKI, E., & AKAO, T. (2008) *Bacillus thuringiensis* strain, crystal gene and crystal protein and uses thereof. United States Patent Office: US 7329733 B2
- CRAWSHAW, A. D., SERRANO, M., STANLEY, W. A., HENRIQUES, A. O., & SALGADO, P. S. (2014) A mother cell-to-forespore channel: current understanding and future challenges. *FEMS Microbiology Letters*, **358**(2), 129–136. DOI: [10.1111/1574-6968.12554](https://doi.org/10.1111/1574-6968.12554)
- CRICKMORE, N. (2006) Beyond the spore - Past and future developments of *Bacillus thuringiensis* as a biopesticide. *Journal of Applied Microbiology*, **101**(3), 616–619. DOI: [10.1111/j.1365-2672.2006.02936.x](https://doi.org/10.1111/j.1365-2672.2006.02936.x)
- CUTTING, S. M. (2013) CDVAX. RETRIEVED SEPTEMBER 28, 2017, FROM [CDVAX.ORG](http://CDVAX.ORG)
- DANQUAH, M. K., & FORDE, G. M. (2007) Growth medium selection and its economic impact on plasmid DNA production. *Journal of Bioscience and Bioengineering*, **104**(6), 490–497. DOI: [10.1263/jbb.104.490](https://doi.org/10.1263/jbb.104.490)
- DELAFIELD, F. P., SOMERVILLE, H. J., & RITTENBERG, S. C. (1968) Immunological homology between crystal and spore protein of *Bacillus thuringiensis*. *Journal of Bacteriology*, **96**(3), 713–20. PMID: 4979101
- DE MEYER, T., MUYLDERMANS, S., & DEPICKER, A. (2014) Nanobody-based products as research and diagnostic tools. *Trends in Biotechnology*, **32**(5), 263–270. DOI: [10.1016/j.tibtech.2014.03.001](https://doi.org/10.1016/j.tibtech.2014.03.001)
- DENG, C., SLAMTI, L., RAYMOND, B., LIU, G., LEMY, C., GOMINET, M., ... SONG, F. (2014) Division of labour and terminal differentiation in a novel *Bacillus thuringiensis* strain. *The ISME Journal*, **9**(2), 286–296. DOI: [10.1038/ismej.2014.122](https://doi.org/10.1038/ismej.2014.122)
- DENG, Y., SUN, M., & SHAEVITZ, J. W. (2011) Direct measurement of cell wall stress stiffening and turgor pressure in live bacterial cells. *Physical Review Letters*, **107**(15), 158101. DOI: [10.1103/PhysRevLett.107.158101](https://doi.org/10.1103/PhysRevLett.107.158101)
- DOBSON, C. L., DEVINE, P. W. A., PHILLIPS, J. J., HIGAZI, D. R., LLOYD, C., POPOVIC, B., ... LOWE, D. C. (2016) Engineering the surface properties of a human monoclonal antibody prevents self-association and rapid clearance in vivo. *Scientific Reports*, **6**(November), 38644. DOI: [10.1038/srep38644](https://doi.org/10.1038/srep38644)
- DU, C., CHAN, W. C., MCKEITHAN, T. W., & NICKERSON, K. W. (2005) Surface display of recombinant proteins on *Bacillus thuringiensis* spores. *Applied and Environmental Microbiology*, **71**(6), 3337–41. DOI: [10.1128/AEM.71.6.3337-3341.2005](https://doi.org/10.1128/AEM.71.6.3337-3341.2005)

- DU, C., & NICKERSON, K. W. (1996) *Bacillus thuringiensis* HD-73 spores have surface-localized Cry1Ac toxin: physiological and pathogenic consequences. *Applied and Environmental Microbiology*, **62**(10), 3722–6. PMID: 16535421
- DUC, L. H., HONG, H. A., FAIRWEATHER, N., RICCA, E., & CUTTING, S. M. (2003) Bacterial spores as vaccine vehicles. *Infection and Immunity*, **71**(5), 2810–2818. DOI: 10.1128/IAI.71.5.2810-2818.2003
- ENGLER, C., KANDZIA, R., & MARILLONNET, S. (2008) A one pot, one step, precision cloning method with high throughput capability. *PLoS ONE*, **3**(11), e3647. DOI: 10.1371/journal.pone.0003647
- ERRINGTON, J. (1993) *Bacillus subtilis* sporulation: regulation of gene expression and control of morphogenesis. *Microbiological Reviews*, **57**(1), 1–33. PMID: 8464402
- EVDOKIMOV, A. G., MOSHIRI, F., STURMAN, E. J., RYDEL, T. J., ZHENG, M., SEALE, J. W., & FRANKLIN, S. (2014) Structure of the full-length insecticidal protein Cry1Ac reveals intriguing details of toxin packaging into in vivo formed crystals. *Protein Science*, **23**(11), 1491–1497. DOI: 10.1002/pro.2536
- EVETT, M. P. (2004) Standard IUB/IUPAC amino and nucleic acid codes. RETRIEVED APRIL 1, 2019, FROM [HTTPS://EMUNIX.EMICH.EDU/~EVETT/BIOINFORMATICTOOLS/IUB%20CODES.HTM](https://emunix.emich.edu/~evett/BIOINFORMATICTOOLS/IUB%20CODES.HTM)
- FABRET, C., DUSKO EHRLICH, S., & NOIROT, P. (2002) A new mutation delivery system for genome-scale approaches in *Bacillus subtilis*. *Molecular Microbiology*, **46**(1), 25–36. DOI: 10.1046/j.1365-2958.2002.03140.x
- FOROUHAR, F., SU, M., SEETHARAMAN, J., FANG, F., XIAO, R., CUNNINGHAM, K., ... NORTHEAST STRUCTURAL GENOMICS CONSORTIUM (NESG) (2010) Crystal structure of Stage V sporulation protein AD (spoVAD) from *Bacillus subtilis*. PDB: 3LM6, version 1.1. DOI: 10.2210/pdb3LM6/pdb
- GHOSH, A., MANTON, J. D., MUSTAFA, A. R., GUPTA, M., AYUSO-GARCIA, A., REES, E. J., & CHRISTIE, G. (2018) Proteins encoded by the *gerP* operon are localized to the inner coat in *Bacillus cereus* spores and are dependent on GerPA and SafA for assembly. *Applied and Environmental Microbiology*, **84**(14), 1–18. DOI: 10.1128/aem.00760-18
- GHOSH, S., ZHANG, P., LI, Y.-Q., & SETLOW, P. (2009) Superdormant spores of *Bacillus* species have elevated wet-heat resistance and temperature requirements for heat activation. *Journal of Bacteriology*, **191**(18), 5584–91. DOI: 10.1128/JB.00736-09
- GIBSON, D. G., GLASS, J. I., LARTIGUE, C., NOSKOV, V. N., CHUANG, R.-Y., ALGIRE, M. A., ... VENTER, J. C. (2010) Creation of a bacterial cell controlled by a chemically synthesized genome. *Science (New York, N.Y.)*, (May). DOI: 10.1126/science.1190719

- GIBSON, D. G., YOUNG, L., CHUANG, R.-Y., VENTER, J. C., HUTCHISON, C. A., & SMITH, H. O. (2009) Enzymatic assembly of DNA molecules up to several hundred kilobases. *Nature Methods*, **6**(5), 343–5. DOI: [10.1038/nmeth.1318](https://doi.org/10.1038/nmeth.1318)
- GIEGÉ, R. (2017) What macromolecular crystallogeneses tells us – what is needed in the future. *IUCrJ*, **4**(4), 340–349. DOI: [10.1107/S2052252517006595](https://doi.org/10.1107/S2052252517006595)
- GLARE, T. R., & O'CALLAGHAN, M. (2000) *Bacillus thuringiensis: Biology, ecology and safety*, John Wiley & Sons. New York, NY: Wiley & Sons, Inc. ISBN: 978-0-471-49630-4
- GLICK, B. R. (1995) Metabolic load and heterologous gene expression. *Biotechnology Advances*, **13**(2), 247–261. DOI: [10.1016/0734-9750\(95\)00004-A](https://doi.org/10.1016/0734-9750(95)00004-A)
- GOLOVANOV, A. P., HAUTBERGUE, G. M., WILSON, S. A., & LIAN, L.-Y. (2004) A simple method for improving protein solubility and long-term stability. *Journal of the American Chemical Society*, **126**(29), 8933–9. DOI: [10.1021/ja049297h](https://doi.org/10.1021/ja049297h)
- GOULD, G. W. (1969) Germination. In: G. W. Gould & A. Hurst (Eds.), *The bacterial spore* (pp. 397–444). London, UK: Academic Press Inc. (London) Ltd.
- GOULD, G. W. (2006) History of science – Spores: Lewis B Perry Memorial Lecture 2005. *Journal of Applied Microbiology*, **101**(3), 507–513. DOI: [10.1111/j.1365-2672.2006.02888.x](https://doi.org/10.1111/j.1365-2672.2006.02888.x)
- GROOT, A. J., MENGESHA, A., WALL, E. VAN DER, DIEST, P. J. VAN, THEYS, J., & VOOIJS, M. (2007) Functional antibodies produced by oncolytic clostridia. *Biochemical and Biophysical Research Communications*, **364**(4), 985–9. DOI: [10.1016/j.bbrc.2007.10.126](https://doi.org/10.1016/j.bbrc.2007.10.126)
- GUÉROUT-FLEURY, A. M., FRANSEN, N., & STRAGIER, P. (1996) Plasmids for ectopic integration in *Bacillus subtilis*. *Gene*, **180**(1-2), 57–61. DOI: [10.1016/S0378-1119\(96\)00404-0](https://doi.org/10.1016/S0378-1119(96)00404-0)
- GUÉROUT-FLEURY, A.-M., SHAZAND, K., FRANSEN, N., & STRAGIER, P. (1995) Antibiotic-resistance cassettes for *Bacillus subtilis*. *Gene*, **167**(1-2), 335–336. DOI: [10.1016/0378-1119\(95\)00652-4](https://doi.org/10.1016/0378-1119(95)00652-4)
- GUIZIOU, S., SAUVEPLANE, V., CHANG, H.-J., CLER E, C., DECLERCK, N., JULES, M., & BONNET, J. (2016) A part toolbox to tune genetic expression in *Bacillus subtilis*. *Nucleic Acids Research*, **44**(10), 7495–7508. DOI: [10.1093/nar/gkw624](https://doi.org/10.1093/nar/gkw624)
- GUPTA, S., USTOK, F. I., JOHNSON, C. L., BAILEY, D. M. D., LOWE, C. R., & CHRISTIE, G. (2013) Investigating the functional hierarchy of *Bacillus megaterium* PV361 spore germinant receptors. *Journal of Bacteriology*, **195**(13), 3045–53. DOI: [10.1128/JB.00325-13](https://doi.org/10.1128/JB.00325-13)
- HARWOOD, C. R., & CUTTING, S. M. (Eds.) (1990) *Molecular biological methods for Bacillus*. New York, NY: John Wiley & Sons. ISBN: 9780471923930

- HEDGES, A. J. (2002) Estimating the precision of serial dilutions and viable bacterial counts. *International Journal of Food Microbiology*, **76**(3), 207–14. PMID: 12051477
- HIMMELREICH, R., & WERNER, S. (2014) Method for isolating and purifying nucleic acids. United States Patent Office: US 8624020 B2. FROM [HTTPS://PATENTS.GOOGLE.COM/PATENT/US8624020](https://patents.google.com/patent/US8624020)
- HUBER, H. E., LÜTHY, P., EBERSOLD, H.-R., & CORDIER, J.-L. (1981) The subunits of the parasporal crystal of *Bacillus thuringiensis*: Size, linkage and toxicity. *Archives of Microbiology*, **129**(1), 14–18. DOI: 10.1007/BF00417171
- ICHIMURA, T., CHIU, L.-D., FUJITA, K., KAWATA, S., WATANABE, T. M., YANAGIDA, T., & FUJITA, H. (2014) Visualizing cell state transition using Raman spectroscopy. *PloS One*, **9**(1), e84478. DOI: 10.1371/journal.pone.0084478
- IUPAC-IUB COMM. ON BIOCHEM. NOMENCL. (1968) A one-letter notation for amino acid sequences. Tentative rules. *Biochemistry*, **7**(8), 2703–2705. DOI: 10.1021/bi00848a001
- JANES, B. K., & STIBITZ, S. (2006) Routine markerless gene replacement in *Bacillus anthracis*. *Infection and Immunity*, **74**(3), 1949–1953. DOI: 10.1128/IAI.74.3.1949-1953.2006
- JANSSEN, F. W., LUND, A. J., & ANDERSON, L. E. (1958) Colorimetric assay for dipicolinic acid in bacterial spores. *Science*, **127**(3288), 26–27. DOI: 10.1126/science.127.3288.26
- JOHLER, S., KALBHENN, E. M., HEINI, N., BRODMANN, P., GAUTSCH, S., BAĞCIOĞLU, M., ... EHLING-SCHULZ, M. (2018) Enterotoxin production of *Bacillus thuringiensis* isolates from biopesticides, foods, and outbreaks. *Frontiers in Microbiology*, **9**, 1915. DOI: 10.3389/fmicb.2018.01915
- JORDAN, E., HUST, M., ROTH, A., BIEDENDIECK, R., SCHIRRMANN, T., JAHN, D., & DÜBEL, S. (2007) Production of recombinant antibody fragments in *Bacillus megaterium*. *Microbial Cell Factories*, **6**, 2. DOI: 10.1186/1475-2859-6-2
- KAIEDA, S., SETLOW, B., SETLOW, P., & HALLE, B. (2013) Mobility of core water in *Bacillus subtilis* spores by (2)H NMR. *Biophysical Journal*, **105**(9), 2016–23. DOI: 10.1016/j.bpj.2013.09.022
- KIRCHHOFER, A., HELMA, J., SCHMIDTHALS, K., FRAUER, C., CUI, S., KARCHER, A., ... ROTHBAUER, U. (2010) Modulation of protein properties in living cells using nanobodies. *Nature Structural & Molecular Biology*, **17**(1), 133–138. DOI: 10.1038/nsmb.1727
- KNOWLES, B. H., & ELLAR, D. J. (1987) Colloid-osmotic lysis is a general feature of the mechanism of action of *Bacillus thuringiensis*  $\delta$ -endotoxins with different insect specificity. *BBA - General Subjects*, **924**(3), 509–518. DOI: 10.1016/0304-4165(87)90167-X

- KOOPMANN, R., CUPELLI, K., REDECKE, L., NASS, K., DEPONTE, D. P., WHITE, T. A., ... DUSZENKO, M. (2012) *In vivo* protein crystallization opens new routes in structural biology. *Nature Methods*, **9**(3), 259–262. DOI: [10.1038/nmeth.1859](https://doi.org/10.1038/nmeth.1859)
- KORNELI, C., DAVID, F., BIEDENDIECK, R., JAHN, D., & WITTMANN, C. (2013) Getting the big beast to work—Systems biotechnology of *Bacillus megaterium* for novel high-value proteins. *Journal of Biotechnology*, **163**(2), 87–96. DOI: [10.1016/j.jbiotec.2012.06.018](https://doi.org/10.1016/j.jbiotec.2012.06.018)
- KRUSCHKE, J. K. (2013) Bayesian estimation supersedes the *t* test. *Journal of Experimental Psychology: General*, **142**(2), 573–603. DOI: [10.1037/a0029146](https://doi.org/10.1037/a0029146)
- KUDLA, J., & BOCK, R. (2016) Lighting the way to protein-protein interactions: recommendations on best practices for bimolecular fluorescence complementation (BiFC) analyses. *The Plant Cell*, **28**(iii), 1–13. DOI: [10.1105/tpc.16.00043](https://doi.org/10.1105/tpc.16.00043)
- LERECLUS, D., ARANTÉS, O. M. N., CHAUFaux, J., & LECADet, M.-M. (1989) Transformation and expression of a cloned  $\delta$ -endotoxin gene in *Bacillus thuringiensis*. *FEMS Microbiology Letters*, **60**(2), 211–217. DOI: [10.1111/j.1574-6968.1989.tb03448.x](https://doi.org/10.1111/j.1574-6968.1989.tb03448.x)
- LEUSCHNER, R. G., & LILLFORD, P. J. (2000) Effects of hydration on molecular mobility in phase-bright *Bacillus subtilis* spores. *Microbiology (Reading, England)*, **146**(1), 49–55. PMID: 10658651
- LI, Y., DAVIS, A., KORZA, G., ZHANG, P., LI, Y.-Q., SETLOW, B., ... HAO, B. (2012) Role of a SpoVA protein in dipicolinic acid uptake into developing spores of *Bacillus subtilis*. *Journal of Bacteriology*, **194**(8), 1875–84. DOI: [10.1128/JB.00062-12](https://doi.org/10.1128/JB.00062-12)
- LIN, H. H. (2017) *Surface display of heterologous proteins on Bacillus subtilis spores* (PhD thesis). University of Cambridge
- LIU, L., LIU, Y., SHIN, H.-D., CHEN, R. R., WANG, N. S., LI, J., ... CHEN, J. (2013) Developing *Bacillus* spp. as a cell factory for production of microbial enzymes and industrially important biochemicals in the context of systems and synthetic biology. *Applied Microbiology and Biotechnology*, **97**(14), 6113–27. DOI: [10.1007/s00253-013-4960-4](https://doi.org/10.1007/s00253-013-4960-4)
- LOSICK, R. (2015) A love affair with *Bacillus subtilis*. *Journal of Biological Chemistry*, **290**(5), 2529–2538. DOI: [10.1074/jbc.X114.634808](https://doi.org/10.1074/jbc.X114.634808)
- MAGGE, A., GRANGER, A. C., WAHOME, P. G., SETLOW, B., VEPACHEDU, V. R., LOSHON, C. A., ... SETLOW, P. (2008) Role of dipicolinic acid in the germination, stability, and viability of spores of *Bacillus subtilis*. *Journal of Bacteriology*, **190**(14), 4798–807. DOI: [10.1128/JB.00477-08](https://doi.org/10.1128/JB.00477-08)
- MANETSBERGER, J. (2015) *Investigating the Bacillus megaterium QM B1551 spore coat and exosporium* (PhD thesis). University of Cambridge

- MANETSBERGER, J., MANTON, J. D., ERDELYI, M. J., LIN, H., REES, H. D., CHRISTIE, G., & REES, E. J. (2015) Ellipsoid localisation microscopy infers the size and order of protein layers in *Bacillus* spore coats.
- MANNING, M. C., CHOU, D. K., MURPHY, B. M., PAYNE, R. W., & KATAYAMA, D. S. (2010) Stability of protein pharmaceuticals: an update. *Pharmaceutical Research*, **27**(4), 544–75. DOI: 10.1007/s11095-009-0045-6
- MARGOSCH, D., GÄNZLE, M. G., EHRMANN, M. A., & VOGEL, R. F. (2004) Pressure inactivation of *Bacillus* endospores. *Applied and Environmental Microbiology*, **70**(12), 7321–8. DOI: 10.1128/AEM.70.12.7321-7328.2004
- MCCOOL, G. J., & CANNON, M. C. (2001) PhaC and PhaR are required for polyhydroxyalkanoic acid synthase activity in *Bacillus megaterium*. *Journal of Bacteriology*, **183**(14), 4235–43. DOI: 10.1128/JB.183.14.4235-4243.2001
- MCKENNEY, P. T., DRIKS, A., & EICHENBERGER, P. (2012) The *Bacillus subtilis* endospore: assembly and functions of the multilayered coat. *Nature Reviews Microbiology*, **11**(1), 33–44. DOI: 10.1038/nrmicro2921
- MCKENNEY, P. T., & EICHENBERGER, P. (2012) Dynamics of spore coat morphogenesis in *Bacillus subtilis*. *Molecular Microbiology*, **83**(2), 245–260. DOI: 10.1111/j.1365-2958.2011.07936.x
- MILES, A. A., MISRA, S. S., & IRWIN, J. O. (1938) The estimation of the bactericidal power of the blood. *The Journal of Hygiene*, **38**(6), 732–49. PMID: 20475467
- MIZUKI, E., OHBA, M., AKAO, T., YAMASHITA, S., SAITOH, H., & PARK, Y. S. (1999) Unique activity associated with non-insecticidal *Bacillus thuringiensis* parasporal inclusions: In vitro cell-killing action on human cancer cells. *Journal of Applied Microbiology*, **86**(3), 477–486. DOI: 10.1046/j.1365-2672.1999.00692.x
- MOCK, M., & FOUET, A. (2001) Anthrax. *Annual Review of Microbiology*, **55**(1), 647–671. DOI: 10.1146/annurev.micro.55.1.647
- MOHAMED, M. Y. H. (2015) *Bacillus* spores as oral delivery carriers of therapeutic proteins and vaccines (PhD Thesis). University of Cambridge
- MOIR, A. (2003) Bacterial spore germination and protein mobility. *Trends in Microbiology*, **11**(10), 452–454. DOI: 10.1016/j.tim.2003.08.001
- MONTGOMERY, D. C. (2012) *Design and analysis of experiments* (8th ed.). Wiley. ISBN: 978-1-118146-92-7



- MORISHITA, M., GOTO, T., NAKAMURA, K., LOWMAN, A. M., TAKAYAMA, K., & PEPPAS, N. A. (2006) Novel oral insulin delivery systems based on complexation polymer hydrogels: Single and multiple administration studies in type 1 and 2 diabetic rats. *Journal of Controlled Release*, **110**(3), 587–594. DOI: [10.1016/j.jconrel.2005.10.029](https://doi.org/10.1016/j.jconrel.2005.10.029)
- MURRELL, W. G. (1969) Chemical composition of spores and spore structures. In: G. W. Gould & A. Hurst (EDS.), *The bacterial spore* (pp. 215–273). London, UK: Academic Press Inc. (London) Ltd.
- MURRELL, W. G., & SCOTT, W. J. (1966) The heat resistance of bacterial spores at various water activities. *Microbiology*, **43**(3), 411–425. DOI: [10.1099/00221287-43-3-411](https://doi.org/10.1099/00221287-43-3-411)
- NAIR, M. S., LEE, M. M., BONNEGARDE-BERNARD, A., WALLACE, J. A., DEAN, D. H., OSTROWSKI, M. C., ... CHAN, M. K. (2015) Cry protein crystals: A novel platform for protein delivery. *PLoS ONE*, **10**(6). DOI: [10.1371/journal.pone.0127669](https://doi.org/10.1371/journal.pone.0127669)
- NICHOLSON, W. L. (2002) Roles of *Bacillus* endospores in the environment. *Cellular and Molecular Life Sciences*, **59**(3), 410–416. DOI: [10.1007/s00018-002-8433-7](https://doi.org/10.1007/s00018-002-8433-7)
- NICHOLSON, W. L., & SETLOW, P. (1990) Sporulation, germination and outgrowth. In: C. R. Harwood & S. M. Cutting (EDS.), *Molecular biological methods for Bacillus* (pp. 391–450). New York, NY: John Wiley & Sons
- NIEMELÄ, S. I. (2003) Measurement uncertainty of microbiological viable counts. *Accreditation and Quality Assurance*, **8**(12), 559–563. DOI: [10.1007/s00769-003-0709-6](https://doi.org/10.1007/s00769-003-0709-6)
- OEDA, K., INOUE, K., IBUCHI, Y., OSHIE, K., SHIMIZU, M., NAKAMURA, K., ... OHKAWA, H. (1989) Formation of crystals of the insecticidal proteins of *Bacillus thuringiensis* subsp. aizawai IPL7 in *Escherichia coli*. *Journal of Bacteriology*, **171**(6), 3568–3571. PMID: 2656661
- OHBA, M., MIZUKI, E., & UEMORI, A. (2009) Parasporin, a new anticancer protein group from *Bacillus thuringiensis*. *Anticancer Research*, **29**(1), 427–433. PMID: 19331182
- OPTUM INC. (2017) *Imfinzi™ (durvalumab) – New drug approval*. RETRIEVED FROM [GOO.GL/KRvFY1](https://www.goo.gl/KRvFY1)
- ORSBURN, B. C., MELVILLE, S. B., & POPHAM, D. L. (2010) EtfA catalyses the formation of dipicolinic acid in *Clostridium perfringens*. *Molecular Microbiology*, **75**(1), 178–86. DOI: [10.1111/j.1365-2958.2009.06975.x](https://doi.org/10.1111/j.1365-2958.2009.06975.x)
- PAIDHUNGAT, M., RAGKOUSI, K., & SETLOW, P. (2001) Genetic requirements for induction of germination of spores of *Bacillus subtilis* by Ca<sup>2+</sup>-dipicolinate. *Journal of Bacteriology*, **183**(16), 4886–93. DOI: [10.1128/JB.183.16.4886-4893.2001](https://doi.org/10.1128/JB.183.16.4886-4893.2001)
- PAIDHUNGAT, M., SETLOW, B., DRIKS, A., & SETLOW, P. (2000) Characterization of spores of *Bacillus subtilis* which lack dipicolinic acid. *Journal of Bacteriology*, **182**(19), 5505–5512. DOI: [10.1128/JB.182.19.5505-5512.2000](https://doi.org/10.1128/JB.182.19.5505-5512.2000)

- PALMA, L., MUÑOZ, D., BERRY, C., MURILLO, J., & CABALLERO, P. (2014) *Bacillus thuringiensis* toxins: An overview of their biocidal activity. *Toxins*, **6**(12), 3296–3325. DOI: [10.3390/toxins6123296](https://doi.org/10.3390/toxins6123296)
- PANZA, P., MAIER, J., SCHMEES, C., ROTHBAUER, U., & SOLLNER, C. (2015) Live imaging of endogenous protein dynamics in zebrafish using chromobodies. *Development*, **142**(10), 1879–1884. DOI: [10.1242/dev.118943](https://doi.org/10.1242/dev.118943)
- PARDO-LÓPEZ, L., SOBERÓN, M., & BRAVO, A. (2013) *Bacillus thuringiensis* insecticidal three-domain Cry toxins: Mode of action, insect resistance and consequences for crop protection. *FEMS Microbiology Reviews*, **37**(1), 3–22. DOI: [10.1111/j.1574-6976.2012.00341.x](https://doi.org/10.1111/j.1574-6976.2012.00341.x)
- PARDES-SABJA, D., SETLOW, B., SETLOW, P., & SARKER, M. R. (2008) Characterization of *Clostridium perfringens* spores that lack SpoVA proteins and dipicolinic acid. *Journal of Bacteriology*, **190**(13), 4648–59. DOI: [10.1128/JB.00325-08](https://doi.org/10.1128/JB.00325-08)
- PATRON, N. J., ORZAEZ, D., MARILLONNET, S., WARZECHA, H., MATTHEWMAN, C., YOULES, M., ... HASELOFF, J. (2015) Standards for plant synthetic biology: a common syntax for exchange of DNA parts. *New Phytologist*, **208**(1), 13–19. DOI: [10.1111/nph.13532](https://doi.org/10.1111/nph.13532)
- PEARSON, D., & WARD, O. P. (1987) Purification of the parasporal crystals of *Bacillus thuringiensis* subsp. *israelensis* and development of a novel bioassay technique. *Biotechnology Letters*, **9**(11), 771–776. DOI: [10.1007/BF01028282](https://doi.org/10.1007/BF01028282)
- PEDRAZA-REYES, M., RAMÍREZ-RAMÍREZ, N., VIDALES-RODRÍGUEZ, L. E., & ROBLETO, E. A. (2012) Mechanisms of bacterial spore survival. In: E. Abel-Santos (Ed.), *Bacterial spores: Current research and applications* (pp. 73–88). Norfolk, UK: Caister Academic Press
- PERANI, M., BISHOP, A. H., & VAID, A. (1998) Prevalence of  $\beta$ -exotoxin, diarrhoeal toxin and specific  $\delta$ -endotoxin in natural isolates of *Bacillus thuringiensis*. *FEMS Microbiology Letters*, **160**(1), 55–60. DOI: [10.1016/S0378-1097\(98\)00010-X](https://doi.org/10.1016/S0378-1097(98)00010-X)
- PIGGOT, P. J., & COOTE, J. G. (1976) Genetic aspects of bacterial endospore formation. *Microbiology and Molecular Biology Reviews*, **40**(4), 908–962. PMID: 12736
- PIGOTT, C. R., KING, M. S., & ELLAR, D. J. (2008) Investigating the properties of *Bacillus thuringiensis* cry proteins with novel loop replacements created using combinatorial molecular biology. *Applied and Environmental Microbiology*, **74**(11), 3497–3511. DOI: [10.1128/AEM.02844-07](https://doi.org/10.1128/AEM.02844-07)
- POMPIDOR, G., D'ALÉO, A., VICAT, J., TOUPET, L., GIRAUD, N., KAHN, R., & MAURY, O. (2008a) Protein crystallography through supramolecular interactions between a lanthanide complex and arginine. *Angewandte Chemie (International Ed. In English)*, **47**(18), 3388–91. DOI: [10.1002/anie.200704683](https://doi.org/10.1002/anie.200704683)
- POMPIDOR, G., VICAT, J., & KAHN, R. (2008b) Lysozyme cocrystallized with tris-dipicolinate Eu complex. PDB: 2PC2, version 1.2. DOI: [10.2210/pdb2PC2/pdb](https://doi.org/10.2210/pdb2PC2/pdb)

- PÓSFAL, G., KOLISNYCHENKO, V., BERECZKI, Z., & BLATTNER, F. R. (1999) Markerless gene replacement in *Escherichia coli* stimulated by a double-strand break in the chromosome. *Nucleic Acids Research*, **27**(22), 4409–4415. DOI: [10.1093/nar/27.22.4409](https://doi.org/10.1093/nar/27.22.4409)
- REESE, M. G. (2001) Application of a time-delay neural network to promoter annotation in the *Drosophila melanogaster* genome. *Computers and Chemistry*, **26**(1), 51–56. DOI: [10.1016/S0097-8485\(01\)00099-7](https://doi.org/10.1016/S0097-8485(01)00099-7)
- ROBINSON, C. R., & SAUER, R. T. (1998) Optimizing the stability of single-chain proteins by linker length and composition mutagenesis. *Proceedings of the National Academy of Sciences*, **95**(11), 5929–5934. DOI: [10.1073/pnas.95.11.5929](https://doi.org/10.1073/pnas.95.11.5929)
- ROBINSON, M.-P., KE, N., LOBSTEIN, J., PETERSON, C., SZKODNY, A., MANSELL, T. J., ... BERKMEN, M. (2015) Efficient expression of full-length antibodies in the cytoplasm of engineered bacteria. *Nature Communications*, **6**, 8072. DOI: [10.1038/ncomms9072](https://doi.org/10.1038/ncomms9072)
- ROH, J. Y., LI, M. S., CHANG, J. H., CHOI, J. Y., SHIM, H. J., SHIN, S. C., ... JE, Y. H. (2004) Expression and characterization of a recombinant Cry1Ac crystal protein with enhanced green fluorescent protein in acrySTALLIFEROUS *Bacillus thuringiensis*. *Letters in Applied Microbiology*, **38**(5), 393–399. DOI: [10.1111/j.1472-765X.2004.01505.x](https://doi.org/10.1111/j.1472-765X.2004.01505.x)
- ROTMAN, Y., & FIELDS, M. L. (1968) A modified reagent for dipicolinic acid analysis. *Analytical Biochemistry*, **22**(1), 168. DOI: [10.1016/0003-2697\(68\)90272-8](https://doi.org/10.1016/0003-2697(68)90272-8)
- SACKS, L. E. (1969) Modified two-phase system for partition of *Bacillus macerans* spores. *Applied Microbiology*, **18**(3), 416–419. PMID: 4907003
- SANSINENEA, E. (ED.) (2012) *Bacillus thuringiensis Biotechnology*. Dordrecht: Springer Netherlands. ISBN: 978-94-007-3020-5
- SARMENTO, B., RIBEIRO, A., VEIGA, F., FERREIRA, D., & NEUFELD, R. (2007) Oral bioavailability of insulin contained in polysaccharide nanoparticles. *Biomacromolecules*, **8**(10), 3054–3060. DOI: [10.1021/bm0703923](https://doi.org/10.1021/bm0703923)
- SAWAYA, M. R., CASCIO, D., GINGERY, M., RODRIGUEZ, J., GOLDSCHMIDT, L., COLLETIER, J.-P., ... EISENBERG, D. S. (2014) Protein crystal structure obtained at 2.9 Å resolution from injecting bacterial cells into an X-ray free-electron laser beam. *Proceedings of the National Academy of Sciences of the United States of America*, **111**(35), 12769–74. DOI: [10.1073/pnas.1413456111](https://doi.org/10.1073/pnas.1413456111)
- SCHALLMEY, M., SINGH, A., & WARD, O. P. (2004) Developments in the use of *Bacillus* species for industrial production. *Canadian Journal of Microbiology*, **50**(1), 1–17. DOI: [10.1139/w03-076](https://doi.org/10.1139/w03-076)
- SCHNEIDER, C. P., SHUKLA, D., & TROUT, B. L. (2011) Arginine and the Hofmeister Series: the role of ion-ion interactions in protein aggregation suppression. *The Journal of Physical Chemistry. B*, **115**(22), 7447–58. DOI: [10.1021/jp111920y](https://doi.org/10.1021/jp111920y)

- SCHNEPF, H. E., & WHITELEY, H. R. (1981) Cloning and expression of the *Bacillus thuringiensis* crystal protein gene in *Escherichia coli*. *Proceedings of the National Academy of Sciences of the United States of America*, **78**(5), 2893–7. DOI: [10.1007/s11033-008-9366-5](https://doi.org/10.1007/s11033-008-9366-5)
- SCHÖNHERR, R., RUDOLPH, J. M., & REDECKE, L. (2018) Protein crystallization in living cells. *Biological Chemistry*, **399**(7), 751–772. DOI: [10.1515/hsz-2018-0158](https://doi.org/10.1515/hsz-2018-0158)
- SETLOW, B., ATLURI, S., KITCHEL, R., KOZIOL-DUBE, K., & SETLOW, P. (2006) Role of dipicolinic acid in resistance and stability of spores of *Bacillus subtilis* with or without DNA-protective alpha/beta-type small acid-soluble proteins. *Journal of Bacteriology*, **188**(11), 3740–7. DOI: [10.1128/JB.00212-06](https://doi.org/10.1128/JB.00212-06)
- SETLOW, B., PENG, L., LOSHON, C. A., LI, Y.-Q., CHRISTIE, G., & SETLOW, P. (2009) Characterization of the germination of *Bacillus megaterium* spores lacking enzymes that degrade the spore cortex. *Journal of Applied Microbiology*, **107**(1), 318–28. DOI: [10.1111/j.1365-2672.2009.04210.x](https://doi.org/10.1111/j.1365-2672.2009.04210.x)
- SETLOW, P. (2006) Spores of *Bacillus subtilis*: their resistance to and killing by radiation, heat and chemicals. *Journal of Applied Microbiology*, **101**(3), 514–25. DOI: [10.1111/j.1365-2672.2005.02736.x](https://doi.org/10.1111/j.1365-2672.2005.02736.x)
- SETLOW, P. (2014) The germination of spores of *Bacillus* species: what we know and don't know. *Journal of Bacteriology*, **196**(7), 1297–1305. DOI: [10.1128/JB.01455-13](https://doi.org/10.1128/JB.01455-13)
- SETLOW, P. (2016) Germination of spores of *Bacillus* and *Clostridium* species: surprises and challenges. In: *7th European Spores Conference*. Egham
- SETLOW, P., LIU, J., & FAEDER, J. R. (2012) Heterogeneity in bacterial spore populations. In: E. Abel-Santos (Ed.), *Bacterial spores: Current research and applications* (pp. 199–214). Norfolk, UK: Caister Academic Press
- SHAH, I. M., LAABERKI, M.-H., POPHAM, D. L., & DWORKIN, J. (2008) A eukaryotic-like Ser/Thr kinase signals bacteria to exit dormancy in response to peptidoglycan fragments. *Cell*, **135**(3), 486–496. DOI: [10.1016/j.cell.2008.08.039](https://doi.org/10.1016/j.cell.2008.08.039)
- SHAO, X., JIANG, M., YU, Z., CAI, H., & LI, L. (2009) Surface display of heterologous proteins in *Bacillus thuringiensis* using a peptidoglycan hydrolase anchor. *Microbial Cell Factories*, **8**, 48. DOI: [10.1186/1475-2859-8-48](https://doi.org/10.1186/1475-2859-8-48)
- SHI, T., WANG, G., WANG, Z., FU, J., CHEN, T., & ZHAO, X. (2013) Establishment of a markerless mutation delivery system in *Bacillus subtilis* stimulated by a double-strand break in the chromosome. *PLoS ONE*, **8**(11), e81370. DOI: [10.1371/journal.pone.0081370](https://doi.org/10.1371/journal.pone.0081370)
- SHIBATA, H., YAMASHITA, S., OHE, M., & TANI, I. (1986) Laser Raman spectroscopy of lyophilized bacterial spores. *Microbiology and Immunology*, **30**(4), 307–313. DOI: [10.1111/j.1348-0421.1986.tb00947.x](https://doi.org/10.1111/j.1348-0421.1986.tb00947.x)

- SOBERÓN, M., PARDO-LÓPEZ, L., LÓPEZ, I., GÓMEZ, I., TABASHNIK, B. E., & BRAVO, A. (2007) Engineering modified Bt toxins to counter insect resistance. *Science*, **318**(5856), 1640–1642. DOI: [10.1126/science.1146453](https://doi.org/10.1126/science.1146453)
- SOTO, O., BAÑUELOS, E. A., & ALMANZA, G. M. (2014) Insecticide Cry proteins of *Bacillus thuringiensis* with anti-cancer activity. United States Patent Office: US 2014/0073582 A1. FROM [HTTPS://PATENTS.GOOGLE.COM/PATENT/US20140073582A1](https://patents.google.com/patent/US20140073582A1)
- STEWART, G. C. (2015) The exosporium layer of bacterial spores: a connection to the environment and the infected host. *Microbiology and Molecular Biology Reviews*, **79**(4), 437–457. DOI: [10.1128/MMBR.00050-15](https://doi.org/10.1128/MMBR.00050-15)
- STEWART, G. S. A. B., JOHNSTONE, K., HAGELBERG, E., & ELLAR, D. J. (1981) Commitment of bacterial spores to germinate., **198**(1), 101–106. DOI: [10.1042/bj1980101](https://doi.org/10.1042/bj1980101)
- SUNDE, E. P., SETLOW, P., HEDERSTEDT, L., & HALLE, B. (2009) The physical state of water in bacterial spores. *Proceedings of the National Academy of Sciences of the United States of America*, **106**(46), 19334–9. DOI: [10.1073/pnas.0908712106](https://doi.org/10.1073/pnas.0908712106)
- SØEBORG, T., RASMUSSEN, C. H., MOSEKILDE, E., & COLDING-JØRGENSEN, M. (2012) Bioavailability and variability of biphasic insulin mixtures. *European Journal of Pharmaceutical Sciences*, **46**(4), 198–208. DOI: [10.1016/j.ejps.2011.06.005](https://doi.org/10.1016/j.ejps.2011.06.005)
- TAM, N. K. M., UYEN, N. Q., HONG, H. A., DUC, L. H., HOA, T. T., SERRA, C. R., ... CUTTING, S. M. (2006) The intestinal life cycle of *Bacillus subtilis* and close relatives. *Journal of Bacteriology*, **188**(7), 2692–2700. DOI: [10.1128/JB.188.7.2692-2700.2006](https://doi.org/10.1128/JB.188.7.2692-2700.2006)
- TERPE, K. (2006) Overview of bacterial expression systems for heterologous protein production: from molecular and biochemical fundamentals to commercial systems. *Applied Microbiology and Biotechnology*, **72**(2), 211–22. DOI: [10.1007/s00253-006-0465-8](https://doi.org/10.1007/s00253-006-0465-8)
- THOMAS, W. E., & ELLAR, D. J. (1983) *Bacillus thuringiensis* var *israelensis* crystal  $\delta$ -endotoxin: effects on insect and mammalian cells *in vitro* and *in vivo*. *Journal of Cell Science*, **60**, 181–197. PMID: 6874728
- TIBURSKI, J. H., ROSENTHAL, A., GUYOT, S., PERRIER-CORNET, J.-M., & GERVAIS, P. (2014) Water distribution in bacterial spores: A key factor in heat resistance. *Food Biophysics*, **9**(1), 10–19. DOI: [10.1007/s11483-013-9312-5](https://doi.org/10.1007/s11483-013-9312-5)
- TING, Y. T., HARRIS, P. W. R., BATOT, G., BRIMBLE, M. A., BAKER, E. N., & YOUNG, P. G. (2016) Peptide binding to a bacterial signal peptidase visualized by peptide tethering and carrier-driven crystallization. *IUCrJ*, **3**, 10–19. DOI: [10.1107/S2052252515019971](https://doi.org/10.1107/S2052252515019971)
- TRAUTH, S., & BISCHOFFS, I. B. (2014) Ectopic integration vectors for generating fluorescent promoter fusions in *Bacillus subtilis* with minimal dark noise. *PLoS ONE*, **9**(5), e98360. DOI: [10.1371/journal.pone.0098360](https://doi.org/10.1371/journal.pone.0098360)

- ULANOWSKI, Z., LUDLOW, I. K., & WAITES, W. M. (1987) Water content and size of spore components determined by laser diffractometry. *FEMS Microbiology Letters*, **40**(2-3), 229–232. DOI: [10.1111/j.1574-6968.1987.tb02030.x](https://doi.org/10.1111/j.1574-6968.1987.tb02030.x)
- UMER, B., GOOD, D., ANNÉ, J., DUAN, W., & WEI, M. Q. (2012) Clostridial spores for cancer therapy: targeting solid tumour microenvironment. *Journal of Toxicology*, **2012**, 8. DOI: [10.1155/2012/862764](https://doi.org/10.1155/2012/862764)
- VANDERMARLIÈRE, M. (2016) cGMP production of recombinant spores: a challenge. In: *7th European Spores Conferences*. Egham
- VELÁSQUEZ, J., SCHUURMAN-WOLTERS, G., BIRKNER, J. P., ABEE, T., & POOLMAN, B. (2014) *Bacillus subtilis* spore protein SpoVAC functions as a mechanosensitive channel. *Molecular Microbiology*, **92**(4), 813–23. DOI: [10.1111/mmi.12591](https://doi.org/10.1111/mmi.12591)
- VEPACHEDU, V. R., & SETLOW, P. (2007) Role of SpoVA proteins in release of dipicolinic acid during germination of *Bacillus subtilis* spores triggered by dodecylamine or lysozyme. *Journal of Bacteriology*, **189**(5), 1565–72. DOI: [10.1128/JB.01613-06](https://doi.org/10.1128/JB.01613-06)
- WALLE, C. F. VAN DER (2016) Personal communications. [wallec@MedImmune.com](mailto:wallec@MedImmune.com)
- WALSH, G. (2005) Therapeutic insulins and their large-scale manufacture. *Applied Microbiology and Biotechnology*, **67**(2), 151–159. DOI: [10.1007/s00253-004-1809-x](https://doi.org/10.1007/s00253-004-1809-x)
- WARRINER, K., & WAITES, W. M. (1999) Enhanced sporulation in *Bacillus subtilis* grown on medium containing glucose:ribose. *Letters in Applied Microbiology*, **29**(2), 97–102. DOI: [10.1046/j.1365-2672.1999.00593.x](https://doi.org/10.1046/j.1365-2672.1999.00593.x)
- WEBB, C. D., DECATUR, A., TELEMAN, A., & LOSICK, R. (1995) Use of green fluorescent protein for visualization of cell-specific gene expression and subcellular protein localization during sporulation in *Bacillus subtilis*. *Journal of Bacteriology*, **177**(20), 5906. DOI: [10.1128/jb.177.20.5906-5911.1995](https://doi.org/10.1128/jb.177.20.5906-5911.1995)
- WESTPHAL, A. J., PRICE, P. B., LEIGHTON, T. J., & WHEELER, K. E. (2003) Kinetics of size changes of individual *Bacillus thuringiensis* spores in response to changes in relative humidity. *Proceedings of the National Academy of Sciences of the United States of America*, **100**(6), 3461–6. DOI: [10.1073/pnas.232710999](https://doi.org/10.1073/pnas.232710999)
- WITTCHEN, K. D., & MEINHARDT, F. (1995) Inactivation of the major extracellular protease from *Bacillus megaterium* DSM319 by gene replacement. *Applied Microbiology and Biotechnology*, **42**(6), 871–877. DOI: [10.1007/BF00191184](https://doi.org/10.1007/BF00191184)
- XU ZHOU, K., IONESCU, A., WAN, E., HO, Y. N., BARNES, C. H. W., CHRISTIE, G., & WILSON, D. I. (2018) Paramagnetism in *Bacillus* spores: Opportunities for novel biotechnological applications. *Biotechnology and Bioengineering*, **115**(4), 955–964. DOI: [10.1002/bit.26501](https://doi.org/10.1002/bit.26501)

- XU ZHOU, K., WISNIVESKY, F., WILSON, D. I., & CHRISTIE, G. (2017) Effects of culture conditions on the size, morphology and wet density of spores of *Bacillus cereus* 569 and *Bacillus megaterium* QM B1551. *Letters in Applied Microbiology*, **65**(1), 50–56. DOI: [10.1111/lam.12745](https://doi.org/10.1111/lam.12745)
- YAN, X., YU, H.-J., HONG, Q., & LI, S.-P. (2008) Cre/lox system and PCR-based genome engineering in *Bacillus subtilis*. *Applied and Environmental Microbiology*, **74**(17), 5556–62. DOI: [10.1128/AEM.01156-08](https://doi.org/10.1128/AEM.01156-08)
- YANG, M. X., SHENOY, B., DISTTLER, M., PATEL, R., MCGRATH, M., PECHENOV, S., & MARGOLIN, A. L. (2003) Crystalline monoclonal antibodies for subcutaneous delivery. *Proceedings of the National Academy of Sciences*, **100**(12), 6934–6939. DOI: [10.1073/pnas.1131899100](https://doi.org/10.1073/pnas.1131899100)
- YOU, C., ZHANG, X.-Z., & ZHANG, Y. H. P. (2012) Simple cloning via direct transformation of PCR product (DNA multimer) to *Escherichia coli* and *Bacillus subtilis*. *Applied and Environmental Microbiology*, **78**(5), 1593–1595. DOI: [10.1128/AEM.07105-11](https://doi.org/10.1128/AEM.07105-11)
- YOUNG, I. E., & FITZ-JAMES, P. C. (1959) Chemical and morphological studies of bacterial spore formation II. Spore and parasporal protein formation in *Bacillus cereus* var. *alesti*. *J. Biophysics and Biochem. Cytol.*, **6**(3), 483–498
- ZHENG, L. B., DONOVAN, W. P., FITZ-JAMES, P. C., & LOSICK, R. (1988) Gene encoding a morphogenic protein required in the assembly of the outer coat of the *Bacillus subtilis* endospore. *Genes & Development*, **2**(8), 1047–1054. DOI: [10.1101/gad.2.8.1047](https://doi.org/10.1101/gad.2.8.1047)
- ZHU, Y., JI, F., SHANG, H., ZHU, Q., WANG, P., XU, C., ... SUN, M. (2011) Gene clusters located on two large plasmids determine spore crystal association (SCA) in *Bacillus thuringiensis* subsp. *finitimus* strain YBT-020. *PLoS ONE*, **6**(11). DOI: [10.1371/journal.pone.0027164](https://doi.org/10.1371/journal.pone.0027164)





# Chapter A1

## Appendix

## A1.1 DPA Assay

Figure A1.1 shows the standard curve for DPA assays. Table A1.1 shows the details of the paired comparisons calculation in section 3.2.1. Table A1.2 shows the details of the second paired comparisons calculation in section 3.2.2. Table A1.3 shows the data used to plot figure 3.3.

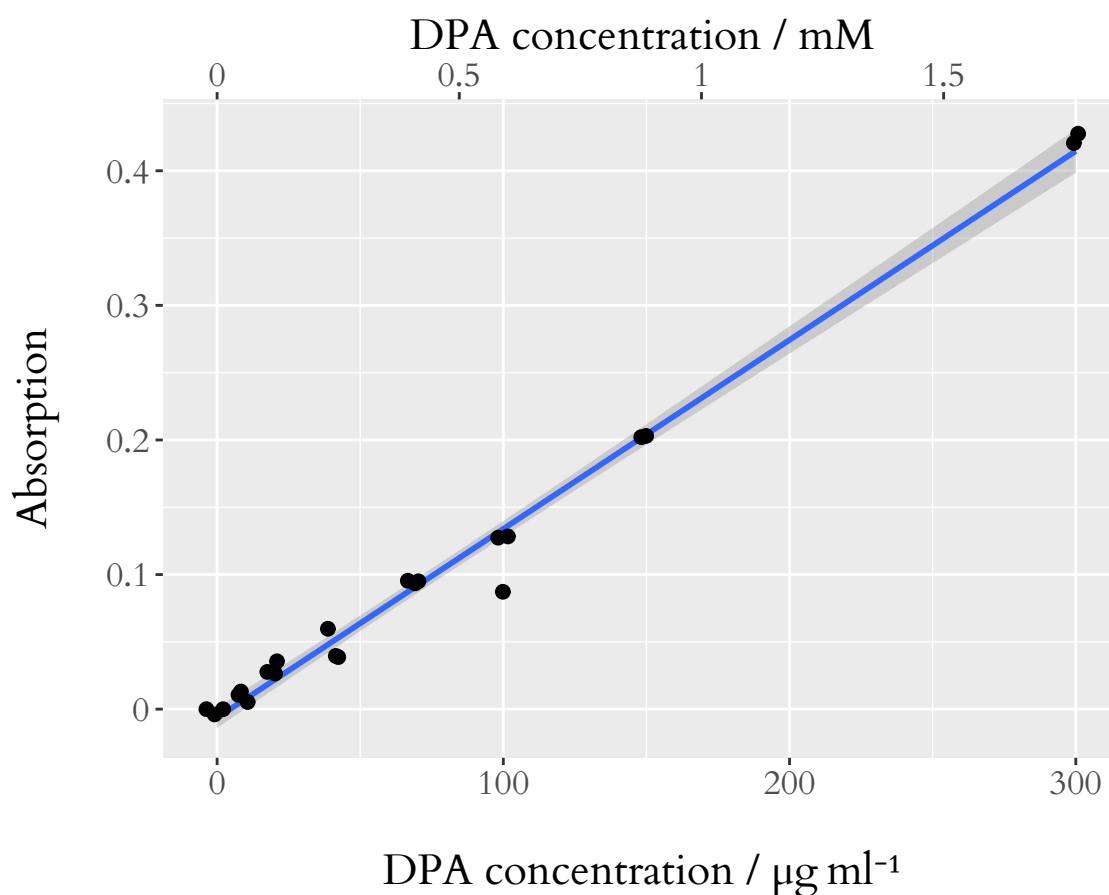


Figure A1.1: Calibration curve for DPA assay. Values are jittered so coincident points can be resolved. Data are from multiple batches of standard solution.

Table A1.1: Paired comparisons test, of differences in DPA content with or without  $\Delta spoVF$  mutation. Values presented are averages of the readings in each category: with (+) or without (-)  $spoVF$  or  $sleB$ . The resulting test statistic,  $t_0$ , is 20.4 (mean difference divided by error in mean), giving a p-value of 0.016.

Normalized DPA concentration	+ $spoVF$	- $spoVF$	Difference
+ $sleB$	0.986	0.212	0.775
- $sleB$	0.729	0.026	0.702
Mean	0.858	0.119	0.738
Sum of error squares			1.093
Standard deviation	0.182	0.131	0.051
Error in mean	0.129	0.093	0.036

Table A1.2: Paired comparisons test of differences in DPA content with ( $\checkmark$ ) or without ( $\times$ ) exogenous DPA. The resulting test statistic,  $t_0$ , is 5.95 (mean difference divided by error in mean), giving a p-value of  $9.6 \times 10^{-4}$ .

Normalized DPA concentration	Batch	$\checkmark$	$\times$	Difference
QM B1551	1	1.174	1.000	0.174
QM B1551	2	1.862	1.000	0.862
1462::21s	1	0.941	0.008	0.933
1462::21s	2	0.949	0.000	0.949
1551::21s+	1	0.888	0.277	0.611
1551::21s+	2	1.076	0.155	0.921
Mean		1.148	0.407	0.742
Sum of error squares				3.765
Standard deviation		0.365	0.471	0.305
Error in mean		0.149	0.192	0.125

Table A1.3: Data, for DPA assay plot.

Strain	DPA added?	SXO	Batch	Coded	Normalized	Concentration / $\mu\text{g ml}^{-1}$
QM B1551	x	x	1	0.1203	1	85.9
QM B1551	x	x	2	0.1065	1.03	76.1
QM B1551	x	x	2	0.1007	0.97	71.9
QM B1551	x	x	3	0.1385	1	98.9
QM B1551	✓	x	1	0.1412	1.17	100.9
QM B1551	✓	x	3	0.2579	1.86	184.2
PS1462	x	x	2	0.0867	0.84	61.9
PS1462	x	x	2	0.0685	0.66	48.9
1551::21s+	x	✓	1	0.0333	0.28	23.8
1551::21s+	x	✓	2	0.0189	0.18	13.5
1551::21s+	x	✓	2	0.0253	0.24	18.1
1551::21s+	x	✓	3	0.0215	0.16	15.4
1551::21s+	✓	✓	1	0.1068	0.89	76.3
1551::21s+	✓	✓	3	0.1490	1.08	106.4
1462::21s	x	x	1	0.0010	0.01	0.7
1462::21s	x	x	2	0	0	0
1462::21s	x	x	2	0	0	0
1462::21s	x	x	3	0	0	0
1462::21s	✓	x	1	0.1132	0.94	80.9
1462::21s	✓	x	3	0.1315	0.95	93.9

## A1.2 *B. megaterium* colony counts

Table A1.4 shows colony count data for figures 3.5, 3.6. The PS1462 value for the former is based on slightly different raw data to that corresponding to no shock for the latter.

Table A1.4: Colony count data for *B. megaterium* mutants.

Strain	DPA added?	Shock	Shape	Rate	Maximum likelihood estimator
PS1462	✗	70°C 20min	31	$3.3 \times 10^{-7}$	$9.09 \times 10^7$
PS1462	✗	80°C 20min	121	$3.333 \times 10^{-5}$	$3.60 \times 10^6$
PS1462	✗	90°C 20min	11	0.00333333	3000
PS1462	✗	none	232	$6.99 \times 10^{-6}$	$3.30 \times 10^7$
1551::21s+	✓	70°C 20min	142	$3.33 \times 10^{-6}$	$4.23 \times 10^7$
1551::21s+	✓	80°C 20min	29	$3.33 \times 10^{-6}$	$8.41 \times 10^6$
1551::21s+	✓	90°C 20min	61	$3.333 \times 10^{-5}$	$1.80 \times 10^6$
1551::21s+	✓	none	201	$3.66 \times 10^{-6}$	$5.46 \times 10^7$
1462::21s	✗	70°C 20min	19	$3.33 \times 10^{-6}$	$5.41 \times 10^6$
1462::21s	✗	80°C 20min	57	$3.333 \times 10^{-5}$	$1.68 \times 10^6$
1462::21s	✗	90°C 20min	33	0.00333333	9600
1462::21s	✗	none	107	$6.666 \times 10^{-5}$	$1.59 \times 10^6$
1462::21s	✓	70°C 20min	111	$3.33 \times 10^{-6}$	$3.30 \times 10^7$
1462::21s	✓	80°C 20min	186	$3.333 \times 10^{-5}$	$5.55 \times 10^6$
1462::21s	✓	90°C 20min	46	$3.3333 \times 10^{-4}$	$1.35 \times 10^5$
1462::21s	✓	none	185	$6.66 \times 10^{-6}$	$2.76 \times 10^7$
QM B1551	✗	none	442	$3.99 \times 10^{-6}$	$1.11 \times 10^8$

### A1.3 Spores grown with DPA analogues

Figure A1.2 shows micrographs of  $\Delta spoVF$  mutant spores grown with various DPA analogues. They appear just as the spores grown with no supplement.

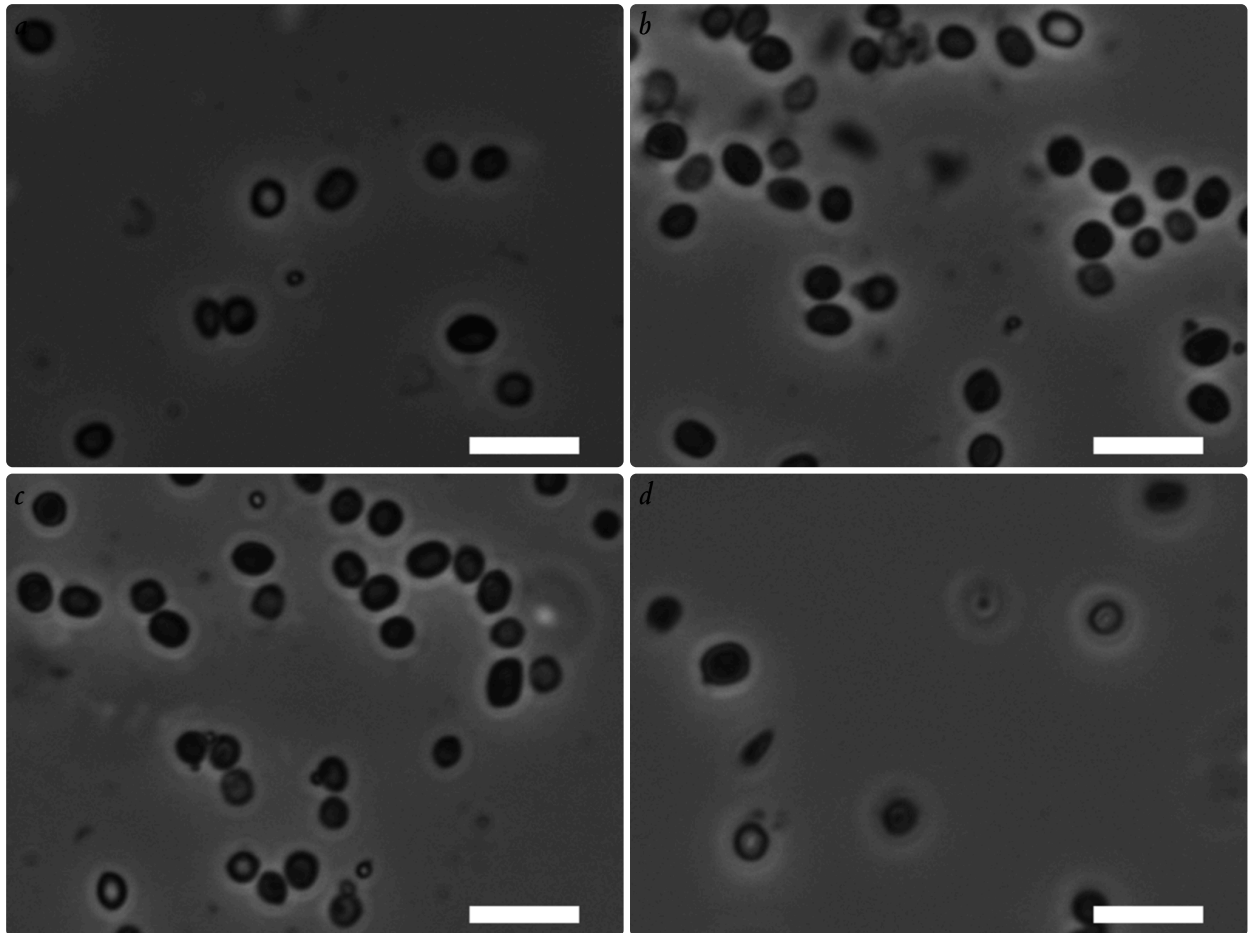


Figure A1.2: Micrographs of *B. megaterium* 1551::21s+, sporulated in DPA analogue-supplemented SNB. (a) shows the culture supplemented with IPA; (b) PA; (c) IDA; (d) NTA. Spores grown in these media looked no different to those grown in standard medium. Strain 1551::21s has the  $\Delta spoVF$  mutation. Cultures were induced to sporulate via nutrient exhaustion. Scale bars are  $5\mu\text{m} \times 1\mu\text{m}$ .

## A1.4 Pop-out calculation

To estimate the pop-out proportion from the pop-out frequency, one need only consider the cells which do not revert.

Let  $f$  denote the pop-out frequency (i.e. the probability that any one cell division results in excision of the plasmid); assume this is small ( $\sim 10^{-6}$ ). Let  $g$  denote the number of generations. Let  $a_i$  denote the proportional growth of the culture in generation  $i$ . Let  $n$  denote the number of cells in the culture. Let  $N$  denote the number of cells in the initial inoculum; assume this is large ( $\gtrsim 10^3$ ).

The inoculum contains  $N$  cells, initially. After 1 generation, the expectation of  $n$  is  $a_0 N$ ; after 2,  $a_0 a_1 N$ ; etc. After  $g$  generations, this is  $N \prod_{i=0}^{g-1} a_i$ , where the product runs from  $a_0$  to  $a_{(g-1)}$ .

The inoculum contains  $N$  non-revertants, initially. After 1 generation, the expected number of non-revertants is  $a_0(1-f)N$ ; after 2,  $a_0 a_1 (1-f)^2 N$ ; etc. After  $g$  generations, this is  $(1-f)^g N \prod_{i=0}^{g-1} a_i$ , where the product runs as above.

Thus the expected proportion of non-revertants, after  $g$  generations, is the quotient:  $(1-f)^g$ . The expected proportion of revertants, after  $g$  generations, is  $1 - (1-f)^g \simeq fg$ .

This Poisson process corresponds to a Gamma distribution, with shape parameter  $g$  and scale parameter  $f$ . The mean is  $fg$ ; the variance is  $f^2 g$ . Distributions are plotted in figure A1.3.

Spore crops in SNB have number densities of the order of  $10^9$  spore  $\text{ml}^{-1}$ . A 200 ml culture, resuspended in 4 ml, gives an  $\text{OD}_{600}$  of 1 when diluted 500 $\times$ . This means if diluted to  $500 \times 4 \text{ ml} = 2000 \text{ ml}$  the whole sample would have an  $\text{OD}_{600}$  of 1, corresponding to  $10^8$  spore  $\text{ml}^{-1}$ . As that is 10 $\times$  the original volume, the original culture must have had 10 $\times$  the number density, i.e.  $10^9$  cfu  $\text{ml}^{-1}$ . The 200 ml culture would contain  $10^{11}$  spores.



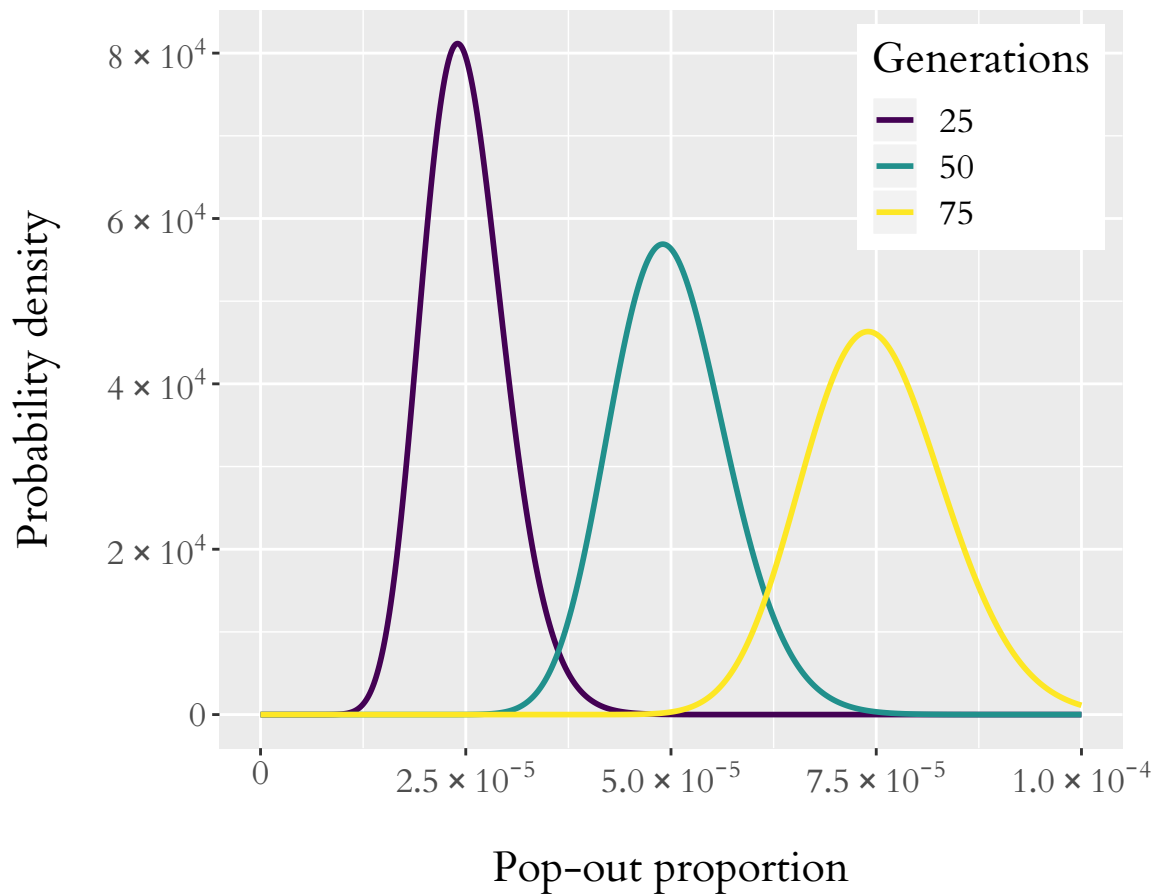


Figure A1.3: Probability density distributions, for fraction of cells undergoing pop-out. The mean (and maximum likelihood estimator) grows linearly with the number of generations, and linearly with the pop-out frequency. The pop-out frequency used here is  $10^{-6}$ .

## A1.5 Fusions

Listing A1.1 shows amino acid sequences of fusion domains.

*Listing A1.1: Amino acid sequences of antibody fusions. Sequences are presented in FASTA format.*

```

> AL11 linker
GTAAAGAGAAGGAAAGAAG

> Chromobody Linker
RNSISSLSIPSTVPRARDPPVD

> Fluorescent Protein mCherry
RGVSKGEEDNMAIIKEFMRFKVHMEGSVNGHEFEIEGEGEGRPYEGTQTAKLKVTKGGPL
PFAWDILSPQFMYGSKAYVKHPADIPDYLKLSFPEGFKWERVMNFEDGGVVTVTQDSSLQ
DGEFIYNVKLRGTNFPDGPVMQKKTMGWEASSERMYPEDGALKGEIKQRLKLDGGHYD
AEVKTTYKAKKPVQLPGAYNVNIKLDITSHNEDYTIVEQYERAEGRHSTGGMDELYK

> GFP
SKGEELFTGVVPILEVELDGDVNGHKFSVSGEGEGDATYGKLTCLKFICTTGKLPVPWPTLV
TTLTYGVCFSRYPDHMKQHDFFKSAMPEGYVQERTIFFKDDGNYKTRAEVKFEGLTLVN
RIELKGIDFKEDGNILGHKLEYNYNVSHNVYIMADKQKNGIKVNFKIRHNIEDGSVQLADH
YQNTPIGDGPVLSPDNHYLSTQSALSKDPNEKRDHMLLEFVTAAGITHGMDELYK

```

## A1.6 Nanobodies

Listing A1.2 shows amino acid sequences of nanobodies. These use using single letter notation.

*Listing A1.2: Amino acid sequences of nanobodies. Sequences are presented in FASTA format.*

```

> VHHGFP4
DQVQLVESGGALVQPGGSLRLSCAASGFPVNRYSMRWYRQAPGKEREWVAGMSSAGDRSS
YEDSVKGRFTISRDDARNTVYLQMNSLKPEDTAVYYCNVNVGFEYWGQGTQTVSS

> BcII10
QVQLVESGGGSVQAGGSLRLSCTASGGSEYSYSTFSLGWFRQAPGQEREAVAAIASMGL
TYYADSVKGRFTISRDNKNTVTLQMNNLKPEDTAIYYCAAVRGYFMRLPSSHNFRYWGQ
GTQTVSS

> TEM02
QVQLVESGGGSVQAGGSLRLSCARSGSTDSRNCMGWFRQAPGKERESVASIYASGSTLYA
DSVEDRFTISQDNNKNTVYLQMNSLKPDDTAMYYCAAGRSRLGCSTERNSDYWGQGTQVT
VSS

> TEM13
QVQLVESGGGSVQAGGSLRLSCAASGYDYSTNCMAWFRQAPGKEREWVATIYTAGYTRYA
DSVKGRFTISQESAKNTVYLQMNILKPEDTAMYYCAEGRWDCSSAPNHWGQGTQTVSS

```

## A1.7 Inducibly (super-)competent *B. subtilis*

Multiple methods were used to attempt to transform *B. subtilis* 168 to the desired genotype.

- Plasmid pDBT690 was used to transform wild type chemically competent *Bacillus subtilis* 168 to 5-fluorouracil<sup>r</sup>.
- A 200 µl aliquot of chemically competent *B. subtilis* 168 was transformed to chloramphenicol resistance with 230 ng of a 4527 bp PCR fragment corresponding to the operon shown in figure A1.6, otherwise according to the standard protocol from section 2.3.5.
- *B. subtilis* 168 was transformed to chloramphenicol<sup>r</sup> with pDBT69d, and selected on LB plates containing chloramphenicol, as described in section 2.4.

Plasmid pDBT690 matches pST, used by Shi *et al.* (2013) with the purpose of converting *B. subtilis* subsp. *subtilis* 168 to *B. subtilis* BUK (figure A1.4). The construct replicated here uses their same homologous regions, but a backbone from pDG1662.

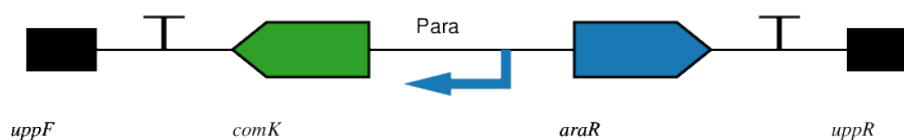


Figure A1.4: The *upp* locus, following a successful indel mutation. This mutation would generate an inducibly (super-)competent strain of *B. subtilis*. The locus corresponds to a double crossover integration of plasmid pDBT690 into the *B. subtilis* 168 genome. The *uppF*(orward) and *uppR*(everse) elements correspond to loci just 5' and 3' of the wild type *upp* respectively. The *comK* gene and terminator, which encode the competence master regulator, are assembled facing upstream. The *araR* gene, terminator and the  $P_{ara}$  (arabinose inducible) promoter at its 5' are assembled downstream of that. Thus  $P_{ara}$  drives *comK*, and arabinose induces competence.

Strain 168::69c lacks *upp*, and can therefore be a positive control for *upp* counter-selection. Thanks to its *cat* cassette, it can also be isolated using chloramphenicol selection. Like pDBT690, pDBT69c has homology with regions at the *upp* locus. When integrated by double-crossover, it would also knock out *upp*. Rather than introducing the aforementioned *comK* machinery to induce competence, though, it simply adds a chloramphenicol resistance cassette.

Plasmid pDBT69d introduces the *comK* machinery and a chloramphenicol cassette, at the *upp* locus (figures A1.5, A1.6). The upstream region of homology, like in pDBT690, matches the region just upstream of *upp*. Here, however, the downstream region of homology matches a region that is *also* upstream of *upp* — as opposed to a region downstream of *upp*. The plasmid would thereby insert its payload immediately upstream of *upp*, with minimal deletion. At this point, there would now be two 30 bp regions of homology: one from the insert, one in the region just downstream of *upp*. The chloramphenicol resistance gene, *cat*, and *upp* are now located between these two 30 bp repeats. An *I-SceI* restriction site is situated such that recombination at these two repeating regions, following *I-SceI* digestion, will excise the marker (*cat*, from pDBT69d) and the counter-selection marker (*upp*, already present in the genome).

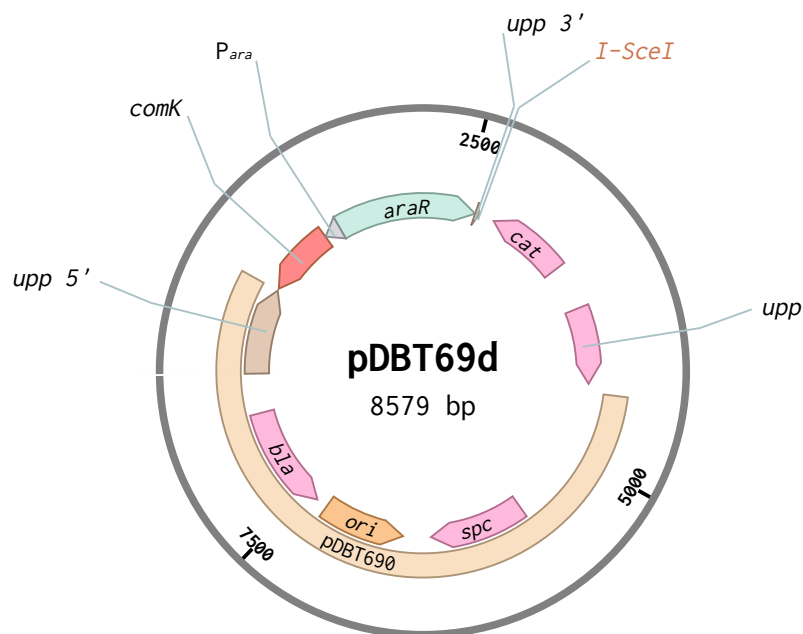


Figure A1.5: Plasmid pDBT69d for construction of 168::690 via dual cassette strain 168::69d. Labels indicate: *araR*, arabinose repressor; *comK*, master competence regulator; *upp*, uracil phosphoribyl-transferase; *bla*,  $\beta$ -lactamase (carbenicillin resistance); *spc*, spectinomycin adenylyltransferase; *cat*, chloramphenicol acetyltransferase; *ori*, *E. coli* origin of replication; *P<sub>ara</sub>*, arabinose-inducible promoter; *I-SceI*, restriction site.

Following transformation of *B. subtilis* 168 with pDBT69d, two of the twelve screened colonies showed bands, consistent with those predicted at 898 bp and 1261 bp. Strain 168::69d was then transformed with pEBS-cop1, and eight of the resulting colonies were screened for marker excision, by multiplex PCR. The subsequent phenotypic screen indicated Colony 4 had the chloramphenicol<sup>s</sup> 5-FU<sup>r</sup> erythromycin/lincomycin<sup>s</sup> properties

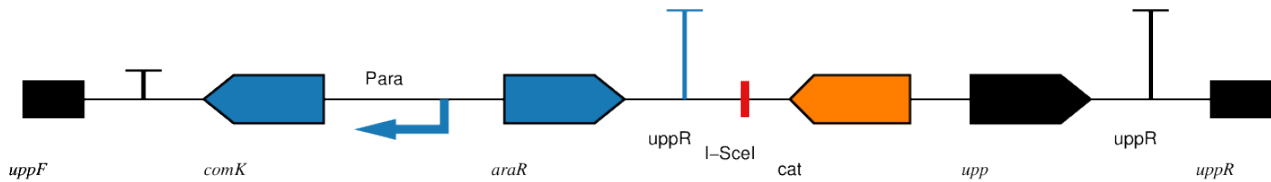


Figure A1.6: The *upp* locus following a successful double crossover integration of plasmid pDBT69d into the *B. subtilis* 168 genome. The native elements (in black) are disrupted by a) the *comK*–*araR* cassette and 30 bp of the *upp* terminator region from pDBT690, b) the *I-SceI* recognition site TAGGG|ATAA\_CAGGGTAAT, and c) the *cat* cassette (chloramphenicol resistance). The aforementioned 30 bp region is present twice; flanking the recombinant *cat* and native *upp*. Following *I-SceI* digestion, recombination between these regions excises the full selection-counter-selection cassette.

associated with having lost the plasmid pEBS-cop1 — this before having cultured the strain at 50 °C. Colony 4, when cultured at 50 °C, resulted in colony a, chosen as 168::690; colony PCR verification of strain 168::690 was performed using multiplexed and simple PCR.

Additionally, a 2138 bp fragment was amplified from gDNA using primers y188 and y192 (table 2.31); this region was designed to cross the region from which the marker had been excised. Sanger sequencing was used to confirm the fragment had the correct sequence.

A1.8  $\Delta cotE$  mutants

Table A1.5 shows the details of the paired comparisons calculation in section 4.2.2.

*Table A1.5: Paired comparisons test, of differences in  $OD_{600}$  in  $\Delta cotE$  strains. The resulting test statistic,  $t_0$ , is 15.4 (mean difference divided by error in mean), giving a p-value of  $5.9 \times 10^{-4}$ .*

Equivalent $OD_{600}$	690:: <u>_</u>	71e:: <u>_</u>	Difference	
—	784	415	369	47%
611l	554	152	402	73%
611h	571	176	395	69%
611s	622	324	298	48%
Mean	633	267	366	59%
Sum of error squares			542594	
Standard deviation	105	125	47.5	
Error in mean	52.4	62.4	23.8	